From the
Institute of Veterinary Pathology
Chair of General Pathology and Pathological Anatomy

Head: Prof. Dr. W. Hermanns
Ludwig-Maximilians-University, Munich, Germany

and the
Department of Internal Medicine
Division of Nephrology

Head: Prof. Dr. F. Brosius III
University of Michigan, Ann Arbor, United States of America

Under the supervision of
Prof. Dr. R. Wanke and Prof. Dr. M. Kretzler

Common patterns of glomerular gene expression profiles in different murine models of early nephropathy

Inaugural - Dissertation
to achieve the doctor title of veterinary medicine
at the Faculty of Veterinary Medicine of the
Ludwig-Maximilians-University, Munich

Andreas Falko Blutke
from Stuttgart

Munich 2007

Gedruckt mit Genehmigung der Tierärztlichen Fakultät

der Ludwig-Maximilians-Universität München

Dekan:	Univ.-Prof. Dr. Braun
Berichterstatter:	Univ.-Prof. Dr. Wanke
Korreferent/en:	Univ.-Prof. Dr. Hartmann
	Univ.-Prof. Dr. Kaspers
	Univ.-Prof. Dr. Müller
	Univ.-Prof. Dr. Poulsen-Nautrup

Tag der Promotion: 8. Februar 2008

Meinem Bruder

Table of contents

1 Introduction

Development of glomerulosclerotic alterations is a common feature of various chronic kidney diseases leading to a progressive loss of functioning kidney parenchyma and finally resulting in terminal renal failure (Klahr et al. 1988). Manifold mechanisms involved in the pathogenesis of distinct aspects of glomerulosclerotic lesions have been studied in a large variety of different chronic kidney diseases in humans, as well as in diverse experimental animal models. Virtually independent of the respective aetiology of the underlying disease, the earliest stages of these different disease entities are characterized by common morphological and functional alterations of the glomeruli. These consist of development of glomerular hypertrophy and subsequent appearance of micro-albuminuria, both identified as key determinants of the progression of disease (Fogo and Ichikawa 1991, Remuzzi 1995, Wiggins 2007). Various studies have focussed on the characterization of disease specific properties, allowing for definition and segregation of single disease entities on the molecular level, which is seen as a prerequisite for identification of pathogenetic mechanisms, potential disease markers, new therapeutic targets and the development of individually adjusted therapies (Schmid et al. 2006). To achieve these goals, additional functional insights into the individual disease processes, as well as into common aspects of the pathophysiology of chronic kidney diseases on the glomerular level are required. Nephrology has greatly benefited from recent technical improvements in generation (Takemoto et al. 2002) and preservation of sample materials derived from human renal biopsies or from kidney tissues of experimental animal models. Modern research methods as transcript profiling or proteomic analysis are now applicable even on samples of isolated kidney glomeruli and represent valuable and promising approaches to study the pathogenetic mechanisms of glomerular gene expression regulation and alterations of the glomerular proteome in chronic renal diseases (Kretzler et al. 2002, Sitek et al. 2006, Yasuda et al. 2006). The present study was performed within the framework of the superordinated project "Cluster growth and differentiation - molecular pathogenesis of glomerulosclerosis in transgenic mouse models" of the graduate college "Functional genomics in veterinary medicine" (grk 1029), supported by the Deutsche Forschungsgemeinschaft, DFG.

The overriding hypothesis to be tested was, if the common patterns of morphological and functional glomerular alterations in the early stages of different chronic kidney diseases would also find a reflection in common glomerular gene or protein expression profiles. Therefore, both differential transcript profiling (present study) and proteomic analyses (Diss. med.vet., Block 2008, grk1029) were performed on samples of isolated kidney glomeruli of transgenic animals and their associated non-transgenic wild-type littermate control animals of two different transgenic mouse models of nephropathy. In order to ensure the comparability of data generated from glomerular samples derived from these different models, investigations were performed in two stringently defined early stages of comparable glomerular alteration: glomerular hypertrophy and onset of micro-albuminuria. Differential glomerular gene expression profiles from these stages of glomerular alteration were identified by microarray analysis in each investigated mouse model and compared to each other. The purpose of the present study was to identify transcripts displaying a congeneric differential expression in the respective stages of investigation in both mouse models. These common glomerular gene expression profiles are presumably independent of the different genetic backgrounds of the investigated animal models and of the identities of the different transgenes expressed in these models. The generated datasets provide the basis for further detailed studies of altered glomerular gene expression profiles related to distinct parameters of glomerular morphology and function in the single animal models, as well as evaluation of common molecular mechanisms implicated in the pathogenesis of glomerulosclerotic lesions, disease pathways and the regulatory networks underlying differential gene expression.

2 Scientific background

2.1 Importance of chronic kidney diseases (CKD)

The world's disease profile is changing, and chronic diseases now account for the majority of global morbidity and mortality (Atkins 2005). Supported by changed lifestyles, chronic kidney diseases are emerging as a major health problem worldwide, not only within the developed, but also increasingly within the emerging world (Atkins 2005, Fogo 2006). Following the US National Kidney Foundation, chronic kidney diseases are generally defined through either appearance of albuminuria or proteinuria, or a loss of kidney function, distinguished by a decline of the glomerular filtration rate of more than 40%, or the diagnosis of structural kidney alterations persisting for more than three months. Virtually independent of the initial insult, a common character of the various different disease entities, which are summarized under the term of chronic kidney diseases, is their tendency towards progression to end stage renal disease (ESRD), defined as the need for dialysis, receipt of a renal transplant, or death from chronic kidney failure (Remuzzi et al. 2006, White et al. 2005). Recent studies revealed the tremendous dimensions of CKD and end stage renal disease. Assuming continuation of previous trends in ESRD incidence and prevalence, alone in the US, the numbers of patients suffering from ESRD will raise from 382,000 in the year 2000 to over 700,000 in 2015, while the number of incident ESRD patients per year is expected to increase by 44% to 136,166 with more than 100,000 ESRD deaths annually (Gilbertson et al. 2005). Worldwide, chronic kidney disease (CKD) is increasing at an annual growth rate of 8% (Alebiosu and Ayodele 2005). While success of therapeutic treatment is often limited, the increasing number of patients with CKD or kidney failure requiring replacement therapy is burdening public health care systems with immense costs, consuming a significant proportion of health care budgets (Eknoyan et al. 2004, Schieppati and Remuzzi 2005). Separate from the economic magnitude of the problem, CKD has a significant impact on life expectancy and quality of life of affected patients and also comprises an increased risk for subsequent diseases (Tarnow et al. 2000, Young et al. 2003). Concerning the reasons identified to be responsible for the development of CKD, it is evident that a major cause of these diseases are glomerular disorders (Johnstone and Holzman 2006).

Data from the United States Renal Data Systems (USRDS) show, that 56% of incident patients with ESRD have glomerular diseases secondary to diabetic nephropathy, primary glomerulonephritis, vasculitis, or AIDS nephropathy (USRDS 2004). In most Western countries, diabetic nephropathy (DN) has become the single most common condition found in patients with CKD leading to ESRD (Alebiosu and Ayodele 2005, Mitka 2005, Wolf and Ziyadeh 2007). DN manifests as a clinical syndrome that is composed of albuminuria, progressively declining GFR, and increased risk for cardiovascular disease (Tarnow et al. 2000, Young et al. 2003). While the worldwide prevalence of diabetes mellitus is steadily increasing and estimated to reach 4.4% in 2030 (Wild et al. 2004), 20 to 40% of all diabetic patients are prone to develop kidney failure, suggesting also significant genetic influences on risk for development of DN (Krolewski 1999, Seaquist et al. 1989, USRDS 2004).

2.1.2 Common pathological features of CKD

The slow and persistent progressive loss of kidney function is characteristic for the chronological sequence in development of chronic renal failure. Apart from classifications according to etiological or morphological aspects of different chronic progressive nephropathies into distinct disease entities, and regardless of the underlying cause, chronic kidney diseases are commonly characterized by a progressive loss of functioning kidney nephrons. Histological, this is commonly marked by development of glomerulosclerosis, tubular atrophy and interstitial fibrosis, a progressive scarring that ultimately affects all structures of the kidney and finally leads to ESRD (Fogo and Ichikawa 1989, Fogo 1999, Mauer et al. 1992). In that context, it is most remarkable that the tendency of a once established chronic renal insufficiency to progression towards ESRD is not only independent of the respective nature of the initiating nephropathy, but also not necessarily depending on the persistence of that initial insult (Baldwin 1982, Brenner et al. 1982, el Nahas 1989, Klahr et al. 1988, Olson and Heptinstall 1988). The activation of unspecific mechanisms leading to a progressive loss of functioning kidney parenchyma is considered to be only dependent of the severity of the initial damage. Terminal renal failure is then the result of a vicious circle maintained by these mechanisms (Baldwin 1982, Brenner et al. 1982, Fogo and Ichikawa 1989, Hostetter et al. 1981, Ichikawa et al. 1991, Shimamura and Morrison 1975). Using different animal models, the pathomechanisms implicated in the progression of diverse chronic renal diseases have been studied in great detail through the last decades.

Throughout the different postulated hypotheses concerning the nature of the initiating events, which had been subject of intense discussions, the central common pathogenetic role of glomerulosclerotic alterations for the progression of chronic nephropathies has clearly emerged (Klahr et al. 1988): development of progressive glomerulosclerotic alterations results in loss of functioning nephrons and thereby leads to damage and progressive destruction of the remaining nephrons, finally resulting in terminal renal failure. Within the majority of the diverse chronic kidney diseases, the first alterations are detectable in the renal glomeruli. It is remarkable that all glomerular diseases implicated in the development of CKD, share the common features of proteinuria and effacement of podocyte foot processes (Johnstone and Holzman 2006). Glomerulosclerotic alterations as a consequence of podocyte damage are considered to play a key role in the progression of chronic kidney diseases to terminal renal failure (Klahr et al. 1988, Kriz 2002, Kriz et al. 1994, Mauer et al. 1992, Zoja et al. 2006). Therefore, the following sections will focus on the development of progressive glomerulosclerotic kidney alterations and their proposed implication in the progression of chronic renal disease to ESRD.

2.2 Glomerulosclerosis

Originally the term „glomerulosclerosis" was embossed by Kimmelstiel and Wilson in 1936, who employed it to describe the morphological alterations of glomeruli they found in kidney sections of patients with diabetes mellitus (Kimmelstiel and Wilson 1936). Since then, several authors provided different definitions of glomerulosclerosis, due to various aspects of the polymorphic occurrence of glomerular lesions and their respective properties (Churg and Sobin 1982, Fries et al. 1989, Romen 1976, Rumpelt and Thoenes 1974, Shimamura and Morrison 1975, van Goor et al. 1991). However, today it has generally become accepted to use the term glomerulusclerosis to designate the complexity of glomerular alterations associated with obliteration of glomerular capillaries, which typically affect single glomeruli to a variable extent. Due to the advance of (progressive) glomerulosclerotic alterations, these alterations comprise glomerular capillary lesions, glomerular extracapillary and exsudative lesions and extraglomerular lesions.

These lesions include increases of extracellular mesangial matrix (referred to as mesangial sclerosis), mesangial hypercellularity, collapse of glomerular capillary lumina, hyalinosis and synechial attachments of the glomerular tuft to the capsule of Bowman (Floege et al. 1992, Grone et al. 1989, Olson et al. 1985, Rennke and Klein 1989, Shimamura and Morrison 1975). In addition, the thickening of the glomerular basement membrane is a typical finding in diabetic glomerulopathy (Chavers et al. 1989). Nevertheless, "glomerulosclerosis" is a pathological diagnosis, which is based on morphological criteria of glomerular alterations. As glomerulosclerosis occurs in various different disease entities, it is not pathognomonic and therefore does not refer to the aetiology or pathogenesis of the lesions (Romen 1976, Schwartz and Lewis 1985). Histopathologically, denotation of glomerular lesions enunciates the extent to which single or different glomeruli are affected by the respective glomerulosclerotic alterations (Churg and Sobin 1982). "Diffuse glomerulosclerosis" refers to an affection of more than 80% of investigated glomeruli; otherwise it is termed "focal". "Global" and "segmental" describe complete or partial extensions of sclerotic lesions of single glomeruli, respectively. The literature provides a comprehensive documentation of glomerulosclerotic kidney alterations in humans and in experimental animal models. As glomerulosclerosis occurs in a variety of glomerular diseases, the spectrum of glomerulosclerotic disorders is traditionally classified into primary and secondary sclerosing glomerulopathies, depending on the recognition of the underlying disease. In human disease, the clinical entity of the so-called primary or idiopathic "focal and segmental glomerulosclerosis" (FSGS), is an important cause for an idiopathic nephrotic syndrome and represents the group of primary glomeruloscleroses (Habib 1973, Waldherr and Derks 1989). In FSGS, sclerosis involves some, but not all glomeruli (focal) and affects a portion, but not the entire glomerular tuft (segmental). The sclerotic process is defined by glomerular capillary collapse with increase in mesangial matrix (Fogo 2001). The term "secondary glomerulosclerosis" summarizes the by far more frequent glomerulosclerotic lesions appearing in the context of a large number of diseases of different aetiologies (Goldszer et al. 1984, Rennke and Klein 1989). A further subdivision of secondary glomeruloscleroses is performed due to either their preferential focal or diffuse appearance, or in accordance to a primarily renal, or systemic character of the underlying disease.

Concerning the primarily renal diseases that may lead to development of diffuse glomerulosclerosis, inflammatory glomerular diseases as diffuse glomerulonephritis are to mention (Klahr et al. 1988). Among the group of systemic diseases which have been associated with the development of progressive glomerulosclerosis of diffuse character, vascular and hereditary diseases, systemic autoimmunopathies and metabolic disorders are the most important (Rennke and Klein 1989). The by far single most common disease in humans that is prone to development of glomerulosclerotic alterations is diabetic nephropathy. In nephrology great emphasis is attributed to the study of the pathogenesis of glomerulosclerosis and the mechanisms which might induce its development. Among the various distinct lesions that can be observed in affected glomeruli, glomerular hypertrophy is the common property preceeding the development of any further damage that might lead to albuminuria and later to extended alterations (Ichikawa et al. 1991, Seyer-Hansen et al. 1980, Steffes et al. 1978).

2.3 Pathogenesis of progressive glomerulosclerosis

2.3.1 Glomerular hypertrophy

There is general agreement that a common pathomechanism exists, which determines the progredient loss of functioning nephrons by progressive glomerulosclerosis in CKD. However, concerning the nature of the initiating event responsible for the induction of development of glomerulosclerotic lesions, different pathogenetic concepts exist. The process is characterized by a self-perpetuating vicious cycle, which passes on the glomerulosclerotic damage from once lost and/or damaged nephrons to the remaining (Ichikawa et al. 1991, Kriz and LeHir 2005). In these nephrons, compensatory mechanisms are induced, which increase their vulnerability to any further challenge and thereby result in development of further glomerulosclerotic alterations. Thus the process proceeds, affecting a steadily increasing number of yet undamaged nephrons, finally resulting in ESRD. The search after the determinant pathomechanism resulted in postulation of different key concepts, from which glomerular hyperfunction (Brenner 1983), glomerular hypertrophy (Fogo and Ichikawa 1989) and disturbance of the glomerular permselectivity (Remuzzi and Bertani 1990) are the most appreciated. In the early eighties of the last century, Brenner and co-workers studied the pathophysiology of renal adaptation to nephron loss in the rat (Brenner 1983).

Using micropuncture techniques, as well as morphological investigations, they found that after removal of renal mass in a rat model of subtotal nephrectomy, arteriolar resistance lowered and plasma flow increased in remnant glomeruli (Hostetter et al. 1981), leading to more filtrate formed per nephron. They reasoned, that adaptive glomerular hyperperfusion and hyperfiltration in the remnant glomeruli represented the responsible factors for initiation of self destructive processes leading to development of glomerulosclerosis and progression of chronical renal failure (Brenner 1983). Later they amended their initial hypothesis and found increased pressures in the glomerular capillaries to be the determinant key mediator (Anderson et al. 1985, Lafferty and Brenner 1990). The hypothesis of glomerular hyperfiltration and hypertension then was able to explain the progression of chronic renal failure as a consequence of capacity overload in glomeruli due to renal ablation, primary renal disease, diabetes mellitus (Zatz et al. 1985) and aging, resulting in development of glomerulosclerotic alterations. The importance of hemodynamic factors in the pathogenesis of glomerulosclerotic kidney lesions was supported by experiments, in which pharmacological reduction of glomerular hypertension reduced the dimensions of development of glomerulosclerosis and decelerated the progression of chronic renal failure (Anderson et al. 1985, Anderson et al. 1986). However, at the end of the eighties, the universal validity of this „hyperfiltration"-hypothesis was criticized, as it could not explain all observed differences of development of glomerulosclerotic alterations and chronic renal failure in different animal models. The studies in the model of the subtotal nephrectomized rat performed by Yoshida and colleges included serial measurements of intraglomerular pressures by micropuncture of single nephrons and morphological investigations of these glomeruli (Fogo et al. 1988, Yoshida et al. 1988). They found, that either glomerulosclerotic lesions did not preferentially develop in glomeruli which displayed the uppermost increase of capillary pressures after subtotal nephrectomy, and that there was no detectable positive correlation between the magnitude of early glomerular capillary pressure and the severity of glomerulosclerosis in these glomeruli. Thus, they concluded that hypertension would be a rather minor contributor to the development of glomerulosclerotic alterations and therefore other factors than hemodynamic changes would predominantly promote glomerular sclerosis (Yoshida et al. 1988). In further experiments, they were able to demonstrate a direct linkage between an increase in size of glomeruli and the severity of subsequently developing glomerulosclerotic alterations.

They reasoned that glomerulosclerosis is caused by glomerular hypertrophy and not by increased pressures in glomerular capillaries, and that glomerular hypertrophy itself is dependent on an effective loss of functioning kidney parenchyma (Yoshida et al. 1989). The term „glomerular hypertrophy" refers to not only an overall increase of size or volume of the glomerular tuft due to an increase of the volume of glomerular cells and/or extracellular matrix, but also to a hyperplasia of mesangial and endothelial cells. Whereas the numbers of glomerular mesangial and endothelial cells increase in hypertrophied glomeruli, podocytes only display hypertrophy while their numbers per glomerulus remain unchanged (Wanke et al. 2001, Wiggins et al. 2005). The increase of the volume of the glomerular tuft, appearing during physiological growth is almost exclusively related to an increase of length of the glomerular capillaries (Schwartz and Bidani 1993), whereas pathological glomerular hypertrophy is also marked by an increase of the diameter of the glomerular capillaries (Amann et al. 1993, Lax et al. 1992, Osterby and Gundersen 1975, Schwartz and Bidani 1993), which is considered to be an additional determinant factor of development of glomerulosclerosis (Daniels and Hostetter 1990, Olson and Heptinstall 1988). Glomerular hypertrophy, as well as the numbers of glomerular cells can be estimated in kidney sections, using different means of stereological investigation (Hirose et al. 1982, Nyengaard 1999, Sanden et al. 2003, Sterio 1984, Weibel 1979, Weibel 1980, Weibel and Gomez 1962). Additionally, the availability of markers enables the identification of single glomerular cell types in these sections (Pavenstadt et al. 2003, Sanden et al. 2003). In 1989, Fogo and Ichikawa phrased their " hypertrophy" hypothesis (refer to figure 2.1), that has at its central proposition the loss of a critical number of nephrons through an initial insult leading to compensational, growth factor mediated glomerular hypertrophy, which is a determinant for the development of glomerulosclerosis and therefore for the progression of kidney damage (Fogo and Ichikawa 1989, Fogo and Ichikawa 1991, Ichikawa et al. 1991). The consequences of glomerular enlargement itself then lead to glomerulosclerosis. The distinct, invariable association, as well as the pathogenetic relevance of glomerular hypertrophy for the development of glomerulosclerosis, independent of alterations of systemic or glomerular pressures, has been shown by several authors in various animal experimental studies, as well as in investigations of human disease (Daniels and Hostetter 1990, Doi et al. 1990, Fogo and Ichikawa 1991, Fogo 2000, Fries et al. 1989, Klahr et al. 1988, Olson 1992 (a), Olson 1992 (b), Olson and Heptinstall 1988, Wanke et al. 1991).

The " hypertrophy" hypothesis is also congruent with studies of pharmacological or dietary intervention, as these do not only evolve anti-hypertensive effects, but also were shown to influence compensatory glomerular growth (Amann et al. 1993, Dworkin et al. 1993, O'Donnell et al. 1990, Yoshida et al. 1989). More than being just a result of compensatory mechanisms arising in the remnant glomeruli of a kidney that has been affected by a loss of a critical number of functioning nephrons by an initial result, glomerular hypertrophy also provides a possible explanation for the initiation and progression of chronic kidney diseases, that appear without a prior loss of nephrons. Such diseases include diabetes mellitus associated nephropathy (DN) and primary focal and segmental glomerulosclerosis (Fogo and Ichikawa 1989). In diabetes of man, as well as in experimental rat models of streptozotozin (STZ) induced diabetes, the first obvious kidney associated changes after onset of diabetes are renal and glomerular hypertrophy (Mogensen et al. 1983). In this context, the development of renal hypertrophy is seen more as a prerequisite than a consequence of renal hyperfunction (Cortes et al. 1987). Using morphometric analysis, glomerular hypertrophy can be detected in kidney sections of diabetic human patients as early as within one week after manifestation of diabetes (Osterby and Gundersen 1975), and in animal experimental models of the rat within 4 days after application of STZ, a commonly used method to induce diabetes mellitus (DM) in rats and mice (Cortes et al. 1987, Seyer-Hansen et al. 1980). The reason responsible for development of glomerular hypertrophy itself yet remains unclear. As underlying hemodynamic changes became improbable, increased effects and/or activities of both local and circulating growth factors were supposed (Fogo and Ichikawa 1989), either as a consequence of loss of functioning nephrons due to a previous insult, or, as an effect of aberration of regulation of glomerular growth in diseases that appear without prior loss of functioning kidney parenchyma (e.g. diabetic glomerulosclerosis or primary focal segmental glomerulosclerosis, FSGS). The potential to affect renal and glomerular growth processes has been documented for several hormones and local growth factors. Especially the effects of members of the growth hormone system, including insulin like growth factors (IGF) and IGF-binding proteins, which partially mediate growth hormone actions but also exhibit systemic, para- and autocrine effects independent of GH, have been investigated in detail (Bellush et al. 2000, Fisch 2004, Gowri et al. 2003, Hammerman 1989, Moerth et al. 2007).

As well, the high recurrence rate of FSGS in kidney transplant recipients suggests that such patients might have a circulating factor that alters glomerular capillary permeability. This factor has been partially identified as a protein (Sharma et al. 1999), whose removal by plasmapheresis decreases proteinuria (Carraro et al. 2004, Garcia et al. 2006). However, due to the various possible interactions of different factors under different circumstances of kidney disease, a single circulating or local factor responsible for the development of glomerular hypertrophy in chronic kidney disease has not yet been identified. Direct consequences of glomerular hypertrophy include the development of podocyte damage and successional impairment of the glomerular filtration process (Kriz et al. 1994, Wanke et al. 2001), which trigger the development of glomerulosclerosis as explicated in the following section.
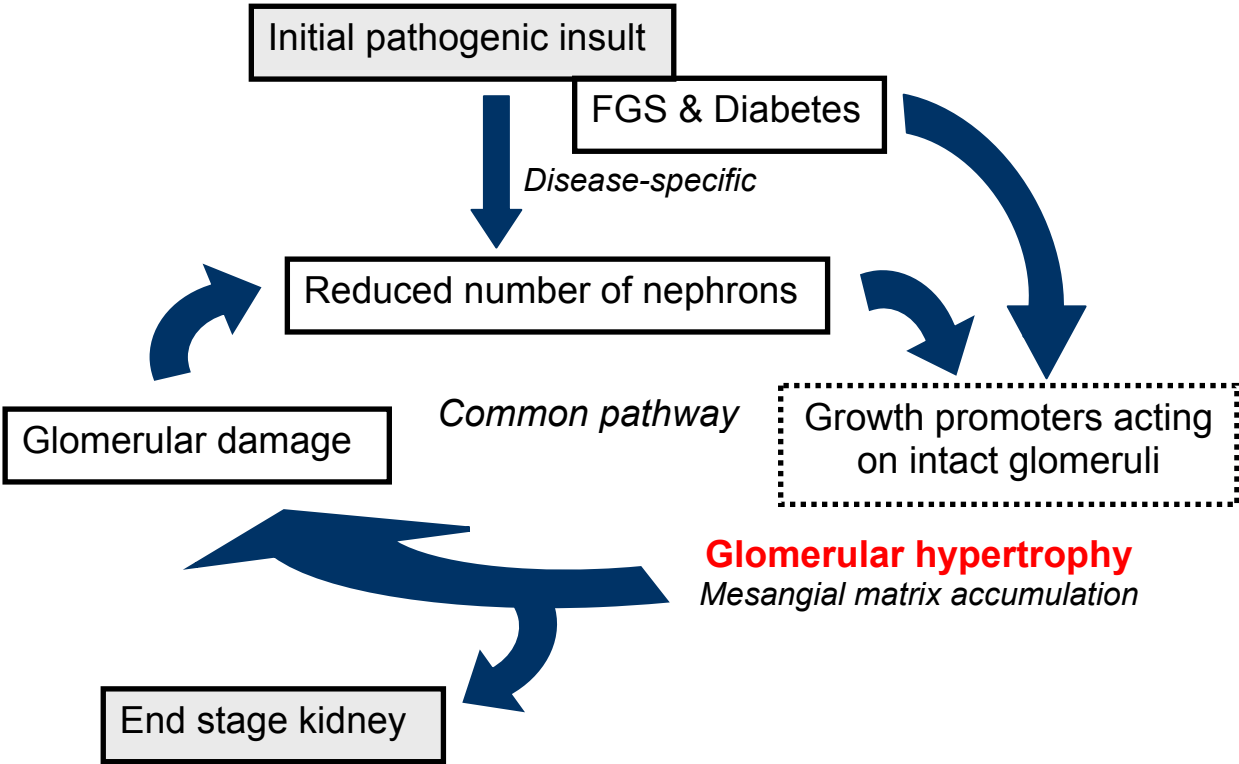
Figure 2.1: Proposed concept of glomerular hypertrophy caused by growth promoters acting on intact glomeruli being the central pathogenetic mechanism underlying the self perpetuating vicious cycle of progressive destruction of glomerular architecture in chronic renal disease.
From Fogo A, Ichikawa I: Semin Nephrol 1989; 9:329-342.

2.3.2 Podocyte function and the importance of podocyte damage for the development of glomerulosclerosis

The efficiency of glomerular filtration is a fundamental prerequisite for physiological kidney function. Structurally, the glomerular filter is composed of three parts: a layer of endothelial cells separated by large fenestrations of 50–100 nm, the glomerular basement membrane (GBM) that is about 300 nm thick (human kidney glomeruli), and the podocyte slit diaphragm spanning roughly 40 nm between interdigitating tertiary foot processes of adjacent podocytes that cover the GBM (Deen et al. 2001, Madsen and Tisher 1996). The function of mesangial glomerular cells, which provide structural support to the glomerulus, as well as an efficient interaction of all structural components of the glomerular filtration barrier is essential for the physiological filtration process. Next to physical interactions, also paracrine cross talks between podocytes, mesangial and endothelial cells have been identified to play crucial roles for development and maintenance of the glomerular filtration barrier (Eremina et al. 2007, Eremina et al. 2006). The glomerular filter has a remarkable and well described selectivity for macromolecules based on both charge and size (D'Amico and Bazzi 2003, Deen et al. 2001, Haraldsson and Sorensson 2004, Tryggvason and Wartiovaara 2005). Under physiological conditions, it provides free permeability for water and small solutes, whereas proteins like serum albumin or larger molecules are efficiently retained. Smaller proteins are partially filtered before passing into the primary ultra-filtrate, where they can be reabsorbed in the proximal tubules. Podocytes are crucially involved in establishing the specific permeability properties of the glomerular filter. The by far most selective part of the glomerular filter, responsible for the ultimate size selectivity of the filtration process for proteins and about 50% of its hydraulic resistance, is represented by the slit diaphragm, a highly specialized gap junction between interdigitating foot processes of neighboured podocytes (Pavenstadt et al. 2003, Shankland 2006). Studies concerning the structure of the slit diaphragm (slit membrane) have significantly increased the understanding of the molecular physiology of the filtration process (Karnovsky and Ainsworth 1972, Wartiovaara et al. 2004), as well as the implication of podocyte damage in the development of proteinuria in various kidney diseases (Holzman et al. 1999, Kestila et al. 1998, Pavenstadt et al. 2003, Ruotsalainen et al. 1999, Shankland 2006).

The slit membrane is composed of extracellular domains of podocyte derived nephrin molecules, regularly arranged in a unique "zipper-like" structure, forming a molecular sieve with pores slightly smaller than albumin (Wartiovaara et al. 2004). Podocytes themselves are unique, highly differentiated epithelial cells with a complex cytoarchitecture (Pavenstadt et al. 2003). Next to their function in the process of glomerular filtration, where they provide a size and charge barrier to proteins, they also are responsible for the maintenance of the capillary loop shape and the counteraction to the intraglomerular pressure, as well as for the synthesis and maintenance of the glomerular basement membrane (Shankland 2006) and therefore play a central role in development and maintenance of normal glomerular structure and function. The structural integrity of the foot process is crucial for establishing stability between the cell-cell and the cell-matrix contact of podocytes. This unique challenge has resulted in the development of a specialized cytoskeletal organization of podocyte foot processes (Pavenstadt et al. 2003). The primary function of the foot process cytoskeleton is the coupling of the slit membrane complex with the podocyte-GBM contacts in their close proximity. The cytoskeleton of the major processes also has to maintain contact with the metabolic machinery of the podocyte cell body to allow vesicular transport along the process. Because the glomerular capillary wall undergoes cyclic distensions with each heart beat, a combination of mechanical strength and flexibility is also required. The cytoskeleton therefore has to serve static and dynamic functions. Foot processes contain all elements required to generate a tensile strength to oppose the distensible forces of the capillary wall (Drenckhahn and Franke 1988, Kriz et al. 1995, Kriz et al. 1994). Podocytes also share common properties with neurons (Kobayashi et al. 2004, Kobayashi and Mundel 1998, Rastaldi et al. 2006, Rastaldi et al. 2003) and exert indirect influence on endothelial and mesangial cells by excretion of signalling molecules exhibiting paracrine actions (e.g. vascular endothelial growth factor), which are required for their function and integrity (Eremina et al. 2006, Eremina et al. 2003, Pavenstadt et al. 2003). To fulfil all these highly specialized functions, podocytes express a variety of different unique proteins with very complex patterns of interaction and architecture (Pavenstadt et al. 2003, Shankland 2006). Due to this high grade of differentiation, their capacity for cell division and replacement is extremely limited, except for few glomerular diseases in humans (Barisoni et al. 1999, Griffin et al. 2003, Kriz 2002, Mundel and Shankland 2002, Nagata et al. 1998, Pavenstadt et al. 2003, Valeri et al. 1996).

During development and progression of glomerular hypertrophy, podocytes gradually fail to functionally adapt to the increased size of the glomerulus. Whereas numbers of mesangial and endothelial cells per glomerulus increase during development of glomerular hypertrophy (refer to 2.3.1), the number of cells displaying a podocytic phenotype remains unchanged, reflecting the inability of these highly differentiated cells to undergo functional proliferation, leading to a relative depletion of podocyte in the respective glomeruli. Exposed to the challenge to maintain their functions under the circumstances of increasing areas of glomerular basement membrane to cover, podocytes are unable to maintain their normal cell shape but change in appearance in a fairly stereotyped manner (Kerjaschki 2001, Kriz et al. 1999, Kriz et al. 1996, Wanke et al. 2001, Wiggins 2007). The early stages of this characteristic sequence of structural alterations include cell hypertrophy and foot process effacement. Biochemically, hypertrophy is defined as an increase in the cell's protein to DNA ratio, accompanied by increased cell volume, but not number (Shankland 2006). Both, analyses of human biopsies, as well as studies in animal models show that podocytes can undergo significant hypertrophy but to a limited extent (Bhathena 2003, Chen et al. 2006, Gross et al. 2004, Wiggins et al. 2005). Thus, podocyte hypertrophy initially seems to be adaptive, representing the attempt of a cell that is relatively incapable of proliferating, to cover the underlying GBM. However, with time, it is likely that podocyte hypertrophy becomes maladaptive. In a model system, as podocytes continue to enlarge, they express different proteins reflecting this 'adaptation' stage and subsequently a 'decompensation' stage before becoming lost from the glomeruli (Wiggins et al. 2005). Foot process effacement is a consequence of retraction, widening, and shortening of the processes of each podocyte, finally resulting in a reduction of the frequency of filtration slits (Drumond et al. 1994). These uniform phenotypical changes represent a stereotypical reaction of podocytes to injury or damage and can be observed throughout a large variety of different glomerular diseases (Shankland 2006, Shirato et al. 1996). Later stages of podocyte damage include cell body attenuation and pseudocyst formation. Finally, detachment of podocytes from the GBM leads to severe proteinuria, glomerular hyalinosis, formation of synechial adhesions between the glomerular tuft and the capsule of Bowman and collapse of glomerular capillaries (Pavenstadt et al. 2003, Shankland 2006, Wanke et al. 2001).

This characteristic sequence of anatomic events resulting from podocyte injury has been comprehensively described in multiple animal model systems (Kretzler et al. 1994, Kriz 2002, Wanke et al. 2001): Podocyte damage leads to appearance of denuded areas of GBM, which is followed by formation of adhesion to Bowman's capsule (synechia formation), focal segmental glomerulosclerosis, and global glomerulosclerosis associated with misdirected filtration into the interstitial compartment contributing to interstitial injury and fibrosis. Herein, the loss of the separation between the tuft and Bowman's capsule in affected glomeruli by formation of cell bridges between the glomerular and the parietal basement membranes by proliferating parietal epithelial cells and/or altered podocytes (Moeller et al. 2004), or by misdirected filtration represents a crucial event for the further development of glomerulosclerosis and the possible progression towards ESRD. A primary glomerular injury is transferred onto the tubulointerstitium, either by direct encroachment of extracapillary lesions, or by protein leakage into tubular urine, resulting in injury to the tubule and the interstitium (Kriz and LeHir 2005). The loss of nephrons then leads to compensatory mechanisms in the remaining nephrons (e.g. glomerular hypertrophy), which increase their vulnerability to any further challenge and may again cause further podocyte damage. An additional further possible mechanism would be that tubulointerstitial inflammation and fibrosis, caused by misdirected filtration, account for the further deterioration of renal function (Remuzzi 1995). Thus, podocyte injury, due to glomerular hypertrophy or other factors, as well as the consequences of impaired podocyte function, depletion or loss of podocytes are seen as the central initial pathogenetic features in the development and the progression of glomerulosclerotic kidney alterations, including DN (Hayden et al. 2005, Lemley 2003, Pagtalunan et al. 1997, Steffes et al. 2001, White et al. 2002, Wolf et al. 2005). They provide a possible explanation for the development of proteinuria (Shankland 2006), as well as for the development of the various histological features of glomerulosclerosis and their progression (Wanke et al. 2001). The key role of podocyte dysfunction, injury and loss from the glomerulus, as initiators of processes that lead to the development and self perpetuating progression of glomerulosclerotic alterations, is also increasingly supported by various experimental animal models (Asanuma and Mundel 2003, Kretzler et al. 1994, Kriz 2002, Mundel and Shankland 2002, Wanke et al. 2001, Wharram et al. 2005), including rat models of regulated podocyte depletion (Kim et al. 2001, Wharram et al. 2005).

Recent studies also indicate that serum proteins which pass the glomerular filter into the Bowmans' space as a consequence of podocyte damage, may exhibit toxic effects on other podocytes of the same glomerulus. Thus, the leakage of those proteins into the Bowmans space is not only a result, but may also be a cause of podocyte damage (Ichikawa et al. 2005). All these findings have led to the postulation of the "podocyte depletion hypothesis" for glomerulosclerosis that has as its central tenet the concept that a failure of podocytes to cover the available GBM filtration surface area results in denuded areas of GBM, which in turn triggers glomerulosclerosis (Wiggins 2007). If progressive podocyte depletion is allowed to occur over time, then this will inevitably be associated with progressive glomerulosclerosis leading to progressive loss of renal function culminating in ESRD (Kriz 1996, Wiggins 2007). This hypothesis also considers other mechanisms than glomerular hypertrophy to be the initial cause of development of podocyte damage, including direct podocyte loss because of necrosis, apoptosis, or detachment and by a switch of the podocyte phenotype to one which cannot maintain normal glomerular structure and function (Wiggins 2007).

2.3.3 Proteinuria

Generally, serum proteins of the size of albumin and larger are efficiently excluded from glomerular filtration. Smaller proteins that pass the intact glomerular filter are reabsorbed in different parts of the renal tubular system. In humans, the common definition of proteinuria is a urinary protein excretion exceeding 150 mg/day (adults) (Bergstein 1999). In human urine samples, protein concentrations can be detected very easily, using so called dip stick tests as a routinely used diagnostic method, even though the measurement has a rather semi-quantitative character and detects predominantly albumin (Bergstein 1999). As mice are commonly used as animal models in nephrological research, the use of dip stick tests to determine albumin concentrations in urine samples of murine origin is probably inaccurate, if not totally condemned to fail (Breyer et al. 2005), as adult mice, predominantly male animals, physiologically display significant urine concentrations of small proteins, so-called major urinary proteins (MUPs) (Beynon and Hurst 2004, Finlayson et al. 1965, Shahan et al. 1987). MUPs are liver synthesized pheromone-binding proteins, which are physiologically excreted in the urine and play complex roles in chemosensory signalling among rodents (Cavaggioni and Mucignat-Caretta 2000).

The inaccuracy of the dipstick proteinuria test in mouse urine may be a consequence of sensitivity of the assay to these abundant major urinary proteins. In mouse urine, albuminuria is detected using gel-electrophoresis (Doi et al. 1990, Yamada et al. 1994) or other specific methods, such as Enzyme- Linked Immunosorbent Assay (ELISA). SDS-PAGE (sodium dodecyl sulphate-polyacrylamide gel electrophoresis) provides an excellent diagnostic aid for early detection of nephropathy. Characteristic protein profiles, detected by SDS-PAGE based urine protein analyses, allow for separation of different origins of proteins appearing in the urine (Oser and Boesken 1993). If urine samples collected over 24-hours are not available, urinary protein excretion can also be estimated semiquantitatively by measuring the ratio of urinary protein (ELISA) to creatinine concentrations in spot urine samples (Abitbol et al. 1990, Doi et al. 1990). Persistent proteinuria can be the first sign of kidney disease and commonly results from disorders associated with increased glomerular permeability or tubular disorders. Traditionally, evaluation of the molecular size of proteins occurring in the urine is used to draw conclusions concerning their origin and the supposable localization of kidney damage. If postrenal serum or blood contamination can be excluded, large proteins prove a glomerulopathy. The appearance of urine proteins with molecular weights of 68 – 350 kDa, termed unselective glomerular proteinuria, is linked to an (additional to podocyte damage) affection of the glomerular basement membrane or the mesangium and is regarded to reflect an established kidney damage (Bergstein 1999, Oser and Boesken 1993, Stierle et al. 1990). Small proteins reflect tubular or interstitial injury, resulting in insufficient reabsorption of microproteins. Depending on the grade of alteration, an incomplete micro-proteinuria (40-70 kDa) or a complete micro-proteinuria (10-70 kDa) can occur. Tubular proteinuria can be observed in patients with interstitial nephritis, rejected kidney transplants and others. Many nephropathies damage both, glomeruli and tubules and therefore mixed types of glomerular and tubular proteinuria can be found (Marshall and Williams 1998). According to the size selectivity of the different layers of the glomerular filtration barrier, alterations selectively affecting the glomerular filtration barrier first result in occurrence of proteins of 68-150 kDa (transferrin, albumin, dimeric albumin), termed selective glomerular proteinuria (Bergstein 1999, Stierle et al. 1990). The first clinically detectable signature of damage of the glomerular filtration barrier, with or without loss of renal function owing to glomerulosclerosis, is the appearance of low, yet abnormal levels of albumin in the urine, referred to as microalbuminuria.

However, a causative linkage of appearance of microalbuminuria with the morphological equivalent of early podocyte damage, foot process effacement, is still subject of discussion (Shankland 2006, Shumway and Gambert 2002). Irrespective the reasons of its origin, the degree of proteinuria was found to correlate with the progression of glomerulosclerosis and tubulointerstitial fibrosis and was shown to predict the progression and the expected outcome (Remuzzi et al. 2002, Risdon et al. 1968, Wolf and Ziyadeh 2007) in diabetic and nondiabetic renal disease (Iseki et al. 2004, Peterson et al. 1995). Next to that predictive value of proteinuria as a renal risk factor, it was shown that reduction of urinary protein levels by various medications and a low-protein diet limits renal function decline towards ESRD in human and in various animal models (Gaspari et al. 1995, Ikoma et al. 1991, Lewis et al. 1993, Marinides et al. 1990, Maschio et al. 1996, Remuzzi et al. 1999, Remuzzi et al. 2002, Remuzzi et al. 2006). These findings strongly support the thesis, that proteinuria itself is not only a symptom, but also has a central pathogenetic importance for the progression of CKD. Development of glomerulosclerosis and tubulointerstitial lesions are seen as the consequences of disturbed glomerular filtration (Remuzzi 1995, Remuzzi et al. 2006, Remuzzi and Bertani 1990). Due to the development of podocyte damage, an accelerated plasma protein leakage across the GBM into Bowman' space and the mesangium participates in the initiation glomerulosclerosis (Wolf and Ziyadeh 2007). Proliferation of mesangial cells and increased synthesis of extracellular mesangial matrix are seen to result from a "protein overload" of the mesangium. Urinary proteins may exhibit intrinsic renal toxicity and contribute to the progression of renal damage by induction proinflammatory and profibrogenic injury in tubular cells which can facilitate the development of interstitial inflammation and fibrosis, leading to tubular atrophy (Benigni et al. 2004, Bertani et al. 1986, Eddy 1989, Eddy and Michael 1988, Remuzzi 1995, Remuzzi et al. 2006, Wolf and Ziyadeh 2007). Also, recent findings suggest toxic effects of plasma proteins on the function of podocytes (refer to 2.3.2) and are currently thought to play a key role in the perpetuation and progression of glomerulosclerotic lesions (Abbate et al. 2002, Ichikawa et al. 2005).

2.4.1 Animal models of glomerulosclerosis

In nephrological research, great efforts have been employed to generate suitable animal models of nephropathy displaying patterns of glomerulosclerotic alterations comparable to those found in the various forms of CKD of humans. Traditionally, predominantly rats have been used as conventional animal models to study the pathogenesis of glomerulosclerotic lesions and the progression of chronic nephropathies. Due to its "comfortable" size, this species evolved as an ideal experimental model for appliance of different in vivo manipulations, like direct micropuncture of single glomeruli or performance of repeated kidney biopsies from the same animal. As performance of experimental techniques steadily improved, and since the introduction of transgenic technologies lead to a revolution of new possibilities to study the effects and implications of various genetic modifications on glomerular disease in models of defined genetic backgrounds, also a large number of relevant mouse models has been established in experimental nephrology (Breyer et al. 2005, Fogo 2003). Due to the respective mode of introduction of nephropathy, different groups of animal models of glomerulosclerosis can be distinguished: animal models that do spontaneously develop glomerulosclerotic alterations, conventional experimental models and models established via gene transfer (Anders and Schlondorff 2000, Wanke 1996). Spontaneous development of glomerulosclerotic kidney lesions has been described for various rat strains. The "obese-Zucker" rat for example, develops progressive glomerulosclerosis in association with obesity and hyperlipidaemia (Kasiske et al. 1985). Other rat models, used to study glomerulosclerotic alterations, develop nephropathy in the context of hypertension, partially inducible by administration of a high salt diet (Chen et al. 1993, Raij et al. 1984). In the group of conventional models, nephropathy is induced by pharmacological induction, experimental manipulation as chirurgical intervention, or by combinations of different approaches, including enforcement of development of glomerular lesions by additional dietary interventions. Pharmacological induction of a biphasic nephrotic syndrome in the rat uses the nephrotoxic effects of puromycin-aminonucleoside or adriamycin (Bertani et al. 1986, Diamond and Karnovsky 1986, Glasser et al. 1977, Grond et al. 1984). Application of STZ is commonly used to induce diabetes mellitus (DM) in rats and mice. As STZ exhibits cytotoxicity not only on pancreatic beta-cells, multiple low-dose STZ injections have been established to induce diabetes.

However, apart from few exceptions (Nakagawa et al. 2007, Zhao et al. 2006), reports of renal failure resulting from diabetes in mice or rats are lacking (Breyer et al. 2005) and only a minority of mouse strains (e.g., KK, KK-Ay) develop evidence of arteriolar hyalinosis, mesangial proliferation or glomerulosclerosis, mirroring the strong impact of genetic background on the susceptibility to development of DN (Camerini-Davalos et al. 1968, Gurley et al. 2006, Liao et al. 2003, Reddi et al. 1977, Reddi et al. 1990, Reddi et al. 1988, Suto et al. 1998). Various models based on surgical intervention have been studied and established in nephrology. One principle of induction of nephropathy is the removal of a "critical mass" of kidney tissue. Most commonly, the so-called remnant kidney model is used, in which more than 50% (75-90%) of renal tissue is removed, using different surgical techniques (Heptinstall 1992, Lafferty and Brenner 1990). After an initial stage of acute renal failure, surviving animals proceed to develop compensational hypertrophy of the remaining kidney tissue, followed by the stages of chronic and finally terminal renal failure, characterized by proteinuria, progressive glomerulosclerosis, tubulo-interstitial and possibly vascular alterations (Kleinknecht et al. 1988, Koletsky and Goodsitt 1960, Romen 1976). Yet, the difficulties to standardize the experimental conditions (Elema et al. 1988, Gretz et al. 1988, Ritz et al. 1978) have led to a controversial discussion concerning the validity of these models (Schwartz et al. 1987). Transgenic mice account for a great part of the most relevant animal models used in nephrological research. In these models, expression of a transgene is the causative principle responsible for the development of nephropathy. Growth hormone-transgenic mice represent a well characterized model of progressive glomerulosclerosis (Doi et al. 1990, Doi et al. 1988, Wanke 1996, Wanke et al. 1993, Wanke et al. 2001). Transgenic mice expressing a dominant negative glucose dependent insulinotropic polypeptide receptor represent a novel model of diabetic nephropathy (Herbach 2002, Herbach et al. 2003, Schairer 2006). Studies in transgenic mouse models have contributed to improve the understanding of single factors that exacerbate glomerular disease, as well in DN (Breyer et al. 2005, Yamamoto et al. 2001). The availability of murine embryonic stem cells has provided the ability to disrupt the expression and function of specific preselected genes (Babinet 2000, Bronson and Smithies 1994, Mansouri 2001).

Today, generation of mice with specific gene knockouts and even podocyte specific gene knockouts, or podocyte specific transgene expression resulting in development glomerular alterations, represent promising approaches towards an improved understanding of the detailed molecular mechanisms implicated in the single aspects of pathogenesis of CKD (El-Aouni et al. 2006, Ichikawa et al. 2005, Moeller et al. 2004, Pavenstadt et al. 2003, Shankland 2006, Wharram et al. 2005).

2.4.2 GIPR^{dn}-transgenic mice: a novel mouse model of diabetes mellitus

GIP (glucose-dependent insulinotropic polypeptide, gastric inhibitory polypeptide) is a so-called incretin hormone, released from endocrine cells of the small intestine after food intake. As part of the enteroinsular axis (Creutzfeldt 1979), GIP promotes its endocrine effects on insulin secretion upon nutritient ingestion via binding to its receptor (GIPR) expressed on the surface of pancreatic beta-cells (Usdin et al. 1993). Via different domains in its third intracellular loop, the GIP receptor is coupled to a heterodimeric G-protein (Mayo et al. 2003), through which predominantly intracellular cAMP (cyclic adenosine monophosphate) production is stimulated upon ligand binding (Tseng and Zhang 1998). This leads to increased intracellular Ca^{++} concentrations, that trigger the exocytosis of insulin (Habener 1993, Kieffer and Habener 1999, Lu et al. 1993). Next to the enhancement of glucose-mediated insulin secretion, GIP produces multiple physiological effects, including stimulation of insulin gene transcription in pancreatic beta-cells (Creutzfeldt and Nauck 1992, Fehmann et al. 1995), as well as mitogenic and antiapoptotic effects on beta-cells (Trumper et al. 2001, Trumper et al. 2000).

Transgenic mice expressing a dominant negative glucose dependent insulinotropic polypeptide receptor (GIPR^{dn}) under the control of the rat pro-insulin gene promoter in pancreatic beta-cells were created by Volz in 1997 (Volz 1997). The aim was to generate a mutated GIP receptor that shows unchanged binding affinities to GIP but is unable to induce signal transduction. Elimination of induction of further intracellular signal transduction according to an unaltered ligand binding is a functional characteristic of a dominant negative receptor. Sequences of cDNA, encoding for the third intracellular loop of the human GIP receptor, which is essential for the downstream intracellular signal transduction, were mutated through insertion of a point mutation (position 1018-1020), resulting in an altered amino acid sequence at position 340 of the protein (Ala→Glu) and deletion of 24 base pairs (position 955-978), resulting in a deletion of eight amino acids (position 319-326).

In cell culture experiments, using CHL (Chinese hamster lung) cells stably transfected with the mutated GIP receptor, binding affinities to GIP remained unchanged, whereas the induction of signal transduction upon binding of GIP to the mutated receptor was eliminated, as no increase of intracellular cAMP levels was detectable. It is important to point out, that GIPR[dn]-transgenic mice still co-express the endogenous GIP receptor. Recent clinical and pathomorphological characterisations of GIPR[dn]-transgenic mice by Herbach et al. revealed the phenotypic consequences of the expression of the mutated GIP receptor (Herbach 2002, Herbach et al. 2005, Herbach et al. 2003). GIPR[dn]-transgenic mice develop an absolute insulin deficiency, resulting in a severe diabetic phenotype, characterized by hyperglycaemia and glucosuria, starting as early as from day 14 to 21 on, as well as hypoinsulinaemia, hyperphagia, polydipsia and polyuria. After onset of diabetes, both fasting and postprandial serum glucose levels were found to be significantly higher and insulin values significantly decreased in GIPR[dn]-transgenic animals compared to their non-transgenic littermate controls. Quantitative stereological studies of pancreatic islets and their endocrine cell types revealed a significant reduction of the total islet and total beta-cell volume of transgenic mice, as well as a disturbed islet neogenesis. The respective average life spans of GIPR[dn]-transgenic mice were drastically reduced compared to non transgenic animals. Additionally to these findings, GIPR[dn]-transgenic mice also develop kidney lesions in succession of diabetes mellitus, characterized by renal and glomerular hypertrophy and onset of albuminuria (Herbach 2002, Herbach et al. 2003, Schairer 2006). These renal alterations are marked by typical glomerular lesions like mesangial expansion, attended by accumulation of mesangial matrix, hyalinosis and, indicating podocyte damage, formation of synechiae between the glomerular tuft and the capsule of Bowman. In advanced stages, the glomerular alterations were accompanied by focal atrophy of tubuli, focal interstitial fibrosis and signs of proteinuria. Development, dimensions and histological patterns of glomerular/kidney alterations detected in GIPR[dn]-transgenic mice show similarities to early diabetes associated kidney lesions of humans, thus making GIPR[dn]-transgenic mice an promising animal model of early diabetic nephropathy (Herbach 2002, Herbach et al. 2003, Schairer 2006).

2.4.3 Growth hormone (GH)-transgenic mice

Mice expressing the human growth hormone (hGH) gene were among the first of transgenic animals (Palmiter et al. 1982). Since then, several strains of transgenic mice overexpressing different heterologous GH genes under the transcriptional control of various regulatory elements have been developed (Brem et al. 1989). The PEPCKbGH-transgenic mice investigated in the present study, overexpress the bovine growth hormone (bGH) under the transcriptional control of the rat phosphoenolpyruvate-carboxykinase (PEPCK) gene promoter in the liver and kidneys (McGrane et al. 1988). Using in situ hybridisation for analysis of the cellular distribution of transgene expression in the kidneys, bGH mRNA expression could be detected in tubular epithelia of the renal cortex, but not in glomeruli (Ehrlein 1993). In non-transgenic adult mice, secretion of endogenous growth hormone from the pituitary gland follows a gender specific, pulsatile pattern of ultradian rhythm with average plasma concentrations ranging from 10 ng/ml in male to 16 ng/ml in female animals (MacLeod et al. 1991). In PEPCKbGH-transgenic mice however, both genders display permanently high serum levels of bovine GH, with average concentrations above 1,200 ng/ml (Wolf et al. 1993). The phenotypical, clinical and pathomorphological changes associated with the expression of heterologous GH-transgenes in GH-transgenic mice have been studied intensively. The most obvious phenotypic effect is the development of a markedly stimulated overall body growth, starting from three weeks of age onwards and increased body weights, which are almost doubled in adult animals versus wild-type controls (Wanke et al. 1992). Apart from visceromegaly and disproportionate skeletal gigantism, GH-transgenic mice exhibit a wide variety of pathomorphological alterations of organs, including characteristic sequences of liver changes (Wanke et al. 1996) and sex dependent alterations of skin growth (Wanke et al. 1999). Furthermore, GH-transgenic mice develop a spectrum of typical kidney lesions, which reproducibly occur in an age dependent manner and finally lead to end stage kidney disease with terminal renal failure (Wolf and Wanke 1997), which is the primary cause for the shortened life span of these animals (Wolf et al. 1993). Detailed studies revealed a characteristic sequence of kidney alterations in GH-transgenic mice, concordant with the postulated pathogenetic principle of evolution of glomerulosclerotic lesions in these animals resulting from podocyte damage (Wanke 1996, Wanke et al. 2001).

The earliest detectable alteration of kidney morphology in GH-transgenic mice is the hypertrophy of glomeruli, assessed by quantitative stereological investigations (Doi et al. 1990, Wanke et al. 1992). Glomerular hypertrophy in these animals is overproportional both in relation to both kidney and body weight (Wanke et al. 1991) and progresses with the age of animals. Progression of glomerular hypertrophy in GH-transgenic mice is associated with the development of glomerulosclerotic lesions, including mesangial extracellular matrix expansion due to an increased extracellular matrix synthesis and a decreased extracellular matrix degradation (Jacot et al. 1996), as well as proliferation of both endothelial and mesangial glomerular cells, whereas the number of podocytes per glomerulus remains unchanged. In the early stages, podocytes display typical lesions as hypertrophy and foot process effacement (Wanke et al. 2001), which are associated with onset of albuminuria. As the process of glomerular hypertrophy progresses, podocytes display severe maladaptive lesions, including detachment of podocytes from the glomerular basement membrane. The resultant denudation of the glomerular basement membrane is associated with severe proteinuria, glomerular hyalinosis, formation of cellular synechiae and collapse of glomerular capillaries, subsequently leading to glomerular obsolescence with consecutive atrophy of the adjacent tubule and development of interstitial fibrosis (Wanke et al. 2001). Atrophy of nephrons, interstitial fibrosis and tubulocystic alterations are the characteristic histological findings in the terminal stages of renal lesions, while remnant glomeruli demonstrate diffuse-segmental or focal-global sclerosis and/or hyalinosis (Brem et al. 1989, Wanke et al. 1991). Therefore, GH-transgenic mice represent an established, valuable and well characterized model for studying the pathogenesis of glomerulosclerosis and the mechanisms involved in the progression of chronic renal failure (Wanke and Wolf 1996). Furthermore, although GH-transgenic mice are not diabetic, the glomerular lesions, developing in response to high levels of circulating GH in these mice, mimic those observed in human diabetes mellitus (Doi et al. 1988).

2.5.1 Transcript profiling analysis in nephrology

As the quantity of available efficient therapeutic agents for treatment of CKD is still very limited, the understanding of the molecular mechanisms involved in the pathogenesis and progression of glomerular lesions in CKD is seen as a prerequisite for identification of potential new therapeutic targets, molecular diagnostic markers and development of individually adjusted therapies (Schmid et al. 2006, Yasuda et al. 2006). Therefore, additional functional insights into the individual disease processes, as well as into common aspects of the pathophysiology of CKD on the glomerular level are required, regarding the revelation of both common and disease specific pathogenetic key mechanisms and disease pathways (Yasuda et al. 2006). Due to the various possible and partially yet unknown mechanisms of interactions between different glomerular cells, as well as the impact of other local and systemic factors involved in the pathogenesis of glomerular lesions in CKD, experimental data derived from cell culture experiments is not fully capable to reflect the in vivo situation. Especially cultured podocytes display extensive differences in phenotype and function compared to podocytes under the glomerular microenvironment in the kidney (Pavenstadt et al. 2003). Therefore, only renal tissue can provide critical information on the disease processes, which are not available by non-tissue-based approaches. In human medicine, currently histological examination of renal biopsies provides the key information for the diagnosis and effective therapeutic management of progressive renal disease. However, the present histology-based analysis yields mainly descriptive diagnostic categories and gives limited prognostic information (Madaio 1990). The development of molecular biological tools for performance of gene expression analyses has opened new windows to evaluate the pathophysiology of CKD in human patients or in animal models of nephropathy, even if only limited amounts of sample materials, as kidney biopsies or samples of isolated glomeruli are available. Several techniques have been developed, including nonamplifying methods of mRNA expression analysis as Northern blotting and in-situ hybridization (ISH), as well as methods that include amplification of mRNA transcripts based on polymerase chain reaction (PCR) and enable for investigation of minimal amounts of sample material. Finally, introduction of novel mRNA expression-profiling technologies, such as microarray analyses have offered the possibility to simultaneously profile the whole transcriptome of a species.

Combination of different methods of transcript profiling analyses and confirmation of results by histology, immunohistochemistry as well as additional cell culture and animal experimental approaches then provide the opportunity to test and confirm the biological significance of obtained data. Northern blotting has been the standard in quantitative gene expression analysis. As this technique requires a considerable amount of RNA and can analyze only a single transcript per hybridization, it is suitable for in vivo or in vitro experiments, where larger amounts of sample material are available (Yasuda et al. 2006). ISH is an effective technique for localizing specific mRNA expression in cells and tissues, but a time-consuming process and it has an only limited ability to quantitate expression levels or compare multiple transcripts. However, this technology has successfully been applied on biopsy materials to demonstrate the significant role of for example inflammatory cytokines, growth factors, extracellular matrix metabolism and specific transcription factors in diabetic nephropathy (Suzuki et al. 1997, Suzuki et al. 1995, Toyoda et al. 2004). Compared to non-amplifying methods of mRNA expression analysis, PCR is a powerful tool for detecting the mRNA expression of multiple genes in a small amount of sample RNA. Quantitative real-time PCR enables the exact quantification of a target mRNA in a given sample (Gibson et al. 1996, Heid et al. 1996). The study of transcriptomics, also called genome-wide expression profiling, examines the expression levels of all mRNAs in a given cell population and is therefore a global way of looking at gene expression patterns, used to improve the understanding of genes and pathways involved in biological processes. The transcriptome itself is defined as the set of all messenger RNA (mRNA) transcripts, present in one, or a population of cells at any one time. It is therefore reflecting the genes that are being actively expressed in a given organism, tissue, or in a particular cell type at any given time. Conversely to the genome, which is, at least to its most extent, roughly fixed for a given cell line, the transcriptome varies considerably under different circumstances due to different patterns of gene expression and is therefore extremely dynamic. Today, the human, as well as the genomes of the species most commonly used in animal experimental studies are fully sequenced. Together with recent advances in genome-wide profiling techniques, this allows for a comprehensive analysis of renal disease-associated transcriptional programs in both human disease, as well as in animal experimental models (Alcorta et al. 2000, Kretzler et al. 2002).

Evaluation of gene expression patterns in renal specimens, with oligonucleotide DNA array and quantitative real-time reverse transcription (RT) PCR techniques provides novel insights into both physiological and pathogenetic mechanisms of gene expression regulation and serves as a starting point for novel molecular diagnostic tools in nephrology (Yasuda et al. 2006).

2.5.2 Real-time polymerase chain reaction (real-time PCR)

Real-time quantitative polymerase chain reaction is a technique, used to simultaneously quantify and amplify a specific sequence (target) of a given DNA molecule. For the purpose of evaluation of expression levels of mRNA transcripts by real-time PCR, total RNA is isolated from the sample material, reverse transcribed into cDNA and then investigated in the real-time PCR reaction. The real-time PCR procedure follows the general pattern of the polymerase chain reaction, but the DNA is quantified during each round of amplification. This quantification can be performed by measurement of all double stranded DNA (Morrison et al. 1998), or as indirect quantization of only the target sequence (Arya et al. 2005). Using fluorescent reporter probes is considered to be the most accurate and most reliable of the various methods that can be applied for quantification of PCR products (Ding and Cantor 2004). The so-called TaqMan® PCR method employs a probe technology that exploits the 5'-3' nuclease activity of the Taq (thermus aquaticus) DNA Polymerase (Holland et al. 1991) to allow direct detection of PCR product by the release of a fluorescent reporter during the PCR (Arya et al. 2005). The probe consists of an oligonucleotide with a 5'–reporter dye and a 3'–quencher dye covalently linked to the probe. When the probe is intact, the proximity of the reporter dye to the quencher dye results in suppression of the reporter fluorescence, primarily by Förster-type energy transfer through space (Cardullo et al. 1988, Förster 1948, Lakowicz 1983). During PCR, if the target of interest is present, the probe specifically anneals between the forward and reverse primer sites. The 5'–3' nucleolytic activity of the Taq DNA Polymerase cleaves the hybridized probe between the reporter and the quencher, whereas free probe is not digested. The probe is then displaced from the target, and polymerization of the strand continues. This process occurs in every cycle and does not interfere with the exponential accumulation of product. The separation of the reporter dye from the quencher dye is a direct consequence of specific target amplification during PCR and results in an increase of fluorescence of the reporter. This increase in fluorescence is measured.

Quantification of the target sequence can then either be performed as an absolute quantification, using standard dilutions of known concentrations of plasmid cDNA of the target sequence, or as relative quantification by relating the signal intensity measured in a given sample to that of an internal or external reference (Cohen and Kretzler 2003). For that purpose, expression levels of the molecule of interest (target) are related to the amount of mRNA analyzed, using reference RNAs (so-called housekeeping transcripts) with assumed stable, comparable and indifferent expression levels in the different samples to be compared (Cohen and Kretzler 2003). Frequently used housekeepers are for example 18S rRNA, beta-actin, Cyclophyllin or Gapdh (glyceraldehyde-3-phosphate dehydrogenase). The choice of an internal reference is critical, as regulation of these "housekeepers" will confound the expression ratio with the mRNA of interest. Therefore, if the reference gene expression in a particular sample has not previously been characterized, the evaluation of several housekeepers in parallel will reduce the danger of confounding studies by reference gene regulation (Cohen and Kretzler 2003). Because real-time PCR provides an accurate, reproducible and sensitive determination of mRNA expression levels, it has become the standard among all PCR-based gene expression analysis techniques. Recent advances in RNA preservation techniques have facilitated the implementation of expression studies using small amounts of kidney tissue processed for generation of sample materials, such as isolated glomeruli. Apart from detection of differences in abundance of special transcripts in different samples, real-time PCR also provides an exceptional good method for performance of confirmation studies on results obtained by microarray experiments (Schmid et al. 2004). Additionally, real-time PCR can be performed to identify infecting pathogens (Schmid et al. 2005) and profile the cellular composition of the specimen, as it contains multiple intrinsic and immigrating cell types with different expression signatures (Cohen et al. 2005). Furthermore, application of real-time PCR allows for performance of so-called "in-silico microdissection" (Schmid et al. 2003). Evaluation of gene expression regulation of a specific intrinsic renal cell type is confounded by simultaneously detected expression signals derived from other cell types in the sample. Even after microdissection of the glomerular compartment, different cell types, including mesangial cells, podocytes and glomerular endothelial cells can contribute to the expression signal.

Therefore, the use of a housekeeping reference gene that is exclusively expressed in a distinct glomerular cell type and not differentially expressed under circumstances of nephropathy, as for example synaptopodin as a podocyte-specific transcript, allows for evaluation of other podocyte specific transcripts that do undergo differential expression in renal disease (Schmid et al. 2003). A remaining limitation of real-time RT-PCR studies is the still limited number of mRNAs to be assayed in parallel, even if the latest technologies, so called low density arrays or microfluidic cards, allow for simultaneous performance of up to 384 parallel real-time PCR reactions with only minimal amounts of sample cDNA (Goulter et al. 2006, Steg et al. 2006).

2.5.3 Microarray analysis

High-throughput techniques based on DNA microarray technology can profile the whole transcriptome of a tissue and therefore provide a practical and economical tool for studying the gene expression of a multitude of genes in parallel (Schena et al. 1995). The underlying principle of DNA microarray technology is based on detection of hybridisation of labeled cDNAs (targets, which are obtained through extraction of mRNAs of a respective sample, followed by reverse transcription and optional amplification steps) to DNA probes of known sequence and position (array) on a chip surface, allowing for determination of the identities and abundances of the complementary target sequences. In the literature there exist at least two confusing nomenclature systems for referring to hybridization partners. According to the nomenclature recommended by B. Phimister of Nature Genetics, a "probe" is the tethered nucleic acid with known sequence, whereas a "target" is the free nucleic acid sample whose identity and abundance is being detected (Phimister 1999).

Performance of transcript profiling analysis, using oligonucleotide DNA microarray technology, allows for detection of genome-wide differences in the expression level of genes, meaning both identification and detection of differences in the abundance of nearly all mRNA transcripts present in the cells of these samples at a given point of time. An oligonucleotide cDNA microarray is an array of oligonucleotide (20~80-mer oligos) probes, chemically synthesized at specific locations (in situ = on-chip) on a coated quartz surface.

An alternative method of fabrication of gene arrays by high density in-situ synthesis of oligonucleotides by photolithography and combinatorial chemistry on wavers provides the basis for commercial available microarray technology and was developed by Steve Fodor and colleges at Affymetrix[®] Inc., USA (Pease et al. 1994), which sells its products under the GeneChip[®] trademark. Affymetrix's GeneChip[®] methodology is limited to hybridization with single samples, and depends on the inclusion of quality control probe sets to allow intra-array data normalization and inter-array data comparability by complex statistical models (Bottinger et al. 2003). Affymetrix's GeneChips[®] use so-called probe sets, containing multiple short oligonucleotide DNA sequences (probes) of each 25 bases, derived from different regions of a single target transcript. The precise location where each probe is synthesized is called a feature. One feature is composed of a large number of identical oligonucleotide probes. In modern Affymetrix's GeneChips[®], the feature size is 11 μm and up to 1.6 millions of features are contained on one array. A probe set consists of eleven pairs of oligonucleotide probes (=22 different oligonucleotide probes). The individual probes of a probe set are located close to the 3' end of the respective mRNA sequence. Each pair consists of a perfect match (PM) oligonucleotide (complementary to the target sequence of interest), that provides measurable fluorescence when target sequences binds to it and a mismatch (MM) oligonucleotide, identical to its PM counterpart except for one mismatch base inserted at its central position. The paired mismatch probe serves as an internal control for its perfect match partner. False or contaminating fluorescence, for example derived from non-specific cross hybridizations, can efficiently be quantified and subtracted from a gene expression measurement. The difference in detected hybridization signals between the PM and MM partners, as well as their intensity ratios serve as indicators of specific target abundance, allowing for consistent discrimination between signal and background noise and for generation of accurate data sets (Affymetrix Manual). The availability of sequence descriptions and annotations of all probes present on the Affymetrix arrays also allows for approaches of analyses of microarray raw data different from the original "probe-set" approach by Affymetrix[©] (e.g. ChipInspector 1.2, Genomatix). Sequences of all probes are blasted against the entire mouse genome, thereby using the latest sequences information available to identify the transcripts, represented through the respective probes on the array. Following image acquisition and quality controls of scanned chips, generated microarray raw data are normalized to allow for inter- and intra-array comparability.

For his purpose, Affymetrix's GeneChips® include a set of maintenance genes (normalization controls) to facilitate the normalization and scaling of array experiments prior to performing data comparisons. Expression levels of individual probe sets detected in the respective samples of an experiment are then compared. "Differentially expressed transcripts or probe sets" are then functionally annotated and further bioinformatical analyses are performed for revelation of their biological function, using software tools for pathway mapping analysis and generation of functional networks. To avoid misleading and confusing nomenclatures, it is important to point out clearly, that the described approaches of analysis of microarray data are designed for detection and identification of "differentially expressed transcripts", not "genes". Under optimal conditions, the cDNA samples hybridized to the probes on the surface of the respective arrays, would be regarded to represent the entire population of all mature mRNA-transcripts, present in all cells of the original sample material (e.g. glomerulus isolates) at the respective time point of investigation. Thus, the performance of a microarray experiment is basically capable of providing information concerning both identity and abundance (the frequency of occurrence) of each single transcript, detectable in the respective sample material. The term "differentially expressed or regulated transcript" is used for denomination of a single mRNA species whose abundance was experimentally found to be significantly altered in samples of one investigated group, relative to its abundance detected in samples of another group in the experiment, but does not automatically also refer to any regulatory processes of differential gene expression. The terms "differentially expressed transcript" and "differentially expressed gene" should actually not be used synonymously, since transcription of one single gene might result in the presence of more than a single species of mRNA-transcripts (e. g. by different post-transcriptional modifications of the primary transcript). However, a synonymous denomination of an identified transcript with a detected differential abundance in investigated samples in a given experiment and its corresponding gene is commonly performed.

In nephrology, early studies using DNA array technology were able to describe the basal expression profiles of whole renal tissues in normal human kidney (Yano et al. 2000) and in an animal model of diabetic nephropathy (Wada et al. 2001). However, the number of genes on the membrane-based high-density cDNA arrays was still very limited and critical questions concerning probe design and array quantification remained.

Later experiments benefited from matured technology and comprehensive gene expression analyses could be performed in various acute renal failure animal models, such as ischemia-reperfusion, unilateral ureter obstruction, and adriamycin-induced nephropathy, using whole renal tissue (Higgins et al. 2003, Kieran et al. 2003, Sadlier et al. 2004, Yoshida et al. 2002). Interestingly, a comparison of the gene expression signatures of these murine renal failure models was able to identify a shared transcriptome of 49 differentially expressed genes. Three renal disease-associated genes found in mice were also differentially expressed in human kidney biopsies, and correlated with renal disease stage and/or disease progression. These cross-species expression signatures are consistent with an evolutionarily conserved response of renal tissue, irrespective of the initial renal insult (Yasuda et al. 2005). In 2004, Susztak and colleges (Susztak et al. 2004) performed microarray analysis on samples of whole kidney tissues from different mouse models of diabetic nephropathy with comparable levels of hyperglycemia and albuminuria but different degrees of glomerular mesangial matrix expansion, which is considered to be a valuable indicator for the development of end stage renal disease in humans (Caramori et al. 2000). Comparison of the renal expression profiles of these different models allowed for the identification of a couple of genes whose differential expression was associated with specific steps of diabetic glomerulopathy, regardless of the investigated mouse model, the type of diabetes, its experimental induction as well as the presence or absence of obesity. In human nephrology, the use of oligonucleotide microarray based approaches on total kidney tissue has led to identification of novel diagnostic and prognostic parameters in patients with diverse renal diseases or renal transplants (Akalin et al. 2001, Sarwal et al. 2003, Takahashi et al. 2001). Expression array studies of renal disease can also facilitate the prediction of the disease course over time by definition of disease specific marker profiles that allow for the segregation of patients with a rather progressive or a stable disease course (Henger et al. 2004). The feasibility of such gene expression-based disease categorization in human renal biopsy samples was supported by clinical follow-up investigations, which revealed a stringent correlation between the respective expression fingerprint and the progression of renal disease. Besides molecular diagnostics or identification of candidates of potential therapeutic targets, gene expression profiling can also identify activated molecular pathways in the development of chronic renal diseases.

To gain insight into the molecular programs activated in diabetic nephropathy, for example, genome-wide gene expression profiling was performed in a disease stage-specific manner, using tubulo-interstitial compartments of human renal biopsies. Pathway mapping of the genes activated in DN was consistent with nuclear factor (NF)-κβ pathway activation, and allowed the identification of the promoter models enriched in DN-regulated genes (Schmid et al. 2006). Similar approaches also led to the identification of yet unknown members of the glomerular slit membrane (Cohen et al. 2006). In summary, the present cDNA array technology provides a powerful tool to analyze expression profiles from minimal amounts of renal tissue. This is seen as a prerequisite to identify the molecular processes involved in the pathogenesis of progressive chronic kidney diseases of various origins (Yasuda et al. 2006). However, in comparison to experiments on the respective animal models, comprehensive gene expression analyses in human native renal biopsy materials are still limited. These experiments principally suffer from the high degree of heterogeneity within the samples in the investigated cohorts of human patients and the restricted availability of sufficient amounts of sample materials for performance of different experiments on the same sample materials.

2.6 Methods of glomerulus isolation

As the early stages in development of chronic renal diseases characterized by glomerulosclerotic lesions begin at the renal glomerulus, a predominant interest of nephrological research focuses on the revelation of the molecular mechanisms implicated in the development of glomerular damage. As mentioned above, performance of transcript profiling analyses is applied to reveal such molecular mechanisms associated with, or causative for the development of glomerulosclerotic lesions on the transcriptional level. As glomeruli constitute only < 5% of the total renal cortex (Artacho-Perula et al. 1993, Nyengaard and Bendtsen 1992, Wanke 1996), the use of homogenates of total kidney tissue results in a low representation of glomerular cells in the sample material. Due to the high sensitivity of the analytical methods applied for performance of transcript profiling analyses, the interpretation of data obtained from investigation of total or cortical kidney tissue always inherits the danger of nonobservance of signals actually derived from glomerular cells, as those signals become overlaid by stronger signals derived from other kidney cell types.

Furthermore, it is nearly impossible to address the origin of a detected signal to a distinct single type of cells, except for single transcripts with known cell type specific patterns of expression. Resulting from the inability of glomerular cells to retain their differentiated features in cell culture, investigations of cultured glomerular cells are not capable to reflect the complexity of circumstances of developing glomerular damage in vivo (Pavenstadt et al. 2003). In order to overcome these problems, various different methods for the isolation of glomeruli from kidney tissue of different species were developed, allowing for performance of investigations on the glomerular level. Primarily three different methodological principles of glomerulus isolation are distinguished: Microdissection techniques (Peten et al. 1992), differential sieving techniques (Krakower and Greenspon 1951, Misra 1972, Spiro 1967, Striker and Striker 1985), including those combined with differential density gradient centrifugation (Norgaard 1976) and magnetic isolation of glomeruli from kidneys perfused with magnetic particles (Baelde et al. 1990, Baelde et al. 1994, Gauthier and Mannik 1988, Takemoto et al. 2002). Dependent on the investigated species, type and extend of scheduled analyses and the availability of kidney tissue, these methods differ with respect to the expectable yield and purity of glomerulus isolates and thus their suitability for performance of gene expression analyses. The availability of samples of human kidney tissue is generally limited. Therefore, appliance of glomerulus isolation methods on human kidney tissue is usually restricted to needle biopsies, using microdissection techniques. Using needle holders, glomeruli are manually microdissected directly from the biopsy under a stereo microscope, stored in RNA stabilization reagent and then processed for real-time RT-PCR or microarray analysis (Cohen and Kretzler 2002). The method is capable to provide maximal yields of isolated glomeruli from a limited given amount of kidney tissue and has also successfully been applied for generation of samples of isolated mouse glomeruli for microarray analyses (Zheng et al. 2004). Amounts of RNA, sufficient for performance of gene expression analysis can even be gathered from glomerular tissue isolated from formaldehyde-fixed archival kidney tissue, paraffin-embedded tissue or cryosections, by using laser microbeam microdissection techniques (Cohen et al. 2002, Fries et al. 2003): under a microscope, glomeruli are individually laser-beam microdissected and subsequently collected from the section, thereby avoiding contamination of glomerular sample material by parietal epithelial cells.

Laser-capture microdissection combined with linear amplification can detect transcription profiles down to the single cell level, but also carries the significant risk of (systematic) sampling errors (Kamme et al. 2003). A major limitation of most microdissection techniques for glomerulus isolation is the relatively low number of glomeruli and the corresponding amounts of mRNA that can be harvested, limiting the potential extent of subsequent analyses performed on these samples. Graded differential sieving is the most commonly applied technique for glomerulus isolation, if larger amounts of kidney tissues are available. After an optional Collagenase digestion, the cortical kidney tissue is pressed through a series of screens of decreasing pore sizes under addition of buffer. Thereby glomeruli are separated from the surrounding adjectant interstitial and tubular tissues and finally collected from the sieve with the pore size slightly smaller than their average diameter. Various modifications of the sieving principle for glomerulus isolation from different species for performance of diverse investigational approaches, including performance of cDNA microarray analyses have been described (Baelde et al. 2004, Higgins et al. 2004, Makino et al. 2006, Wehbi et al. 2001). However, different from other species it is difficult to generate glomerulus isolates of high purities from murine kidneys by using simple sieving techniques, as mouse glomeruli and tubules display similar diameters. As mice are widely used as animal models in nephrological research, performance of different analyses on isolated mouse glomeruli of one animal, or the applicability of investigational methods demanding for large amounts of sample materials requires suitable methods for the isolation of intact glomeruli within acceptable time and under defined temperature conditions. Performance of magnetic isolation of murine glomeruli from kidneys perfused with iron oxide, yielded high numbers of isolated glomeruli (Gauthier and Mannik 1988). Yet, the efficiency of this method, concerning the purity of glomerulus isolates was rather limited, although high quality RNA could be isolated from the generated samples (Baelde et al. 1994). In 2002, Takemoto et al. described a method for large scale isolation of murine glomeruli from kidneys perfused with spherical superparamagnetic beads. Mice are perfused with a suspension of magnetic beads (nominal diameter 4.5 µm) through the heart. These magnetic beads embolize the glomerular capillaries. After Collagenase treatment of the kidney tissue, glomeruli containing beads are isolated in a strong magnetic field.

The method allows for fast isolation of virtually all glomeruli present in a mouse kidney (approx. 12,000 per kidney) (Bonvalet et al. 1977) and provides glomerulus isolates of high purities (97%), suitable for performance of transcript profiling and gene expression analyses (Kiritoshi et al. 2003, Takemoto et al. 2006), as well as for performance of 2D DIGE (two dimensional difference in gel electrophoresis) proteomic analyses, where comparably large amounts of protein are required (Barati et al. 2007, Block et al. 2006, Sitek et al. 2006). The principle of the method is illustrated in figure 2.2. Magnetic isolation of kidney glomeruli, using magnetic beads is currently the only available method providing glomerulus isolates from murine kidney tissue that meets the requirements of a wide range of different investigational approaches. The method itself can be modified, due to the demands of the respective analyses to be performed (Cui et al. 2005), and be it just to remove glomeruli from the remaining kidney tissue (Rouschop et al. 2006). Modifications of the original protocol were also applied in the present study, as the experimental design of the two studies performed in the framework of the superordinated project (refer to chapter 1) scheduled the performance of each transcript profiling analyses and proteomic analyses on samples of isolated glomeruli derived from identical animals. For customization of these demands, extended pilot experiments have been performed (refer to chapter 4.2.1) and described previously (Blutke et al. 2005).

A Magnetic bead

smooth surface
magnetic core
Ø 4.5 µm

B Perfusion

sternum
A. + V. thoracica interna
lung
heart
liver
V. cava caudalis
caecum
diaphragm

C Magnetic beads embolize glomerular capillaries

aorta
perfused kidneys
glomerular capillary convolute
proximal tubulus
Bowman capsule
magnetic bead
vas efferens
vas afferens
A. interlobularis

D Kidneys are minced into 1 mm³ pieces

E Digestion of tissue

Collagenase A
(30 minutes / 37°C)

F Filtration of digested tissue

pestle
100 µm cell strainer
digested tissue

G Magnetic isolation of glomeruli

© Blutke 2007

Figure 2.2: Principle of magnetic isolation of glomeruli.

In **A**, a scheme of a spherical superparamagnetic bead (nominal diameter 4.5 µm) is shown. **B**: Mice are perfused with 40 ml of a suspension of magnetic beads through the left heart ventricle. **C**: In the kidneys, the perfused magnetic beads embolize the glomerular capillaries. **D**: After perfusion, the kidneys are removed, decapsulated and minced into ~1mm³ pieces. **E**: The tissue is then digested with Collagenase A (1mg/ml) at 37°C for 30 minutes. **F**: Under addition of buffer, the digested tissue is pressed through a 100 µm cell strainer, using a flattened pestle. **G**: Glomeruli containing magnetic beads are isolated from the cell suspension in the field of a strong permanent magnet.

3. Research design and methods

3.1 Experimental design

To address the question, if common characteristic patterns of morphological and functional glomerular alterations, displayed by both GIPR^{dn}- or bGH-transgenic mice (refer to chapters 2.4.2 and 2.4.3), would also find a reflection in detectable common glomerular gene expression profiles, differential transcript profiling analyses were performed on samples of isolated kidney glomeruli, generated from male GIPR^{dn}- or bGH-transgenic animals, as well as from their corresponding non-transgenic littermate controls (figure 3.1). The investigated animal models are bred on different genetic backgrounds (chapter 3.2.1) and in both models different mechanisms are responsible for the development of renal alterations (diabetes mellitus vs. overexpression of the GH-transgene). In the context of the present study, the term "group" refers to either GIPR^{dn}-, or bGH-transgenic (tg) animals and their corresponding non-transgenic wild-type littermate controls (wt), respectively the sample materials generated from these animals. Sample materials were generated from pairs of animals of the respective groups and also analyzed pairwise. As a matter of principle, a pair of animals consisted of a transgenic animal and an associated non-transgenic wild-type littermate control (tg/wt-pairs). If the numbers of male transgenic and non-transgenic animals in a respective litter allowed for more than a single possible combination, assignment of transgenic animals and associated littermate controls to tg/wt-pairs was performed by lot. For generation of sample materials, both animals of a respective tg/wt-pair were sacrificed at the same day of age. Sample materials of two cohorts of animals were generated: samples of isolated glomeruli of animals of the "Array Cohort" were investigated by performance of microarray experiments. For performance of real-time PCR confirmation experiments, samples of an additional second independent cohort, termed "Independent Control Cohort" were generated. Investigations were performed in two defined early stages of comparable glomerular alteration, displayed by transgenic animals of both models: First, the stage of glomerular hypertrophy (stage I) and second, the stage of glomerular hypertrophy with onset of micro-albuminuria (stage II). Stringent criteria for assignment of animals to either the first, or the second stage of investigation were defined in order to ensure the comparability of the respective stages in both groups, which was considered to be a crucial prerequisite for meaningful interpretation of analysis results. Assignment to the stages of investigation was performed in

dependency on the degree of glomerular alteration that was detected in the transgenic animal in comparison to its associated wild-type littermate control. In pairs of animals assigned to stage I and II of the Array Cohort, the transgenic mouse was required to display an increase of the mean glomerular volume of at least 40%, compared to its associated control animal. For that purpose, the mean glomerular volume was determined by methods of quantitative stereology, using histological samples of cortical kidney tissue. Since this approach implicated the necessity of accession of kidney tissue of both partners of a respective pair of animals distinguished for assignment to stage I, sacrifice of both mice and glomerulus isolation from their kidneys had to be performed prior to determination of the mean glomerular volumes. In addition to the criterion of glomerular hypertrophy for investigation in stage I, it was required, that neither the transgenic mouse, nor the associated wild-type control displayed albuminuria, verified by recurrent performance of sodium dodecyl sulphate polyacrylamide gel electrophoresis-based urine protein analysis (figure 4.7). In pairs of animals assigned to stage II, the transgenic mouse was required to display glomerular hypertrophy, as well as the onset of persistent albuminuria, whereas the corresponding wild-type mouse was not allowed to show any positive result of albuminuria (figure 4.7). Only sample materials derived from animals that did actually meet the criteria for investigation in the respective stages of glomerular alteration were used for further analyses. After performance of glomerulus isolation from the respective pairs of animals, total RNA was extracted from the glomerulus isolates and routinely processed for microarray analysis, using standard methods. Array data were analyzed to identify transcripts of differentially expressed genes (tg vs. wt) in the respective groups and stages of investigation. Then commonly differentially expressed genes (intersections of congeneric differentially expressed genes in both groups in comparable stages) were identified, representing common patterns of glomerular gene expression profiles in comparable early stages of glomerular alteration, presumably independent of the different expressed transgenes or genetic backgrounds of both different animal models. For revelation of their biological function in the context of molecular pathogenesis of glomerular hypertrophy and albuminuria, bioinformatical analyses were performed. Results from microarray experiments were confirmed, using quantitative real-time PCR. Additionally, sample materials were generated for performance of immunohistochemistry and in situ hybridisation in further studies to demonstrate the cellular distribution of selected proteins and/or transcripts in the glomerulus.

Figure 3.1: Experimental design

Generation and definition of sample material

Animal breeding, determination of gender, genotype and phenotype (3.2).

Screening for absence or onset of albuminuria (3.3) in urine samples of transgenic mice and corresponding wild-type controls in defined intervals.

Pairwise dissection of animals : glomerulus isolation, generation of sample material for histology, electron microscopy, immunohistochemistry and in situ hybridisation (3.4).

Detection of glomerular hypertrophy by determination of the mean glomerular volume (3.5.1). → Selection of each 5 wt/tg littermate pairs of male animals in both groups of investigation per cohort.

glomerulus isolates

Assignment of pairs of animals (generated sample materials) to the respective stages of investigation: stage I & stage II

GIPR[dn]-group   **bGH-group**

Stage I: glomerular hypertrophy

GIPR[dn]-tg   wt   *(5x)*   bGH-tg   wt   *(5x)*

Stage II: glomerular hypertrophy with onset of albuminuria

GIPR[dn]-tg   wt   *(5x)*   bGH-tg   wt   *(5x)*

glomerulus isolates

- samples of isolated glomeruli
- other generated sample materials
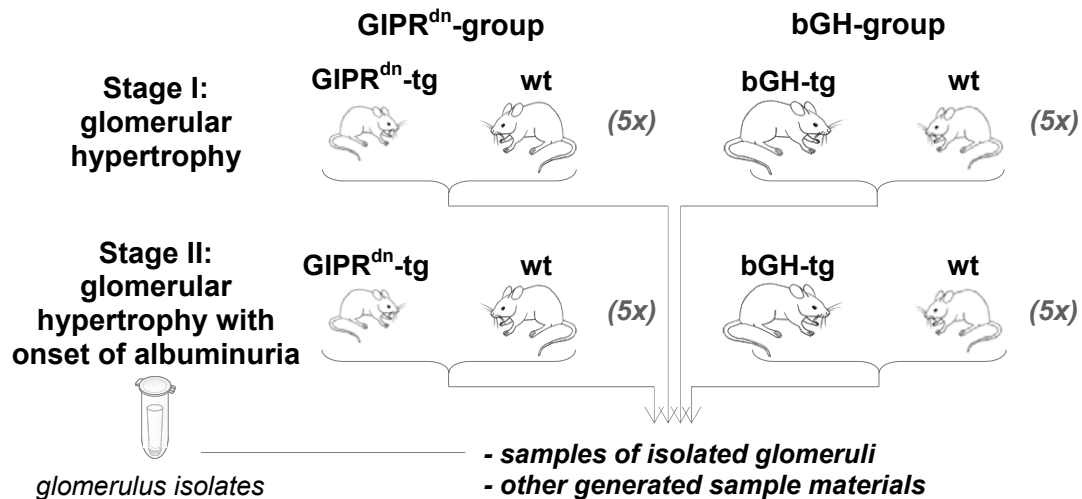
Transcript profiling analyses of samples of isolated glomeruli

Microarray analysis (3.6):
- **Identification of differentially regulated transcripts in the respective groups (tg vs. wt) of both stages of investigation.**
- **Identification of commonly congeneric differentially regulated transcripts in both groups (inter- and intrastadial comparision)**

Confirmation of results by real-time PCR (3.9.)
Bioinformatical analysis (3.10)
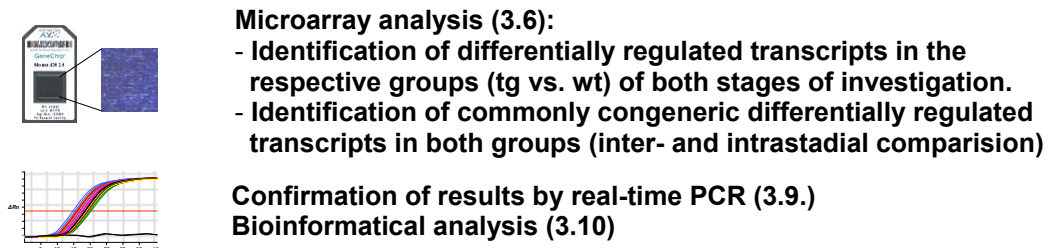
Further analyses: Confirmation of albuminuria by ELISA (3.3.3.3) and Western blot (3.3.3.2); estimation of numbers of cells per glomerulus (3.5.2), determination of the filtration slit frequency (3.5.3) and glomerular basement membrane thickness (3.5.4).

Figure 3.1 (page 40): Experimental design. Numbers given in brackets refer to the respective sub-chapters in „Research design and methods". Transcript profiling analyses were performed, using sample materials of isolated kidney glomeruli from male heterozygous GIPR^{dn}- and bGH-transgenic (**tg**) mice and their respective male non-transgenic wild-type littermate controls (**wt**) in comparable stages of renal alteration (**stage I and stage II**). Sample materials generated from 5 pairs of animals (each consisting of a transgenic mouse and a corresponding control mouse) of each group (**GIPR^{dn}-group and bGH-group**), stage and cohort, that met the respective criteria for assignment to a certain stage of investigation were analyzed.

3.2 Animals

3.2.1 Breeding, animal husbandry and numbers of mice used for analyses

Transgenic mice, expressing a dominant negative glucose-dependent insulinotropic polypeptide receptor (GIPR^{dn}) under the transcriptional control of the rat insulin gene promoter were generated as previously described (Herbach 2002, Herbach et al. 2005, Volz 1997) and maintained on the genetic background of the CD1 outbred stock. Transgenic mice overexpressing bovine growth hormone (bGH) under the transcriptional control of the rat phosphoenolpyruvate carboxykinase (PEPCK) gene promoter (McGrane et al. 1988) and their associated controls were maintained on the genetic background of the NMRI outbred stock (Wolf et al. 1993). In both groups of animals, male hemizygous transgenic animals were mated to female wild-type mice (Charles River Laboratories, Germany) of the respective genetic background (CD1, NMRI respectively). From the offspring, wt/tg-littermate pairs of male animals were selected for further investigations (refer to chapter 3.1). The breeding regimes are illustrated in figure 3.2.

Breeding regimes

GIPR^{dn}-group: GIPR^{dn} x CD1   *groups of investigation*   **bGH-group: bGH-tg x NMRI**

♂ **GIPR^{dn}-tg**   ♀ **wt**   *mating schemes*   ♂ **bGH-tg**   ♀ **wt**

X   X

♂   ♂   ♀   ♀   *offspring genotypes & genders*   ♂   ♂   ♀   ♀

wt   **tg**   *wt*   *tg*   **wt**   **tg**   *wt*   *tg*

→ **selection of tg/wt-littermate pairs of male animals for analysis**
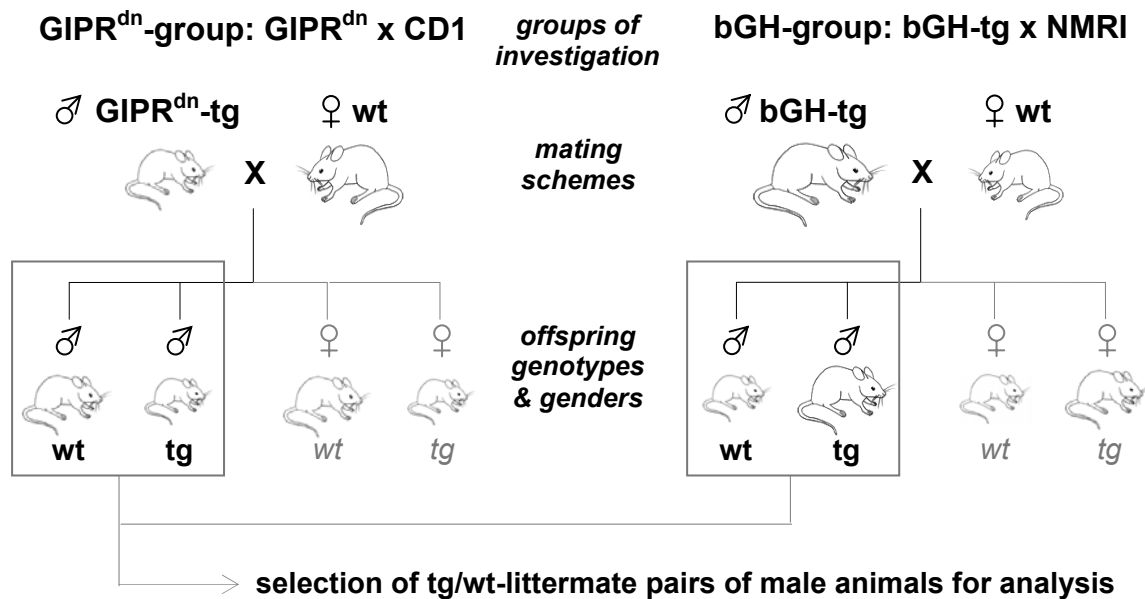
Figure 3.2: Breeding regimes. In both investigated groups of animals (GIPR^{dn}-group and bGH-group), male hemizygous transgenic (**tg**) animals were mated to wild-type (**wt**) female mice of the respective genetic backgrounds (CD1, NMRI respectively).

At an age of three weeks, animals were weaned, separated according to gender, marked by piercing the ears, and tail tip biopsies for genotype analyses were taken. The animals were maintained under standard (non-barrier) conditions (21 ± 1°C, 55 ± 3% relative humidity; 12/12-hours light/dark cycle) and fed standard rodent chow (Altromin C1324, Germany) and tap water ad libitum. All animal experiments were performed in accordance with institutionally approved and current animal care guidelines. The total number of animals investigated in each stage of nephropathy (stage I and stage II) was 20 (GIPR^{dn}-group and bGH-group: each 5 GIPR^{dn}-transgenic and 5 non-transgenic littermate controls). Samples of isolated glomeruli of these 40 mice (Array Cohort) were analyzed in the microarray experiments. For validation of the results of the array-experiments by real-time PCR, an additional second cohort of samples (Independent Control Cohort) of at least same size was generated, applying similar, but less stringent criteria for assignment of the transgenic animals to the respective stages of investigation (stage I: detection of glomerular hypertrophy and absence of albuminuria; stage II: detection of onset of albuminuria). In the Independent Control Cohort also age-matched non-littermate controls were paired to transgenic animals for analyses. The total number of animals investigated in the Independent Control Cohort was n = 50 (tables 3.1 and 3.2).

Numbers of animals in investigated cohorts

Stage	Array Cohort				Independent Control Cohort			
	GIPR^{dn}-group		bGH-group		GIPR^{dn}-group		bGH-group	
	wt	tg	wt	tg	wt	tg	wt	tg
Stage I stage of glomerular hypertrophy	5	5	5	5	5	5 (4 lmp)	5	5 (4 lmp)
Stage II stage of glomerular hypertrophy with onset of albuminuria	5	5	5	5	7	7 (5 lmp)	8	8 (5 lmp)

Table 3.1. Numbers of animals in investigated cohorts. All mice were of male gender; **tg**: transgenic animals; **wt**: non-transgenic wild-type controls. All animals investigated in the Array Cohort were littermate pairs. Numbers of littermate pairs (**lmp**) investigated in the Independent Control Cohort are indicated. A total number of 90 animals were investigated in both cohorts.

Table 3.2	Array Cohort								Independent Control Cohort							
	GIPR^{dn}-group				bGH-group				GIPR^{dn}-group				bGH-group			
Analysis	S I		S II		S I		S II		S I		S II		S I		S II	
	wt	tg	wt	tg	wt	tg	wt	tg	wt	tg	wt	tg	wt	tg	wt	tg
Genotyping	+	+	+	+	+	+	+	+	+	+	+	+	+	+	+	+
Detection of glucosuria	+	+	+	+					+	+	+	+				
Measurement of urine creatinine concentration	+	+	+	+	+	+	+	+	+	+	+	+	+	+	+	+
Urine protein analysis (SDS-PAGE)	+	+	+	+	+	+	+	+	+	+	+	+	+	+	+	+
Albumin ELISA	+	+	+	+	+	+	+	+			+	+			+ (4)	+ (4)
Body weight	+	+	+	+	+	+	+	+	+	+	+	+	+	+	+	+
Kidney weight	+	+	+	+	+	+	+	+	+	+	+	+	+	+	+	+
Relative kidney weight	+	+	+	+	+	+	+	+	+	+	+	+	+	+	+	+
Glomerulus isolation	+	+	+	+	+	+	+	+	+	+	+	+	+	+	+	+
Kidney histology (LM)	+	+	+	+	+	+	+	+	+	+	+	+	+	+	+	+
Kidney histology (TEM)	+	+	+	+	+	+	+	+								
Determination of the mean glomerular volume	+	+	+	+	+	+	+	+	+	+			+	+		
Estimation of numbers of glomerular cells	+	+	+	+	+	+	+	+								
Measurement of the FSF			+	+			+	+								
Measurement of the GBM-thickness			+	+			+	+								
Microarray analysis	+	+	+	+	+	+	+	+								
Real-time PCR analysis	+ (4)	+ (4)	+	+	+	+	+	+	+	+	+	+	+	+	+	+
Generation of samples for performance of Immunohistochemistry (IHC) and in situ hybridisation (ISH) in further studies.																

Table 3.2 (page 43): Performed analyses of single parameters.
If not stated otherwise (as indicated in brackets), in each group (GIPR[dn]-group and bGH-group) and stage (**S**) of investigation, a scheduled number of at least 5 transgenic animals and 5 corresponding non-transgenic wild-type controls (Array Cohort: tg/wt-littermate pairs of identical age; Independent Control Cohort: tg/wt-littermate pairs of identical age and age matched tg/wt-pairs) was investigated. "+" indicates the analysis of the respective parameter. **tg**: transgenic animals; **wt**: non-transgenic wild-type controls; **LM**: light microscopy; **TEM**: transmission electron microscopy; **FSF**: glomerular filtration slit frequency; **GBM**: glomerular basement membrane.

3.2.2 Identification of transgenic mice by PCR

Transgenic mice were identified by polymerase chain reaction as previously described (Herbach et al. 2005, Hoeflich et al. 2001), using DNA extracted from tail tips, according to standard protocols.

3.2.2.1 Primers

For the detection of GIPR[dn]-transgenic mice, oligonucleotide primers with the following sequence were used:

-5'- ACA GNN TCT NAG GGG CAG ACG NCG GG-3' sense (Tra1)

-5'- CCA GCA GNC NTA CAT ATC GAA GG-3' antisense (Tra3)

(Synthese, Ludwig-Maximilians-University, Munich, Germany)

These primers bind to the human cDNA of the mutated GIP receptor and also to the endogenous murine GIP receptor. The primers were chosen from areas where the known DNA sequence of the human, rat, mouse and hamster GIP receptor is highly conserved. Wherever the sequence varies in these animals, oligonucleotide synthesis was performed to allow all nucleotides ("N" in primer sequence) to integrate (Herbach et al. 2005, Volz 1997). The mutated human GIP receptor and the endogenous murine receptor can be distinguished in the PCR by their number of base pairs. The PCR product of the murine GIP receptor contains about 500 base pairs, whereas the PCR-product of the mutated human GIP receptors consists of about 140 base pairs. For the detection of bGH-transgenic mice, oligonucleotide primers (Synthese, Ludwig-Maximilians-University, Munich, Germany) with the following sequence were used:

-5'- GGG ACA GAG ATA CTC CAT CC –3' sense (bGH # 1)

-5'- ATG CGA AGC AGC TCC AAG TC -3' antisense (bGH # 2)

The PCR-product of the bGH-transgene consists of 343 base pairs (~pos. 1379-1722 of the bGH-transgene) (Hoeflich et al. 2001).

3.2.2.2 DNA isolation

At weaning of mice, tail tip biopsies were taken and stored at -20°C until assayed. For DNA extraction, a tail tip of approximately 0.5 cm length was incubated in 400ul Mastermix over night in a heating block (Biometra TB1 Thermoblock, Whatman, Germany) at 55°C. Thereafter, undigested components were separated by centrifugation for two minutes at 15,000 rpm (Sigma 1K15, Sigma, Germany). The supernatant was poured into another tube (Eppendorf safe lock tube, Eppendorf AG, Germany) and 400µl isopropanol (Roth, Germany) were added to precipitate DNA. The DNA pellet was washed twice with 900µl 70% ethanol (Roth, Germany), the liquid phase was discarded and the DNA pellet was dried at room temperature. DNA was suspended in 100 – 200µl 1xTE buffer, according to the size of the pellet when dried. To make sure that the DNA was dissolved completely it was stored at 4°C for at least 24 h before proceeding with the PCR.

Mastermix

Cutting buffer	375 µl
SDS 20% (Sodiumdodecylsulfate Ultra Pure, Roth, Germany)	20 µl
Proteinase K (20mg/ml) (Boehringer Ingelheim, Germany)	5 µl

Proteinase K
20 mg/ml were dissolved in aqua bidest., aliquoted and stored at –20°C.

Cutting buffer

1 M Tris-HCl (pH 7.5, Roth, Germany)	2.5 ml
0.5 M EDTA (pH 8.0, Sigma, Germany)	5.0 ml
5 M NaCl (Roth, Germany)	1.0 ml
1 M DTT (Roth, Germany)	250µl
Spermidine (500mg/ml, Sigma, Germany)	127 µl
Aqua bidest	ad 50ml
Storage at 4°C	

TE-buffer
10 mM Tris-HCl (pH 8.0, Roth, Germany)
1 mM EDTA
Storage at 4°C.

3.2.2.3 Polymerase chain reaction (PCR)

One µl of the suspended DNA was mixed with 19µl of the Master Mix in PCR-analysis cups (Kisker, Germany). DNA and components of the Mastermix were kept on ice during the procedure. The Taq DNA polymerase was stored at -20°C until it was added to the Mastermix. (Taq DNA polymerase and Mastermix reagents were from the Taq PCR Master Mix Kit (Qiagen, Germany).

Until further use, the PCR samples were stored at either 4°C (short-term) or at -20°C (long-term). DNA of a transgenic mouse was used as positive control, DNA of a wild-type mouse was used as negative control and H_2O served as quality (no template) control. The PCR was run in a Biometra® Uno II Thermocycler (Biometra, Germany), programmed as described:

Mastermix (GIPR^{dn}- PCR)		PCR-conditions (GIPR^{dn}- PCR)			
Aqua bidest.	3.65 µl	denaturation	94 °C	4 min	
Q-solution	4.00 ul	denaturation	94 °C	1 min	
10 x buffer	2.00 µl	annealing	60 °C	1 min	39 x
MgCl2	1.25 µl	extension	72 °C	2 min	
dNTP's (1mM)	4.00 µl	final extension	72 °C	10 min	
sense primer (Tra 1: 10 pM)	2.00 µl				
antisense primer (Tra 3: 10 pM)	2.00 µl				
Taq Polymerase	0.10 µl				
template	1.00 µl				

Mastermix (bGH- PCR)		PCR-conditions (bGH- PCR)			
Aqua bidest.	5.65 ul	denaturation	94 °C	4 min	
Q-solution	4.00 ul	denaturation	94 °C	1 min	
10 x buffer	2.00 µl	annealing	60 °C	1 min	34 x
MgCl2	1.25 µl	extension	72 °C	1 min	
dNTP's (1mM)	4.00 µl	final extension	72 °C	10 min	
sense primer (bGH#1: 2 µM)	1.00 µl				
antisense primer (bGH#2: 2 µM)	1.00 µl				
Taq Polymerase	0.10 µl				
template	1.00 µl				

3.2.2.4 Gel electrophoresis

DNA fragments were separated by size via electrophoresis in a TAE agarose (1.5%) gel (1.5 g agarose (Gibco BRL, Germany)/100 ml 1xTAE buffer), containing 9 µl/l ethidiumbromide (0.1%, Merck, Germany), casted in a Easy Cast® gel chamber (PeqLab, Germany) and filled with 1x TAE running buffer. The TAE running buffer also contained 9 µl/l ethidiumbromide (0.1%). Ethidiumbromide binds to double stranded DNA by interpolation between the base pairs and fluorescence may be seen when irradiated in the UV part of the spectrum. DNA samples were coloured with 4 µl of 6x loading dye (MBI Fermentas, Germany). At the beginning of each sample well row, 12 µl PUC Mix Marker #8 (MBI Fermentas, Germany) were placed in order to allow estimation of amplified fragment size. The remaining wells were filled with 24 µl of the samples.

Then electrophoresis was run for approximately 45 minutes at 90 V with an output of approximately 200 mA (Biorad Power PAC 300, Biorad, USA). Subsequently, the amplified products were visualized (Eagle Eye II, Stratagene, Germany) under UV light (306 nm) and a digital picture was taken to document the result (figure 3.3).

50x TAE stock solution

Tris base (Roth, Germany)	121 g
glacial acetic acid (Sigma, Germany)	28.55 ml
EDTA, 0.5 M, pH 8.0 (Sigma, Germany)	50 ml
ad 500 ml distilled water	

1x TAE-buffer
10 ml 50x TAE-buffer ad 500 ml distilled water
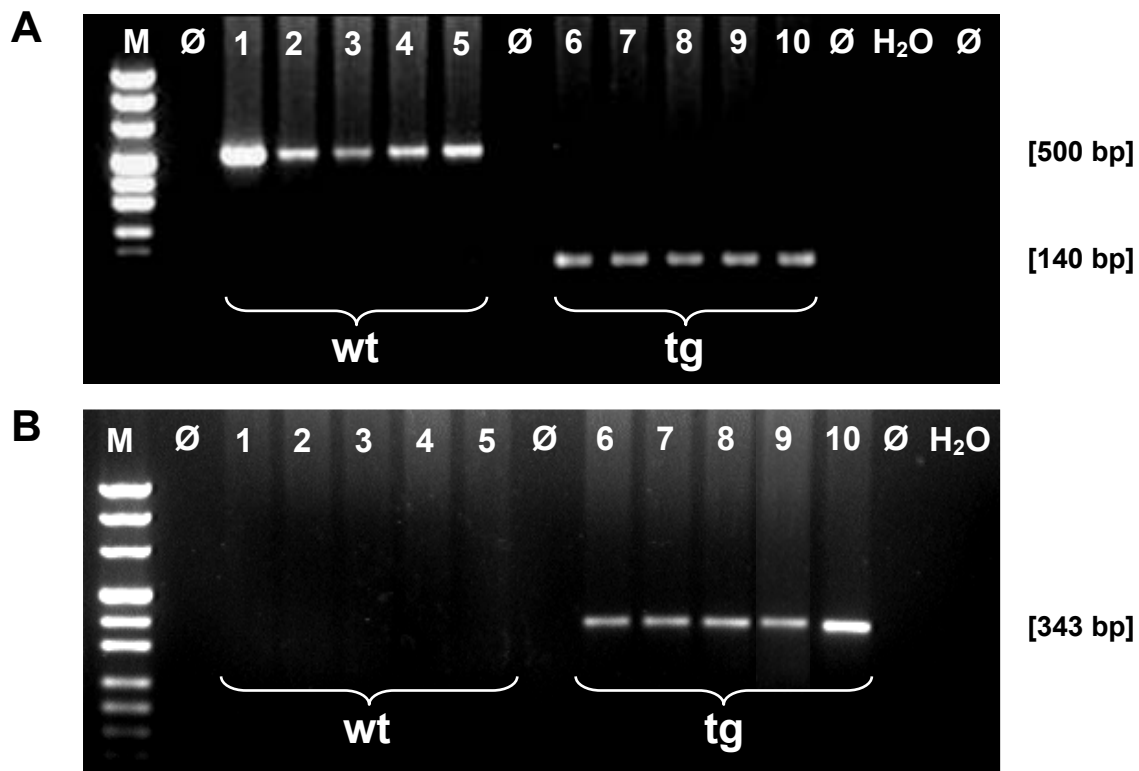
Figure 3.3: Genotyping by PCR. A: PCR-result of GIPR^{dn}-transgenic (**tg**) and non-transgenic wild-type control mice (**wt**). Samples of wild-type animals show a PCR-product of 500 base pairs (endogenous GIP receptor, lanes 1-5). Transgenic animals exhibit a DNA-fragment of 140 base pairs (mutated GIP-receptor, GIPR^{dn}, lanes 6-10). **B**: PCR-result of bGH-transgenic (**tg**) and non-transgenic wild-type control mice (**wt**). Samples of wild-type animals show no PCR-product (lanes 1-5). Transgenic animals exhibit a DNA-fragment of 343 base pairs (lanes 6-10). PCR-results for a "housekeeping gene" are not shown in this figure. **M**: Fragment size marker (pUC Mix Marker #8, Fermentas, USA). Visible marker-bands indicate fragment sizes of 1118, 881, 692, 489, 404, 331, 242, 190 and 147 base pairs from top to bottom. **Ø**: spacing lane. **H$_2$O**: no template control.

3.3 Urine analysis

3.3.1 Definition of stages, time points and intervals of investigation

According to the experimental design of this study, transgenic animals of both groups (GIPR^{dn} and bGH) were investigated either in the stage of glomerular hypertrophy without albuminuria (stage I) or in the stage of onset of albuminuria (stage II). We defined the stage of onset of albuminuria (stage II) as that point of time, at which the transgenic animals first displayed albuminuria twice within 48 hours after a first negative result, verified by Sodium dodecyl sulphate polyacrylamide gel electrophoresis (SDS-PAGE) analysis. Glomeruli from these animals and their corresponding non-transgenic littermate controls were then isolated 24 hours after the second positive result. Transgenic animals to be investigated in stage I, as well as the corresponding controls of both stages were required to show two negative results for albuminuria within 72 hours prior to dissection. Urine samples were collected weekly (GIPR^{dn}- transgenic mice and corresponding controls), or in 48-hour intervals (bGH- transgenic mice and corresponding controls) and every 48 hours after a first positive result. The schedules of time points and intervals of investigation of urine samples and time points of dissections are illustrated in figure 3.4. In order to exclude potential differences in urine protein excretion over the day, spot urine samples were taken constantly between 4 and 5 pm. by the same investigator. The urine samples were immediately frozen and stored at -80°C until assayed. Usually, spontaneous urine could be obtained. If this was not the case, samples were taken by carefully squeezing the bladder with two fingers. SDS-PAGE analyses, Western-blot analyses and quantification of urine albumin concentrations by Enzyme-linked Immunosorbent Assay (ELISA) were performed using aliquots of identical urine samples.
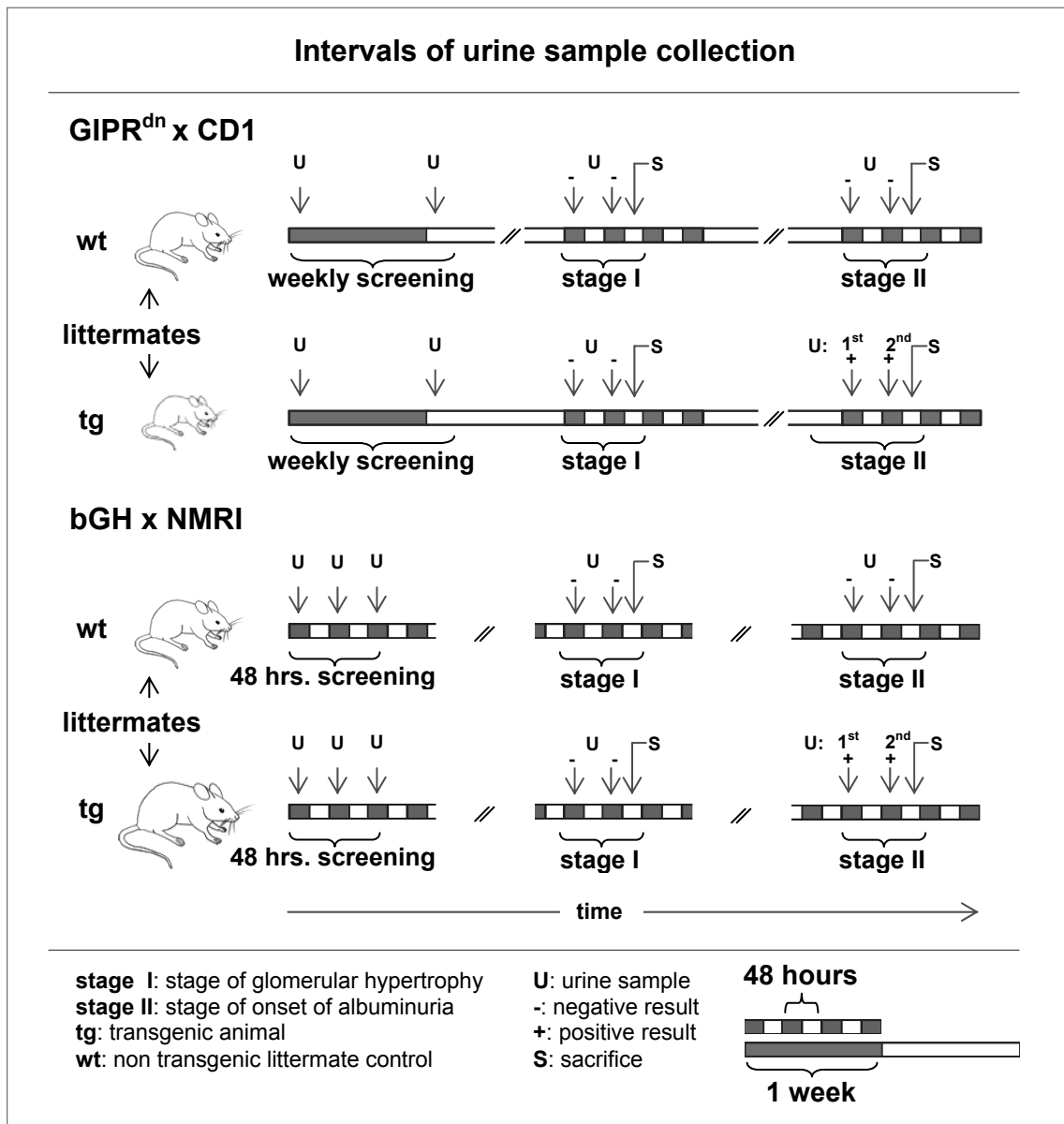
Figure 3.4: Intervals of urine sample collection. Screening for onset or absence of albuminuria by SDS-PAGE. Urine samples (**US**) of transgenic mice (**tg**) and their corresponding non-transgenic wild-type littermate controls (**wt**) were collected in weekly intervals (**GIPR**^{dn}-group), respectively every 48 hours (**bGH**-group). Animals to be investigated in **stage I** (stage of glomerular hypertrophy without albuminuria), as well as **wt**-animals of **stage II** (stage of onset of albuminuria) were required to show two negative results for albuminuria within 72 hours prior to dissection (**S**). **Stage II** was defined as that point of time, at which the transgenic animals first displayed albuminuria twice (**1**st **+**, **2**nd **+**) within 48 hours, following to a first negative result (**US -**). Pairs of animals in **stage II** were sacrificed 24 hours after the second positive result of the respective transgenic animal.

3.3.2 Detection of glucosuria in GIPR[dn]-transgenic mice

The diabetic phenotype of GIPR[dn] -transgenic mice was reconfirmed by detection of glucosuria in urine samples, using the Ratiomed EASY Screen Glucose® sticks (Megro, Germany). Spot urine samples were recurrently taken from GIPR[dn]-transgenic mice, as well as from their non-transgenic wild-type littermate controls from day 21 on (time point of weaning) and investigated, until glucosuria was detected in samples of GIPR[dn]-transgenic mice.

3.3.3 Urine protein analysis

3.3.3.1 Detection of absence or onset of albuminuria (SDS-PAGE)

Urine creatinine concentration was measured, using an automated analyzer technique (Hitachi, Merck, Germany). Urine samples were then standardized by dilution with reducing sample buffer to constant creatinine concentrations. As GIPR[dn]-transgenic animals display massive hyposthenuria and polyuria, their urine samples, as well as those of their corresponding control animals were diluted to a creatinine content of 1.5 mg/dl for silver staining, whereas urine samples derived from animals of the bGH-group were diluted to 3 mg creatinine/dl for Coomassie staining. A mouse albumin standard (1 mg/ml; Biotrend, Germany) was diluted 1:50 (= 20ng/µl) for silver staining or 1:25 (= 40 ng/µl) for Coomassie staining with reducing sample buffer. Both samples and mouse albumin standards were subsequently denatured at 96°C for 10 minutes in a heating block (Biometra, Goettingen, Germany). A 12% separating SDS-polyacrylamide gel was casted in a Mini-Protean III gel-casting chamber (Biorad, Germany), overlayed with distilled water and allowed to polymerise for 45 minutes. After polymerisation, a 5% stacking SDS-polyacrylamide gel was casted onto the 12% SDS gel; a comb for forming sample wells was immediately placed in the still fluid stacking gel. The stacking gel was allowed to polymerise for 45 minutes. The comb was removed then and the gel was placed into an electrophoresis cell (Protean III, Biorad, Germany), which was then filled with running buffer to the top of the inside cell. A volume of each 10 µl of the samples, molecular weight standards, (Broad Range (Biorad, Germany) for Coomassie stained gels, Precision Plus (Biorad, Germany) for silver stained gels) and the mouse albumin standards (Biotrend, Germany) were then run on 12% SDS-PAGE gels at 200 V for 50 minutes (Biorad Power PAC 300, Biorad, USA).

Subsequently, the gel was removed from the glass frame and either silver staining, or Coomassie blue staining was performed. Silver staining was performed due to a standard protocol (given in chapter 9.1). For Coomassie staining, the gel was at first stained with the Coomassie blue staining solution for 30 min and destained in the Coomassie destaining solution for approximately 1.5 hours until clearing of the gel background. In silver- and Coomassie stained gels, all clearly visible gel bands were registered, gels were scanned for documentation (OfficeJet G55, Hewlett Packard, Germany) and then dried according to the manufacturer's protocol, using the DryEase^{TM} Mini-Gel Drying System (Novex, Germany) for long term storage (drying of SDS-PAGE gels is described in the appendix). For detection of albuminuria, the intensities of gel bands of approximately 69 kDa in the SDS-PAGE, reflecting murine albumine, were compared between samples of transgenic animals and those of the corresponding wt-animals and the murine albumin standard on the same gel. In order to demonstrate the comparability of detected results of SDS-PAGE urine protein analyses, using a silver staining of gels (GIPR^{dn}-group), and respective results of Coomassie blue stained gels (bGH-group), urine samples of pairs of animals that had finally been selected for further investigations in the respective stages of analysis were analyzed a second time, now using the silver staining method for all gels. Materials used for performance of SDS-PAGE analyses are indicated below.

Tris/HCL 0.5 M pH 6.8
Tris base (Roth, Germany)   6.075 g
ad 100 ml distilled water

Sample buffer
Distilled water   1 ml
Tris/HCl 0.5 M pH 6.8   0.25 ml
Glycerol (Merck, Germany)   0.2 ml
SDS 10 % (Sigma, Germany)   0.4 ml
Bromphenol blue 0.05 % (Sigma, Germany)   0.125 ml

Reducing sample buffer
Sample buffer   475 µl
ß mercapto-ethanol (Sigma, Germany)   25 µl

Tris/HCL 0.5 M pH 8.8
Tris base (Roth, Germany)   18.5 g
ad 100 ml distilled water
adjust pH with 1N HCl (Merck, Germany)

SDS-12% polyacrylamide gel

Distilled water	3.5 ml
Tris / HCl 1.5 M, pH 8.8	2.5 ml
SDS 10 % (Sigma, Germany)	100 µl
Acrylamide 30% (Roth, Germany)	4.0 ml
Ammonium persulfate 10 % (Biorad, Germany)	50 µl
Tetraethylethylenediamine (TEMED) (Roth, Germany)	5 µl

5% SDS-polyacrylamide stacking gel

Distilled water	6.1 ml
Tris/HCl 0.5 M, pH 6.8	2.5 ml
SDS 10 % (Sigma, Germany)	100 µl
Acrylamide 30% (Roth, Germany)	1.3 ml
Ammonium persulfate 10 % (Biorad, Germany)	50 µl
Tetraethylethylenediamine (TEMED) (Roth, Germany)	10 µl

Running buffer (stock solution)

Tris base (Roth, Germany)	30.3 g
Glycine (Merck, Germany)	144 g
ad 1 l distilled water	

Running buffer (ready to use)

Stock solution	40 ml
SDS 10 % (Sigma, Germany)	4 ml
ad 400 ml distilled water	

Coomassie staining solution

Coomassie brilliant blue G250 (Merck, Germany)	625 mg
100 % acetic acid (AppliChem, Germany)	12.5 ml
100 % ethanol (Roth, Germany)	125 ml
ad 250 ml distilled water	

Coomassie destaining staining solution

100 % acetic acid (AppliChem, Germany)	17.5 ml
100 % ethanol (Roth, Germany)	12.5 ml
ad 250 ml distilled water	

3.3.3.2 Western-blot analysis

In order to confirm that a lane of approximatively 69 kDa in the SDS-PAGE reflects albumin, Western-blot analyses were performed. Urine samples of two GIPR[dn]-transgenic animals, two bGH-transgenic animals (assigned to stage II) and their corresponding controls were analyzed according to a standard Western blot protocol. A 12% SDS-polyacrylamide gel was run as described above. After electrophoresis, gels were placed on a pre-wetted nitrocellulose membrane (Schleicher & Schüll, Germany) between three layers of absorbent paper imbibed with buffer, and fiber pads each side, and the Sandwich was set in the gel holder cassette. Two cassettes were placed into the electrode module, which was then inserted in the buffer lank along with a frozen cooling unit (Mini Trans-Blot Cell, Biorad, Germany). After filling the tank with Towbin buffer, the transfer was run over night at 30 Volt (Biorad Power PAC 300, Biorad, USA). The next day, the membranes were dyed with ponceau S solution (Sigma, Germany) to confirm blotting was achieved. After washing in Tris-buffered saline (TBS, pH 8.3), blocking was performed in 1% bovine serum albumin (BSA, Sigma, Germany) for one hour to avoid non-specific binding of the antibody probe to the membrane. Then incubation with rabbit anti-mouse albumin antibody probe (Biotrend, Germany; 1:300 in TBS-Tween and 1% BSA) was performed for three hours. The membrane was then incubated with horseradish peroxidase conjugated goat anti-rabbit antibody (DAKO Diagnostika, Germany, 1:1000 in TBS-Tween and 1% BSA) for one hour. After washing three times in TBS-Tween for ten minutes, immunoreactivity was visualized using 3, 3' diaminobenzidine tetra hydrochloride (Biotrend, Germany) as chromogen. Then the membranes were scanned and stored in a cassette. The following materials were used for performance of Western-blot experiments:

Towbin buffer (storage at 4°C)
Tris base (Roth, Germany)	3.03 g
Glycine (Merck, Germany)	14.4 g
Distilled water	800 ml
Methanol (Roth, Germany)	200 ml

Tris buffered saline (TBS) 10x stock solution (storage at 4°C)
Tris base (Roth, Germany)	60.6 g
Sodium Chloride (AppliChem, Germany)	87.6 g

ad 1 l distilled water
adjust to pH 7.4 using 1N HCl (Merck, Germany)

1x TBS-buffer
100 ml 10x TBS ad 1000 ml Aqua bidest.

TBS-Tween
1x TBS with 0.05% Tween 20 (Roth, Germany)

DAB (3,3' diaminobenzidine tetrahydrochloride dihydrate)
DAB (Biotrend, Germany)	5 ml
Tris/HCl 50 mM pH 7.3	25 ml
Hydrogen peroxide 30 % (Roth, Germany)	10 µl

Tris/HCL 0.05 M pH 7.3
Tris base (Roth, Germany)	1.85 g
ad 100 ml distilled water	
adjust pH with 1N HCl (Merck, Germany)	

3.3.3.3 Determination of urine albumin concentrations by ELISA

For determination of urine albumin concentrations, spot urine samples of GIPR^{dn}-transgenic and bGH-transgenic animals and their associated non-transgenic wild-type controls of both cohorts (Array Cohort and Independent Control Cohort) of both investigated stages of glomerular alteration, taken 24 hours prior to sacrifice of mice were examined. These were the same urine samples that had previously been analyzed by performance of SDS-PAGE based urine protein analyses. The creatinine concentrations in these samples were measured, using an automated analyzer technique (Hitachi, Merck, Germany). The numbers of investigated urine samples are indicated in table 3.3.

Group/stage	genotype		lmp	
	wt	tg	AC	ICC
GIPR^{dn} stage I	5	5	5	-
GIPR^{dn} stage II	11	11	5	6
bGH stage I	5	5	5	-
bGH stage II	9	9	5	4

Table 3.3. Numbers of investigated urine samples for determination of urine albumin concentrations by ELISA. wt: non-transgenic wild-type controls; **tg**: transgenic animals. Numbers of investigated littermate pairs (**lmp**) of animals in the Array Cohort (**AC**) and the Independent Control Cohort (**ICC**) are indicated.

Urine albumin concentrations were determined, using the mouse albumin ELISA-kit Bethyl E90-134 (Bethyl, USA), according to the manufacturer's protocol. All steps were performed at room temperature. Coating and blocking of plates was performed according to the manufacturer's recommendations: 1µl (1 mg/ml) of goat anti-mouse albumin capture antibody (A90-134A) was diluted to 100 µl coating buffer for each well to be coated.

The coated plate (Nunc C bottom Immunoplate 96 well, Nunc A/S, Denmark) was incubated for 60 minutes. After incubation, the capture antibody solution was aspirated from each well. Each well was then filled with wash solution, which then was removed by aspiration. These washing steps were repeated for a total of 3 washes. 200 µl of blocking (postcoat) solution were then added to each well and the plate was incubated for 30 minutes. After incubation, the blocking (postcoat) solution was removed and each well was washed for three times as described above. The murine albumin standard (Calibrator) dilutions were prepared due to manufacturer's recommendations (range: 7.8 - 500 ng/ml). Standards were diluted in sample diluent as described in chapter 9.3. The urine samples were diluted with sample diluent, based on the expected concentration of the analytes to fall within the concentration range of the standards. The proper dilution of urine specimens ranged from 1:50-1:6000 (GIPR^{dn}-tg: 1:50 - 1:1.600, associated controls: 1:300 - 1:600; bGH-tg: 1:300 - 1:6.000, associated controls: 1:300 - 1:1.500), as shown by a pilot study. Standards, samples, blanks and controls were analyzed in duplicates. Each 100 µl of standards or samples were transferred to the assigned wells. The plate was then incubated for 60 minutes. After incubation, samples and standards were removed and each well was washed 5 times as described above. The HRP conjugate (goat anti-mouse albumin-HRP conjugate, 1 mg/ml) was diluted in conjugate diluent 1:100,000. 100 µl of diluted HRP conjugate were transferred to each well and the plate was then incubated for 60 minutes. After incubation, the free HRP conjugate was removed and each well was washed for 5 times. Subsequently, bound HRP antibody conjugate was detected through a chromogenic reaction. The substrate solution (TMB/H_2O_2, Kirkegaard and Perry, USA) was prepared by mixing equal volumes of the two-substrate reagents, provided by the manufacturer. 100 µl of substrate solution were added to each well and incubated for seven minutes. The TMB reaction was stopped by adding 100 µl of 1 M H_3PO_4 (Roth, Germany) to each well. The color intensity was measured by determining the absorbance at 450 nm using a computer-assisted (Magellan, Tecan AG, Germany) microplate reader (Sunrise, Tecan AG, Germany). For calculation of results, the duplicate readings from each standard, control and sample were averaged. The zero reading was subtracted from each averaged value above. A standard curve was generated for each set of samples (Magellan, Tecan AG, Germany). The values of the specimen wells were in the linear segment of the calibration curve.

For each group and stage of investigation, the albumin/creatinine ratios were calculated by dividing the measured albumin concentration of a urine sample by its corresponding creatinine concentration. Materials used for performance of ELISA-analyses are indicated below.

Coating buffer
0.05 M Carbonate-bicarbonate (Sigma, Germany)
adjust to pH 9.6

Wash solution
50 mM Tris (Roth, Germany)
0.14 M NaCl (AppliChem, Germany)
0.05% Tween 20 (Roth, Germany)
adjust to pH 8.0

Blocking (postcoat) solution
50 mM Tris (Roth, Germany)
0.14 M NaCl (AppliChem, Germany)
1% Bovine serum albumin in Tris buffered saline (Sigma Chemical, Germany)
adjust to pH 8.0

Sample/conjugate diluent
50 mM Tris (Roth, Germany)
0.14 M NaCl (AppliChem, Germany)
1% Bovine serum albumin in Tris buffered saline (Sigma Chemical, Germany)
0.05% Tween 20 (Roth, Germany)
adjust to pH 8.0

3.4.1 Generation of sample materials and acquisition of additional data

According to the results of the SDS-PAGE urine protein analyses, mice were dissected at defined time points (3.3.1). Both, the transgenic mouse and its associated wild-type littermate control animal of a tg/wt-pair were dissected at the same day. Samples of isolated kidney glomeruli were generated for performance of transcript profiling analyses. As well, samples of kidney tissue were generated for further morphological investigations. In order to exclude potential differences in patterns of glomerular gene expression profiles over the day, dissections were always performed between 8 and 11 am. For every single tg/wt-pair of animals, the order of dissection of the respective transgenic mouse and its associated control animal was decided strictly random by drawing lots.

3.4.2 Kidney perfusion and glomerulus isolation

All mice were weighed prior to sacrifice. Body weight was determined to the nearest 0.1 g, using a precision scale (Kern KB 5000-1, Kern & Sohn GmbH, Germany). Mice were anesthetized by intraperitoneal injection of ketamine (Ketanest[®], 80 mg/kg, Bayer, Germany) and xylacine (8 mg/kg, Rompun[®], Bayer, Germany). Approximately 8 x 10^7 (200 µl) Dnabeads ® M-450 Epoxy (Dynal Invitrogen Corporation, Germany) were blocked according to the manufacturers instructions, diluted in 40 ml of 38°C warm phosphate buffered saline (PBS, pH 7.4; composition indicated below) and perfused through the left heart ventricle. Dynabeads are made of an iron-containing monodisperse polymer and exhibit magnetic properties within a magnetic field (Kemshead, 1985, Magnetic separation techniques). Their surface is smooth with a coated polymer shell that reduces the direct damage to the tissues and protects from toxic exposure to iron when they are perfused. As perfusion technique had pointed out to be the most important prerequisite for the method's success, a self-developed perfusion device (German utility patent no. DE 202006001542 U1) was used for performance of perfusion (figure 3.5), which allows for uncomplicated perfusion of nearly all glomeruli in the adult mouse kidney with sufficient numbers of magnetic beads under adjustable pressure conditions, thereby minimizing common problems of conventional perfusion techniques (refer to chapter 4.2.1) (Blutke et al. 2005). An incision in the inferior vena cava, cranial of the diaphragm provided outflow of the perfusate. Perfusion was performed using a perfusion pressure of 70 mm Hg. After perfusion, the kidneys were removed, decapsulated and weight to the nearest 0.1 mg (BP 61 S, Sartorius AG, Germany). For histology and quantitative stereology, IHC and TEM, a sagittal slice of approximatively 1 mm thickness was carefully cut from the middle of each kidney, using a scalpel blade, as illustrated in figure 3.6.

Phosphate-buffered saline (PBS)
potassium dihydrogen phosphate (AppliChem, Germany)   0.25 g
sodium chloride (AppliChem, Germany)   8.0 g
di-sodium hydrogen phosphate dihydrate (AppliChem,Germany)   1.46 g
ad 1 l distilled water, adjust to pH 7.4
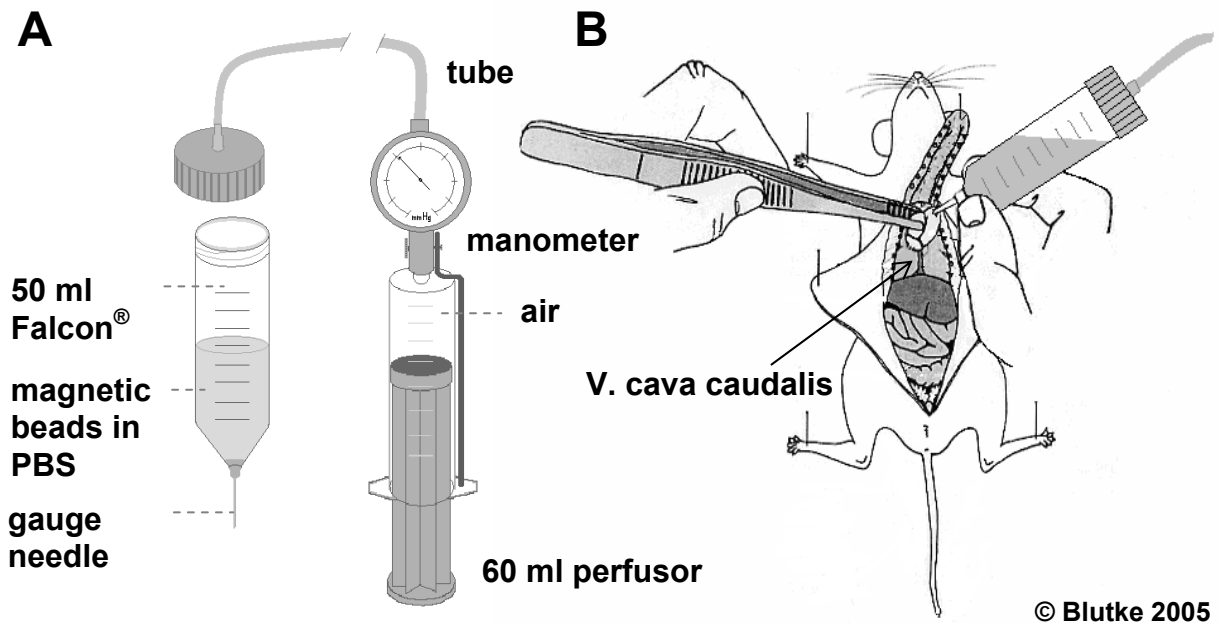
Figure 3.5: Device used for perfusion (A) and perfusion technique (B). A: As the entire perfusion volume is located directly above the perfusion canulla inside the perfusion reservoir (50 ml Falcon ® tube), no dead stock volumes remain inside the system after perfusion and precipitation of beads or formation of air bubbles inside the perfusate are reduced to a minimum. Perfusion can be performed under adjustable pressure conditions. **B**: Perfusion was performed, using a pressure of 70 mm Hg. An incision in the vena cava caudalis (indicated) provided outflow of the perfusate.
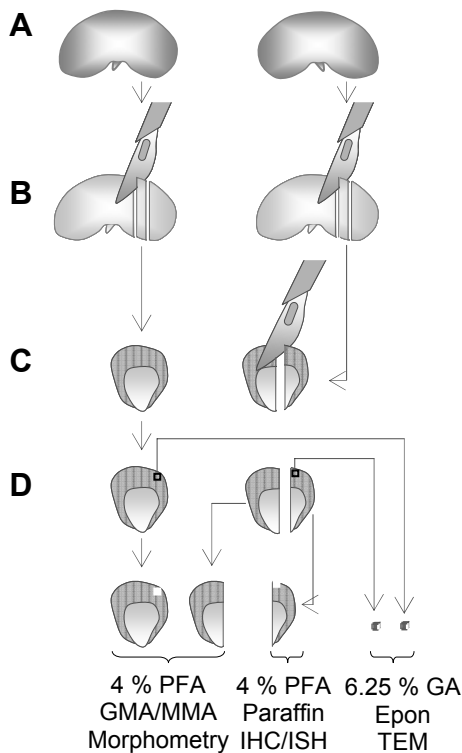
Figure 3.6. Tissue sampling for histology, electron microscopy, immunohistochemistry and in situ hybridisation. A: After perfusion kidneys were decapsulated and weighed. **B**: A slice of approximately 1 mm thickness was cut from the middle of each kidney. Glomeruli were isolated from the remaining tissue. **C**: 1 slice was cut into halves. **D**: 2 cortical samples for electron microscopy (1 mm^3) were taken from 1 ½ kidney slices, fixed in 6.25 % glutaraldehyde (**GA**) and embedded in Epon. A half slice of kidney tissue was fixed in 4 % paraformaldehyde (**PA**) and embedded in paraffin for immunohistochemistry (**IHC**) and in situ hybridisation (**ISH**). 1 ½ slices of kidney tissue were fixed in 4 % paraformaldehyde (**PA**) and embedded in glycolmethacrylate and methyl-methacrylate (GMA/MMA) for histology and and quantitative stereological analyses.

The remaining kidney tissue designated for glomerulus isolation was cut into small pieces of approximately 1 mm^3 and digested with Collagenase A (Roche, Germany) in Hanks' balanced salt solution (Invitrogen, Germany) (1 mg collagenase A/ml HBSS), inside a round-bottomed 2 ml tube (Eppendorf safe lock tube, Eppendorf AG, Germany) at 37°C for 30 minutes with gentle agitation (Biometra TB1 Thermoblock, Whatman, Germany). The digested tissue was gently pressed through a 100-µm cell strainer (Falcon, Germany), using a flattened pestle and the cell strainer was then washed with 7 ml of 4°C phosphate buffered saline (PBS, pH 7.4). The cell suspension was then transferred into a 12 ml tube (Techno Plastic Products AG, Switzerland) and placed into the magnetic field of a strong permanent magnet (BD I Magnet^{TM} Cell Separation Magnet, BD Biosciences, Germany) for 5 minutes. The buffer, containing the non-glomerular kidney-tissues was then removed by careful aspiration and examined for absence of glomeruli, using a photomacroscope (Stemi DV4, Zeiss, Germany) as illustrated in figure 3.7. Isolated glomeruli containing Dynabeads were resuspended in 7 ml of 4°C PBS and filtered through a new 100-µm cell strainer without pressing. The cell strainer was washed with 5 ml of 4°C PBS. Magnetic isolation of glomeruli containing Dynabeads and washing steps were repeated for two times (figure 3.7).
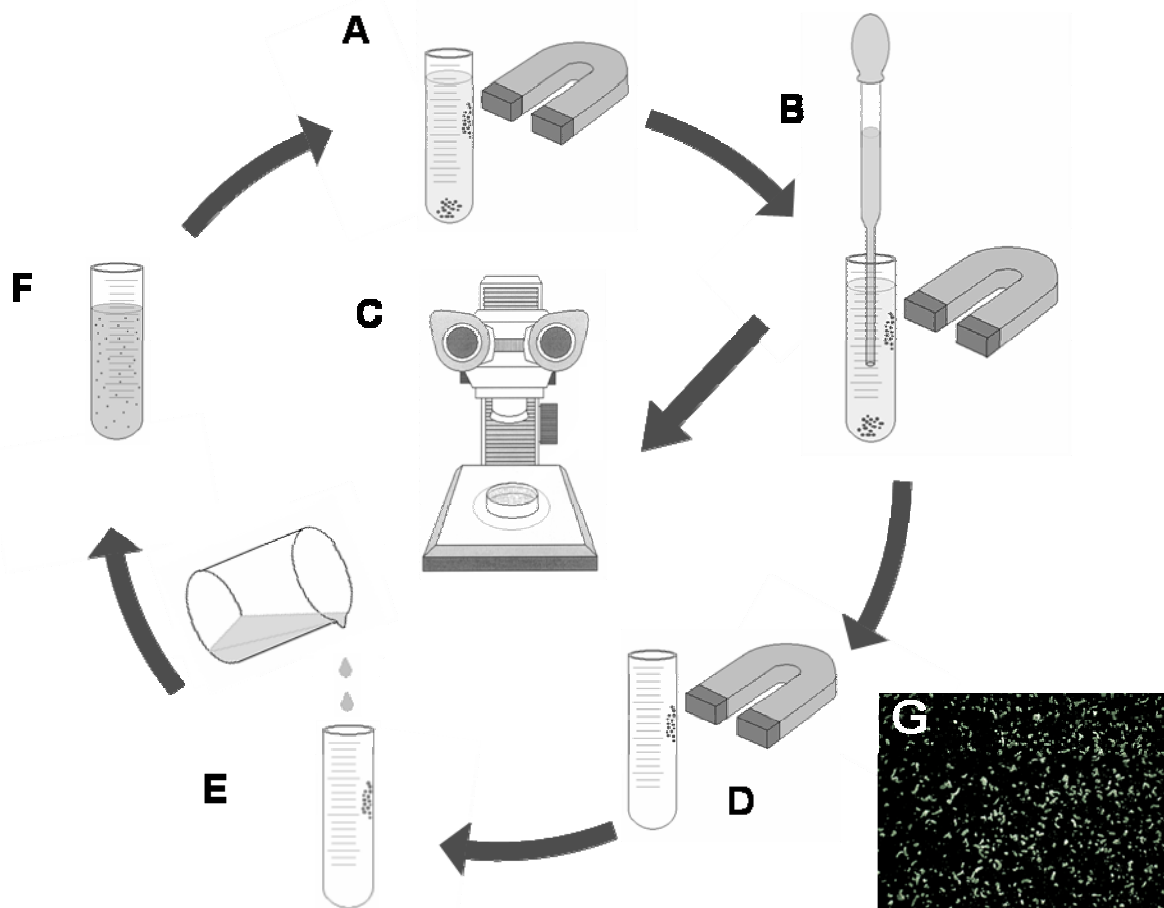
Figure 3.7: Magnetic isolation of glomeruli: Washing steps.

A: During exposure time at the magnet, glomeruli containing magnetic beads are drawn to the cup's wall. **B**: The buffer, containing the non-glomerular tissues, is removed by aspiration. **C**: Examination of the removed buffer for absence of glomeruli, using a photomacroscope. **D**-**F**: After removal of the buffer, the cup is removed from the magnet and new buffer is added. **G**: Wash (of second isolation cycle in this instance): predominantly pieces of tubular tissues [native, 32x].

Isolated glomeruli were then suspended in 10 ml of 4°C PBS and from this volume an aliquot of 1.5 ml, determined for transcript profiling analysis, was transferred into a 1.5 ml Eppendorf-tube and placed at the magnet for 3 minutes. After removal of the buffer, the isolated glomeruli were suspended in 4 ml of 4°C RNA-later$^®$ RNA stabilization reagent (Ambion, Germany) and transferred into a sterile glass platter. From this suspension all identifiable glomeruli (an average number of 1000 per animal), were counted and simultaneously picked under a photomacroscope (magnification: 32x), using a fine-tipped (Micro gel-loader tips 1-200 µl, Peske, Germany) pipette (figures 3.8 and 3.9).

The isolated glomeruli were then concentrated in a volume of 30 µl RNA-later®, using an autoclavable 50 µm mini cell strainer (figures 3.8 and 3.10), developed for this application (Blutke et al. 2005). This device consists of a piece of mesh, derived from a 50 µm cell strainer (BD, Germany), that is attached to a corpus (derived from a 1000 µl pipette tip) by a plastic ring (also derived from a 1000 µl pipette tip) and fixed with super-glue (UHU GmbH & Co. KG, Germany). Prior to use it was treated with 10 % SDS (Sigma, Germany) for two minutes, then washed with distilled water (RNAse-free quality) for 10 minutes and put into a 2 ml round-bottomed Eppendorf-cup and autoclaved. For concentration of isolated glomeruli suspended in RNA-later®, the sample was transferred into the 50 µm mini cell strainer, the isolated intact glomeruli were thereby filtered and remained inside the mini cell strainer, while the RNA-later® flow through the sieve. The flow-through was then examined under a photomacroscope at x 32 factor of magnification, to ensure that no isolated glomeruli passed the filter. The 50 µm mini cell strainer, containing the isolated glomeruli, was then put into the 2 ml round-bottomed Eppendorf-tube, 30 µl of fresh RNA-later® were added and stored at -20°C until further treatment (figure 3.8).
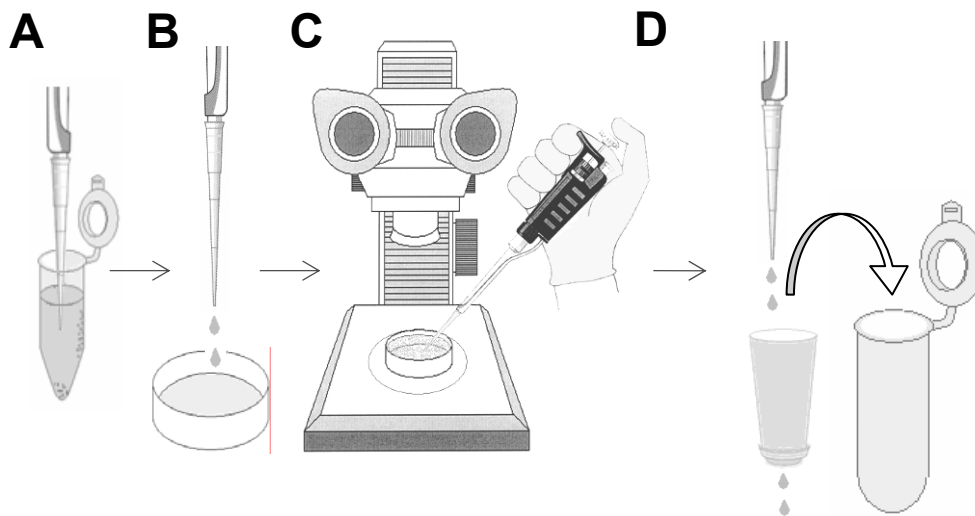
Figure 3.8: Isolation of glomeruli for transcript profiling analysis and concentration of isolated glomeruli in RNA-later®. A-C: Isolated glomeruli, enriched by magnetic isolation (**A**) were transferred into RNA-later® (**B**) and picked under a photomacroscope, using a fine tipped pipette (**C**). **D**: Each 1000 glomeruli per sample were concentrated in 30 µl RNA-later®, using a 50 µm mini cell strainer and stored at -20 °C.
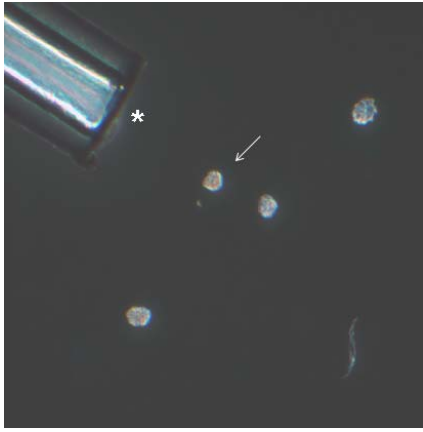
Figure 3.9: Picking of isolated glomeruli in RNA-later®. Asterisk marks the opening of the pipette tip; arrow indicates a glomerulus [native, 40x].

2 ml cup

50 µm mini cell strainer

wall of 50 µm mini cell strainer

wall of 2 ml cup

~1000 isolated glomeruli

50 µm sieve

30 µl RNA-later®

storage at – 20°C
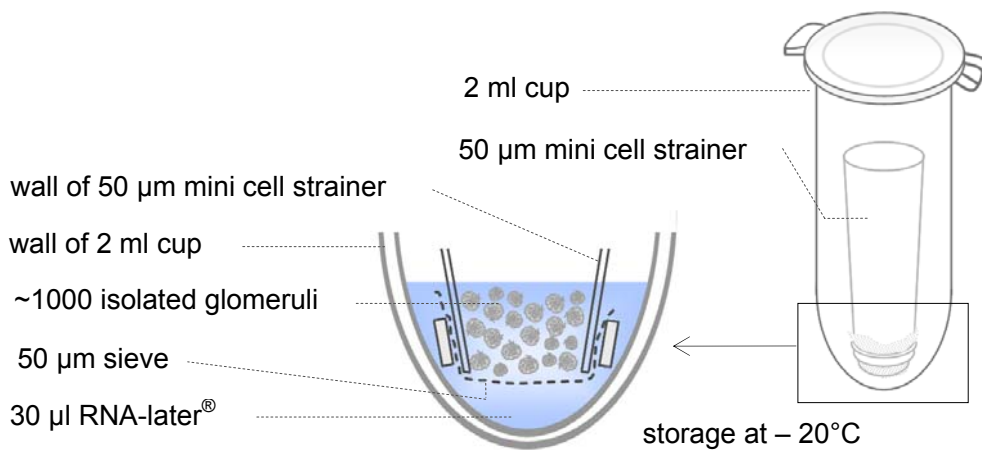
Figure 3.10: Scheme of the 50 µm mini cell strainer.

Quantity and purity (%) of generated glomerulus isolates was estimated by counting the numbers of clearly identifiable isolated glomeruli, as well as the numbers of pieces of non-glomerular tissues in a representative number of aliquots of the respective glomerulus isolates under a photomacroscope at a 32x magnification. The appearance of glomerular losses in the washes was estimated in an analogous manner. During the procedure, kidney tissues were kept at 4°C except for the collagenase digestion at 37°C.

3.4.3 Tissue preparation for histology and electron microscopy

3.4.3.1 Plastic histology

For histology and morphometric analysis 1 ½ slices of kidney tissue of each animal were fixed by immersion in 4% paraformaldehyde (VWR international, Germany) in phosphate buffered saline (PBS pH 7.4) for 24 hours at 8°C and then routinely processed for plastic embedding in a Citadel 1000 (Shandon, Germany), as indicated below. In order to avoid distortions, the kidney slices were fixed with a piece of foam-rubber sponge (Bio Optica, Italy) in the tissue-embedding capsules (Engelbrecht, Germany). Embedding in glycolmethacrylate and methylmethacrylate (GMA/MMA) was performed as previously described (Hermanns et al. 1981). Kidney slices were immersed in a hydroxymethylmethacrylate (Fluka Chemie, Germany) / methylmethacrylate (Riedel de Haën, Germany) solution at 4°C on a shaker for 18 hours. The kidney slices were then shifted into "solution A", composed of benzoylperoxide (338 mg; Merck, Germany), methylmethacrylate (20 ml), hydroxymethylmethacrylate (60 ml), ethyleneglycol monobutylether (16 ml; Merck, Germany) and polyethylene glycol 400 (2 ml; Merck, Germany). After immersion at 4°C on a shaker for four hours, the kidney slices were placed in plastic cups and embedded using 60 µl of dimethylanilin (Merck, Germany) in 40 ml of "solution 1" as starter for polymerisation. Embedding cups were immediately placed into a water bath (4°C) and polymerisation took place at 4°C over night. Sections of approximately 1.5 µm thickness were cut using a Microm HM 360 rotary microtome (Microm, Germany), dried on a heating plate (OTS 40, Meditel, Germany) and stored in an incubator (Memmert, Germany) at 64°C over night before staining. Sections were stained with PAS (Periodic Acid Schiff stain) and H&E (Hematoxilin & Eosin), as indicated below.

4% paraformaldehyde in PBS (pH 7.2)
PBS, pH 7.4   1000 ml
paraformaldehyde (Serva, Germany)   40 g
adjust to pH 7.2 with 1 n NaOH (Roth, Germany)

Processing of paraformaldehyde fixed tissue for plastic histology:

Chemical	Time
Rinsing solution	3 hours
Ethyl alcohol 30 % (Bundesmonopolverwaltung für Branntwein, Germany)	2 x 1 hour
Ethyl alcohol 56 %	2 x 1 hour
Ethyl alcohol 70 %	2 x 1 hour
Ethyl alcohol 96 %	2 hours
Ethyl alcohol 96 %	2 x 3 hours

HE staining of plastic sections

Reagents	Time
Mayer's Hemalaun (AppliChem, Germany)	20 min
running tap water	10 min
1% HCl-ethyl alcohol (Roth, Germany)	10 sec
running tap water	10 min
heating plate	5 min
Eosin-Phloxin (Merck, Germany)	20 min
Aqua dest.	2 x 2 min
heating plate	5 min
Xylol (SAV LP, Germany)	2 min

Covering with glass coverslips (Menzel GmbH & Co KG, Germany), using Histofluid® (Superior, Germany).

PAS staining of plastic sections

Reagents	Time
Periodic acid 1% (AppliChem, Germany)	15 minutes
Aqua dest.	3 x 3 sec
Schiffs reagent (Merck, Germany)	30 – 60 min
running tap water	30 minutes
dry	
Mayer's Hemalaun (AppliChem, Germany)	35 minutes
running tap water	10 minutes
1% HCl-ethyl alcohol (Roth, Germany)	1 sec
running tap water	10 minutes
dry	

Covering with glass coverslips (Menzel GmbH & Co KG, Germany), using Histofluid® (Superior, Germany)

3.4.3.2 Tissue preparation for transmission electron microscopy (TEM)

For transmission electron microscopy (including quantitative stereological analysis) two cubes ($1mm^3$) of cortical kidney tissue from each animal were fixed by immersion in 6.25% glutaraldehyde (Serva, Germany) in PBS (pH 7.4) at 8°C for 48 hours, postfixed in 1% osmiumtetroxide (OsO_4, Merck, Germany), dehydrated and embedded in Epon (syn. "glycid ether 100", Serva, Germany) according to standard procedures: The samples were washed for 3 hours in Sörensen phosphate buffer at room temperature, postfixed in 1% osmium tetroxide (Caulfield 1957) for 2 hours at 4°C, and washed in Sörensen phosphate buffer three times for 2 min at room temperature. Subsequently, the specimens were dehydrated through a series of acetone (Roth, Germany) solutions at 4°C. Then they were infiltrated with a 100% acetone/Epon mixture for 1 hour, and twice with pure Epon for 30 min, each, at room temperature. Then, the Epon infiltrated samples were embedded in Epon-embedding mixture in dried gelatin capsules (Plano, Germany). Polymerization took place at 60°C for approximately 48 hours. Epon blocks were trimmed with a TM60 Reichert-Jung milling machine (Leica, Germany) and 0.5 µm semi-thin sections were obtained with a Reichert-Jung "Ultracut E" (Leica, Germany). Sections were then stained with Azur II/Safranin, as indicated below. The following materials were used for Epon histology:

Sörensen phosphate buffer 0.067 M, pH 7.4

Solution I	80.8 ml
Solution II	19.2 ml
adjust to pH 7.4	

Solution I

potassium dihydrogen phosphate (Roth, Germany)	9.08 g
ad 1 l distilled water	

Solution II

di-sodium hydrogen phosphate dihydrate (Roth, Germany)	11.88 g
ad 1 l distilled water	

veronal acetate buffer, pH 7.6

sodium veronal (barbitone sodium, Merck, Germany)	2.95 g
sodium acetate (Merck, Germany)	
1.94 g	
ad 100 ml distilled water	

Osmium tetroxide, 1%

osmium tetroxide, 2% (Merck, Germany)	5.0 ml
veronal acetate buffer, pH 7.6	2.0 ml
hydrogen chloride 0.1 M (Merck, Germany)	2.0 ml
distilled water	1.0 ml
Saccharose (Merck, Germany)	0.45 g

Solution A

glycid ether 100 (Serva, Germany)	62 ml
2-dodecenyl succinicacid anhydride (Serva, Germany)	100 ml

Solution B

glycid ether 100 (Serva, Germany)	100 ml
methylnadic anhydride (Serva, Germany)	89 ml

Epon-embedding mixture

solution A	3.5 ml
solution B	6.5 ml
para-dimethyl aminomethyl phenol (Serva, Germany)	0.15 ml

Azur II/Safranin staining protocol for semithin sections

Azur II solution

Disodium tetraborate (Merck 6306, Germany)	1.0 g
Aqua dest.	100 ml
Azur II (Merck 9211, Germany)	1.0 g
37% Formaldehyde (Roth, Germany)	250 µl

Dissolve borate in aqua dest., then add Azur II and stir for approximately two hours before adding formaldehyde. Filter prior to use.

Safranin O solution

Disodium tetraborate (Merck 6306, Germany)	1.0 g
Aqua dest.	100 ml
Safranin O (Chroma 1B 463, Germany)	1.0 g
Saccharose (Merck, Germany)	40.0 g
37% Formaldehyde (Roth, Germany)	250 µl

Dissolve borate in aqua dest., then add Safranin and saccharose. Stir for approximately two hours before adding formaldehyde. Filter prior to use.Stain sections in Azur II solution for 15-20 seconds at 55°C on a heating plate (Meditel, Germany) and rinse with distilled water. Dry. Then stain sections for 15-20 seconds at 55°C on a heating plate (Meditel, Germany) and rinse with distilled water. Dry. Cover sections with glass coverslips (Menzel GmbH & Co KG, Germany) using Histofluid® (Superior, Germany).

3.5.1 Estimation of the mean glomerular volume

The mean glomerular volume was estimated, using a model-based method, as previously described in detail (Hirose et al. 1982, Wanke 1996, Weibel and Gomez 1962). In this model-based stereological approach, the glomeruli were considered as rotation ellipsoids. The mean glomerular area was obtained from planimetric measurements of glomerular profile areas. In the calculation, a shape coefficient and a size distribution coefficient were considered. The results were corrected for embedding shrinkage. The values for the shape and size distribution coefficient as well as for the shrinkage correction factor for plastic embedded murine renal tissue were taken from Wanke (1996). Morphometric evaluation was carried out on a Videoplan$^{®}$ image analysis system (Zeiss-Kontron, Germany) coupled to a light microscope (Orhoplan; Leitz, Germany) via a color video camera (CCTV WV-CD132E; Matsushita, Japan). Images of PAS stained GMA/MMA sections were displayed on a color monitor at a 400x final magnification. The profiles of all glomeruli present in the sections of one animal (mean 123 ± 25) were measured planimetrically by circling their contours with a cursor on the digitizing tablet of the image analysis system after calibration with an object micrometer (Zeiss, Germany). The mean glomerular volume was calculated using equation 1 (Hirose et al. 1982, Wanke 1996).

$$\hat{\overline{v}}_{(glom)(s)} = \frac{ß}{k} \cdot \overline{a}_{(glom)}^{1.5}$$

equation 1

$\hat{\overline{v}}_{(glom)(s)}$: stereologically estimated mean glomerular volume (referring to GMA/MMA embedded tissue)

$ß$: shape coefficient

k : size coefficient

$\overline{a}_{(glom)}$: arithmetic mean of areas of glomerular profiles

The stereologically estimated mean glomerular volume was calculated as the product of the mean glomerular area to the power of 1.5 and the shape coefficient (ß=1.40), divided by the size distribution coefficient (k=1.04) (Weibel 1980). Results were corrected for embedding shrinkage, using the linear tissue shrinkage correction factor (fs = 0.91) for murine kidney tissue embedded in GMA/MMA (Wanke 1996), using equation 2.

equation 2

$$\overline{V}_{(glom)} = \hat{\overline{V}}_{(glom)(s)} / f_s^{\,3}$$

$\hat{\overline{V}}_{(glom)}$: stereologically estimated mean glomerular volume (prior to embedding)

f_s : linear tissue shrinkage correction factor for murine kidney tissue embedded in GMA/MMA

3.5.2 Estimation of numbers of glomerular cells

The number of cells per glomerulus was estimated by applying the physical disector principle. The disector is a three dimensional stereologic probe, which allows unbiased and assumption free counting and sizing of particles (Sterio 1984). The physical disector, which consists of a pair of physical section planes separated by a known distance was used to estimate the numerical density of glomerular cells (C), subdivided into the respective glomerular cell types of podocytes (P) as well as mesangial (M) and endothelial (E) cells. In each case eight serial semithin sections (nominal thickness 0.5µm) of the Epon-embedded samples of cortical kidney tissue were cut with an Ultracut E microtome (Leica, Germany), mounted on glass slides and stained with Azur II/Safranin. Photographs of complete profiles of identical glomeruli, present in the centre of two semithin sections (reference section and look-up section; disector height:1.5µm), were taken at a magnification of x 630 using a Leica DFC 320 camera (Leica, Germany) connected to a microscope (Orthoplan, Leitz, Germany). At the beginning of each set, an object micrometer (Zeiss, Germany) was photographed under the same conditions for calibration. Prints of all pictures were made at a constant setting of the enlarger. Prints of pictures of 6 pairs of glomerular profiles from each animal (n=40) were analyzed. In these prints, the area of the glomerular cross-sections was measured using a Videoplan® image analysis system (Zeiss-Kontron, Germany). The areas of the glomerular profiles were measured planimetrically by circling their contours with a cursor on the digitizing tablet of the image analysis system after calibration. All nuclei of glomerular cells (subdivided into podocytes (P), endothelial (E) and mesangial (M) cells) sampled in the reference section, which were not present in the look-up section, were counted ($Q^-_{(C)}$, $Q^-_{(P)}$, $Q^-_{(E)}$, $Q^-_{(M)}$). The process of counting was then repeated by interchanging the roles of the reference and look-up section, thereby increasing the efficiency by a factor of two. Figures 3.11 and 3.12 illustrate the work-flow and the principle of counting of nuclei of glomerular cells for application of the disector method.

Stereological estimation of numbers of cells per glomerulus (disector principle)
Schematic work-flow

A Eight serial semithin sections (nominal thickness 0.5 μm)

| 1 | 2 | 3 | 4 | 5 | 6 | 7 | 8 |

EL 4292 / 1 (×8)

B Reference section   Look-up section

Measurement of areas of glomerular profiles
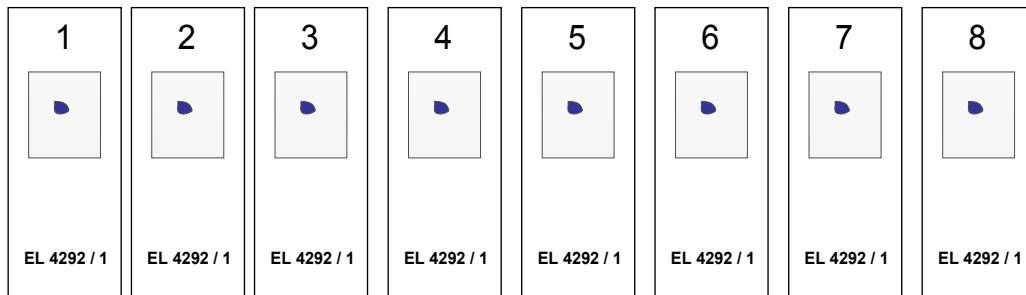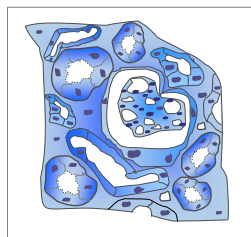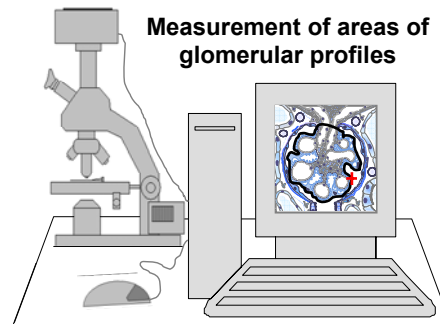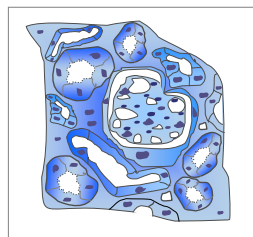
C Photography of the respective glomerular profiles in the primary and reference section

Reference section   Look-up section

◄P   ◄M   ◄P   ◄M

E►   P

10 μm   10 μm
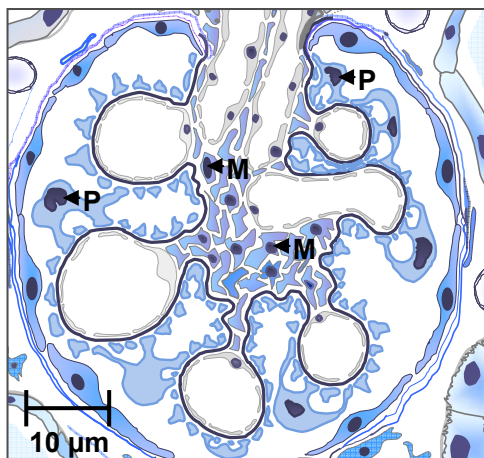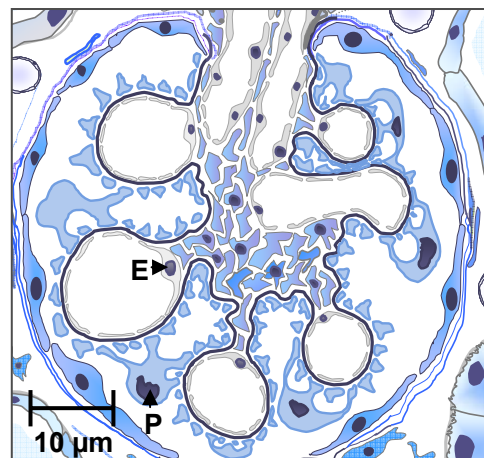
To increase the efficiency of the disector, separate counts are made in both directions, i.e. by first using one section of the physical disector as a reference section and the other as a look-up section and then swopping the roles played by the reference and look-up sections. (Q⁻): P: Podocyte nuclei; M: Nuclei of mesangial cells; E: Nuclei of endothelial cells.

Figure 3.11: Stereological estimation of numbers of cells per glomerulus (disector principle). Schematic work-flow. A: Two semithin sections of known distance (reference and look-up section; disector height h = 1.5 μm) with profiles of identical glomeruli. **B**: The total areas of cross sections of these identical glomeruli in the reference and look-up section are measured and used as disector area, i.e. no subsampling with an unbiased counting frame is performed. **C**: Counting of Q⁻ in photographies of these glomerular profiles.

Figure 3.12: Stereological estimation of numbers of cells per glomerulus (disector principle). Example for counting of Q⁻. Detail enlargements of a reference section (**A**) and a corresponding look-up section (**B**) from the periphery of an identical glomerulus of a NMRI wild-type mouse are shown. Disector height: 1.5 µm; semithin section (Epon); Azur II/Safranin staining; magnification: 630x; **U**: urinary space; **Cap.**: glomerular capillary; **P**: podocyte nucleus present in the reference section (arrow), which is absent in the look-up section. Nuclei present in both sections are indicated by identical symbols (♠,♣,♦).

Since a reliable differentiation of endothelial vs. mesangial nuclei would require electron microscopic pictures of high magnifications and since the subdivision of glomerular cell types into podocytes and non-podocyte glomerular cells was of main interest, the sum of endothelial and mesagial nuclei ($Q^-_{(E+M)}$) was used for further calculations. On the average, a number of 66 ±19 nuclei (Q^-) was counted per individuum. To determine the disector height, the nominal thickness of the sections was controlled, using a resectioning technique. Four sections, which were not used for sampling, were selected from different section series and vertically reembedded in Epon. In electron microscopic pictures (TEM, 32.000x), the thickness of sections was obtained by two-point distance measurement on a Videoplan® image analysis system after calibration. The measured mean thickness of the sections was 0.47 ± 0.02µm. A value of 0.5 µm was taken for calculations. The numerical density of glomerular cells was calculated using equation 3 (Sterio 1984).

$$\hat{N}_{V(C/glom)(s)} = \frac{\sum\limits_{i=1}^{n} Q(C)i}{h \cdot \sum\limits_{i=1}^{n} a(glom)i}$$

$\hat{N}_{V(C/glom)(s)}$: stereologically estimated numerical density of all cells (nuclei) C
(= podocytes, mesangial and endothelial cells) in the glomerulus
(referring to embedded tissue)

$Q(C)$: number of nuclei counted in disector i

h : distance between the primary and the reference section (disector height)

n : number of disectors analyzed per case

$a(glom)i$: area of the glomerular cross section i

Since calculation of numerical densities of glomerular cells is influenced by tissue shrinkage due to the embedding procedure, results were corrected for embedding shrinkage, using the linear tissue shrinkage correction factor (fs = 0.95) for murine kidney tissue embedded in Epon (equation 4). The number of the respective cell types per glomerulus was calculated as the product of their numerical volume density and the mean glomerular volume (equation 5) (Wanke 1996, Weibel 1979).

$$\hat{N}_{V(Y/glom)} = \hat{N}_{V(Y/glom)(s)} \cdot f_s^3$$

$\hat{N}_{V(Y/glom)}$: stereologically estimated numerical density of glomerular cells
(corrected for embedding shrinkage), all glomerular cell types, Y=C;
Podocytes, Y=P; endothelial and mesangial cells, Y=E+M

f_s : linear tissue shrinkage correction factor for murine kidney tissue
embedded in Epon

$$\hat{N}_{(Y,glom)} = \hat{N}_{V(Y/glom)} \cdot \hat{\bar{V}}_{(glom)}$$

$\hat{N}_{(Y,glom)}$: stereologically estimated number of cells per glomerulus
(all glomerular cell types, Y=C; Podocytes, Y=P;
endothelial and mesangial cells, Y=E+M

$\hat{\bar{V}}_{(glom)}$: stereologically estimated mean glomerular volume

3.5.3 Determination of the filtration slit frequency (FSF)

The filtration slit frequency (FSF) was determined using ultrathin sections of the identical samples used for estimation of the number of glomerular cells. Azur II/Safranin blue-stained sections of Epon embedded samples were surveyed, to locate patent glomeruli entirely within the block. Ultrastructural analysis was performed on six (5-7) glomerular profiles for each animal of both groups (GIPR[dn]-transgenic, bGH-transgenic, as well as the corresponding controls; each n=5) of stage II (stage of onset of albuminuria). Ultrathin sections (60 to 70 mm) of the glomeruli were cut with an Ultracut E microtome (Leica, Germany) mounted on uncoated copper grids (SSI, Science Services, Germany) and routinely contrasted with uranyl-acetate (Serva, Germany) and lead citrate (Serva, Germany) prior to examination (Reynolds 1963). Transmission electron microscopy (TEM) was performed using a Zeiss EM 10 electron microscope (Zeiss, Germany). Six to eight images of peripheral capillary loops from each of the glomerular profiles were photographed at 8000x magnification in a predetermined manner by whole turns of the stage handle (for details refer to chapter 9.1). For calibration, photographs of a standard cross-grating grid (S 107, TAAB; USA) with 2,160 lines/mm were taken with every set. For evaluation of the FSF, photographs were developed to a final print magnification of 22,500x. The FSF ($n_{(FS)}$/mm) was determined by counting the total number of epithelial filtration slits (figure 3.13) and dividing that value by the total length of the peripheral capillary wall at the epithelial interface (Jani et al. 2002, Remuzzi et al. 1995). The length of the peripheral capillary wall was measured using a Videoplan® image analysis system (Zeiss-Kontron, Germany). On the average 1,117±215 filtration slits were counted (range 689-1570) per animal.

P: podocyte
FP: foot process
FS: filtration slit
GBM: glomerular basement membrane
E: endothelial cell
U: urinary space

⊢ – ⊣ measured length of the peripheral capillary wall at the epithelial interface
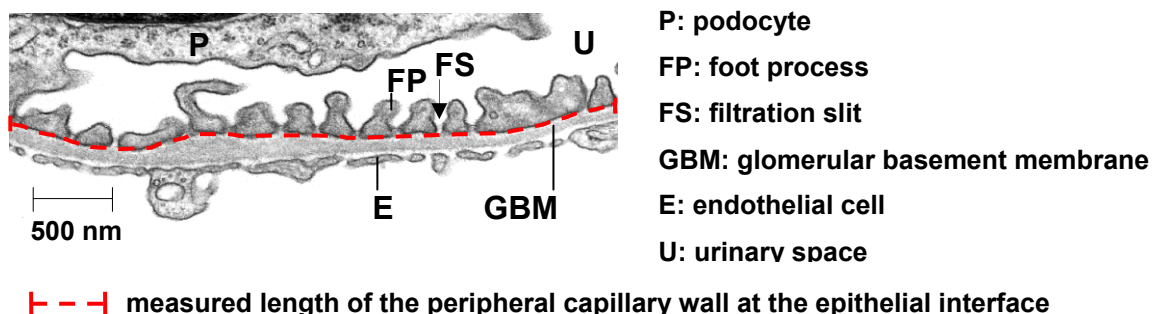
Figure 3.13: Determination of filtration slit frequency (TEM, 8000x). The number of filtration slits (twelve in this instance) per measured length of the peripheral capillary wall at the epithelial interface is determined.

3.5.4 Determination of the true harmonic mean thickness (Th) of the glomerular basement membrane (GBM)

In samples of animals assigned to stage II, the glomerular basement membrane (GBM) thickness was determined by the orthogonal intercept method (Dische 1992, Hirose et al. 1982, Jensen et al. 1979, Ramage et al. 2002). Pictures of transmission electron microscopic photographs, which had previously been examined for determination of the FSF, were developed to a final print magnification of 45,000x, covered by a transparent 2.5 x 2.5 cm grid. The shortest distance between the endothelial cytoplasmatic membrane and the outer lining of the lamina rara externa underneath the cytoplasmatic membrane of the epithelial foot processes was measured where gridlines transected the endothelial surface of the GBM. Measurements were made using a transparent logarithmic ruler provided by Ewald Freitag (Institute of Thermodynamics, TU Munich), generated according to the description by Ramage et al. (2002). In this ruler, 0.75 is used as a multiplier of the harmonic (inverse) value for each division, with calibration undertaken, when no measured areas of the GBM lay within the initial division (marked A on figure 3.14). Figure 3.15 demonstrates the use of the transparent ruler for measurement of the GBM thickness. The exact dimensions of the ruler (chapter 9.5.1), as well as a work example (chapter 9.5.2) are shown in the appendix. The apparent harmonic mean thickness was calculated, from which the true harmonic mean thickness (Th) was estimated.

Apparent harmonic mean thickness ($\bar{l}_h$), *mm*

$$\bar{l}_h = \frac{\sum(\text{N° of Observations})}{\sum(\text{Midpoints x N° of Observations})}$$

Harmonic mean thickness (T_h), *nm*

$$T_h = \frac{8}{3\pi} \times \frac{10^6}{\text{Magnification (M)}} \times \bar{l}_h$$

8/3 π (= 0.8488) is used as correction factor for oblique sectioning, M represents the final print magnification factor. On average 215 ± 42 intercepts per animal (range: 117-289) were measured.

Figure 3.14: Logarithmic ruler. "A" denotes the initial division in which no measurements of the glomerular basement membrane (GBM) can be contained. Numbers 1 through 11 are classes of ruler into which measurements are placed (according to Ramage et al. 2002).
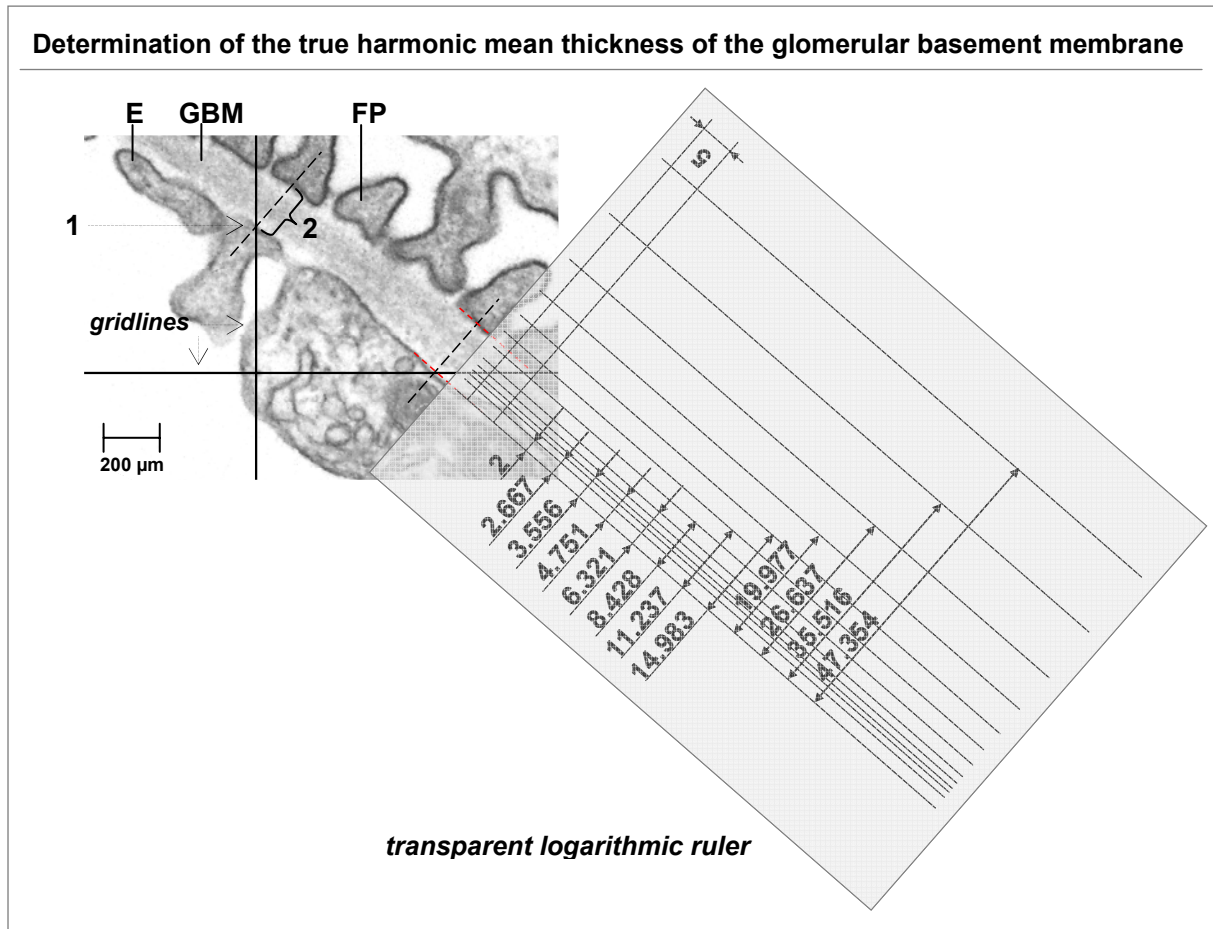
Figure 3.15: Determination of the true harmonic mean thickness (Th) of the GBM. Measurements are performed using prints of electron microscopic photographs. **E**: Endothelial cell. **GBM**: Glomerular basement membrane. **FP**: Podocyte foot process. **1**: Gridline (transparent 2.5 x 2.5 cm grid), transecting the endothelial surface of the GBM. **2**: Measurement of the shortest distance between the attachment of the endothelial cytoplasmatic membrane to the outer lining of the lamina rara externa underneath the cytoplasmatic membrane of the epithelial foot process, using a transparent logarithmic ruler. The ruler is laid over the electron micrograph and the GBM-width is read off at right angles in terms of "classes" (class 6 in this instance).

3.6 Microarray analyses of samples of isolated glomeruli

3.6.1 Work-flow of microarray analysis

Microarray analysis was performed on 40 samples of isolated glomeruli of the "array-Cohort" (AC) (= each 5 samples derived from GIPR[dn]-, respectively bGH-transgenic animals and 5 samples of the corresponding non transgenic wild-type littermate controls per stage of investigation), each consisting of approximately 1000 purified glomeruli, concentrated in RNA-later® RNA stabilization reagent. The basic work-flow of the array experiment is illustrated in figure 3.16. First, total RNA was extracted from the glomerular samples (chapter 3.6.2), yield, purity and quality of isolated RNA were controlled using a microfluid electrophoresis technology (chapter 3.6.3). Identical amounts of high quality RNA were then reverse transcribed into cDNA, amplified, fragmented and labelled with biotin (chapter 3.6.4). After target preparation for GeneChip® Analysis, each sample was hybridised to a GeneChip® Mouse Genome 430 2.0 Array (Affymetrix, USA). Then the arrays were washed, subsequently stained with phycoerythrin-conjugated streptavidin (SAPE) and washed again. The fluorescent intensity emitted by the labelled targets was measured by an Affymetrix GeneChip Scanner. Scanned hybridization images were translated into so-called ".CEL files" (Affymetrix© Microarray Suite version 5.0.1). Each .CEL-file contains the average signal intensity of all pixels of every single feature of probes on an Affymetrix © GeneChip Array. After scanning of the chips the efficiency of hybridisation, as well as the quality of hybridized targets was evaluated. For identification of differentially expressed transcrips in samples derived from transgenic animals, compared to those of the respective control cohort, .CEL file data were analyzed using the Genomatix® ChipInspector® 1.2 software (Genomatix®, Germany) (chapter 3.7.2). Measurements of RNA (respectively cDNA) quantity and quality, RNA amplification and biotin labelling for preparation of cDNA for gene expression analysis and the array experiments (target preparation, hybridisation and scan of chips) were performed by the University of Michigan Comprehensive Cancer Center (UMCCC) Affymetrix and Microarray Core Facility, Cancer Centre, University of Michigan, Ann Arbor, Michigan, USA, according to the manufacturer's instructions, as described in the respective protocols.

Workflow of microarray experiment

A RNA Extraction from each 1000 isolated glomeruli per sample, concentrated in RNA-later®
(RNeasy® Kit, Qiagen)

B Reverse transcription of mRNA, amplification, fragmentation and biotin labeling of cDNA
(Ovation™, NuGen)

C RNA and cDNA quantity and quality analyses
(Agilent Bioanalyzer®)

total RNA *cDNA* *fragmented cDNA*

D Hybridisation to probes on array, detection and quantitation of signal intensity
(GeneChip® Mouse Genome 430 2.0 Array, Affymetrix)

oligonucleotide probes *hybridisation* *washing and staining*

GeneChip® Expression Array *scanning and quantitation*

1.25 cm

E Microarray analysis
(ChipInspector® 1.2)
→ **identification of differentially expressed transcripts**

F Bioinformatical analysis
(BiblioSphere®, Genomatix®; Ingenuity PA®)

Figure 3.16: Workflow of microarray experiment. A: Total RNA was isolated from each sample of isolated glomeruli. Quality and quantity of total RNA were controlled (**C**). **B**: From the total RNA, mRNA was reverse transcribed (RT) into cDNA, amplificated, fragmented and biotynilated (-B) **C**: Again, quantity and integrity of cDNA and fragmented cDNA were controlled **D**: The fragmented and biotynilated cDNA was hybridized to Affymetrix© Mouse GeneChip© Arrays. **E**, **F**: Hybridisation results were statistically analyzed in order to identify differentially expressed transcripts. Bioinformatical analysis was performed, using software tools as BiblioSphere© (Genomatix©) and Ingenuity Pathway analysis©.

3.6.2 RNA preparation

Total RNA was isolated from the glomerular samples (each ~1000 isolated glomeruli per sample/animal) using a commercially available silica-gel based isolation protocol (RNeasy Mini Kit, Qiagen, USA) including an on-column DNAse digestion. Additionally, two samples of total RNA lysates were generated from freshly dissected snap frozen (liquid nitrogen) cortical kidney tissue of a male wild-type mouse as a "total renal cortex control" to glomerular samples. For RNA-isolation, a modified version of the "RNeasy Mini Protocol for isolation of total RNA from animal tissues" was used. All steps were performed at room temperature (20-25°C). In order to avoid losses of sample material during the first steps of the RNA-isolation process, disruption and homogenisation of glomeruli was performed inside the 2ml cup containing the 50 µm mini cell strainer with approximately 1000 isolated glomeruli, concentrated in 30 µl RNA-later$^®$ RNA stabilization reagent. Therefore 350 µl of buffer RLT were added and incubated for 30 minutes on a shaker (Thermomixer R, Eppendorf, USA) running at maximum speed. Afterwards 350 µl of 70% ethanol were added to the lysate and mixed by pipetting. The sample was then applied to an RNeasy mini spin column placed in a 2 ml collection tube; the tube was closed gently and centrifuged for 30 sec at ≥8000 x g (Sigma 1 K 15, Sigma, Germany). The flow-through was discarded. 350 µl Buffer RW1 were pipetted into RNeasy mini spin column and centrifuged for 30 sec at ≥8000 x g. The flow-through was discarded. For the on-column DNAse digestion, the RNase-free DNAse set (Qiagen, USA) was used. DNAse I stock solution was prepared by adding 550 µl of RNAse-free water to the solid DNAse I (1500 Kunitz units) and gentle mixing. Per sample 80 µl of DNase I incubation mix were prepared by adding 10 µl of DNAse I stock solution to 70 µl buffer RDD and gentle mixing. The DNase I incubation mix was pipetted directly onto the RNeasy silica gel membrane and placed on the benchtop for 15 minutes. Then 350 µl Buffer RW1 were pipetted into RNeasy mini spin column and centrifuged for 30 sec at ≥8000 x g. The flow-through and the collection tube were discarded. The RNeasy mini spin column was transferred into a new 2 ml collection tube. 500 µl buffer RPE were added onto the RNeasy mini spin column; the tube was closed gently and centrifuged for 30 sec at ≥8000 x g to wash the column. The flow-through was discarded. Another 500 µl buffer RPE were added onto the RNeasy mini spin column; the tube was closed gently and centrifuged for 2 minutes at ≥8000 x g to dry the RNeasy silica gel membrane. The flow-through and the collection tube were discarded.

The RNeasy mini spin column was placed into a new 2 ml collection tube and centrifuged for 1 minute at full speed. The flow-through and the collection tube were discarded. For elution of total RNA, the RNeasy mini spin column was then placed into a 1.5 ml collection tube, 40 µl of RNAse-free water were pipetted directly onto the RNeasy silica gel membrane. The tube was closed gently, placed on the benchtop for 1 minute and then centrifuged for 1 minute at ≥8000 x g to elute the RNA. To increase the RNA yield, the elution step was repeated by adding the first eluate directly onto the RNeasy silica gel membrane. The tube was closed gently, placed on the benchtop for 2 minutes, and then centrifuged for 2 minutes at ≥8000 x g. Afterwards the RNA was immediately stored at -80°C until further investigation. Additionally to the Kits contents the following reagents and equipments are used: 14.3 M beta-mercaptoethanol (beta-ME, Sigma Aldrich, USA), RNAse-free pipette tips, sterile (Fisher Scientific, USA), Ethanol 96-100% (Sigma Aldrich, USA), and Ethanol 70%.

3.6.3 Determination of quantity and quality of isolated total RNA by microfluid electrophoresis

For determination of RNA quantity and quality, an aliquot (1 µl) of each of the respective RNA-samples was diluted (1:1-1:5) with RNAse-free water (Qiagen, USA). Until investigation specimens were stored at -80°C. RNA quantity and quality was controlled by microfluid electrophoresis using the RNA 6000 Pico LabChip® (Agilent Technologies, USA) on a 2100 Bioanalyzer (Agilent Technologies, USA), according to the manufactorer's instructions. The Agilent Bioanalyzer system performs electrophoretic separation of total RNA by means of a microfluidic system (Mueller et al. 2000). It utilizes a network of microfluid electrophoresis channels and wells that are etched onto polymer chips (figure 3.17). Sample components are electrophoretically separated and each of their absorbances at 260 nm (and 280 nm) at a certain time is detected by a spectrophotometer. Readings are translated into gel-like images (bands) and electropherograms (peaks), as illustrated in figure 3.18.

Figure 3.17: **Mcrofluid electrophoresis chip**
(RNA 6000 Pico LabChip®, Agilent Technologies, USA)

RNA Concentration: 21.876 pg/µl

rRNA Ratio [28S/18S]:   1.8
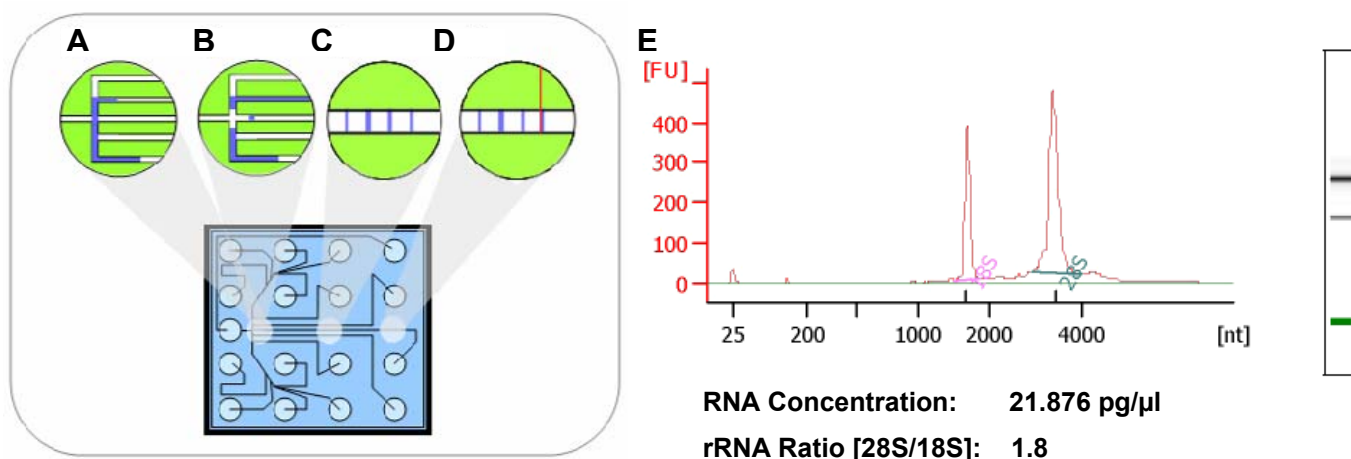
Figure 3.18: Principle of measurement of RNA quality and quantity by microfluid electrophoresis (RNA 6000 Pico LabChip® on a 2100 Bioanalyzer, Agilent Technologies, USA)

A: The sample moves through the microchannels from the sample well.

B: The sample is injected into the separation channel.

C: Sample components are electrophoretically separated.

D: Components are detected by their fluorescence.

E: Graphical output of results: measured values are translated into gel-like images (bands) and electropherograms (peaks). Example shows results of total RNA measurement of a sample of isolated RNA from a glomerulus isolate of a bGH-transgenic animal. The high quality of RNA is confirmed by circumscribed ribosomal peaks in the electrophoresis read-out, with no additional signals below the ribosomal bands and no shift to shorter fragments.

3.6.4 Preparation of amplified, biotin-labeled cDNA from total RNA

Amplified, biotin-labelled cDNA for gene expression analysis was prepared from each 75 ng of glomerular total RNA in 5 µl of RNase-free water (Qiagen, USA) per sample, using the Ovation™ Biotin-RNA Amplification and Labeling System (NuGen Inc., USA), according to the manufacturers instructions. A schematic description of the single steps of the procedure is illustrated in chapter 9.6. Amplified cDNA was purified using DyeEx columns (QIAGEN, USA). The amplified SPIA™ cDNA product was purified prior to fragmentation and biotin-labeling, using the NucleoSpin® Extract Kit (Clontech Laboratories, USA), according to the manufacturer's instructions. cDNA product yield and purity was measured, using the Agilent 2100 Bioanalyzer® and RNA 6000 Nano LabChip® (Agilent Technologies, USA). For quality control of the amplified, fragmented cDNA product, ~100 ng of each sample of fragmented/biotinylated cDNA were analyzed on an RNA 6000 Nano LabChip® (Agilent Technologies, USA). The fragmented, biotin labeled product was used immediately after preparation.

3.6.5.1 DNA microarray experiments

DNA microarray experiments (hybridization, washing and scanning of arrays) were performed by the UMCCC (University of Michigan Comprehensive Cancer Center, Affymetrix and Microarray Core Facility, Cancer Centre, University of Michigan, Ann Arbor, Michigan, USA), using the GeneChip® Mouse Genome 430 2.0 Array (Affymetrix, USA; see figure 3.16 in chapter 3.6.1). The Affymetrix pan genomic mouse arrays, used in the experiments of the present study contain probes, covering the entire transcribed mouse genome on a single array. The array area of a Mouse Genome 430 2.0 Array GeneChip® is ~1.6 cm^2 in size. It contains 1.6 millions of features, each with a size of eleven μm in diameter. 45,000 probe sets are present on this chip, used to analyze the expression level of over 39,000 transcripts and variants from over 34,000 well characterized mouse genes. The probe sets were selected from sequences derived from multiple databases in the public domain (GenBank®, dbEST, and RefSeq). The sequence clusters were created from the UniGene database (June 2002) and then refined by analysis and comparison with the publicly available draft assembly of the mouse genome from the Whitehead Institute Center for Genome Research (MSCG, April 2002). All experiments were performed, using arrays of the identical production lot number. 10 μg of prepared target cDNA were hybridized to each array. Hybridization, washing and scanning of chips were performed according to the Affymetrix GeneChip® Expression Analysis Technical Manual (revision 4).

3.6.5.2 Quality controls of microarrays and cluster analyses

Each processed microarray was controlled for any material or technical defects. Before normalization and for verification of the quality of each experiment itself, a "density plot" and a "degradation plot" were generated (Affymetrix© Microarray Suite version 5.0.1). The Density plot (refer to chapter 4.3.2.1) is used to visualize differences in the distribution of the arrays. It shows the density of the probe match intensity for each chip (each line corresponds to an individual array). These should be positively skewed (long right tail) and similar to each other in a sample set. The RNA digestion plot (refer to chapter 4.3.2.1) was generated by calculating and plotting the array-wide mean intensities of ordered probe match probe sets, where the position 0 corresponds to the most 5' probe and position 10 the most 3' probe. In a RNA sample degradation of mRNAs by RNAses preferably starts at the 5' site of large mRNA molecules of high abundance.

Thus, the described processing of a single, partially degraded mRNA will result in a lower number of biotinylated cDNA fragments derived from the 5' region than from the 3' region. Array hybridization of these cDNAs will then result in the detection of lower hybridization signal intensities at features containing probes complementary to cDNA fragments representing the 5' regions of the target molecule. Cluster dendrograms and the principal component analysis (PCA) plot were generated after normalisation of .CEL files data. Normalization of .CEL files was performed using the RMAExpress (Robust Multichip Average) software (Irizarry et al. 2003). For identification of expressed glomerular genes, a "cut-off value" was defined, using the expression values of internal Affymetrix control probe sets. All probe sets that displayed expression values below this cut-off in all samples were discarded. These data were then used for generation of Cluster dendrograms, the PCA plot, as well as for performance of the Monte Carlo simulations (refer to chapter 3.7.4). Principal component analysis (refer to chapter 4.3.2.2) is commonly used as a cluster tool in microarray research. It is designed to capture the variance in a dataset in terms of principle components. Samples are expected to cluster into treatment groups and/or sample source. Unbiased cluster dendrograms, using Ward's minimum variance were generated from expression data of each 45101 genes (refer to chapter 4.3.2.2), using the RACE analysis tools (Remote Analysis Computation for gene Expression data, DNA Array Facility, Faculté de biologie et de medicine, Lausanne, Switzerland).

3.7 Statistical analysis of microarray data

3.7.1 Nomenclature of "differentially expressed transcripts" and "genes"

In the present study, the terms "differentially abundant transcript" and "differentially expressed transcript" are used synonymously for description of each single transcript that is displaying a statistically significant difference of its measured relative abundance in the respective groups of samples that were compared to each other (tg vs. wt). Each of these differentially expressed transcripts is identifiable through a unique accession number. The number of single transcripts found to be differentially expressed in the performed experiments partially reached the limits of capacity for performance of calculations.

To reduce the intricacy of generated datasets, all differentially expressed transcripts derived from a common single gene, were summarized together and assigned to the identifier (Entrez Gene ID) of that respective gene (table 4.7, chapter 4.3.3.1). None of the different differentially expressed transcripts derived from a common single gene displayed a different direction of regulation in the compared groups of the experiment. The indicated numbers of "differentially and commonly differentially expressed genes" in figure 4.17 (chapter 4.3.3) refer to the numbers of gene-IDs of single genes, whose respective transcripts displayed a differential expression of congeneric direction in the experiment. So far the term "(commonly) differentially expressed gene" is used to describe the entirety of all transcripts of a single gene that displayed a congeneric differential abundance in the investigated samples.

3.7.2 Identification of differentially expressed transcripts (tg vs. wt)

Transcripts, displaying a statistically significant differential abundance in the samples derived from transgenic animals (tg), compared to the corresponding samples derived from non transgenic wild-type littermate controls (wt) were identified in both groups (GIPR^{dn} and bGH) in each stage of investigation (stage I and stage II), using the ChipInspector 1.2 software (Genomatix$^{©}$, Germany) for statistical analysis of the microarray .CEL file data. This approach uses the availability of all probe sequences descriptions and annotations, including PM probes as well as MM probes present on the Affymetrix arrays for an analysis of microarray raw data different from the original "probe-set" approach by Affymetrix$^{©}$. The microarray raw data of each single group and stage of investigation (stage I: GIPR^{dn}-tg vs. -wt; stage I: bGH-tg vs. -wt; stage II: GIPR^{dn}-tg vs. -wt and stage II: bGH-tg vs. -wt) were uploaded into the software and subsequently analyzed. For data analysis, ChipInspector evaluates expression levels of single probes derived from Affymetrix CEL-files. Previous annotations of the single oligonucleotide probes by Affymetrix were disregarded, together with the grouping of the probes in probe sets. Probes were assigned correctly to transcripts by mapping the sequence of each single probe against the current genome annotation of the target organism (mus musculus) (National Center for Biotechnology Information [NCBI]) and against ElDorado, Genomatix$^{®}$' database of transcripts. Only probes that met quality criteria such as uniqueness in the genome, mismatch proof and other criteria were used for the analysis. For the Affymetrix GeneChip® Mouse Genome 430 2.0 Array, 426,824 probes, representing 90,827 annotated transcripts, fulfil these quality criteria.

Statistical analysis was carried out after calculating the base 2 logarithm of the fold-changes (ratios of the single probe signals) between corresponding probes in samples derived from transgenic mice and their associated wt-controls in the respective groups and stages of investigation. For normalization, a linear total-intensity normalization algorithm was used. Significant probes were discovered by a standard single sided permutation T-test analysis with false discovery rate (FDR) calculation, performed at the single probe level, using the significance analysis of microarray (SAM) algorithm (Tusher et al. 2001). The probes determined to be significantly regulated in the experiment were subsequently matched with the transcripts that they describe and the coverage of regulated probes was calculated for each of these transcripts. As default value, three significant probes were reqired to detect a transcript as being significantly regulated in the experiment. Analyses were performed, applying settings of analysis parameters as specified in table 3.4. An FDR of < 0.049% was chosen in the statistical analysis. The respective statistics curves (shown in figure 4.16, chapter 4.3.3.1) display the results of the performed statistical analyses as a plot of the observed expression ratio over an artificial background based on randomized expression ratios (expected ratio) for each perfect match probe. The diagonal line passing through the origin represents observed ratio = expected ratio; two more lines represent observed ratio = expected ratio + Delta (+) and observed ratio = expected ratio + Delta (-). Delta (+/-) are threshold values; the change in the expression of a single probe (feature) is considered significant if observed ratio > expected ratio + Delta (+) (up-regulated features), or, if observed ratio < expected ratio + Delta (-) (down-regulated features). The FDR is estimated for a given delta by dividing the average number of features that are called significant in the background data (falsely called features) by the number of significant features resulting from the experimental assignment. Delta values were adjusted manually in order to adjust the FDR. The lists of regulated features (or transcripts) including the respective (mean) expression ratio logs were then saved in a MS Excel format for further calculations and for export in pathway mapping softwares. Congeneric differentially expressed transcripts of a single gene were assigned to their corresponding Entrez gene ID.

Settings of analysis parameters	Group			
	GIPR^{dn} stage I tg vs. wt	bGH stage I tg vs. wt	GIPR^{dn} stage II tg vs. wt	bGH stage II tg vs. wt
chosen Delta value for up-regulation	1.685	1.637	1,698	2.239
False Discovery Rate (up-regulation)	< 0.049%	< 0.049%	< 0.049%	< 0.049%
chosen Delta value for down-regulation	-1.622	-1.551	-1.710	-2.228
False Discovery Rate (down-regulation)	< 0.049%	< 0.049%	< 0.049%	< 0.049%
Treatment/Control pairing; number of unique single probes: 35081; random seed: 2359				

Table 3.4: Significance analysis of microarray data: settings of analysis parameters

3.7.3 Identification of commonly differentially expressed genes

3.7.3.1 Identification of commonly differentially expressed genes in the single stages of investigation

In both stages of investigation (stage I and stage II) the lists of differentially expressed transcripts (summarized under their respective Entrez gene ID, = genes; see above) between samples derived from transgenic and their corresponding wt-control mice of the GIPR^{dn}-group and the bGH-group were compared for identification of commonly differentially expressed genes, as illustrated in figure 4.17. Therefore, the respective lists of differentially expressed genes and their mean expression ratio logs were compared (MS Excel) and genes displaying a congeneric differential expression in both groups (identical annotation and direction of regulation) of one stage (intrastadial comparison: differentially expressed genes GIPR^{dn} stage I vs. bGH stage I and differentially expressed genes GIPR^{dn} stage II vs. bGH stage II) were identified. The mean expression ratio logs for these commonly differentially expressed genes were calculated as the artithmetic mean of the respective mean expression ratio logs that the commonly differentially expressed genes displayed in the respective groups (wt vs. tg). Functional annotation of these genes was performed on a computer, using the publicly available NCBI database (National Center for Biotechnology Information), the BiblioSphere Pathway Edition software (Genomatix®, Germany) and the Ingenuity Pathways Analysis 5.0 software (IPA, Ingenuity® Systems, USA).

3.7.3.2 Identification of commonly differentially expressed genes in both stages of investigation

Genes that displayed a congeneric differential expression in all groups and stages (inter- and intrastadial comparison: [commonly differentially expressed genes in the GIPR^{dn}- and bGH-group of stage I] vs. [commonly differentially expressed genes in GIPR^{dn}- and bGH-group of stage II]) and their corresponding mean expression ratio logs were identified in an analogous manner (figure 4.17).

3.7.4 Estimation of statistical enrichment of the numbers of commonly differentially expressed genes by Monte Carlo simulation

In order to estimate if the numbers of commonly differentially expressed genes resulting from the comparison of differentially expressed transcripts (tg vs. wt) in the respective groups and stages of investigation, displayed a significant statistical enrichment between these groups, a mathematical method of statistical sampling called "Monte Carlo simulation" was performed (Robert and Casella 2004). This statistical approach is applied to estimate the likelihood with that a certain number of identical values can be found within two independent and different sized lists of values, under purely randomly conditions. Thus, this approach does not regard any of the molecular functions of the respective transcripts/genes, nor their potential biological significance. Here, performance of Monte Carlo simulations basically provides the information, if a given number of commonly differentially expressed genes, derived from the comparison of two different sized groups of differentially expressed genes is likely to be just the result of coincidence or not. The numbers of differentially expressed glomerular genes (tg vs. wt) were both detected using the identical settings of parameters in the significance analysis of microarray data. Thus, the numbers of differentially expressed genes (each distinctively identifiable by its corresponding EntrezGene ID) in these two different groups both derive from the total number of expressed glomerular genes in the respective samples, which was determined to be approximately 26,000 (after normalisation, averagely 26,000 probe-sets on the arrays displayed detected hybridisation signal intensities above the cut-off threshold). The program, which was especially designed for the application of Monte Carlo simulations in this study, was programmed by Timothy Wiggin, Dept. of Neurology, University of Michigan, Ann Arbor, USA.

The program each generates a number of unique random numbers, equal to the number of observed differentially expressed genes in both groups to be compared, ranging from 1 to 26,000 and compares these numbers to each other. The number of identical unique random numbers found present in both groups of random numbers is detected by the program and saved. This operation is repeated for 10,000 times. The arithmetic mean, as well as the standard deviation of these 10,000 values is then calculated. The average number of identical unique random numbers found present in both groups, as well as the standard deviation of values can be regarded as the result to be expected under purely randomly conditions, displaying a normal distribution of single values. The probability of observing a distinct single value (observed number of commonly differentially expressed genes) within this distribution is calculated, using a Z-Test (left-tailed statistical test for population mean; MS Excel function "Normdist-true"). This probability is indicated by a p-value. P-values < 0.05 were considered statistically significant. Monte Carlo simulations were performed for the estimation of probabilities of observing the respective numbers of commonly differentially expressed genes in stage I and II, as well as the numbers of commonly differentially expressed genes resulting from the interstadial comparison. A calculation example illustrating the performance of the Monte Carlo is provided in the appendix (chapter 9.8).

3.8 Cluster analyses

Common differential gene expression profiles of wt-/tg-pairs of animals were clustered using a euclidian distance metric hierarchical clustering software tool (MultiExperiment Viewer 4.0 software). Average linkage clustering (Eisen et al. 1998) was performed to cluster the samples and the expression ratios of commonly differentially expressed transcripts in both stages of investigation.

3.9.1 Confirmation of array data by quantitative real-time PCR

To confirm the common differential expression of selected transcripts detected in the array experiment, real-time PCR was performed on cDNA samples obtained through reverse transcription of total RNA of samples of glomerulus isolates from animals of the Array Cohort and the Independent Control Cohort. Numbers of animals/samples investigated in the real-time PCR confirmation experiments are indicated in table 3.5.

Numbers of samples investigated in the real-time PCR confirmation experiments					
Group / stage	**Array cohort**		**Independent control cohort**		
	wt	**tg**	**wt**	**tg**	**littermate pairs**
GIPR^{dn} stage I	4	4	5	5	4
GIPR^{dn} stage II	5	5	7	7	5
bGH stage I	5	5	5	5	4
bGH stage II	5	5	8	8	5

Table 3.5: tg: transgenic animal; **wt**: corresponding non-transgenic wild-type control. The numbers of littermate pairs in the Independent Control Cohort are indicated.

3.9.2 Reverse transcription of RNA into cDNA

Approximately 100 ng (where available) of each sample of total RNA were reverse transcribed (RT+) in a 40 µl volume, containing 8 µl first strand buffer (5x), 2 µl 100 mM DTT (both Invitrogen, USA), 0.8 µl 25 mM dNTP (Amersham Pharmacia, USA), 1 µl ribonuclease inhibitor (RNasin, Promega, USA), 0.5 µl linear acrylamid (15 µg/ml; Ambion, USA), 0.43 µl random hexamers (Hexanucleotide Mix, 10x conc., Roche, USA) and 0.86 µl reverse transcriptase (Superscript, 200 U/µl, Invitrogen, USA) for 1 hour at 42 °C. Resulting cDNAs (RT+) were then diluted 1:10 in TRIS-EDTA buffer [10 mM Tris-HCl, 1 mM EDTA, pH 8.0]. For genomic DNA-contamination control (RT-), the same reaction was applied, using 10 ng of total RNA, but without addition of reverse transcriptase. All samples were stored at -20°C until further investigation.

3.9.3 Performance of real-time PCR

Real time PCR was performed on a 7900HT Fast Real-Time PCR System with Fast 96-Well Block Module TaqMan ABI 7900 Sequence Detection System® (Applied Biosystems, USA) and SDS Software v2.2.2. Expression of 5 selected transcripts was analyzed, using predesigned gene-specific TaqMan Gene Expression Assays (Applied Biosystems, USA), as summarized in table 3.6. Each assay consists of two unlabeled PCR primers (final concentration of 900 nM each) and a TaqMan MGB (minor groove binder) probe (final concentration of 250 nM) with a reporter dye (6-FAM, 6-carboxy-fluorescein) linked to the 5´ end and a nonfluorescent quencher (NFQ) at the 3´ end of the probe. Detection of specific amplification of target cDNA is achieved by using probes that cross exon-exon junctions of the respective target

sequences and therefore will not detect genomic DNA. Using non fluorescent quenchers reduces background noise signals and allows for a more accurate measurement of reporter dye contributions. The use of MGB probes (dihydropyrroloindole-tripeptides conjugated to the probe), allows for the design of shorter probes, as MGBs increase the melting temperature without increasing probe length (Afonina et al. 1997, Kutyavin et al. 1997).

For each sample and run, 2 µl of the suspended cDNA (RT+, diluted 1:10 in TE buffer) were mixed with 10 µl of the TaqMan Fast Universal PCR Master Mix (2x), No AmpErase® UNG (which contains the hot-start AmpliTaq Gold® DNA Polymerase system, deoxyribonucleotides, $MgCl_2$, and buffers; Applied Biosystems, USA; storage at 4-8°C), 7 µl of H_2O and 1 µl of the respective TaqMan Gene Expression Assay (storage at -20°C). Each 10 µl were transferred into two wells of an ABI PRISM 96-well optical reaction plate (Applied Biosystems, USA). Components were kept on ice during the procedure. Samples consisting of distilled H_2O served as negative controls; samples, in which distilled H_2O was used instead of the cDNA template served as no template controls (NTC). Next to Cyclophyllin A, also 18S rRNA and Gapdh served as housekeeping (internal reference) transcripts. The probe of the predesigned gene-specific TaqMan Gene Expression Assay for detection of 18S rRNA expression (accession number: X03205) was labeled with VIC® reporter dye and TAMRA (6-carboxy-tetramethylrhodamine) quencher dye. Single primers and FAM-labelled probes (AppliedBiosystems, USA) were used for real-time PCR detection of Gapdh expression (accession number: M32599). As these primers do not cross exon-exon junctions of the Gapdh target sequence, the genomic DNA-contamination control (RT-) samples were run in parallel with the cDNA (RT+) samples and the no template controls. For each sample and run, 2 µl of the suspended cDNA (RT+) or the respective genomic DNA-contamination control (RT-) were mixed with 10 µl of the TaqMan Fast Universal PCR Master Mix (2x), 6.4 µl of H_2O, 0.4 µl probe and each 0.6 µl of the forward and the reverse primer (each 10 pM) and transferred into two wells of the optical reaction plate as described above.

To confirm the effectiveness of tissue separation in investigated glomerulus isolates, real-time PCR was performed for detection of nephron specific gene expression patterns, using Wilm's tumor antigen 1, a marker for podocytes. The WT-1/Gapdh ratios of glomerular specimens (Cohen et al. 2002, Cohen and Kretzler 2003) and samples of total cortical kidney tissue were compared to confirm the enrichment of podocytes in samples of isolated glomeruli.

Assay ID	Gene Symbol	Gene Name
Mm00445880_m1	**Fabp4**	Fatty acid binding protein 4, adipocyte
Mm00514455_m1	**Ctsh**	Cathepsin H
Mm00446214_m1	**Msr1**	Macrophage scavenger receptor 1
Mm00436454_m1	**Cx3cl1**	Chemokine (C-X3-C motif) ligand 1
Mm01277159_m1	**Cd44**	CD44 antigen
Custom TaqMan® GEA	**WT1**	Wilm's Tumor 1 (acession N°: M55512)
Custom TaqMan® GEA	**PPIA**	Cyclophyllin A (acession N°: NM_008907)

Table 3.6: TaqMan real-time PCR Gene Expression Assays (GEA, Applied Biosystems, USA).

All measurements were performed in duplicates. If possible, all samples belonging to the respective groups to be compared (wt vs. tg) were run on identical plates. The reaction plates were covered with ABI PRISM optical adhesive covers (Applied Biosystems, USA) and centrifuged for 5 seconds at 1000 rpm (Kendro® SORVALL® Legend™ T EASYset™, USA). Prepared plates were then inserted into the Fast 96-Well Block Module of the real-time PCR instrument and runs were performed in the fast mode: after an initial hold of 20 seconds at 95°C, the samples were cycled 40 times at 95°C for 1 sec and 60°C for 20 sec. Negative controls, no template controls and genomic DNA-contamination controls (RT-) were negative in all runs. For comparison of expression levels, relative quantification of results was performed, using the ΔC_T method (Cohen and Kretzler 2003). For all runs to be compared, identical threshold lines were manually set in the exponential phase of the amplification. For each sample, the expression abundance of each target transcript, relative to the expression of the housekeeping transcript was calculated: The mean C_T (= threshold cycle) was calculated from the duplicate measurements of each sample, both for the target transcript, as well as for the housekeeping transcript. By subtraction of the mean C_T value of the target transcript from the mean C_T value of the housekeeping transcript of the respective sample, the respective ΔC_T value was calculated as: ΔC_T = mean C_T (housekeeping transcript) - mean C_T (target transcript). Assuming a comparable amplification efficiency of the primers of the housekeeping and target sequences, copies of the individual target transcript were defined as $2^{mean\Delta C_T}$ copies of housekeeper transcripts. For the respective groups, the means of $2^{mean\Delta C_T}$ values of all samples were calculated and compared (tg vs. wt), using a two sided paired Student's t-test.

For confirmation of common differential expression of transcripts (detected in the array experiments) in samples derived from transgenic animals of all investigated stages and groups, real-time PCR experiments were performed as match pairs analyses, by simultaneously comparing all samples of transgenic animals with their associated controls (refer to chapter 4.3.6). A calculation example is given in the appendix (chapter 9.7).

3.10 Bioinformatical analyses

Bioinformatical analyses were performed in order to gain advanced inside views into the biological and molecular functions, cellular distributions and potential interactions of glomerular transcripts/genes (their deduced proteins, respectively) that displayed a detected congeneric common differential abundance between samples of transgenic animals and their corresponding controls in both investigated groups in stage I or in stage II, as well as in both stages. Functional annotation of these genes and bioinformatical analyses were performed, using the publicly available NCBI database (National Center for Biotechnology Information), the BiblioSphere Pathway Edition software (Genomatix®, Germany) and the Ingenuity Pathways Analysis 5.0 software (IPA, Ingenuity® Systems, USA), as well as by searching publicly available literature databases (pubmed, NCBI) and EST (expressed sequence tag) expression profile (NCBI) databases. These analyses were performed with particular regard to any documented association of these genes and gene products to processes and pathways involved in development or appearance of nephropathies or glomerulopathies.

3.11 Statistical analysis and data presentation

As an essential feature of the experimental design of the present study, sample materials were generated from pairs of animals and also analyzed pairwise. In the respective groups and stages of investigation, means of values were compared (tg vs. wt) by a two-tailed paired Student's t-test (MS Excel, Microsoft®, USA). P values < 0.05 were considered significant. Throughout the study, data are presented as means and standard error of means (SEM) or standard deviations (SD), as indicated. For statistical analysis of microarray data refer to chapter 3.7.2. Presented data-charts were generated, using the GraphPad Prism 3.0 software (GraphPad Software Inc., USA).

4. Results

4.1 Characterisation of investigated stages of nephropathy

4.1.1 Age of animals

According to the experimental design of the present study, tg/wt pairs of animals were assigned to the investigated stages of glomerular alteration, according to either an significant increase of the mean glomerular volume (stage I), or the detection of onset of albuminuria (stage II) of the respective transgenic animal. Thus, a pair of animals dissected at one point of time each consisted of one transgenic animal and its corresponding non transgenic littermate control (wt) of identical age. The average ages of animals of the respective groups and stages of both cohorts of investigation were almost identical (see table 4.1). The ages of GIPR^{dn}-transgenic animals at the time point of onset of albuminuria displayed a greater variance compared to bGH-transgenic mice.

Table 4.1: Age of GIPR^{dn}-transgenic and bGH-transgenic mice and their respective controls in stage I and stage II.

age [d] at day of sacrifice										
Group/stage	**n**		**mean**		**SD**		**min**		**max**	
	AC	ICC	AC	ICC	AC	ICC	AC	ICC	AC	ICC
GIPR^{dn} stage I	10	10	78	74	1	3	77	71	80	80
GIPR^{dn} stage II	10	14	112	111	37	32	70	67	155	151
bGH stage I	10	10	27	28	2	3	25	27	29	33
bGH stage II	10	16	32	35	2	2	30	32	35	38

AC: Array Cohort; **ICC**: Independent Control Cohort; **n**: numbers of animals investigated; **SD**: standard deviation.

4.1.2 Body weight

In both cohorts of investigation, the mean body weight of GIPR^{dn}-transgenic animals compared to their respective controls, measured at the day of dissection, was decreased in both investigated stages, reaching statistical significance in stage II. bGH-transgenic animals in stage I did show a tendency to an increase of body weight compared to their respective controls. These differences were more pronounced in stage II, yet did not reach statistical significance (table 4.2).

Table 4.2: Body weight of GIPR^{dn}-transgenic and bGH-transgenic mice and their respective controls in stage I and stage II.

Body weight [g] at day of sacrifice									
group/stage	**genotype**	**n**		**mean**		**SD**		**significance**	
		AC	ICC	AC	ICC	AC	ICC	AC	ICC
GIPR^{dn} stage I	**wt**	5	5	37.6	35.0	3.2	2.4	ns	**
	tg	5	5	34.6	29.4	4.1	3.4		
GIPR^{dn} stage II	**wt**	5	7	38.0	38.9	2.0	6.6	*	*
	tg	5	7	33.0	31.6	1.1	4.2		
bGH stage I	**wt**	5	5	20.4	18.9	3.7	4.5	ns	*
	tg	5	5	21.6	25.1	1.3	6.3		
bGH stage II	**wt**	5	8	25.8	27.3	1.7	3.4	ns	ns
	tg	5	8	29.2	29.5	2.4	6.0		

AC: Array Cohort; **ICC**: Independent Control Cohort; **tg**: transgenic animals; **wt**: corresponding non-transgenic wild-type controls. **n**: numbers of animals investigated; **SD**: standard deviation; comparison (**tg** vs. **wt**) of groups per stage; level of significance: **ns** = not significant; ***** $p < 0.05$; ****** $p < 0.01$.

4.1.3 Kidney weights and relative kidney weights

Both kidney weights and relative kidney weights (% of body weight) of GIPR^{dn}-transgenic animals were significantly increased in both stages of investigation (AC). In the independent control cohort (ICC) the increase of kidney weights of GIPR^{dn}-transgenic animals assigned to stage II curtly failed to reach statistical significance in comparison to their associated controls, due to a high standard deviation of values. Kidney weights of bGH-transgenic animals were slightly increased vs. controls. These differences were statistically not significant (table 4.3).

Table 4.3: Kidney weights and relative kidney weights of GIPR[dn]-transgenic and bGH-transgenic mice and their respective controls in stage I and stage II.

kidney weight [1] **[mg]**

group/stage	genotype	n AC	n ICC	mean AC	mean ICC	SD AC	SD ICC	significance AC	significance ICC
GIPR[dn] stage I	wt	5	5	672	609	87	62	**	*
	tg	5	5	819	721	103	83		
GIPR[dn] stage II	wt	5	7	656	640	81	207	**	ns
	tg	5	7	855	808	66	120		
bGH stage I	wt	5	5	340	314	53	67	ns	ns
	tg	5	5	361	401	5	171		
bGH stage II	wt	5	8	436	477	53	80	ns	ns
	tg	5	8	485	487	48	134		

relative kidney weight [2] **[%]**

group/stage	genotype	n AC	n ICC	mean AC	mean ICC	SD AC	SD ICC	significance AC	significance ICC
GIPR[dn] stage I	wt	5	5	1.8	1.7	0.1	0.2	**	**
	tg	5	5	2.4	2.5	0.2	0.2		
GIPR[dn] stage II	wt	5	7	1.7	1.6	0.2	0.3	**	**
	tg	5	7	2.6	2.5	0.2	0.3		
bGH stage I	wt	5	5	1.7	1.7	0.2	0.1	ns	ns
	tg	5	5	1.7	1.6	0.1	0.2		
bGH stage II	wt	5	8	1.7	1.7	0.1	0.2	ns	ns
	tg	5	8	1.7	1.6	0.2	0.2		

[1] sum of weight of both kidneys; [2] sum of weight of both kidneys in % of body weight; **AC**: Array Cohort; **ICC**: Independent Control Cohort; **tg**: transgenic animals; **wt**: corresponding non-transgenic wild-type controls; **n**: numbers of animals investigated; **SD**: standard deviation; comparison (**tg** vs. **wt**) of groups per stage; level of significance: **ns** = not significant; ***** $p < 0.05$; ****** $p < 0.01$.

4.1.4 Glomerular histology

Glomerular morphology was evaluated by light microscopy, using the same PAS-stained histological sections that were used for determination of the mean glomerular volume. In all investigated animals, glomeruli displayed a mature phenotype. Irrespective of stage or group affiliation, the areas of cross sections of a considerable fraction of glomeruli of transgenic mice appeared to exceed those of non-transgenic animals (figure 4.1). Concerning conspicuous alterations of glomerular morphology detected in glomeruli of transgenic mice, these frequently showed mesangial expansion and hypercellularity, as well as mild mesangial matrix accumulation, occurring in a predominantly focal pattern with a higher frequency in transgenic animals assigned to stage II. Manifest glomerulosclerotic lesions including hyalinosis, capillary obliteration and synechia formation were exquisitely rare and only observed in single glomeruli of bGH-transgenic animals of stage II. Tubulo-interstitial lesions, such as atrophy of tubuli, interstitial fibrosis and signs of proteinuria were not detected in any of the investigated sections. Performance of transmission electron microscopy (TEM) confirmed the preservation of the structural elements of the glomerular filtration barrier after perfusion with magnetic beads, as no morphological alterations of podocytes, podocyte foot processes or of the endothelium were observed in the investigated samples. However, in samples derived from transgenic animals, the thickness of the glomerular basement membrane (GBM) seemed to be slightly increased compared to the associated non-transgenic controls (figure 4.1).
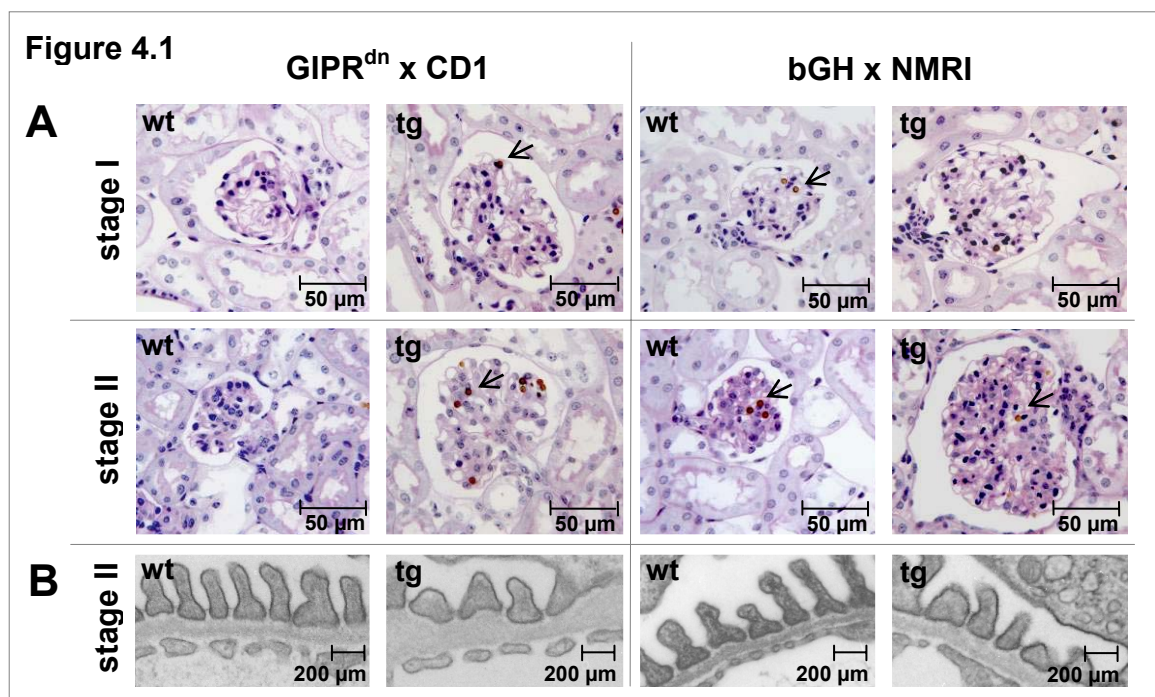
Figure 4.1

Figure 4.1 (page 94): Glomerular histology. Stage I: stage of glomerular hypertrophy; **stage II**: glomerular hypertrophy with onset of albuminuria; **tg**: transgenic animal; **wt**: corresponding non-transgenic littermate control. **A**: Light microscopy of representative cross sections at approximately the glomerular equator (PAS, 250x). The area of glomerular sections is increased in transgenic animals. Arrows mark magnetic beads inside the glomerular capillaries. **B**: Representative electron microscopic pictures of peripheral glomerular capillary loops (TEM, 45,000x). The thickness of the glomerular basement membrane seems to be increased in transgenic animals.

4.1.5 Morphometric analysis and quantitative stereology

4.1.5.1 Mean glomerular volume

In the Array Cohort, the mean glomerular volume of $GIPR^{dn}$- transgenic and bGH-transgenic animals was significantly increased compared to their corresponding non-transgenic littermate controls in both investigated stages of nephropathy. In stage I, the mean glomerular volume of $GIPR^{dn}$-transgenic animals was increased by 45% on the average and by 58% in the bGH-transgenic animals compared to their respective controls. In stage II, the mean glomerular volumes of $GIPR^{dn}$-transgenic animals displayed an enlargement of 59% on the average and of 63% in bGH-transgenic animals compared to their respective corresponding controls. In the Independent Control Cohort, the mean glomerular volume was estimated in samples assigned to stage I (n=5 wt, 5 tg) of investigation and was also significantly increased in transgenic animals in both groups. In the Independent Control Cohort, the mean glomerular volume of $GIPR^{dn}$-transgenic animals was increased by 10% on the average and by 67% in the bGH-transgenic animals compared to their respective controls. Data of animals of the Array Cohort are presented in figure 4.2.

In the investigated samples of the Array Cohort, the mean glomerular volume-to-body weight-ratio ($v_{(glom)}$/body weight) and the mean glomerular volume-to-kidney weight-ratio ($v_{(glom)}$/kidney weight), were significantly increased in all transgenic animals ($GIPR^{dn}$-transgenic mice and bGH-transgenic mice) vs. their associated controls in both investigated stages, indicating an overproportional glomerular growth in the transgenic mice of both groups and stages (table 4.4).

Mean glomerular volume, $\hat{\bar{v}}_{(glom)}$
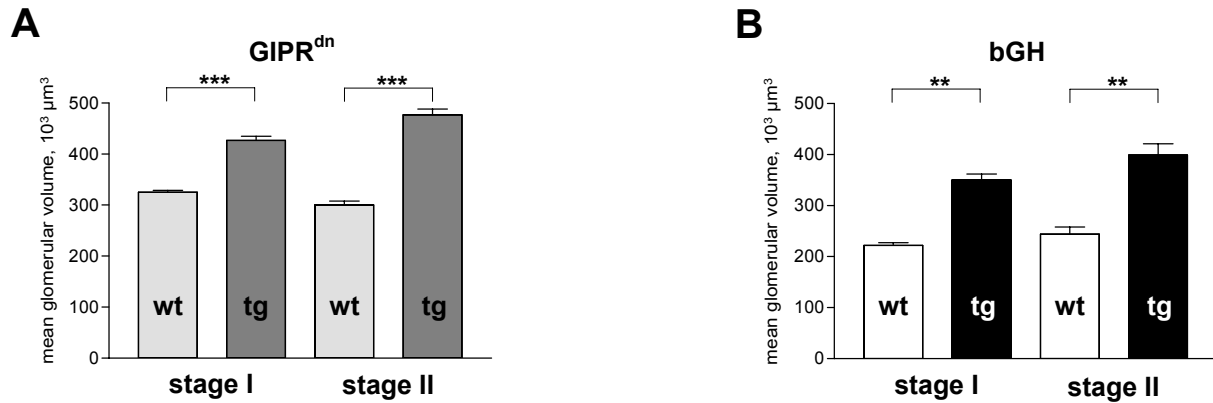
Figure 4.2: Mean glomerular volume (Array Cohort). A: GIPR[dn]-transgenic animals and corresponding controls; **B**: bGH-transgenic animals and corresponding controls. **Stage I**: glomerular hypertrophy; **stage II**: onset of albuminuria; **tg**: transgenic animals; **wt**: corresponding non-transgenic wild-type littermate controls. In both stages of investigation, transgenic mice of both groups displayed a significant increase of their mean glomerular volumes. Data are presented as means ± SEM; level of significance (tg vs. wt): ** = p < 0.01 and *** = p < 0.001 vs. control animals; n = 5 transgenic mice and 5 associated non-transgenic littermate controls per group and stage.

Table 4.4: Stereology of the kidney in GIPR[dn]–transgenic and bGH-transgenic mice and their respective controls in stage I and stage II (Array Cohort):

Mean glomerular volume/body weight; Mean glomerular volume/kidney weight.

Group/stage	genotype	$v_{(glom)}$/body weight [10^3 µm^3/g]			$v_{(glom)}$/kidney weight [10^3 µm^3/g]		
		mean	SD	significance	mean	SD	significance
GIPR[dn] stage I	wt	8.6	0.51	***	0.49	0.05	**
	tg	13.7	0.86		0.58	0.06	
GIPR[dn] stage II	wt	7.9	1.27	***	0.46	0.05	**
	tg	14.4	1.34		0.56	0.08	
bGH stage I	wt	11.0	1.21	**	0.66	0.05	*
	tg	16.1	2.22		0.96	0.13	
bGH stage II	wt	9.5	2.73	***	0.56	0.15	**
	tg	13.6	3.06		0.82	0.19	

tg: transgenic animals; **wt**: corresponding non-transgenic wild-type controls; n = 5 transgenic mice and 5 associated non-transgenic littermate controls per group and stage. **SD**: standard deviation; comparison (**tg** vs. **wt**) of groups per stage; level of significance: **ns** = not significant; * p < 0.05; ** p < 0.01; *** p < 0.001.

4.1.5.2 Numerical density of glomerular cells

In both GIPR^{dn}-transgenic animals, as well as in bGH-transgenic animals of both investigated stages of glomerular alteration, the estimated numerical density of glomerular cells was reduced compared to their respective controls, reaching statistical significance in the bGH-groups. The estimated numerical density of podocytes was significantly reduced in transgenic animals of all groups and stages, except for GIPR^{dn}-transgenic mice of stage II (table 4.5).

Table 4.5: Numerical density of glomerular cells in GIPR^{dn}-transgenic and bGH-transgenic mice and their respective controls in stage I and stage II (Array Cohort).

Group/stage	genotype	$\hat{N}_{V(Y/glom)}$ [10^3/mm^3]			SD			significance		
		C	P	E+M	C	P	E+M	C	P	E+M
GIPR^{dn} stage I	wt	670	202	453	114	45	75	ns	*	ns
	tg	643	148	506	35	16	22			
GIPR^{dn} stage II	wt	803	224	575	81	31	64	ns	ns	ns
	tg	631	144	487	128	56	90			
bGH stage I	wt	1104	350	755	107	26	112	*	***	ns
	tg	890	223	666	148	52	107			
bGH stage II	wt	924	281	636	90	29	70	**	*	*
	tg	759	184	574	89	42	57			

Y = **C**: glomerular cells; Y = **P**: podocytes; Y = **E + M**: endothelial and mesangial cells; **tg**: transgenic animals; **wt**: corresponding non-transgenic wild-type controls; n = 5 transgenic mice and 5 associated non-transgenic littermate controls per group and stage. **SD**: standard deviation; comparison (**tg** vs. **wt**) of groups per stage; level of significance: **ns** = not significant; * $p < 0.05$; ** $p < 0.01$; *** $p < 0.001$

4.1.5.3 Number of cells per glomerulus

In both groups (GIPR^{dn}-group and bGH-group) and stages of nephropathy, the estimated number of endothelial and mesangial cells per glomerulus, was significantly increased in transgenic animals vs. their respective controls, while the number of podocytes per glomerulus remained almost unchanged (figure 4.3).
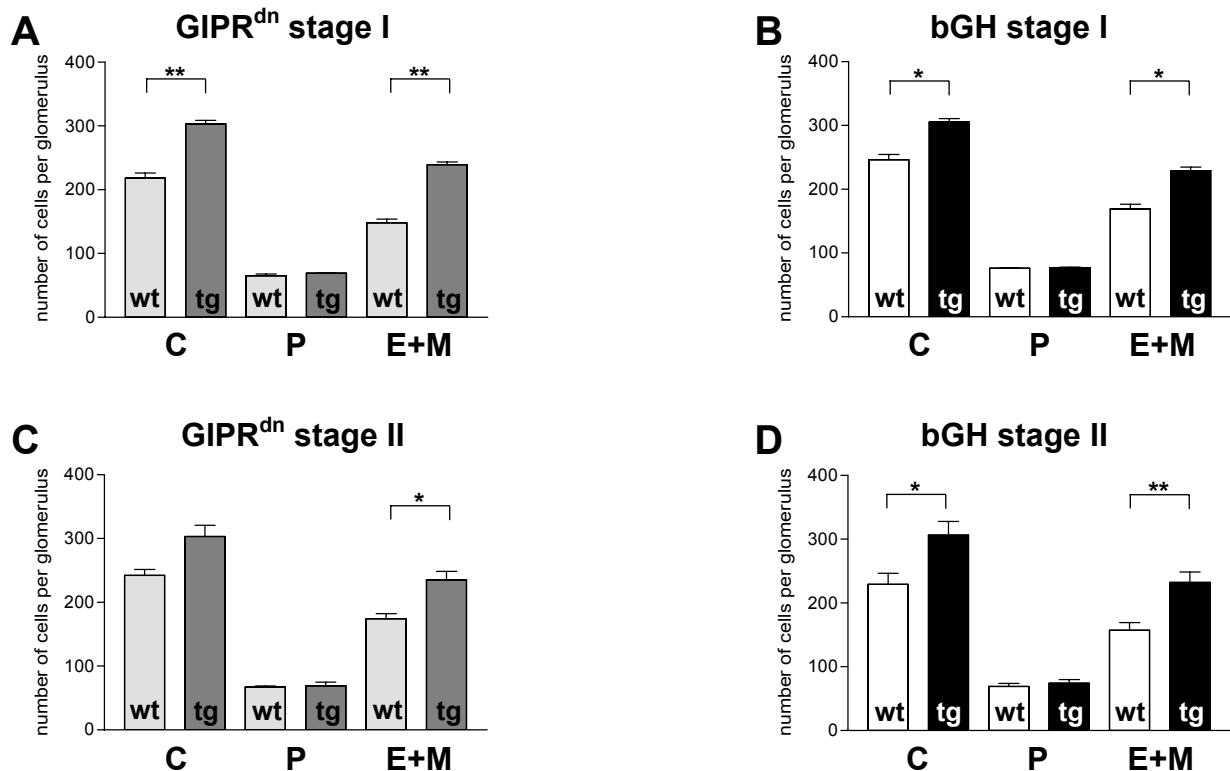
Figure 4.3: Number of cells per glomerulus.
A, C: GIPR^{dn}-transgenic animals and associated controls; **B, D**: bGH-transgenic animals and corresponding controls. **Stage I**: glomerular hypertrophy; **stage II**: onset of albuminuria; **tg**: transgenic animals; **wt**: corresponding non-transgenic littermate controls. n = 5 transgenic mice and 5 associated non-transgenic littermate controls per group and stage. Glomerular cell types: **C**: glomerular cells; **P**: podocytes; **E+M**: endothelial and mesangial cells. Data are presented as means ± SEM; level of significance (tg vs. wt): * $p < 0.05$; ** $p < 0.01$; *** $p < 0.001$.

4.1.5.4 Filtration slit frequency (FSF)

The FSF [FS/mm GBM], determined in peripheral glomerular capillary loops of transgenic animals (Array Cohort) did not show a statistical significant difference to the FSF of the corresponding non-transgenic littermate controls (GIPR^{dn}: -tg: 2550 ± 147 and -wt: 2587 ± 338; bGH: -tg: 2739 ± 175 and -wt: 2803 ± 103) in stage II (figure 4.4).
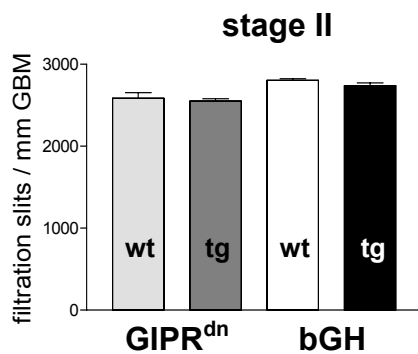
Figure 4.4: Filtration slit frequency (FSF).
Stage II: stage of onset of albuminuria; **tg**: transgenic animals; **wt**: corresponding non-transgenic littermate controls; n = 5 transgenic mice and 5 associated non-transgenic littermate controls per group. Data are presented as means ± SEM.

4.1.5.5 Thickness of the glomerular basement membrane (GBM)

The true harmonic mean thickness (Th) of the glomerular basement membrane of peripheral glomerular capillary loops of transgenic animals (GIPR^{dn}-tg: 156 nm ± 31 and bGH-tg: 126 nm ± 5), compared to their respective controls (GIPR^{dn}-wt: 137 nm ± 28 and bGH-wt: 108 nm ± 10) in stage II was slightly but significantly increased (figure 4.5).
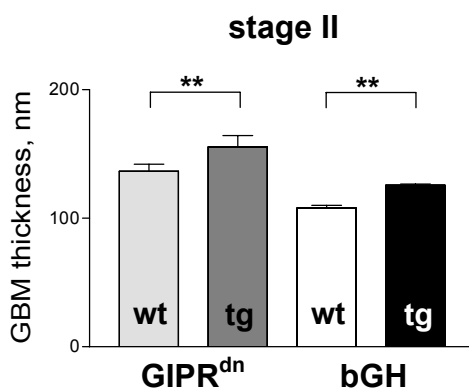
Figure 4.5: True harmonic mean thickness of the glomerular basement membrane (GBM).
Stage II: stage of onset of albuminuria; **tg**: transgenic animals; **wt**: corresponding non-transgenic littermate controls. n = 5 transgenic mice and 5 associated non-transgenic littermate controls per group. Data are presented as means ± SEM; level of significance (tg vs. wt): ** $p < 0.01$. The GBM-thickness was increased by 13.9% in GIPR^{dn}-transgenic animals and by 16.2% in bGH-transgenic animals, compared to their respective controls.

4.1.6 Results of urine analyses

4.1.6.1 Detection of glucosuria in GIPR^{dn} -transgenic mice

The diabetic phenotype of GIPR^{dn} -transgenic mice was reconfirmed by detection of glucosuria in spot urine samples. GIPR^{dn} -transgenic mice displayed glucosuria as early as from day 21 on. At the time point of sacrifice, all GIPR^{dn} -transgenic mice displayed glucosuria, whereas glucosuria was not detected in any of the control animals.

4.1.6.2 Urine creatinine concentrations

As a consequence of the polyuria and hyposthenuria observed in these animals, GIPR^{dn}-transgenic mice of both investigated cohorts (Array Cohort and Independent Control Cohort) displayed significantly lower urine-creatinine concentrations in spot urine samples taken 24 hours prior to dissection compared to their controls in all investigated stages. In stage I, also bGH-transgenic animals exhibited significantly decreased urine-creatinine concentrations in spot urine samples taken 24 hours prior to dissection compared to their controls (table 4.6).

Table 4.6: Urine-creatinine concentrations

Urine-creatinine [mg/dl]

Group/stage	genotype	n	mean	SD	significance
GIPR^{dn} stage I	wt	5	26,7	7,1	**
	tg	5	1,6	0,8	
GIPR^{dn} stage II	wt	11	41,6	13,5	***
	tg	11	2,6	1,3	
bGH stage I	wt	5	23,3	6,1	*
	tg	5	16,4	5,9	
bGH stage II	wt	9	42,1	14,1	ns
	tg	9	15,8	10,0	

Stage I: glomerular hypertrophy; **stage II**: stage of onset of albuminuria; **tg**: transgenic animals; **wt**: corresponding non-transgenic littermate controls; **n**: numbers of animals investigated (Array Cohort and Independent Control Cohort); **SD**: standard deviation; level of significance (tg vs. wt): **ns** = not significant; * $p < 0.05$; ** $p < 0.01$; *** $p < 0.001$.

4.1.6.3 Urine protein excretion patterns (SDS-PAGE)

As scheduled by the study's experimental design, transgenic animals as well as their corresponding non transgenic littermate controls of both investigated cohorts (Array Cohort and Independent Control Cohort), assigned to stage I did not show evidence of albuminuria in the SDS-PAGES at any point of time (figure 4.6, A to F). All transgenic animals assigned to stage II exhibited selective glomerular proteinuria 24 hours prior to dissection (figure 4.6, C and D): bands of approximately 69 kDa, which meets the size of murine albumin, were detected by SDS-PAGE. Excretion of proteins larger than 37 kDa was not detectable in the urine samples of controls (figures 4.6 and 4.7). Bands in the region of approximately 18 kDa reflect major urinary proteins (MUPs), which appear in the murine urine under physiological conditions particularly in male mice. Compared to their control animals, all investigated bGH-transgenic mice exhibited a marked decrease of these MUPs (figure 4.7). In transgenic animals the onset of albuminuria was detected by recurrent SDS-PAGE analysis of urine samples taken in defined intervals. Transgenic animals displayed albuminuria twice within 48 hours prior to dissection, after a first negative result (figure 4.6 E and F). The comparability of results of SDS-PAGE urine protein analyses, using a silver staining of gels (GIPR[dn]-group), and respective results of Coomassie blue stained gels (bGH-group), was confirmed. Results of Coomassie blue stained gels of urine samples of albuminuric (stage II) and non-albuminuric bGH-transgenic mice (stage I), as well as their associated control animals were comparable with the results of silver stained SDS-PAGE gels of the same samples (figure 4.7).

A: GIPR^{dn} stage I: glomerular hypertrophy

M tg tg tg tg wt wt wt wt alb

B: bGH stage I: glomerular hypertrophy

M tg tg tg tg wt wt wt wt alb

C: GIPR^{dn} stage II: onset of albuminuria

M tg tg tg tg wt wt wt wt alb

D: bGH stage II: onset of albuminuria

M tg tg tg tg wt wt wt wt alb

E: GIPR^{dn} : time course of onset of albuminuria

M d_S-7 d_S-3 d_S-1 d_S-7 d_S-3 d_S-1 Ø alb
       tg   wt

F: bGH: time course of onset of albuminuria

M Ø d_S-5 d_S-3 d_S-1 d_S-3 d_S-1 alb
          tg   wt

Figure 4.6: Detection of albuminuria. 12 % SDS-PAGE, silver staining. **M**: Molecular weight marker (Precision Plus, Biorad, Germany): visible marker-bands indicate the molecular weights of recombinant protein standards of 100, 75, 50 and 37 kDa from top to bottom; **alb**: murine albumin standard (400 ng/lane) at approximately 69 kDa; **tg:** transgenic animal; **wt**: wild-type littermate control; **Ø**: spacing lane (H_2O, negative control); **dS**: day of sacrifice. **A**, **C**, **E**: GIPR^{dn}-transgenic mice and corresponding wild-type controls (urine diluted to 1.5 mg/dl [creatinine]). **B**, **D**, **F**: bGH-transgenic mice and corresponding wild-type controls (urine diluted to 3.0 mg/dl [creatinine]). **A**, **B**: **Stage I** (glomerular hypertrophy, 1 day prior to sacrifice). None of the transgenic animals is displaying albuminuria. **C**, **D**: **Stage II** (onset of albuminuria, 1 day prior to sacrifice): all transgenic animals exhibit albuminuria. **E**, **F**: time course of onset of albuminuria (stage II). Transgenic animals displayed albuminuria twice within 48 hours prior to dissection, after a first negative result. **E**: urine samples of a GIPR^{dn}-transgenic animal and the corresponding wild-type control were taken 7, 3 and 1 days prior to dissection (d_S-7, d_S-3, d_S-1). **F**: Urine samples of a bGH-transgenic animal and the corresponding wild-type control were taken 5, 3 and 1 days prior to dissection (d_S-5, d_S-3, d_S-1).
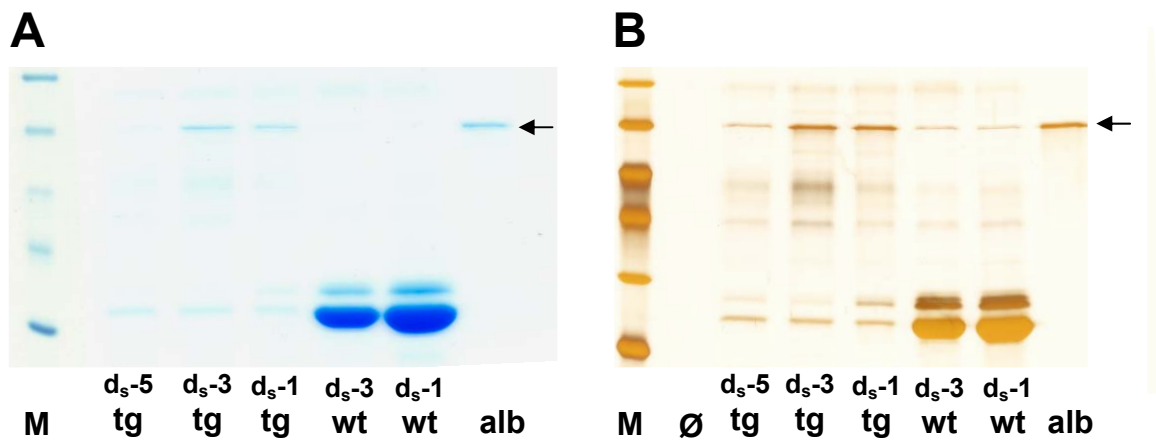
Figure 4.7: Comparability of SDS-PAGE urine protein analysis results of coomassie blue and silver stained gels. Urine samples of a bGH-transgenic animal and the corresponding wild-type control were taken 5, 3 and 1 days prior to dissection (d_S -5, d_S -3, d_S -1). Urine samples were diluted to a creatinine concentration of 3 mg/dl. 12 % SDS-PAGE gels. **A**: Coomassie staining. **B**: Silver stained SDS-PAGE gel of the same samples. **M**: Molecular weight marker; **alb**: murine albumin standard (400 ng/lane) at approximately 69 kDa (arrows). **A**: visible marker-bands (Broad range, Biorad, Germany) indicate the molecular weights of recombinant protein standards of 97, 66, 45, 31, and 14.5 kDa from top to bottom (the marker lane in **A** was superimposed for purpose of illustration); in **B**: visible marker-bands (Precision Plus, Biorad, Germany) indicate the molecular weights of recombinant protein standards of 100, 75, 50, 37, 25 and 10 kDa from top to bottom.

4.1.6.4 Western blot analysis

The presence of albuminuria (as detected in SDS-PAGE-based urine protein analyses) in GIPR^{dn}-transgenic and bGH-transgenic animals investigated in stage II was confirmed by detection of albumin bands of approximately 69 kDA (murine albumin) in Western-blot analysis (figure 4.8).
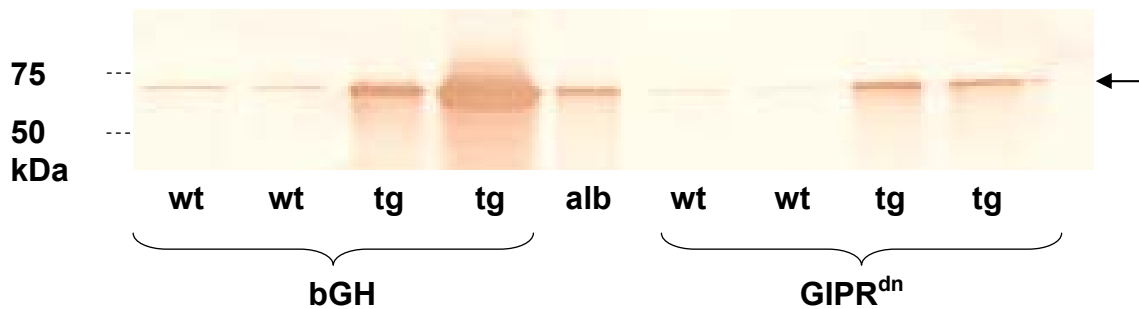
Figure 4.8: Detection of murine albumin in spot urine samples of two bGH-transgenic (tg) and two GIPR^{dn}-transgenic animals and their corresponding wild-type (wt) littermate controls by Western blot. At this point of time (one day prior to sacrifice), transgenic animals displayed albuminuria for 48 hours (stage II: stage of onset of albuminuria). **alb**: mouse albumin standard (400 ng); the positions (75 kDa & 50 kDa) of the molecular weight standard are indicated. Arrow marks albumin bands of approximately 69 kDa.

4.1.6.5 Quantification of urine albumin concentrations by ELISA

In stage II, both GIPR^{dn}- and bGH-transgenic animals displayed a significant increase of urine albumin/creatinine ratios compared to their associated controls, whereas in stage I, the urine albumin/creatinine ratios of transgenic and wild-type animals did not differ significantly (figure 4.9).
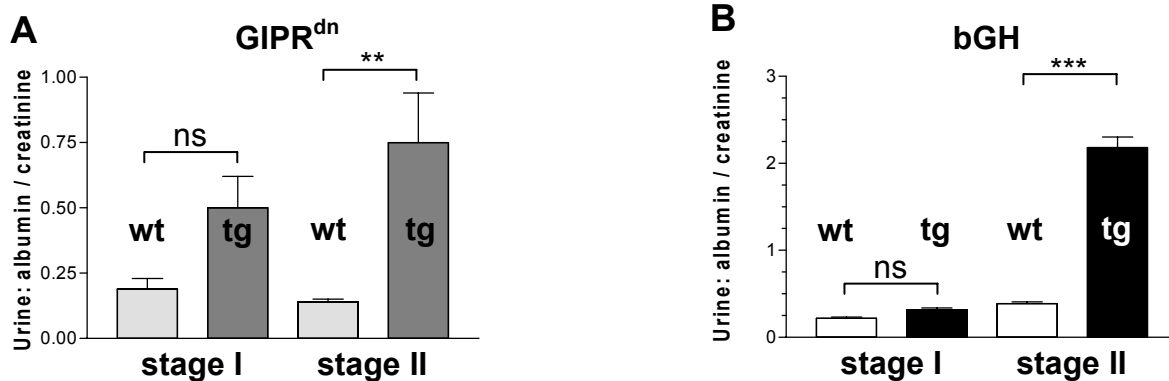
Figure 4.9: Urine albumin/creatinine ratios. **Stage I**: stage of glomerular hypertrophy; **stage II**: stage of glomerular hypertrophy with onset of albuminuria; **tg:** transgenic animals; **wt**: corresponding non-transgenic wild-type littermate controls. **A**: albumin/creatinine ratios were significantly increased in GIPR^{dn}-transgenic mice of stage II, but not in stage I. **B:** albumin/creatinine ratios were also significantly increased in bGH-transgenic mice of stage II, but not in stage I. Numbers of animals investigated: n = 5 transgenic animals and 5 corresponding controls per group in stage I; n = 11 transgenic animals and 11 corresponding controls for the GIPR^{dn}-group of stage II; n = 9 transgenic animals and 9 corresponding controls for the bGH-group in stage II. Data are presented as means ± SEM; level of significance: ** = $p < 0.01$, and *** = $p < 0.001$ vs. control animals.

4.2 Magnetic large scale isolation of kidney glomeruli

4.2.1 Pilot experiments

The perfusion technique pointed out to be the most important prerequisite for the method's success. Common problems using conventional perfusion devices (gauge needle, tube, syringe) were inadjustability and fluctuations of the perfusion pressure, as well as precipitation of magnetic beads, formation of air bubbles and perfusate remaining inside the system used for perfusion. This led to a variable number of glomeruli not being perfused with beads and thereby being inaccessible for magnetic isolation (Blutke et al. 2005). Those problems could be avoided, using a self developed perfusion device (Blutke 2006) (figure 3.5, chapter 3.4.2), which allows uncomplicated perfusion of nearly all glomeruli in the adult mouse kidney with sufficient numbers of beads under adjustable and steady pressure conditions (Blutke et al. 2005). Irrespective of age or genetic background of mice, optimal perfusion results were obtained, using magnetic beads of 4-5 µm diameter (e.g. Dynabeads $^{®}$ M-450 Epoxy, Dynal, Germany) at a perfusion pressure of 70 mm Hg (figure 4.11 B).

Higher perfusion pressures led to glomerular damage, like dilation of glomerular capillaries (figure 4.10 B). Using beads (beadMAG-55, Chemicell, Germany) of smaller diameter (1µm) provided large amounts of isolated glomeruli, as large numbers of beads accumulated inside the glomeruli (figure 4.10 A), but also in low purities of glomerulus isolates, since these small beads accumulated in peritubular vessels as well. Variation in diameters of magnetic beads of a nominal diameter of 4.5 µm (as observed in SIMAG-Oxiran/20 beads, Chemicell, Germany) proved to be a further possible problem, partially causing obstruction of preglomerular vessels by large beads (figures 4.10 C and D). The necessity of concentration of isolated glomeruli in a small volume of RNA stabilization reagent (RNA-later®, Ambion, Germany) for further sample treatment (isolation of total RNA for transcript profiling analyses) led to the development of a device for concentration of glomerulus isolates by sieving. Due to the high density of RNA-later®, centrifugation was ineffective to concentrate the isolated glomeruli into an appropriate volume of RNA-later® after isolation, irrespective of centrifugation time or speed. Furthermore, isolated glomeruli, especially those diluted in RNA-later®, showed strong adhesive properties towards nearly all kinds of surfaces, favoring losses of glomeruli during the further treatment of the samples. These problems could be minimized by the use of a 50 µm mini cell strainer (refer to figure 3.10 in chapter 3.4.2) for removal of surplus RNA-later® and further sample processings of isolated glomeruli.
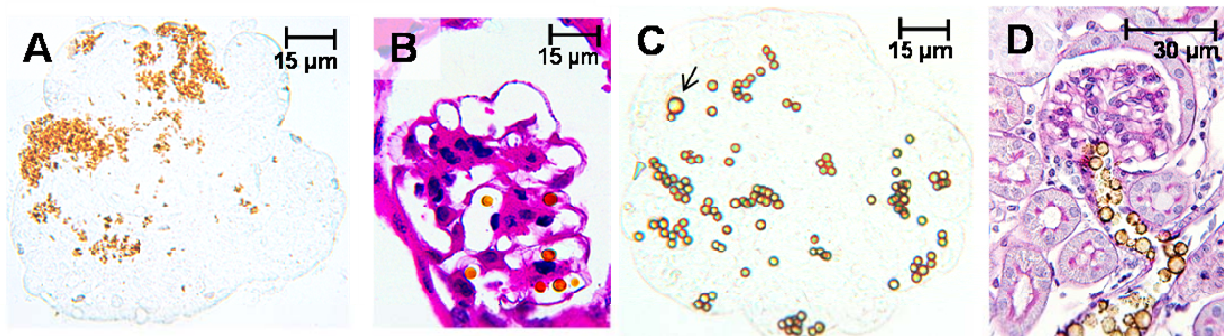
Figure 4.10: Perfusion outcome under varying circumctances. A: Glomerulus, perfused with beads of 1 µm diameter (beadMAG-55, Chemicell, Germany). Note the accumulation of large numbers of beads inside the glomerular capillaries [native, 40x]. **B**: Perfusion with a pressure 120 mm Hg (Dynabeads M-450 Epoxy, Dynal, Germany): dilation of glomerular capillaries [HE staining, 250x]. **C, D**: Variation in magnetic bead diameter. **C**: Isolated glomerulus, perfused with beads of a nominal diameter of 4.5 µm (SIMAG-Oxiran/20, Chemicell, Germany). Note (arrow) the variation of bead diameter [native, 40x]. **D**: Section from the contralateral kidney from **C**. The variation in magnetic bead diameter partially caused obstruction of preglomerular vessels by large beads [PAS staining, 250x].

4.2.2 Quantity and purity of generated glomerulus isolates

Using the developed final protocol (refer to chapter 3.4.2) for large scale glomerulus isolation from kidneys perfused with magnetic beads (Dynabeads ® M-450 Epoxy, Dynal, Germany), an average of ~ 6000 glomeruli per kidney of about 95 % purity were harvested within ~90 minutes. The Collagenase digestion and gentle filtration steps efficiently detached the morphologically intact glomeruli from surrounding tissues. Capillaries of isolated glomeruli were embolized with 10-15 magnetic beads on the average. The glomeruli displayed an intact structure and shape. The maintenance of glomerular morphology was also confirmed by electron microscopic examination of perfused glomeruli (figure 4.11). Glomerulus isolates designated for RNA-isolation for transcript profiling analysis each consisted of about 1000 isolated glomeruli (range 940-1200) and displayed a purity of nearly 100% (absence of non glomerular tissues in the isolate), as these glomeruli were picked under visual control (refer to chapter 3.4.2). About 80% to 95% of these glomeruli were lacking the Bowman's capsule; some of them had part of the afferent and/or efferent arterioles still attached, as verified in preliminary experiments by visual inspection of a representative number of glomerulus isolates. Concerning the percentual share of encapsulated glomeruli, there were no differences between glomerulus isolates derived from transgenic and non-transgenic animals. Isolation time, calculated from the animal's death to the transfer of isolated glomeruli into RNA-later®, was 75 minutes on the average. The effectiveness of tissue separation in investigated glomerulus isolates was also confirmed by real-time PCR for detection of nephron specific gene expression patterns, using Wilm's tumor antigen 1, a marker for glomerular podocytes (Cohen and Kretzler 2003). The WT-1/Gapdh ratio was 362x higher in the glomerular specimens compared to total kidney cortex samples.
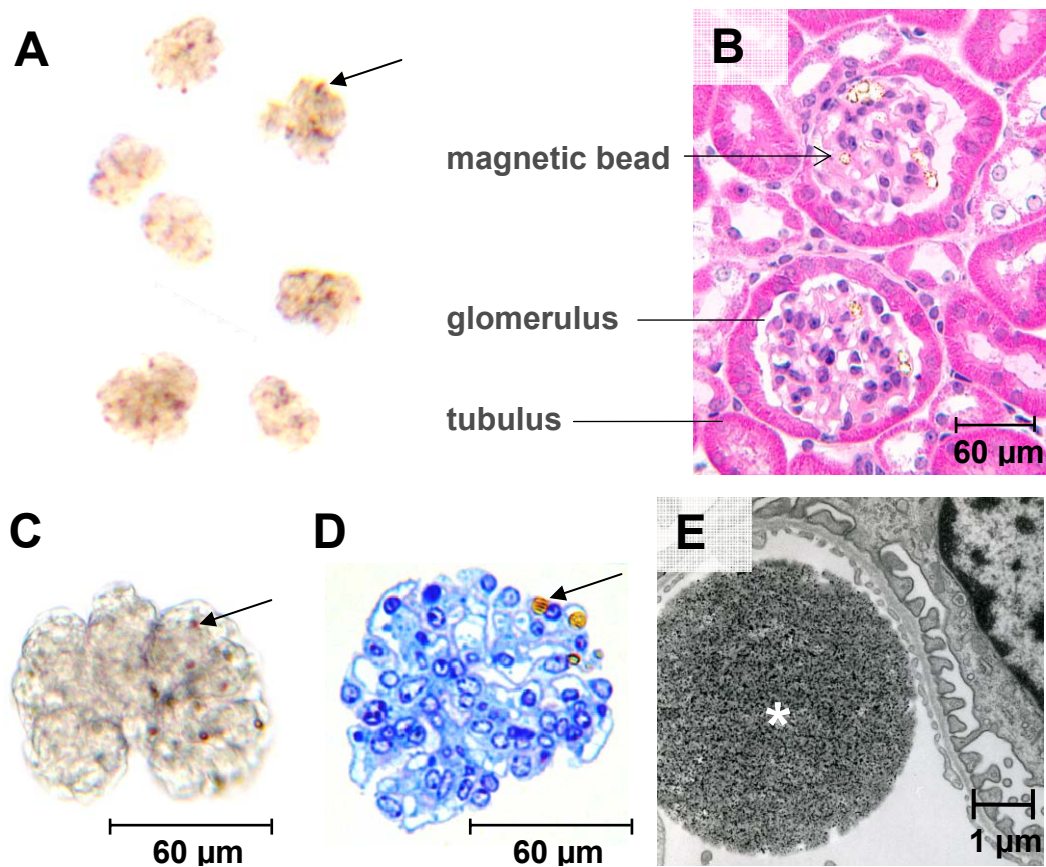
Figure 4.11: Perfusion with spherical superparamagnetic beads: Embolization of glomerular capillaries. A-**E**: Mice were perfused with 40 ml of a suspension of approximately 8 x 107 magnetic beads (Dynabeads® M-450 Epoxy, Dynal, Invitrogen Corporation, Germany; nominal diameter 4.5 µm) through the left heart ventricle, using a perfusion pressure of 70 mm Hg. **A**: Isolated glomeruli [native, 32x, arrow marks magnetic bead]. **B**: Section of perfused kidney displaying an optimal perfusion result: glomeruli are uniformly perfused with sufficient numbers of magnetic beads (indicated by arrow); perfusion pressure 70 mm Hg [GMA/MMA, HE staining, 250x].**C**: Isolated glomerulus [native, 40x, arrow marks magnetic bead]. **D**: Semithin section of isolated glomerulus [Epon, Azur II/Safranin blue staining, 630x, arrow marks magnetic bead]. **E**: Magnetic bead inside a glomerular capillary [TEM, 8000x, asterisk marks magnetic bead].

4.3 Results of transcript profiling analyses

4.3.1.1 Quantities and quality of total glomerular RNA

Quality and quantity of total RNA, extracted from the glomerulus isolates, was controlled for each sample by microfluid electrophoresis (Agilent Technologies, USA). The high quality of RNA was confirmed by circumscribed ribosomal peaks in the electrophoresis read-out, with no additional signals below the ribosomal bands and no shift to shorter fragments (figure 3.18 E in chapter 3.6.3). On the average an amount of ~780 ± 356 ng (range: 196 - 1456 ng) total RNA was isolated from approximately 1000 isolated glomeruli (range 940 -1200) per sample in the Array Cohort. The average concentration of total RNA in these samples was 19.5 ± 8.9 ng/µl (range: 4.9 - 36.4 ng/µl). Concerning the average yields of total RNA extracted from comparable numbers of isolated glomeruli of transgenic animals vs. their corresponding controls, no significant difference was detected, independent of stage- or group-affiliations of the respective sample materials. Interestingly, the average amounts of total RNA isolated from glomerular samples concordantly displayed a strong dependency on genetic backgrounds of mice. Amounts of total RNA extracted from glomerulus isolates of mice of CD1 background (GIPR^{dn}-group) were averagely about 50% of the respective yields attained in samples of mice of NMRI background (bGH-group).

4.3.1.2 Quality of target cDNA

Using microfluid electrophoresis (Agilent Technologies, USA), the high quality of all amplified, as well as all fragmented/biotinylated cDNA products (n = 40) distinguished for hybridisation on the arrays for gene expression analysis was also confirmed (figure 4.12).
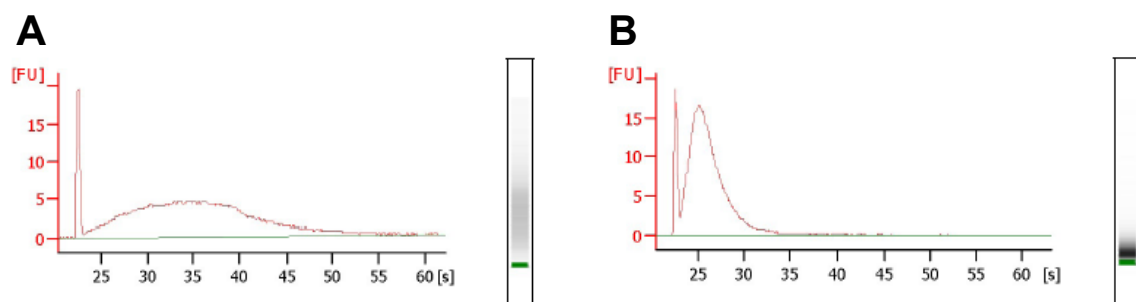
Figure 4.12: Quality of target cDNA. Graphical output of measurement of quantity and quality of amplified (**A**) and fragmented/ biotinylated (**B**) cDNA products of an identical sample (bGH-transgenic animal assigned to stage II).

4.3.2.1 Control of quality and comparability of microarray data

The good overall quality and comparability of array data of the different samples investigated in the experiment was confirmed by evaluation of "density"- and "degradation"-plots (Microarray Suite version 5.0.1 software, Affymetrix, USA). All arrays of the experiment showed similar and comparable patterns of density distributions of overall hybridisation intensities, as well as comparable degrees of only weak degradation of target cDNA (figure 4.13).
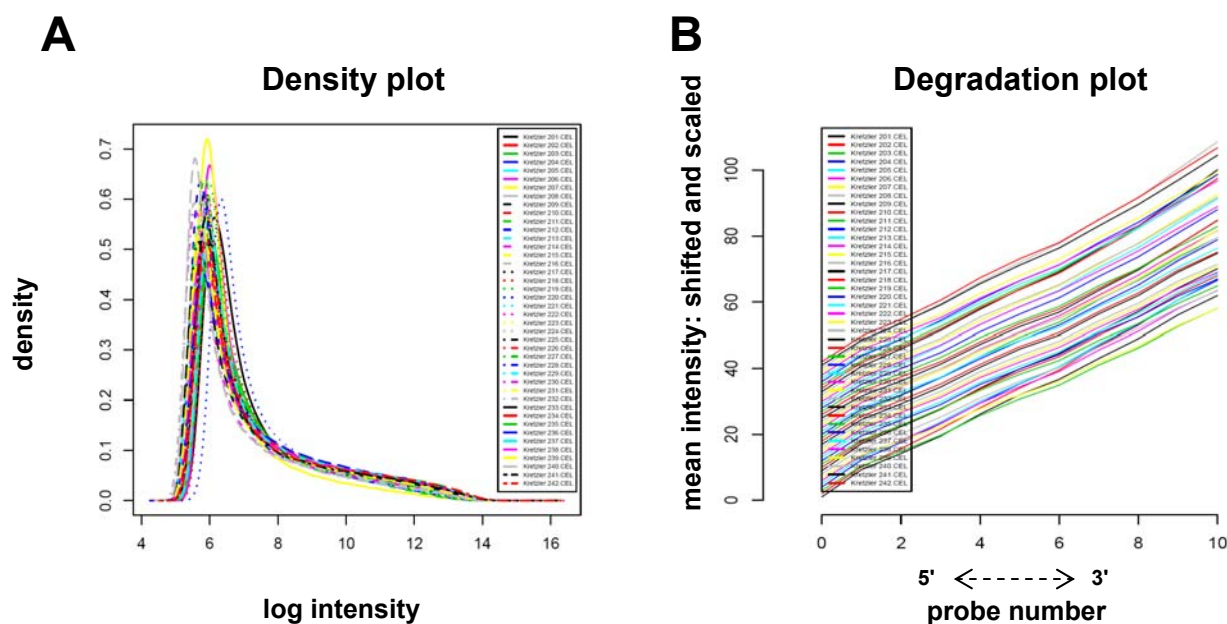
Figure 4.13: Control of quality and comparability of unprocessed microarray data. A: Density plot. B: Degradation plot. Plots were generated from microarray data of all samples in the array experiment (n = 40). Data from each microarray are represented by a different curve. **A: Density plot.** This plot shows the density of the probe intensities to visualize differences in the distributions of the arrays. All curves are congruently positively skewed (long right tail), displaying comparable and similar shapes and slopes. This indicates an optimal comparability of data for differential analyses. **B: Degradation plot.** For each array and within each probe-set, perfect match probes were arranged by their proximity to the 5' end of a respective gene. The plot shows the average intensity of the probes, classified by this order (as a function of 5'-3' position of probes). The slope of each lines' trend indicates potential RNA degradation of the sample material hybridized to the array. The vertical axis is shifted and scaled to highlight the trends of the lines. All curves are roughly parallel and display comparable low slopes, indicating comparable degrees of only minimal degradation of all samples.

4.3.2.2 Cluster analysis of normalized microarray data

The Principle Component Analysis plot (PCA plot, figure 4.14) and the Cluster dendrograms (figure 4.15) illustrate the overall similarity, as well as common differences of detected patterns of hybridisation intensities in normalized microarray data of the different subgroups of samples in the array experiment. In the PCA plot, the patterns of hybridisation intensities detected in samples derived from isolated glomeruli displayed a considerable difference compared to those detected in samples derived from RNA lysates from two samples of total cortical kidney tissue (controls, figure 4.14). Interestingly, glomerular samples always completely clustered into groups of common genetic backgrounds (bGH-group: NMRI background and GIPR^{dn}-group: CD1 background), rather than into groups of wild-type and transgenic animals or common stages of glomerular alteration. Only samples derived from the bGH-group assigned to stage II clustered into distinct groups of wild-type and transgenic animals (figures 4.14 and 4.15).
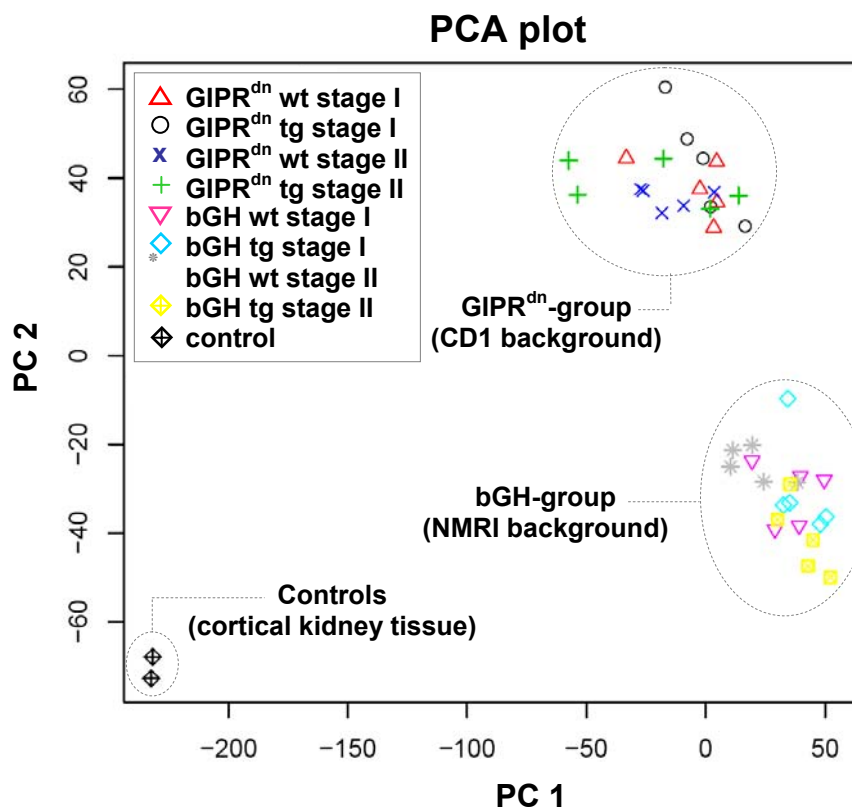
Figure 4.14: PCA plot of normalized microarray data of all samples of the experiment. Note the clear separation between glomerular samples and those derived from total RNA lysates of cortical kidney tissue. Glomerular samples completely clustered into distinct groups of common genetic backgrounds (NMRI and CD1).
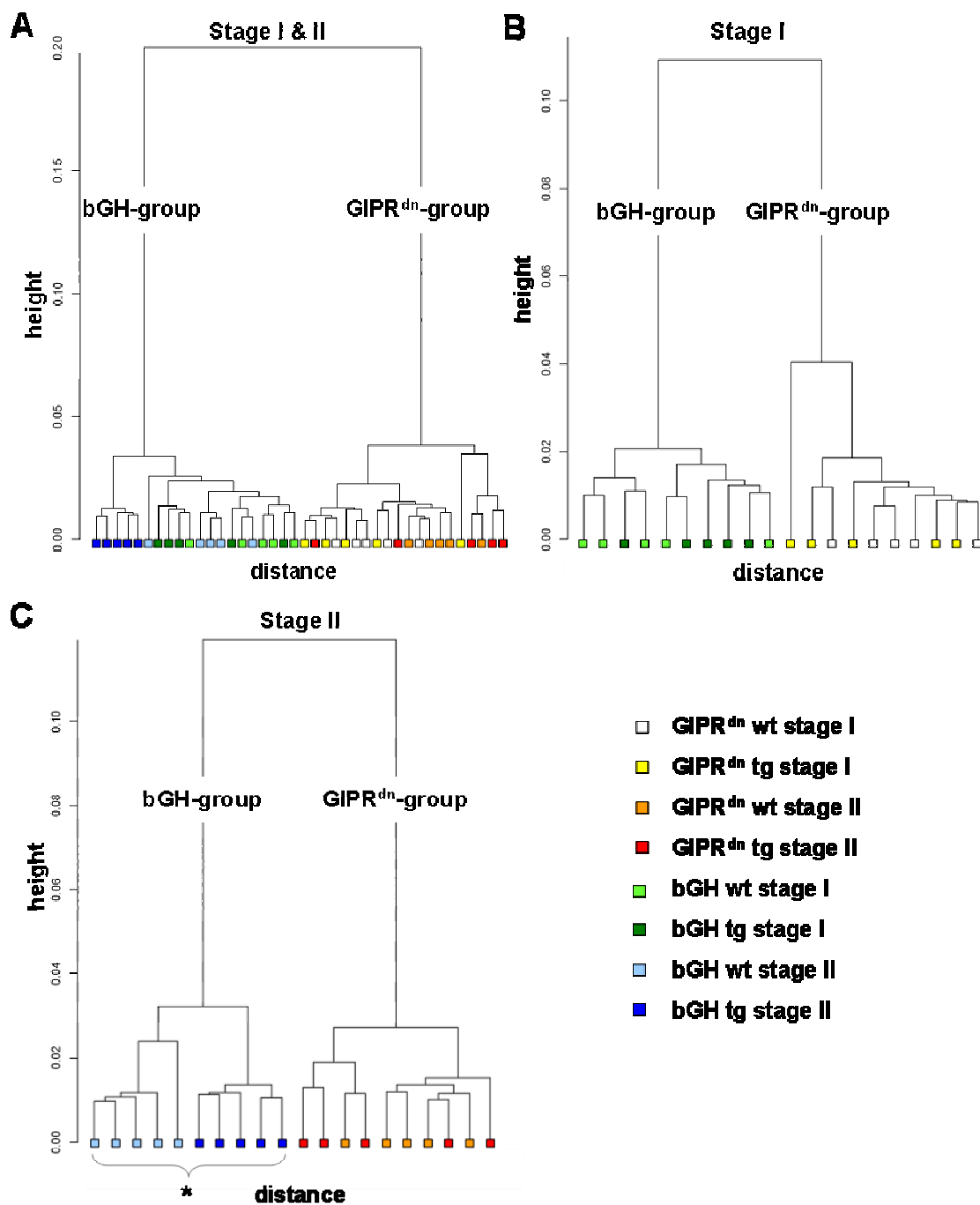
Figure 4.15: Cluster dendrograms. Unbiased cluster dendrograms (Ward's minimum variance) generated from expression data of each 45101 genes per investigated array.) **A**: All glomerular samples (**stages I & II**); **B**: Glomerular samples assigned to **stage I**; **C**: Glomerular samples assigned to **stage II**. Glomerular samples always completely clustered into groups of common genetic backgrounds. Only samples of the bGH-group assigned to stage II clustered into distinct groups of wild-type and transgenic animals (**C**,*).

4.3.3.1 Identification of differentially expressed genes in the single groups and stages of investigation (stage I: GIPR^dn: tg vs. wt; stage I: bGH: tg vs. wt; stage II: GIPR^dn: tg vs. wt and stage II: bGH: tg vs. wt)

Using the ChipInspector 1.2 software with applied settings of analysis parameters (FDR ≤ 0.049 %) as mentioned above (refer to chapter 3.7.2) for performance of statistical analysis of microarray data (figure 4.16), transcripts that displayed a statistical significant differential expression in the respective samples to be compared with each other (5 samples of transgenic animals and 5 samples of their associated wild-type controls per group and stage) were identified. Congeneric differentially expressed transcripts of a single gene were assigned to their common corresponding Entrez Gene ID. The respective numbers of differentially expressed transcripts and corresponding genes are given in table 4.7 and indicated in figure 4.17.
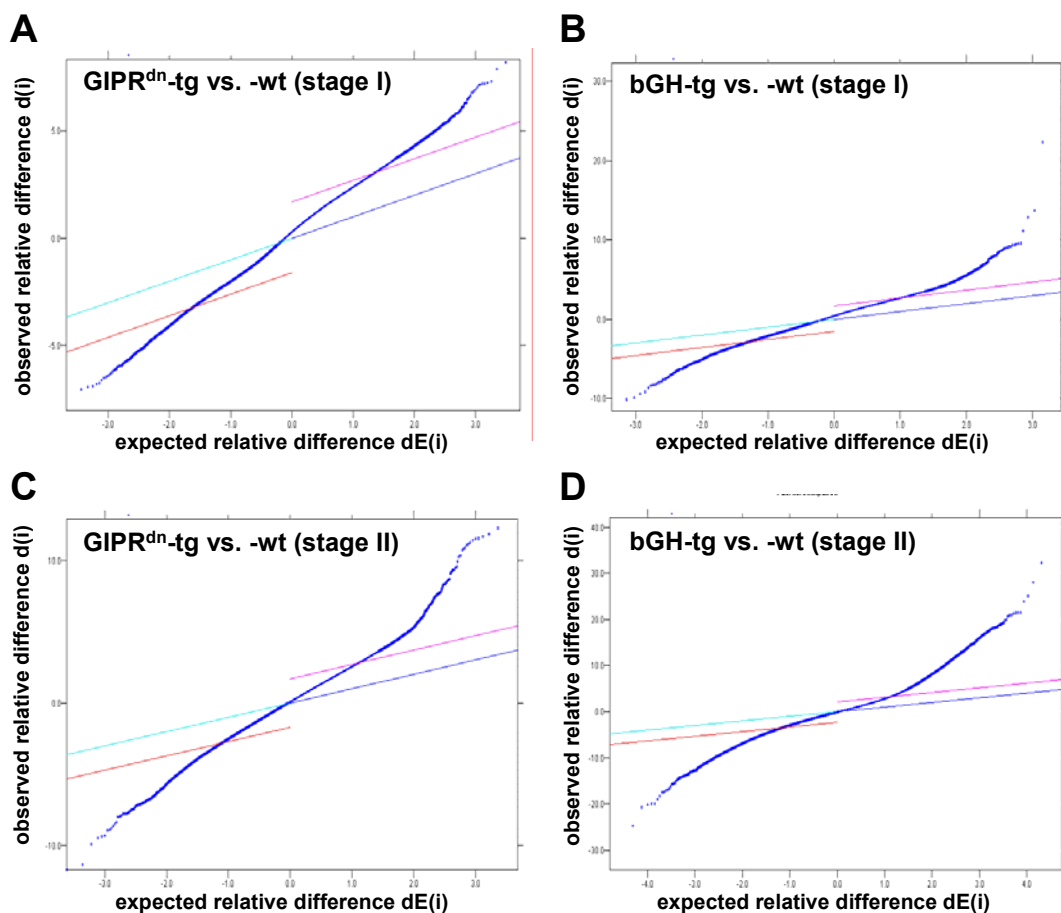
Figure 4.16: Statistics curves from significance analysis of microarray data: Identification of differentially (level of significance: FDR < 0.049 %) expressed transcripts in glomerular samples (each 5 samples of transgenic animals vs. 5 samples of their associated wild-type littermate controls per group and stage). **A**: GIPR^dn-group of stage I. **B**: bGH-group of stage I. **C**: GIPR^dn-group of stage II. **D**: bGH-group of stage II. For interpretation of the statistics curves refer to chapter 3.7.2.

Table 4.7: Numbers of differentially (FDR < 0.049%) expressed glomerular transcripts and corresponding genes in the single groups and stages of investigation.

Group	Stage	Number of differentially expressed transcripts	Number of corresponding genes		
			total number	increased expression	decreased expression
GIPR^{dn}: tg vs. wt	stage I	1946	**531**	302	229
	stage II	5922	**1422**	609	957
bGH: tg vs. wt	stage I	5065	**1566**	986	436
	stage II	17643	**4300**	2059	2241

4.3.3.2 Commonly differentially expressed genes in stage I

(intrastadial comparison: [GIPR^{dn} stage I, tg vs. wt] vs. [bGH stage I, tg vs. wt])

In the defined stage of glomerular hypertrophy before onset of albuminuria (stage I), a number of 86 genes was found to be commonly differentially expressed in both investigated groups (GIPR^{dn}-group and bGH-group, see figure 4.17). These 86 genes independently displayed a congeneric direction of differential expression, observed both in the patterns of differential glomerular gene expression between GIPR^{dn}-transgenic vs. their associated wild-type animals, as well as in those of glomerular samples derived from bGH-transgenic vs. their corresponding wild-type animals. The commonly differentially expressed genes in stage I are listed in the appendix (chapter 9.1), indicating their Entrez Gene IDs, official gene symbols and names (NCBI annotations), as well as their mean expression ratio logs (calculated as arithmetic means of expression ratio log values with identical algebraic signs of the respective differentially expressed genes in the single groups of stage I of investigation).

4.3.3.3 Commonly differentially expressed genes in stage II

(intrastadial comparison: [GIPR^{dn} stage II, tg vs. wt] vs. [bGH stage II, tg vs. wt])

Analogous to the approach mentioned above, a number of 469 genes was found to be independently congeneric commonly differentially expressed in both investigated groups (GIPR^{dn}-group and bGH-group) in the defined stage of glomerular hypertrophy with onset of albuminuria (figure 4.17). These genes are as well listed in the appendix (chapter 9.2).

4.3.3.4 Commonly differentially expressed genes in both stages of investigation (inter- and intrastadial comparison: [stage I: GIPR^{dn} vs. bGH] vs. [stage II: GIPR^{dn} vs. bGH])

A number of 21 genes were identified, that independently displayed a congeneric common differential expression in glomerular samples of both GIPR^{dn}- and bGH-transgenic animals in both investigated stages (stage I and stage II) of glomerular alteration (refer to figure 4.17). These genes are listed in table 4.8, indicating their Entrez Gene IDs, official gene symbols and names (NCBI annotations). The indicated mean expression ratio logs (*) were calculated as arithmetic means of expression ratio log values with identical algebraic signs of the respective commonly differentially expressed genes of stage I and stage II.

Table 4.8: Commonly differentially expressed genes in all stages and groups of investigation.

Entrez Gene ID	official symbol	official full name	mean ratio log [*]
12260	C1qb	complement component 1, q subcomponent, beta polypeptide	0.90
11770	Fabp4	fatty acid binding protein 4, adipocyte	0.86
114332	Xlkd1	extra cellular link domain-containing 1	0.84
60361	Ms4a4b	membrane-spanning 4-domains, subfamily A, member 4B	0.68
14129	Fcgr1	Fc receptor, IgG, high affinity I	0.60
21956	Tnnt2	troponin T2, cardiac	0.57
12505	Cd44	CD44 antigen	0.55
20312	Cx3cl1	chemokine (C-X3-C motif) ligand 1	0.52
68922	Dnaic1	dynein, axonemal, intermediate chain 1	0.51
12983	Csf2rb1	colony stimulating factor 2 receptor, beta 1, low-affinity (granulocyte-macrophage)	0.50
545486	2810484G07Rik	RIKEN cDNA 2810484G07 gene: similar to beta tubulin 1, class VI	0.50
20288	Msr1	macrophage scavenger receptor 1	0.47
14702	Gng2	guanine nucleotide binding protein (G protein), gamma 2 subunit	0.46
70598	Filip1	filamin A interacting protein 1	0.46
13058	Cybb	cytochrome b-245, beta polypeptide	0.46
70065	1700030G11Rik	RIKEN cDNA 1700030G11 gene	0.44
17916	Myo1f	myosin IF	043
101160	AI838057	expressed sequence AI838057	-0.60
13036	Ctsh	cathepsin H	-0.63
223473	Npal2	NIPA-like domain containing 2	-0.63
234564	AU018778	expressed sequence AU018778	-1.11
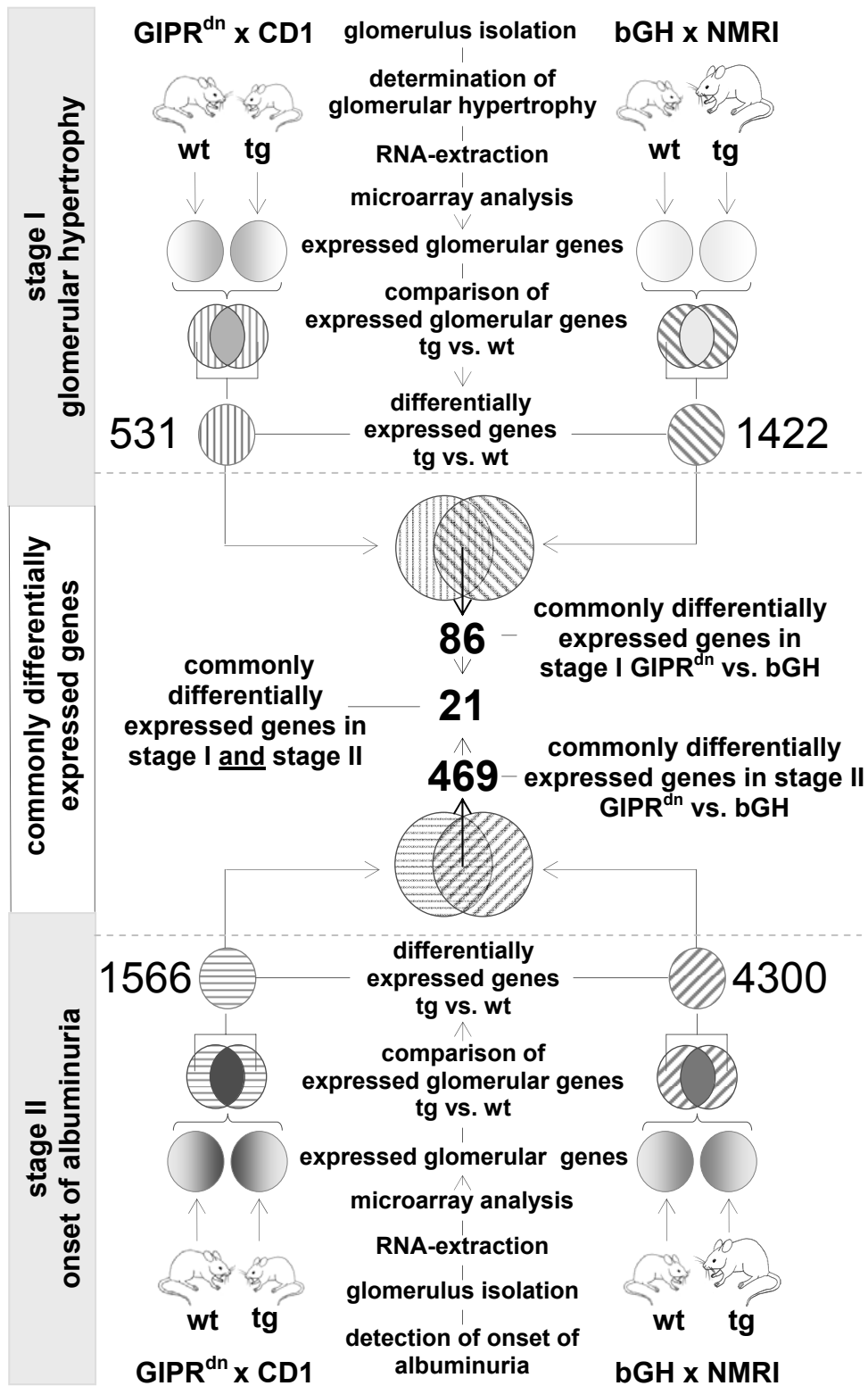
Figure 4.17: Experimental design and numbers of (commonly) differentially expressed genes. Differentially expressed glomerular transcripts (tg vs. wt) were identified in the single stages of investigation in both groups (GIPRdn-group and bGH-group) and assigned to their corresponding genes. Their numbers are indicated as "differentially expressed genes". "Commonly differentially expressed genes", representing the intersections of congeneric differentially expressed genes in both groups in comparable stages) were identified (numbers in bolt), as well as genes that displayed a congeneric common differential expression in all investigated groups and stages (21).

4.3.4 Estimation of statistical enrichment of commonly differentially expressed genes by Monte Carlo simulation

The results of performed Monte Carlo simulations indicate a significant enrichment of numbers of commonly differentially expressed genes within the respective groups and stages of investigation compared to each other. In table 4.9, the settings and results of Monte Carlo simulations are summarized.

Settings and results of Monte Carlo simulations

Comparison		Monte Carlo simulation of random conditions (10,000 simulations per comparision)				observed overlap [6]	Statistical comparison of expected and observed results [7]
		Settings of Monte Carlo simulations		Results of Monte Carlo simulations			
stage	group	[1] Range of source of random numbers	[2] N° of random numbers derived from [1]	Mean of expected random overlaps [5]	Standard deviation of randomly expected overlaps		
I	GIPR^{dn}	1-26,000	**531**	32.36	5.42	86	***
	bGH	1-26,000	**1422**				
II	GIPR^{dn}	1-26,000	**1566**	285.78	14.77	469	***
	bGH	1-26,000	**4300**				
I & II	GIPR^{dn} stage I + bGH stage I	1-26,000	**86** [3]	1.746	1.29	21	***
	GIPR^{dn} stage II + bGH stage II	1-26,000	**469** [4]				

Table 4.9: Settings and results of Monte Carlo Simulations

[1] representing the number of totally expressed glomerular genes

[2] representing the number of differentially expressed glomerular genes (tg vs.wt)

[3] representing the number of commonly differentially expressed genes in stage I

[4] representing the number of commonly differentially expressed genes in stage II

[5] arithmetic mean of the expected number of commonly differentially expressed genes under random conditions(overlaps of 10,000 random simulations)

[6] representing the experimentally observed numbers of commonly differentially expressed genes in the respective intra- and/or interstadial comparisions

[7] level of significance: ***: $p \leq 0.001$

4.3.5 Cluster analyses of common differential expression profiles

Common differential expression profiles of transcripts, detected in glomerular samples derived from tg/wt-pairs of animals assigned to either the first or the second stage of investigation, did not cluster into distinct groups of common genetic backgrounds (figure 4.18). As well, performance of cluster analysis of differential expression profiles of glomerular transcripts that displayed a congeneric common differential expression in all stages and groups of investigation did not allow for separation of distinct subgroups of sample origin (figure 4.19).
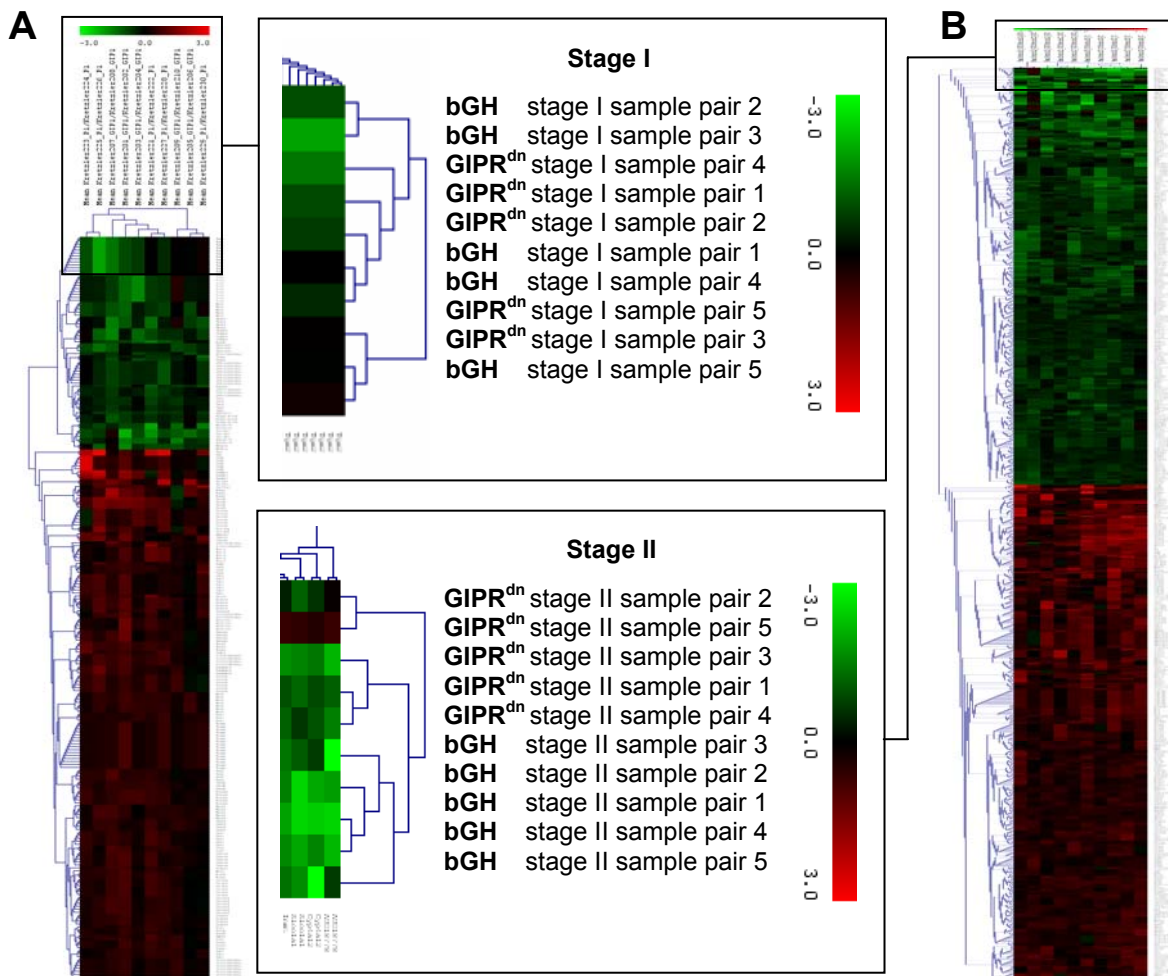
Figure 4.18: Cluster analysis of expression profiles of commonly differentially expressed transcripts in glomerular samples of wt-/tg- pairs of animals of both groups (bGH-group and GIPR^{dn}-group) in stage I (**A**) and stage II (**B**) of investigation. Common differential gene expression profiles were clustered using an Euclidian distance metric hierarchical clustering software tool (MultiExperiment Viewer 4.0). Average linkage clustering was performed to cluster both transcripts and samples. Each raw represents the differential expression profile of one transcript and each column represents the differential expression profile of one pair of animals (wt-/tg). Red squares: transcripts with over-represented abundance in the respective sample of the transgenic animal. Green squares: transcripts with under-represented abundance in the respective sample of the transgenic animal. In both stages of investigation samples did not cluster into distinct groups of common genetic backgrounds.
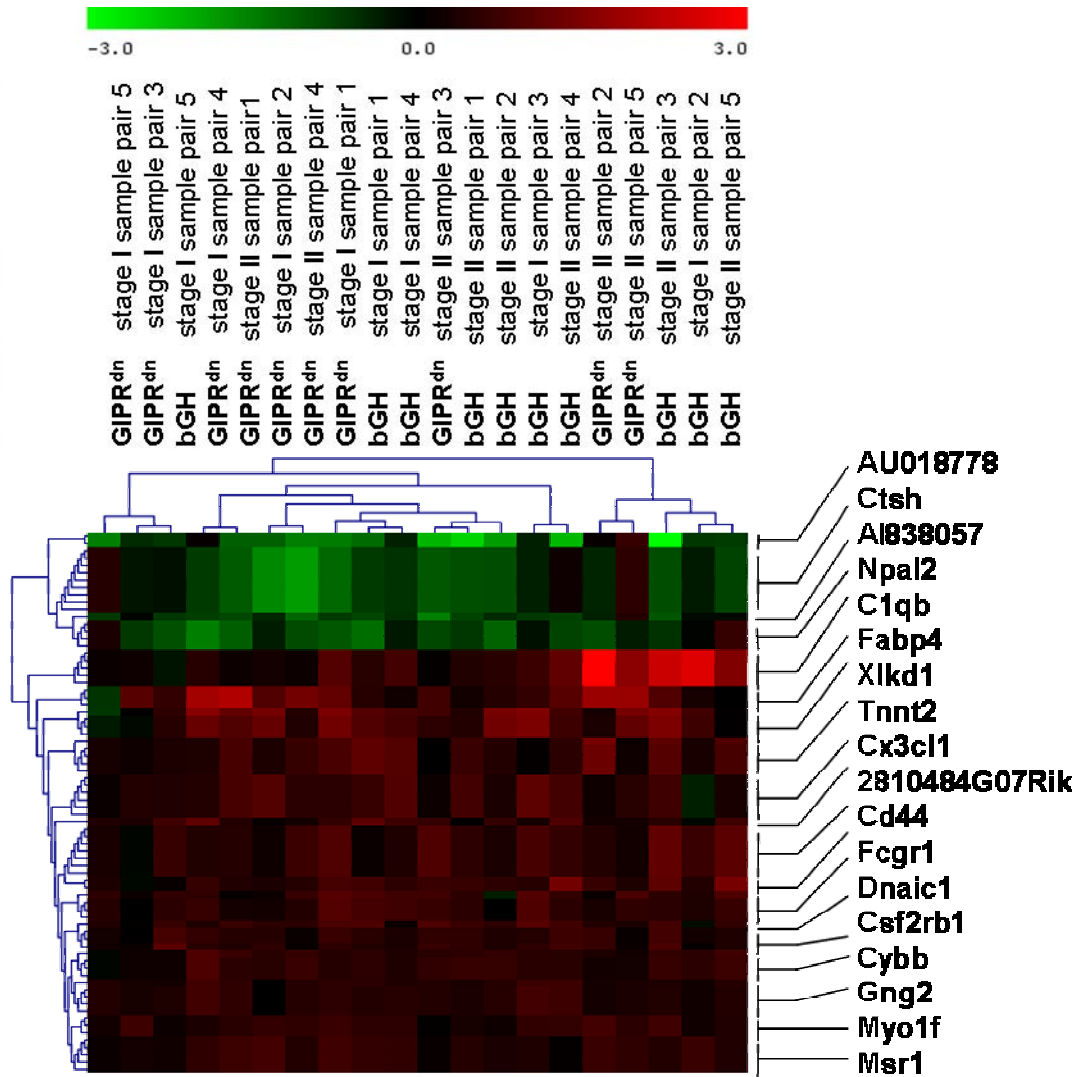
Figure 4.19: Cluster analysis (MultiExperiment Viewer 4.0) of differential expression profiles of commonly differentially expressed transcripts in all stages (stage I and stage II) and groups (bGH-group and GIPR^dn-group) of investigation. Average linkage clustering was performed to cluster both transcripts and samples. Each raw represents the differential expression profile of one transcript and each column represents the differential expression profile of one pair of animals (wt-/tg). Red squares: transcripts with over-represented abundance in the respective sample of the transgenic animal. Green squares: transcripts with under-represented abundance in the respective sample of the transgenic animal. The samples did not cluster into distinct groups of common genetic backgrounds. The names of the 21 commonly differentially regulated genes are indicated by their gene symbols.

4.3.6 Confirmation of array data by real time polymerase chain reaction

The relative expression abundances of five of the 21 genes, that were identified to be commonly differentially expressed in glomerular samples of GIPR^{dn}-transgenic and bGH-transgenic mice (vs. their corresponding non-transgenic wild-type littermate controls) in all investigated stages in the array experiments, were analyzed by performance of quantitative real time PCR, using processed samples of glomerular RNA derived from animals of the Array Cohort and the Independent Control Cohort. Expression levels of three "housekeeping transcripts" (18S rRNA, Gapdh and Cyclophyllin A), were used for calculation of relative expression differences of the respective targets in pairs of samples derived from transgenic animals vs. their associated controls. In the array experiments neither 18S rRNA, nor Gapdh- or Cyclophyllin-mRNA displayed a differential expression in investigated glomerular samples of transgenic mice (vs. controls). Concerning their suitability to serve as reliable "housekeeping genes" for relative quantification of expression abundances of the respective target sequences in real-time PCR experiments, Gapdh and Cyclophyllin concordantly displayed comparable results throughout all investigated samples, whereas glomerular 18S rRNA expressions were found to be relatively heterogeneous. Finally, Cyclophyllin was used as housekeeping transcript in all real-time PCR confirmations of microarray data in the present study. Transcripts coding for FABP4 (fatty acid binding protein 4, adipocyte), MSR1 (macrophage scavenger receptor 1), CX3CL1 (Fractalkine) and the CD44 antigen displayed a significant (FDR < 0.049%) increased expression in the array experiments, whereas Ctsh (cathepsin H) mRNA displayed a decreased expression abundance in glomerular samples of transgenic animals, independent of their different stage- or group-affiliations. The statistically significant congeneric common differential expression of these 5 transcripts was confirmed by real-time PCR (figures 4.20, 4.21 and 4.22). According to the common pattern of differential expression of these transcripts, real-time PCR experiments were performed as "matched-pairs" analyses, by simultaneously comparing all samples of transgenic animals with their corresponding non-transgenic controls (figures 4.21 and 4.22).

Confirmation of array data by real-time PCR: Cx3cl1

Array Cohort

Independent Control Cohort
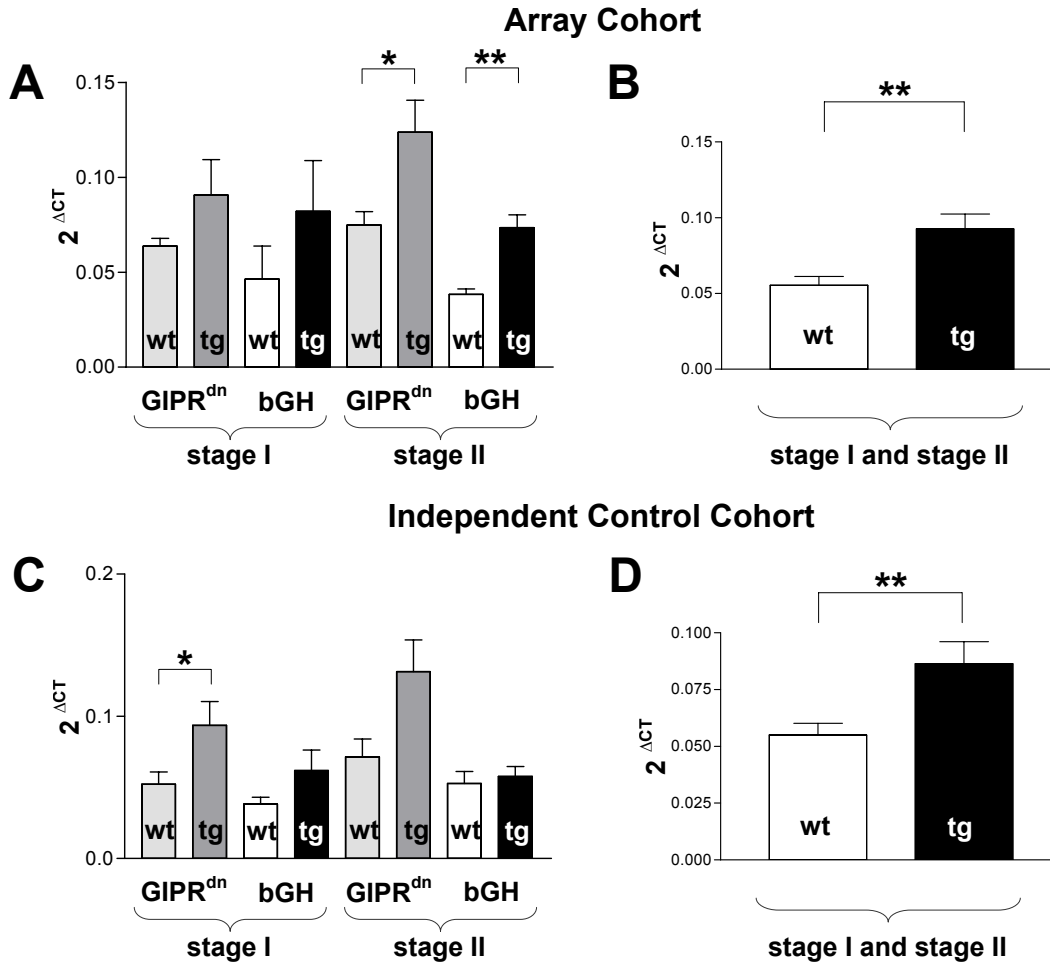
Figure 4.20: Confirmation of array data by real-time PCR: Cx3cl1 (Fractalkine). The applied mode of confirmation of array data by real-time PCR is illustrated. Cyclophyllin served as housekeeping transcript. In the array experiment, Cx3cl1 mRNAs displayed a common differential expression in glomerular samples derived from GIPR^{dn}-transgenic and bGH-transgenic mice (**tg** vs. **wt**) in both stages of investigation in the Array Cohort. In **A**, the result of real-time PCR confirmation for differential expression of Cx3cl1 is shown for each single stage and group of the Array Cohort (n = each 4 samples of GIPR^{dn}-transgenic animals and their associated controls in stage I; n = each 5 samples of GIPR^{dn}-transgenic or bGH-transgenic animals and their associated controls for all other investigated stages), using the same samples of total glomerular RNA analyzed in the array experiments. As Cx3cl1 commonly displayed a significant differential expression between all samples derived from transgenic animals vs. their associated controls in the array experiment, all samples of transgenic animals and all samples derived from their respective controls in the Array Cohort were each merged for performance of a "matched pairs" analysis (**B**). In **C** and **D**, the respective results of real-time PCR confirmation for differential expression of Cx3cl1 in the samples of the Independent Control Cohort are shown (n = each 5 samples of GIPR^{dn}-transgenic, respectively bGH-transgenic animals and their associated controls in stage I; n = each 7 samples of GIPR^{dn}-transgenic animals and their associated controls in stage II; n = each 8 samples of bGH-transgenic animals and their associated controls in stage II). Data are presented as means ± SEM; level of significance: *: p < 0.05; **: p < 0.01 and ***: p < 0.001 vs. controls.

Confirmation of array data by real-time PCR: Cx3cl1

Array Cohort and Independent Control Cohort (merged)
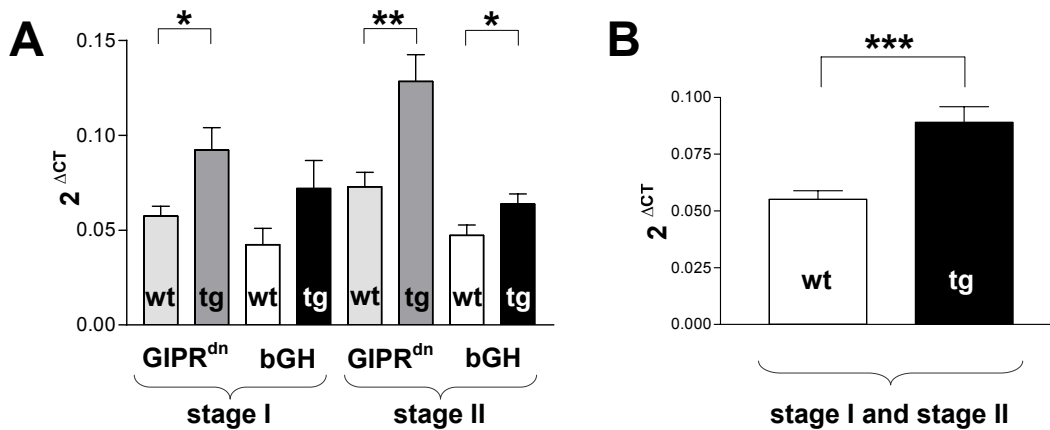
Figure 4.21: Confirmation of array data by real-time PCR: Cx3cl1 (Fractalkine). Detected expression abundances of Cx1cl3 were each related to the expression abundance of Cyclophyllin (housekeeping transcript), detected in the same sample. In **A**, the result of real-time PCR confirmation for differential expression of Cx3cl1 is shown for each single stage and group of all animals investigated in the Array Cohort and the Independent Control Cohort. **B**: Each all samples of transgenic (**tg**) animals and all samples of their respective non-transgenic wild-type controls (**wt**) of the Array Cohort and the Independent Control Cohort were merged for performance of "matched pairs" real-time PCR analysis, confirming the statistically significant differential expression of Cx3cl1. n = 44 samples of transgenic animals (**tg**) and 44 samples of their respective non-transgenic controls (**wt**). Data are presented as means ± SEM; level of significance: *: $p < 0.05$; **: $p < 0.01$ and ***: $p < 0.001$ vs. controls.
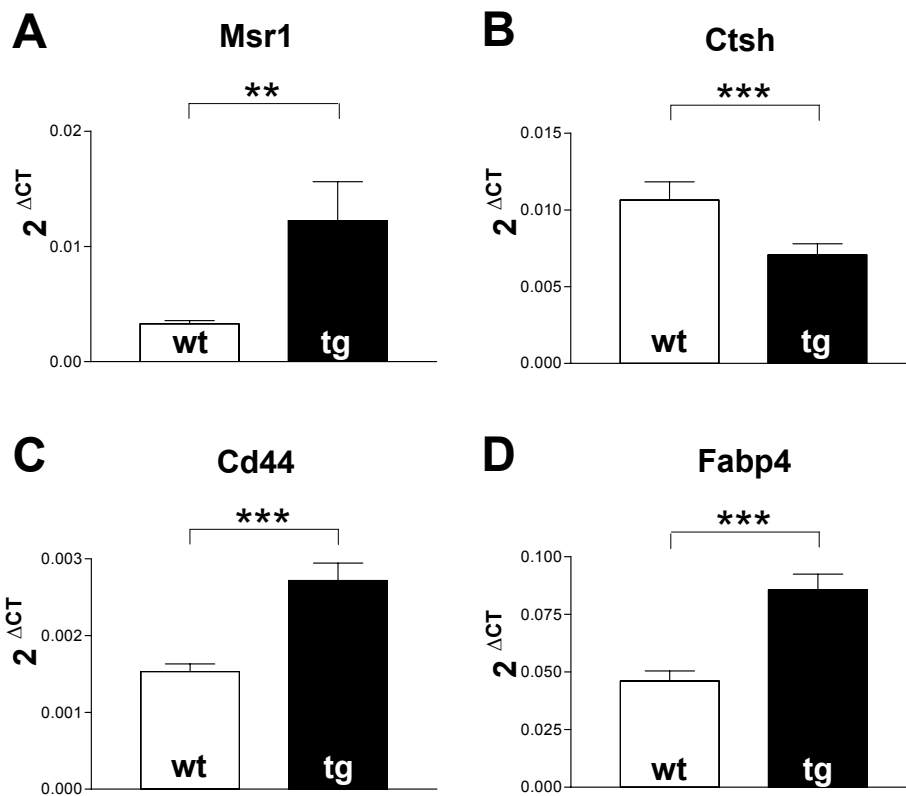
Figure 4.22: Confirmation of array data by real-time PCR. Congeneric common differential expression of selected transcrips, detected in samples of total glomerular RNA of transgenic animals of all groups and stages investigated in the array experiment was confirmed by real-time PCR ("matched pairs" analyses, using samples of total glomerular RNA of animals of the Array Cohort and the Independent Control Cohort). Numbers of samples investigated were each n = 44 samples of transgenic animals (**tg**) and 44 samples of their respective non-transgenic controls (**wt**), except for Cd44: n = 42 samples of transgenic animals and 42 samples of their respective non-transgenic controls. Expression abundances of the respective target-transcripts were each related to the expression abundance of Cyclophyllin (housekeeping transcript), detected in the same sample. Increased expression abundances of macrophage scavenger receptor 1 mRNA (Msr1, **A**), CD44 antigen mRNA (Cd44, **C**) and fatty acid binding protein 4 mRNA (Fabp4, **D**) were confirmed, as well as the decreased expression abundance of cathepsin H mRNA (Ctsh, **B**). Data are presented as means ± SEM; level of significance: **: $p < 0.01$ and ***: $p < 0.001$ vs. controls.

4.3.7 Bioinformatical analysis

4.3.7.1 Molecular functions of gene products of commonly differentially expressed genes in the single stages of investigation

From 86 commonly differentially expressed genes in stage I, 53 could be associated with a known function of their respective gene product. In stage II, 315 from 469 commonly differentially regulated genes were functionally annotated. The diagrams in figure 4.23 and 4.24 illustrate the percentual proportions of the respective molecular functions and subcellular locations of annotated commonly differentially expressed genes (their corresponding proteins, respectively) in stage I and in stage II.
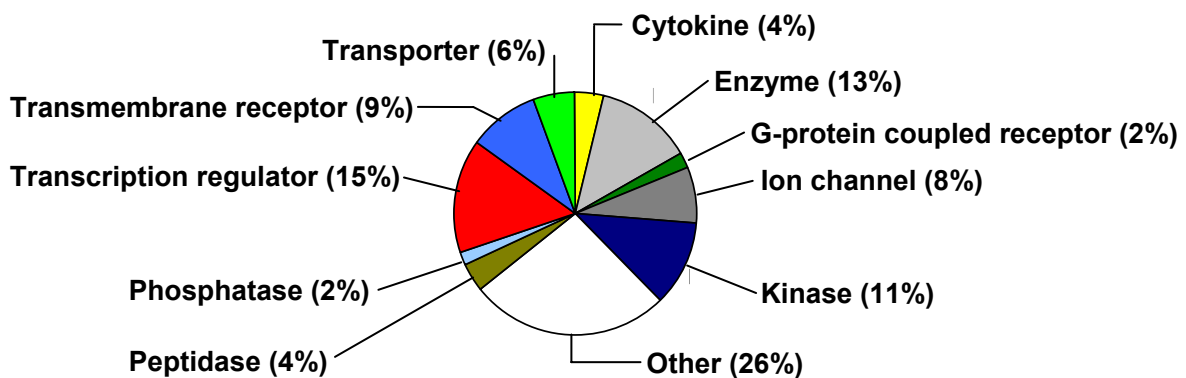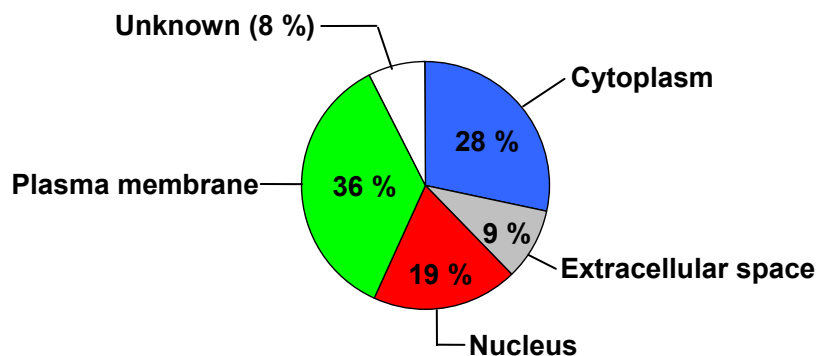
Figure 4.23: Molecular function (A) and subcellular location (B) of commonly differentially expressed genes (their corresponding gene products, respectively) in stage I. Functional annotation of genes was performed, using the Ingenuity Pathways Analysis 5.0 software.

A

Transporter (4%)

Cytokine (3%)

Transmembrane receptor (5%)

Enzyme (14%)

Translation regulator (0%)

G-protein coupled receptor (4%)

Transcription regulator (13%)

Growth factor (4%)

Ion channel (2%)

Phosphatase (2%)

Kinase (5%)

Peptidase (4%)

Ligand dependent nuclear receptor (1%)

Other (39%)

B

Unknown (10 %)

Cytoplasm

23 %

Plasma membrane

27 %

15 %

25 %

Extracellular space

Nucleus
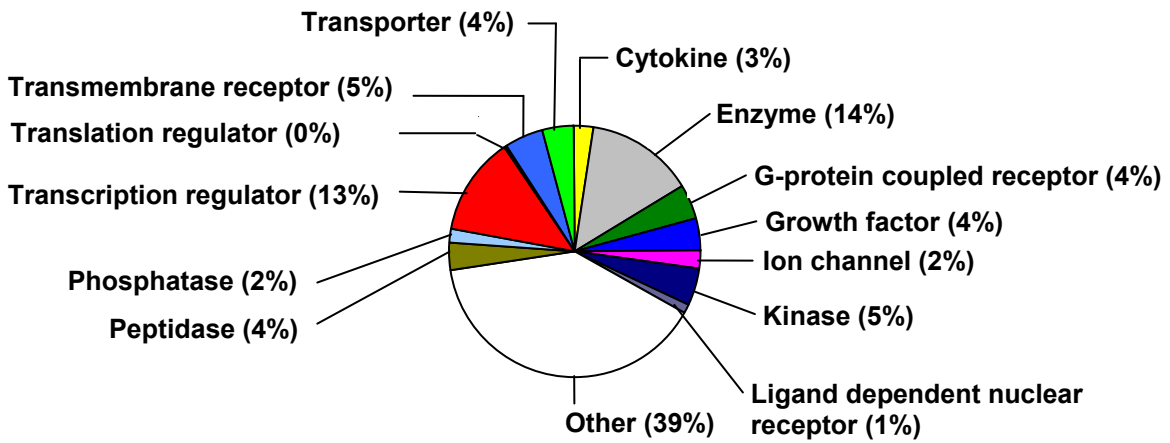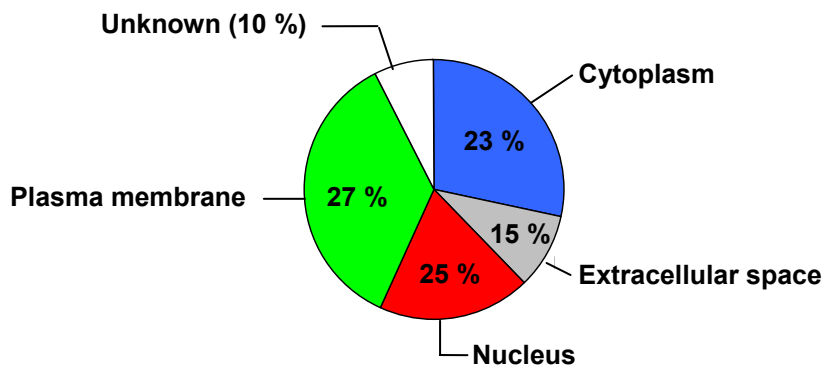
Figure 4.24: Molecular function (A) and subcellular location (B) of commonly differentially expressed genes (their corresponding gene products, respectively) in stage II. Functional annotation of genes was performed, using the Ingenuity Pathways Analysis 5.0 software.

4.3.7.2 Molecular functions and subcellular distributions of gene products of commonly differentially expressed genes in all stages and groups of investigation

From 21 commonly differentially expressed genes in stage I and II, 14 could be associated with a known function of their respective gene product. The diagrams in figure 4.25 illustrate the proportions of the respective molecular functions and subcellular locations of these annotated commonly differentially expressed genes (their corresponding proteins, respecctively) in stage I and II, as well as their numbers and identities.

Molecular function and subcellular location of commonly differentially expressed genes (gene products) in all stages and groups of investigation

A

Other (5):
CD44, C1QB, TNNT2, DNAI1, FILIP1

Cytokine (1): CX3CL1

Enzyme (2): CYBB, GNG2

Peptidase (1): CTSH

Transporter (1): FABP4

Transmembrane receptor (4): XLKD1, CSF2RB, FCGR1A, MSR1

B

Unknown (2): DNAI1, FILIP1

Cytoplasm (4): CYBB, TNNT2, CTSH, FABP4

Plasma membrane (6): GNG2, CD44, XLKD1, CSF2RB, FCGR1A, MSR1
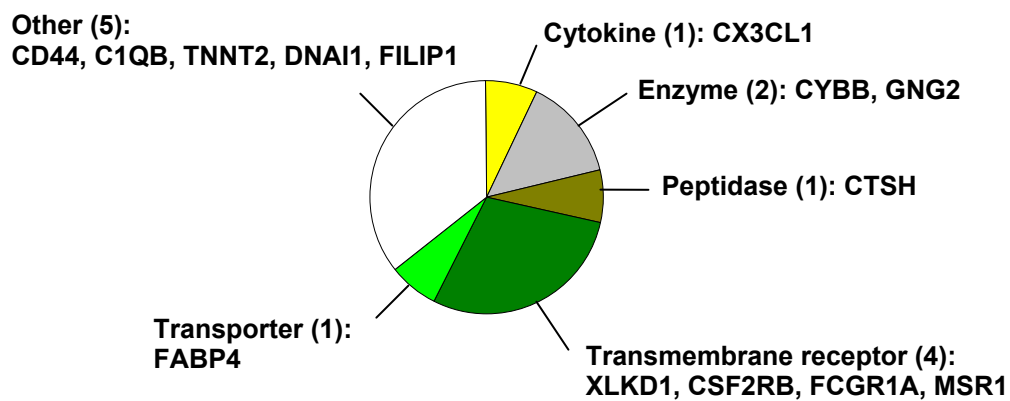
Extracellular space (2): CX3CL1, C1QB
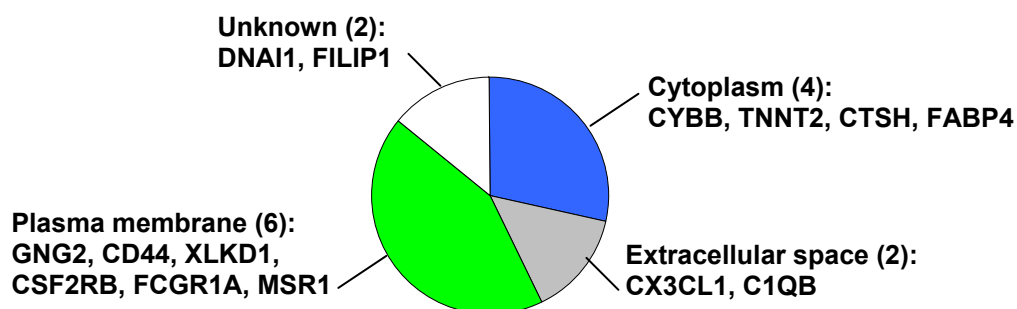
Figure 4.25: Molecular functions (A) and subcellular locations (B) of commonly differentially expressed genes (their corresponding gene products, respectively) in all stages and groups of investigation. The numbers and identities of the respective genes/gene products are indicated.

4.3.7.3 Identification of known interactions of single gene products corresponding to commonly differentially expressed genes in all stages and groups of investigation

Interactions of single gene products with known functions, corresponding to commonly differentially expressed genes in all stages and groups of investigation, which have been described in the literature, were identified, using the BiblioSphere® software. Co-citations of nine of these respective genes or their products, at least on the level of abstracts, were used to generate an interaction network (figure 4.26) of these genes (their corresponding gene products, respectively).
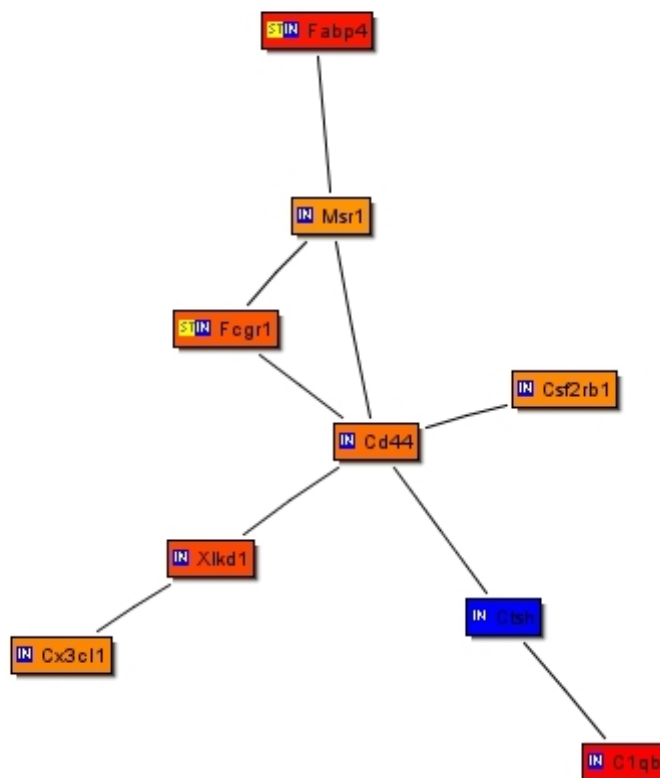
Figure 4.26: Literature based interaction network (BiblioSphere®) of gene products with known function generated from the dataset of commonly differentially expressed genes in all stages and groups of investigation. Gene symbols are indicated. Red colour corresponds to a detected increased abundance of transcripts of the respective genes at the given level of statistical significance (FDR < 0.049%) in glomerular samples derived from transgenic animals, whereas blue colour indicates "down-regulation" (Ctsh). Connections of gene nodes indicate co-citations of the respective genes/gene products in the literature, at least on the level of abstracts.

5. Discussion

5.1 General aspects

The present study addressed the question if common patterns of morphological and functional glomerular alterations, such as glomerular hypertrophy and consecutive development of albuminuria, which represent pathogenetically relevant common characteristic features of early stages of glomerulosclerotic alterations in various progressive kidney diseases (Fogo and Ichikawa 1991, Klahr et al. 1988, Remuzzi 1995, Wiggins 2007), would also find a reflection in detectable common glomerular gene expression profiles. Therefore differential gene expression profiles of samples of isolated kidney glomeruli from two different, well established transgenic mouse models of nephropathy of different genetic backgrounds were identified by performance of microarray analyses. As diabetic nephropathy represents the most common disease in humans that is prone to development of CKD leading to ESRD (Alebiosu and Ayodele 2005, Mitka 2005, Wolf and Ziyadeh 2007) and development of progressive glomerulosclerosis is common to most of the different entities of CKD (Fogo and Ichikawa 1989, Fogo 1999, Mauer et al. 1992), experiments were performed in a mouse model of diabetes mellitus associated nephropathy, GIPR^{dn}-transgenic mice (Herbach 2002, Herbach et al. 2005, Herbach et al. 2003, Schairer 2006, Volz 1997) and in bGH-transgenic mice, a non-diabetic model of progressive glomerulosclerosis (Doi et al. 1990, Doi et al. 1988, Wanke 1996, Wanke et al. 1993, Wanke et al. 2001). According to comparable extents of morphological and functional glomerular alterations of the respective transgenic animals, pairs of male transgenic mice and their corresponding non-transgenic littermate controls of both experimental models were investigated in two early stages of glomerular alteration. These stages were defined as the stage of glomerular hypertrophy (stage I) and the stage of glomerular hypertrophy with onset of albuminuria (stage II). In each investigated model and stage, transcripts that were differentially expressed in glomerular samples of transgenic animals vs. their corresponding controls were identified. Then commonly differentially expressed transcripts, representing the intersections of congeneric differentially expressed transcripts in both investigated models in comparable stages of glomerular alteration were identified. The respective numbers of genes corresponding to these commonly differentially expressed transcripts were found to be significantly enriched between the investigated models of nephropathy.

Thus, the identified common patterns of glomerular gene expression profiles in early comparable stages of glomerular alteration can be considered to be independent of the different mechanisms (diabetes mellitus vs. elevated systemic levels of GH resulting from overexpression of the bGH-transgene) that are responsible for development of glomerular damage in the respective mouse models, as well as independent of their different genetic backgrounds. A number of 21 genes displayed a congeneric common differential expression in glomerular samples of both GIPR[dn]-transgenic and bGH-transgenic mice in both investigated stages of glomerular alteration, representing a shared gene expression profile of glomerular hypertrophy and beginning albuminuria. Finally, the common differential expression of five (Cx3cl1, Ctsh, Fabp4, Cd44 and Msr1) of these 21 genes was confirmed by performance of real-time PCR.

5.2 Experimental design

Standardization of the investigated biological models, as well as characterization and definition of investigated sample materials are most important issues in the experimental design of a transcript profiling experiment. Identification of differential gene expression profiles related to processes of biological significance and meaningful interpretation of obtained microarray data strongly depend on the comparability of investigated sample materials, regarding their origin, mode of generation, processing and quality. Effects of unintended and/or artificial differences concerning these sample characteristics, will probably appear as systematic differences in the detected gene expression profiles but might not be recognized as those and therefore lead to misinterpretations of generated datasets. Therefore, great emphasis was laid on identical treatment of animals and application of stringent criteria on the definition of the respective stages of glomerular alteration, as well as on standardized methods of generation of sample materials of highest qualities. This was considered to be an important prerequisite for assurance of the comparability of the investigated stages of nephropathy in the different animal models, as well as for a meaningful interpretation and linkage of obtained analysis data to distinct morphological and functional glomerular alterations.

Due to the fact that glomeruli represent only a small percentage of the kidney cortex volume (Artacho-Perula et al. 1993, Nyengaard and Bendtsen 1992, Wanke 1996), the interpretation of gene expression data from investigations of total kidney tissue always inherits the danger of nonobservance of signals actually derived from glomerular cells, as those signals become overlaid by stronger signals derived from other kidney cell types (Cohen and Kretzler 2003). To overcome these difficulties, transcript profiling analyses were performed on samples of isolated glomeruli. This strategy allows for a reliable linkage of obtained analysis results to cells of the glomerular compartment (Cohen and Kretzler 2003) and has successfully been applied in several studies of human disease, as well as in various animal experimental models of nephropathy (Baelde et al. 2004, Cohen and Kretzler 2002, Higgins et al. 2004, Makino et al. 2006).

The time points of development of the distinct investigated stages of glomerular alteration (glomerular hypertrophy and glomerular hypertrophy with onset of albuminuria) display considerable individual variances in GIPR^{dn}-transgenic animals (Herbach 2002, Schairer 2006). Thus, the identification of shared glomerular gene expression profiles linked to these defined early stages of glomerular alterations excluded the possibility of performance of investigation of groups of animals of identical ages. Therefore, assignment of littermate pairs of transgenic animals and their associated non-transgenic wild-type controls of both investigated mouse models to either the stage of glomerular hypertrophy or the stage of onset of albuminuria was exclusively performed according to the detected degree of the increase of the mean glomerular volume or the onset of albuminuria in the transgenic mouse vs. its corresponding control. Both parameters, glomerular hypertrophy and onset of albuminuria, were determined using adequate methods of quantitative stereology (Hirose et al. 1982, Sanden et al. 2003, Sterio 1984, Weibel 1979, Weibel 1980, Weibel and Gomez 1962), and SDS-PAGE and ELISA-based approaches of urine protein analysis, respectively (Doi et al. 1990, Yamada et al. 1994). Although the generation of the required numbers of samples demanded for performance of comprehensive morphological and functional investigations in a large number of animals, these efforts allowed for generation of well defined comparable sample materials of isolated glomeruli for performance of transcript profiling analyses.

5.3 Quality of glomerulus isolates

The experimental design of the superordinated project of the present study scheduled the generation of samples of glomerulus isolates from each animal in quantities and qualities allowing for performance of both transcript profiling and proteomic analyses (refer to chapter 1). Currently, the only available method for glomerulus isolation from murine kidney tissue, capable to generate glomerulus isolates in sufficient quantities and purities for performance of these analyses, is based on perfusion of kidneys with spherical paramagnetic beads and subsequent isolation of glomeruli in a strong magnetic field (Barati et al. 2007, Sitek et al. 2006, Takemoto et al. 2002). In the present study, the protocol of the original method was individually modified to meet the respective demands of the different intended analytical procedures under standardized conditions (Blutke et al. 2005). These modifications included the development of a perfusion device (Blutke 2006), allowing for performance of perfusions under defined pressure conditions, and a "mini-cell strainer" for concentration of isolated glomeruli in an adequate volume of RNA stabilization reagent (Blutke et al. 2005). The final protocol reproducibly allowed for fast (~75 minutes) isolation of maximal numbers (~6000) of intact glomeruli under defined temperature conditions. Consistent with the original study (Takemoto et al. 2002), no signs of morphological damage of glomerular structures, as a potential consequence of perfusion with magnetic beads or Collagenase treatment of kidney tissue were observed.

Transcript profiling analyses can successfully be performed on samples consisting of only minimal numbers (~ one dozen) of isolated glomeruli (Cohen and Kretzler 2003) for example derived from biopsies, or even on single glomerular cells (Schroppel et al. 1998). However, these approaches principally suffer from the low amount of available glomerular RNA, which is limiting the number of possible experiments to be performed on these samples (Yasuda et al. 2006). These approaches also inherit the danger of occurrence of systematic sampling errors due to examination of limited numbers of glomeruli derived from only a few locations of the renal cortex (Cohen and Kretzler 2003). Therefore it remains questionable, if transcriptomic data obtained from examination of such low numbers of glomeruli is actually capable to provide a representative snapshot mirroring common alterations of gene expression profiles of the majority of glomeruli present in early stages of chronic kidney disease.

In order to provide samples of sufficient quantities of isolated glomeruli in comparable and highest qualities for performance of transcript profiling analyses, at least 1000 isolated glomeruli per sample were individually picked from a defined aliquot of the total isolate. To avoid systematic sampling errors due to preferential selection of e.g. large glomeruli, all identifiable glomeruli present in a respective aliquot were gathered. The purity of each sample was examined by visual inspection and further analyses were only applied on glomerular samples of highest purities (~ 98-100%). Yet it is important to mention that about 5% to 20% of isolated glomeruli were not lacking the Bowman's capsule and some of them had part of the afferent and/or efferent arterioles still attached. A higher degree of absence of non glomerular tissues in glomerulus isolates can only be achieved by performance of microdissection techniques, which were not applicable in the present study, as they provide only small numbers of glomeruli (Cohen and Kretzler 2002). The effectiveness of tissue separation in investigated glomerulus isolates was also confirmed by real-time PCR analysis of nephron specific gene expression patterns as Wilms' tumor antigen 1, a marker for glomerular epithelial cells. The Wt-1/Gapdh ratio was considerably higher (362x) in the glomerular specimens compared to samples of total cortical kidney tissue, which stands in accordance with findings of other studies (Cohen et al. 2002). The high and comparable quality of all samples of total RNA extracted from glomerulus isolates was confirmed by microfluid electrophoresis.

An interesting finding was that the average amounts of total RNA isolated from glomerular samples of mice of CD1 background (GIPR^{dn}-group) were averagely only about 50% of the respective yields attained in samples of mice of NMRI background (bGH-group). Next to a dependency on the genetic background of investigated animal models, another plausible explanation for that finding might lie in young age of the animals investigated in the bGH-group. This might be responsible for a stronger transcriptional activity in the still growing glomeruli of these animals and therefore a higher content of RNA. Although the glomeruli of transgenic animals were significantly larger than those of their associated control mice, the attained yields of total RNA, isolated from glomerular samples of transgenic animals vs. their associated controls did not display explicit differences in each of the investigated models of nephropathy.

5.4 Morphological and functional investigations

5.4.1 Histology

The histological findings confirmed that the detected glomerular lesions of GIPR^{dn}- and bGH-transgenic animals in both stages of investigation represented very early stages of development of glomerulosclerotic alterations (mesangial expansion and hypercellularity, as well as mild mesangial matrix accumulation), as intended by the experimental design of the study.

5.4.2 Glomerular hypertrophy and numbers of cells per glomerulus

For estimation of the mean glomerular volumes of transgenic mice and their associated non-transgenic controls, GMA/MMA embedded kidney sections were investigated, using a well established, fast model-based stereological approach, in which glomeruli are considered as rotation ellipsoids (Hirose et al. 1982, Wanke 1996, Weibel and Gomez 1962). Compared to assumption free methods of determination of the mean glomerular volume (Cavalieri and disektor methods), the applied Weibel-Gomez approach does not systematically overestimate the obtained values (Pesce 1998). The number of glomerular profiles investigated in each case was sufficient (Hirose et al. 1982, Lane et al. 1992) for generation of robust data and reliably allowed for identification of glomerular hypertrophy in the respective samples of investigated animals. Irrespective of their affiliation to one of the investigated animal models or stages of glomerular alteration, transgenic animals investigated in the microarray experiments displayed significant glomerular hypertrophy compared to their associated controls. This was marked by a significant increase of at least 40% of the mean glomerular volumes, as well as by an overproportional increase of glomerular size in relation to both body or kidney weight. So far, the present findings concerning development of glomerular hypertrophy in GH-transgenic mice are consistent with those of previous studies (Doi et al. 1990, Fisch 2004, Wanke 1996). However, most of these studies were performed on animals of elder age or in models overexpressing different GH-fusion transgenes and thus, the detected absolute values of the estimated mean glomerular volumes in these experiments were partially larger than the respective ones measured in the present study. In mice, approximately 80% of glomeruli continue to form and differentiate after birth, a process completed by two weeks post partum (Gilbert et al. 1987, Yuan et al. 1999).

In mice, the mean glomerular volume physiologically increases continuously up to 7 weeks of age and remains stable thereafter (Doi et al. 1990). In GH-transgenic mice, a significant increase of the mean glomerular volume can already be detected in the juvenile kidney as early as at 4 weeks of age (Doi et al. 1990). In all samples of GH-transgenic mice and their corresponding control animals investigated in the present study, glomeruli displayed a mature phenotype. For these reasons, there was no evidence that the young age of mice investigated in the bGH-groups of the present study might exhibit a distorting unconsidered influence on interpretation of the gene expression profiles assessed by analysis of samples of isolated glomeruli derived from these animals. The development of glomerular hypertrophy, as a characteristic feature of diabetic nephropathy (Cortes et al. 1987, Mogensen et al. 1983, Osterby and Gundersen 1975, Seyer-Hansen et al. 1980), was also observed in the diabetic $GIPR^{dn}$-transgenic animals in both investigated stages of nephropathy. In male $GIPR^{dn}$-transgenic animals, development of absolute (mean $v_{(glom)}$) and relative glomerular hypertrophy (mean glomerular volume to body weight or kidney weight ratios) has been reported to occur between nine and twenty weeks of age (Schairer 2006), which is in line with the findings in the present study. Mirroring the progressive character of development of glomerular hypertrophy in both animal models, the observed differences of the mean glomerular volumes of transgenic animals compared to their associated controls increased on the average from 45% in $GIPR^{dn}$-transgenic animals and 58% in bGH-transgenic animals investigated in stage one, to 59% and 63%, respectively in stage two. Development of glomerular hypertrophy is not only characterized by an increase of the glomerular volume, due to an increase of the volume of glomerular cells and extracellular matrix, or growth of glomerular capillaries, but also by increasing numbers of cells per glomerulus (Wanke 1996, Wiggins et al. 2005). Therefore, quantitative stereological analyses were performed to estimate the total numbers of cells per glomerulus. The respective numbers of cells of distinct glomerular cell types per glomerulus were determined, to allow for a further distinct definition of the degree of glomerular alterations. For estimation of the numbers of glomerular cells in semithin sections of cortical kidney tissue, the so-called "disector" method was applied (Sterio 1984). The disector method is generally accepted to be one of the most accurate and reliable approaches (Gundersen 1986) among the various methods that can be applied for determination of glomerular cell numbers (Sanden et al. 2003).

As a 3-dimensional stereological probe, it allows unbiased and assumption free counting and sizing of particles (Sterio 1984). Reliable results of determined volume densities of different cell types can already be obtained from counting a number of about 50 particles per case (Gundersen 1986). In the present study the differentiation of distinct glomerular cell types was restricted to distinction between podocytes and non-podocytic (mesangial and endothelial) glomerular cells. Since a reliable differentiation of endothelial vs. mesangial cells/nuclei by evaluation of electron microscopic photographs was not in the scope of interest, investigations were performed on the level of light microscopy, accepting the potential risk of accidental non-identification of podocytes localized in the centre of the glomerular tuft, which is rather marginal, as podocytes of rodent glomeruli tend to congregate on the periphery of the glomerular tuft (Sanden et al. 2003). In both investigated groups and stages of nephropathy, the estimated number of endothelial and mesangial cells per glomerulus was significantly increased in transgenic animals vs. their respective controls, while the number of podocytes per glomerulus remained almost unchanged. These findings are characteristic for development of glomerular hypertrophy and have been described to occur in various chronic kidney diseases of man and animal experimental models (Kretzler et al. 1994, Wanke et al. 2001, Wiggins et al. 2005, Wiggins 2007). They also stand in line with the postulated pathogenetic mechanisms for development of glomerulosclerotic lesions and the progression of chronic kidney disease (Kretzler et al. 1994, Kriz 1996, Kriz et al. 1994, Shankland 2006, Wanke et al. 2001), which consider the inability of podocytes to functionally adapt to the circumstances of developing glomerular hypertrophy to be the determinant key mechanism triggering glomerulosclerosis. Concerning the estimated numbers of the respective glomerular cells per glomerulus in bGH-transgenic mice, the relative differences between transgenic mice and their corresponding control animals are confirmed by similar findings of other studies (Wanke 1996), whereas the respective values of these numbers detected in the present study were slightly smaller than in other studies. A supposable explanation for these differences lies in the investigation of GH-transgenic mice overexpressing a different GH-fusion transgene (MTbGH), as well as of animals of different ages (Wanke 1996). Concerning the numbers of glomerular cells in GIPR[dn]-transgenic mice, the present study was the first to examine this parameter.

5.4.3 Thickness of the glomerular basement membrane

The increase of the thickness of the peripheral glomerular basement membrane (GBM) is a characteristic early histopathological finding in human diabetic nephropathy (Chavers et al. 1989, Mauer et al. 1984). GBM-thickening has also been reported in several but not all diabetic mouse models (Carlson et al. 1997, Fujimoto et al. 2003, Hammad et al. 2003, Hong et al. 2001). Possible mechanisms for the thickening of the GBM could be an increased matrix synthesis (Van Vliet et al. 2001) or decreased degradation, deposition of circulating proteins in the GBM (Kerjaschki et al. 1987), or alterations in GBM assembly (Velling et al. 2002). In this context, also podocytes are considered to play a crucial role for GBM dynamics and maintenance in health and disease (Martin et al. 1998, Pavenstadt et al. 2003). The findings concerning the increased true harmonic mean thickness of the peripheral GBM of the diabetic GIPR^{dn}-transgenic animals investigated in stage II of the present study would therefore stand in line with the results of several other studies. Although the detected increase in GBM thickness in GIPR^{dn}-transgenic animals did reach statistical significance, the absolute average increase yet comprised of only 19 nm or approximately 14%, whereas other studies in human diabetic nephropathy or in animal models of podocyte damage associated with increasing GBM thicknesses report of increases of GBM thickness exceeding 20 % (Drummond and Mauer 2002, El-Aouni et al. 2006). Current investigations in GIPR^{dn}-transgenic mice with progressed renal alterations will provide additional results concerning the increase of GBM-thickness in this animal model. In GH-transgenic animals, increases of the glomerular basement membrane thickness have not been detected so far (Wanke 1996). However, in these studies a different method was applied for determination of the GBM-thickness (Osawa et al. 1966), investigated animals were of elder age and overexpressed another GH-fusion-transgene than the PEPCKbGH-transgenic animals investigated in the present study.

5.4.4 Filtration slit frequency

The filtration slit frequency, determined in peripheral glomerular capillary loops of transgenic animals of both investigated animal models did not show a significant difference to the FSF of the corresponding non-transgenic littermate controls in the stage of onset of albuminuria. Decreased filtration slit frequencies, preceeding proteinuria have been reported in various observations of human disease, as well as in animal experiments (Inokuchi et al. 1996, Shirato 2002). The spatial frequency of filtration slits is considered to be a very important determinant of the overall hydraulic permeability, in keeping with observations in several glomerular diseases in humans. Reductions in filtration slit frequency reflect broadening and "effacement" of the epithelial foot processes, a uniform finding in virtually all humans with the nephrotic syndrome, regardless of its aetiology (Drumond et al. 1994). However, there are also reports of human chronic kidney disease as diabetic nephropathy and results from animal experiments, where albuminuria occurred without a change in the frequencies of glomerular filtration slits (Benigni et al. 2004, El-Aouni et al. 2006, Kalluri 2006). Several divergent opinions exist concerning a causative linkage of appearance of microalbuminuria and the morphological equivalents of podocyte damage, which comprise foot process effacement, detectable alterations of the filtration slits, or the FSF (Inokuchi et al. 1996, Seefeldt et al. 1981, Shankland 2006, Shirato 2002, Shumway and Gambert 2002). For determination of the FSF in the present study, a relatively large number of filtration slits (1100) was counted per animal. However, it also has to be taken into consideration that investigations were performed in a very early stage of glomerular alteration. In developing glomerulosclerosis, early alterations typically affect different glomeruli in the diseased kidney to different extents. Therefore, the detection of onset of albuminuria does not require a damage of the glomerular filtration barrier in all glomeruli. Thus, it is obvious that the detection of an unaltered FSF does not exclude a reduction of this parameter in the glomeruli that are affected by a severe impairment of the filtration barriers function and therefore responsible for the detected onset of albuminuria. Thus, an unaltered FSF in the stage of onset of albuminuria actually supports the intended investigation of transgenic animals at the earliest time point at which persistent albuminuria was detectable.

5.4.5 Urine analyses

Occurrence of albuminuria as a consequence of developing glomerulopathy impairing the function of the glomerular filtration barrier, has been documented extensively in several studies for both GIPR[dn]- and bGH-transgenic mice (Doi et al. 1990, Fisch 2004, Herbach 2002, Schairer 2006, Wanke 1996). Thus, in the present study the comprehensive SDS-PAGE analyses of urine protein excretion patterns were performed as a screening method to allow for an accurate definition of a distinct stage of functional glomerular alteration (onset of albuminuria in transgenic animals assigned to stage II and absence of albuminuria in stage I). Assignment of pairs of transgenic animals and their corresponding non-transgenic controls to the respective stages of investigation was performed in accordance to the results of these analyses. The suitability of SDS-PAGE analyses of urine samples for detection of albuminuria and urine protein profiles has been demonstrated in various studies (Doi et al. 1990, Fisch 2004, Herbach 2002, Oser and Boesken 1993, Schairer 2006, Wanke 1996, Yamada et al. 1994). Urine creatinine concentrations of GIPR[dn]-transgenic mice were drastically reduced compared to those of their corresponding controls (by 94% in stage I and stage II). This is a characteristic finding in the transgenic animals of this model of diabetes mellitus, displaying massive polyuria and hyposthenuria (Herbach 2002, Schairer 2006). Consistent with other findings (Herbach et al. 2005), all GIPR[dn]-transgenic mice displayed glucosuria as early as from day 21 onwards. The reduced creatinine concentrations detected in urine samples of PEPCKbGH-transgenic animals (30% in stage I and 62% in stage II vs. controls) are in line with the results of previous studies (Fisch 2004). To allow for a comparison of albumin band intensities detected in SDS-PAGE gels of samples derived from transgenic mice and their associated non-transgenic control animals, urine samples were each diluted to identical urine creatinine concentrations. Urine samples of GH-transgenic animals and their associated controls were diluted to a creatinine concentration of 3 mg/dl for performance of Coomassie blue staining of SDS-PAGE gels, whereas the low creatinine concentrations in urine samples of GIPR[dn]-transgenic animals only allowed for a dilution to a creatinine concentration of 1.5 mg/dl and required for performance of a silver staining of SDS-PAGE gels. The comparability of results of SDS-PAGE urine protein analyses, using a silver staining method of gels and respective results of Coomassie blue stained gels was confirmed.

As staining intensities of bands of identical amounts of albumin may vary from one SDS-PAGE gel to another, urine samples of transgenic mice and their associated controls were run on identical gels and comparisons of albumin band intensities between these samples were also exclusively performed in identical gels. Closely defined intervals of recurrent SDS-PAGE analyses of spot urine samples of both transgenic animals and their associated non-transgenic controls allowed for an accurate determination of the time point of onset of albuminuria in transgenic mice, as well as for confirmation of absence of albuminuria in urine samples of non-transgenic control animals. In order to eliminate the risk of detection of transient albuminuria, both positive and negative results were confirmed by a second congeneric result, detected in an independent urine sample taken from the same animal after 24 hours.

Transgenic animals assigned to stage I, as well as all non-transgenic mice of both investigated experimental models in both stages of glomerular alteration did not display albuminuria in the SDS-PAGE gels at any point of time. Transgenic animals of both investigated groups assigned to stage II displayed albuminuria twice within 48 hours prior to dissection, after a first negative result. Western-blot experiments confirmed the presence of albuminuria detected by SDS-PAGE based urine protein analyses. GIPR^{dn}-transgenic mice reached the stage of onset of albuminuria between 70 to 155 days (average: 112 ± 37 d) of age. This frame of time, as well as the quite broad variance of ages is consistent with previous findings (Herbach 2002, Schairer 2006), and suggests strong impacts of individual, dietary and yet unknown influences on the time point of development of albuminuria in GIPR^{dn}-transgenic mice. Compared to the later onset of albuminuria in GIPR^{dn}-transgenic mice, the respective findings in SDS-PAGE analyses of urine samples of bGH-transgenic mice demonstrate an early and reproducible onset of albuminuria (average: 32 ± 2 d), which is characteristic for the accelerated progression of development of renal alterations in this animal model (Doi et al. 1990, Wanke 1996). As well, the patterns of urine protein profiles detected in SDS-PAGE gels of bGH-transgenic mice accord with previous findings (Fisch 2004, Wanke 1996). Urine of bGH-transgenic mice displayed reduced concentrations of major urinary proteins (MUPs), which is a characteristic finding in male GH-transgenic mice (Wanke 1996). Normal MUP synthesis requires a pulsatile GH secretion, whereas constant high GH levels cause a reduction in hepatic synthesis of MUPs (Johnson et al. 1995, Norstedt and Palmiter 1984).

Although performance of SDS-PAGE analysis of urine samples allows for a sensitive detection of presence of albuminuria, this method has only a qualitative or at most semi-quantitative character. To confirm the presence (or absence, respectively) of albuminuria of animals investigated in the present study, urine albumin concentrations were additionally quantified by ELISA as a second independent methodological approach, using the same urine samples.

Since diabetic GIPR^{dn}-transgenic animals display massive hyposthenuria and polyuria, urine albumin concentrations, measured in spot urine samples of these mice cannot be compared directly to albumin concentrations measured in urine samples of wild-type animals. Comparisons of the absolute urine albumin excretions per day of transgenic animals vs. their corresponding non-transgenic wild-type controls would require the collection of 24-hours urine samples, which was not conformable with the experimental design of the study. Therefore, spot urine albumin/creatinine ratios were used for comparison of the respective urine samples of transgenic vs. control mice (Abitbol et al. 1990, Doi et al. 1990, Fisch 2004). In both investigated murine models of nephropathy, the measured urinary albumin/creatinine-ratios were significantly elevated in samples of transgenic animals assigned to stage II, whereas those of transgenic mice investigated in stage I did not display a significant difference to their corresponding non-transgenic controls. These findings confirmed the results of the SDS-PAGE based screenings and agree with the results of previous studies (Fisch 2004). However, results of the ELISA experiments indicated a beginning tendency towards increased urine albumin/creatinine ratios in urine samples of GIPR^{dn}-transgenic animals assigned to stage I, which was not evident in the SDS-PAGE based screenings. In summary, nearly all applicable approaches for a comprehensive definition of the functional parameter of onset of albuminuria were applied in order to characterize the investigated stage of nephropathy in both different animal models. Regarding this parameter, the sophisticated schedules, as well as the results of the different performed analyses represent a reliable basis for the comparability of the investigated stage of functional glomerular alteration in both animal models of nephropathy.

5.4.6 Ages of animals and further parameters

Following the strategy for performance of investigations in defined comparable stages of glomerular alteration, exclusively characterized by distinct morphological and functional aspects, resulted in the basic necessity of investigation of subgroups, compiled of animals of different and variable ages. Further parameters, as body weight, kidney weight and relative kidney weight (%) were examined to provide an additional characterization of the investigated stages of renal alteration, but were not employed as criteria for assignment to these respective stages. Development of glomerular lesions in growth hormone transgenic mice is characterized by an early onset and stable progression of the morphological and functional lesions of glomeruli that were employed as determinants of stage assignment in the present study (Doi et al. 1990, Wanke et al. 2001). These alterations occur reproducibly in an age dependent manner (Wanke et al. 1996, Wanke et al. 2001). Thus, bGH-transgenic mice were of relative young age when they reached the respective early stages of glomerular hypertrophy (27 ± 2 d) and onset of albuminuria (32 ± 2 d), which were separated by only five days of age in average. As well, the ages of animals of the bGH-group assigned to a respective stage of investigation did not display a great variance. GIPR^{dn}-transgenic mice, however, typically display a slower progression in development of glomerular lesions and the time points of ages at which comparable degrees of these lesions can be detected in those animals display considerable individual differences (Schairer 2006). These conditions are considered to be responsible for the advanced ages, the greater variability of ages of GIPR^{dn}-transgenic mice assigned to a respective stage of investigation and the greater chronological separation of stage I (78 ± 1 d) and stage II (112 ± 37 d). In GH-transgenic mice, the onset of growth promoting effects resulting from overexpression of the GH-transgene starts from three weeks of age onwards (Wanke et al. 1992). Stimulation of body and kidney growth is a characteristic finding in transgenic mice with high systemic GH-levels (Wanke et al. 1996). The differences of body weights, kidney weights and relative kidney weights of GH-transgenic mice investigated in the present study slightly failed to reach statistical significance in comparison to their associated non-transgenic control animals. However, in slightly elder ages, development of significant renal hypertrophy is a characteristic finding in GH-transgenic mice (Wanke et al. 1993). The respective findings in the investigated GIPR^{dn}-transgenic animals stand in line with previous findings (Schairer 2006).

Both kidney weights and relative kidney weights of GIPR^{dn}-transgenic animals were significantly increased in both stages of investigation. These findings indicate that in the different investigated animal models, the different growth promoting mechanisms that lead to development of glomerular and renal hypertrophy might exhibit their effects on different compartments of the renal cortex at different points of time, respectively, that different subunit structures of the kidney may respond differently to a particular growth stimulus (Doi et al. 1990). As also observed in other studies (Fisch 2004), in growth hormone-transgenic mice these effects apparently resulted in detection of increased glomerular growth prior to a measurable effect of induction of growth processes in the other compartments of the kidney. However, the finding that GIPR^{dn}-transgenic animals displayed increased relative kidney weights (kidney weight to body weight ratio) in the investigated stage of glomerular hypertrophy does not implicate that the development of renal hypertrophy does preceede the development of glomerular hypertrophy in this animal model.

5.5 Transcript profiling analyses

5.5.1 Microarray analyses: Patterns of glomerular gene expression

Recurrent controls of quality and quantity of total RNA lysates extracted from the glomerulus isolates, as well as of the deduced target preparations generated for hybridization to the microarrays confirmed the comparable and high quality of investigated samples. Successful performance of the microarray experiments was verified by control of the distribution of the detected hybridization signal intensities on each single array. All 40 arrays of the experiment showed similar and comparable patterns of density distributions of overall hybridisation intensities, as well as comparable degrees of only weakest degradation of target cDNA. Analysis of PCA (principle component analysis) plots, illustrating the similarity of detected patterns of gene expression of the different subgroups of samples investigated in the micro-array experiments, confirmed the effectiveness of tissue separation of samples of glomerulus isolates. Here, samples derived from isolated glomeruli displayed an impressive difference compared to those of two investigated samples of total cortical kidney tissue, indicating strong differences in the gene-expression profiles of total cortical kidney tissue and preparations of pure glomerulus isolates.

Interestingly, Cluster dendrograms and PCA plots also showed that glomerular samples always completely clustered into groups of common genetic backgrounds, rather than into distinct groups of transgenic and non-transgenic control animals or common stages of glomerular alteration. Only samples derived from the bGH-group assigned to stage II completely clustered into distinct groups of transgenic and non-transgenic control animals. Concerning the investigated animal models and early stages of glomerular alteration, this indicates a stronger influence of the respective genetic background of animals on the detected patterns of gene-expression in glomerular samples, than that, caused by differences of transgenic animals and non-transgenic controls or different stages of comparable degrees of glomerular alteration. These findings exactly corresponded to the expected results and confirmed the scheduled mode of comparisons, based on the a priori experimental group design of two different transgenic mouse models of nephropathy with different genetic backgrounds: a strong influence of the genetic background on the detected differences of glomerular gene expression profiles in the different investigated animal models, a comparably weaker genotype-dependent influence on samples derived from transgenic and non-transgenic animals of identical genetic backgrounds, as well as an increasing difference of patterns of glomerular gene expression in transgenic and non-transgenic animals according to the degree of glomerular alteration and progression of disease. These results also indicate that within each of the investigated animal models a significant impact of other processes than those actually related to development of glomerular hypertrophy or onset of albuminuria became present in detected differences of glomerular gene expression profiles in transgenic animals vs. their associated non-transgenic controls. Similar conclusions were drawn from results of independent studies and have been reported previously (Susztak et al. 2004). The relatively small, yet significant differences of patterns of glomerular gene-expression profiles in transgenic and control animals might be explainable through the patterns of development of glomerulosclerotic kidney lesions. At a given point of time, different glomeruli in the kidney display different degrees of alteration. In the investigated early stages of alteration, only a comparably small number of glomeruli exhibits distinct lesions, whereas the number of damaged glomeruli is steadily increasing during the further progressive development of disease (Schairer 2006, Wanke 1996).

This situation was mirrored by increased differences of the overall similarities of glomerular gene-expression profiles of transgenic animals vs. their corresponding non-transgenic controls in the second investigated stage of glomerular alteration.

5.5.2 Microarray analyses: Differential glomerular gene expression profiles

For statistical analysis of microarray data, a sensitive method was applied (ChipInspector, Genomatix), that presents an advanced approach for identification of differentially regulated transcripts using Affymetrix $^{®}$ Gene Chip data, avoiding potentially occurring pitfalls resulting from data analysis following the original "probe-set" approach. This approach has also been successfully applied in previous studies (Gehrig et al. 2007). Statistical analysis was then carried out, using an accredited method of statistical testing (Tusher et al. 2001). A stringent level of statistical significance (FDR < 0.049%) was applied in the analysis, which resulted in detection of numbers of differentially expressed glomerular genes in transgenic vs. control animals in the respective investigated models and stages of nephropathy, allowing for comprehensive further analyses. In a microarray experiment, the numbers of detected differentially expressed genes (tg vs. wt) predominantly depend on the applied level of significance in the statistical analysis of microarray data, as well as on the specific properties of investigated sample materials and methodological aspects of analyses. Thus, direct comparisons of the numbers of differentially expressed genes detected in the present study with results of other studies can not be performed. However, an interesting finding is that, although almost identical settings of statistical analysis parameters were applied, the numbers of differentially expressed glomerular genes in GH-transgenic mice (stage I: 1566, stage II: 4300, vs. wt) robustly exceeded those detected in GIPR^{dn}-transgenic mice (stage I: 513, stage II: 1422, vs. wt). These differences might be related to generally stronger effects of systemically elevated GH-levels on differential glomerular gene expression profiles in GH-transgenic mice, as well as to the comparably fast development of glomerular lesions in young mice of this model of progressive glomerulosclerosis. In both animal models, the numbers of differentially expressed glomerular genes in transgenic mice (vs. non-transgenic controls) in the second stage of investigation were consistently exceeding the respective numbers of differentially expressed genes in the earlier first stage of glomerular hypertrophy. This observation presumably reflects an increased transcriptional activity in glomerular cells of transgenic animals accompanying the progression of development of glomerular alterations.

As well, the detected differences in the relative abundance (expression ratios) of the majority of transcripts that displayed a congeneric differential abundance in both stages of investigation in the respective animal models (tg vs. wt) were increasing from stage I to stage II, possibly indicating both a differential expression of these transcripts in a growing number of glomerular cells and/or their persistent and increasing differential expression in single cells during progression of glomerulopathy.

5.5.3 Microarray analyses: Common differential gene expression profiles

Within the number of transcripts displaying a significant differential abundance in glomerular samples of transgenic vs. control animals of one investigated model and stage, there will be some whose differential expression is actually related to development of glomerular hypertrophy or onset of albuminuria. However, there will also be a presumably large number of transcripts, whose differential expression is assumed to result from other factors, which specifically alter glomerular gene expression profiles in the different investigated mouse models of nephropathy. In GIPR^{dn}-transgenic mice, these factors result from the systemic effects associated with the diabetic phenotype of these animals. In GH-transgenic mice, the systemic effects of permanently elevated GH-levels (Wolf and Wanke 1997) are responsible for the induction of processes leading to alterations of glomerular gene expression profiles. Therefore, the applied mode of comparison of differentially expressed glomerular genes in the different investigated mouse models and well defined distinct stages of glomerular alteration should allow for a significant reduction of the numbers of differentially expressed genes, which are not related to the interested features of glomerular hypertrophy or onset of albuminuria. It therefore should as well allow for identification of relevant genes, whose common differential expression abundance in both GIPR^{dn}- and GH-transgenic animals is assumable independent of the genetic background or the identity of expressed transgenes.

The observed overlaps of numbers of congeneric commonly differentially expressed genes between the different groups in a respective stage of investigation appear to be rather small at first sight (stage I: 86 commonly differentially expressed genes; stage II: 469 commonly differentially expressed genes.) However, for several of the reasons mentioned above, this is a typical finding when comparing transcript profiles of comparable sample materials derived from different animal models (Susztak et al. 2004).

In both stages of investigation, the significant enrichment of detected numbers of commonly differentially expressed glomerular genes between the different models of nephropathy was confirmed by performance of sophisticated statistical tests (Monte Carlo simulations). As well, the number (21) of genes that displayed a congeneric common differential expression in both stages and models was found to be significantly enriched. The successful identification of glomerular genes, whose common congeneric patterns of differential expression can be supposed to be actually related to common molecular processes of development of early stages glomerular alteration, independent of genetic backgrounds or effects of different expressed transgenes, was also confirmed by the results of performed cluster analyses. Differential expression profiles of commonly differentially expressed transcripts in the single stages of investigation (stage I or stage II), did not cluster into distinct groups of common genetic backgrounds, whereas the overall glomerular gene expression profiles of the different investigated models did. As well, cluster analyses of differential expression profiles of transcripts that displayed a congeneric common differential expression in all investigated stages and models of nephropathy did not allow for a separation into distinct subgroups according to common genetic backgrounds or stage affiliations.

5.5.4 Confirmation of array data by real-time PCR

The glomerular 18S rRNA expressions were found to be too heterogeneous for use as internal references ("housekeeping transcripts") in the real-time PCR experiments. This finding is consistent with the experiences of other real-time PCR experiments performed on samples of isolated glomeruli of different species under diverse disease conditions (Prof. Dr. M. Kretzler, personal communication). Evaluation of expression abundances of transcripts coding for GAPDH (glyceraldehyde-3-phosphate dehydrogenase), an enzyme involved in glycolyse metabolism, as an internal reference in real-time PCR experiments performed on samples derived from diabetic animals is not recommended (Schmid et al. 2003). Therefore, cyclophyllin was finally used as housekeeping transcript in all real-time PCR confirmations of microarray data in the present study. The common congeneric differential expressions of five selected genes (including both "up" and "down-regulated" ones), which had been identified in the microarray experiments, were confirmed by performance of real-time PCR as an independent method of gene expression profiling analysis.

In these experiments, the same samples investigated in the array experiment, as well as samples of the Independent Control Cohort were examined. In order to eliminate potential systematic biases resulting from the performed mode of assignment of tg/wt-pairs of mice to certain stages of glomerular alterations, in the Independent Control Cohort, less stringent criteria for assignment of transgenic mice and their corresponding non-transgenic control animals to the respective stages of investigation were applied. The results of the real-time PCR analyses generally stood in accordance with those of the generated array data and confirmed their reliability. As the genes, whose differential expression was examined by real-time PCR, displayed a common congeneric differential expression in glomerular samples of transgenic animals in both investigated models and stages in the microarray experiments, real-time PCR experiments were performed both in each the single stages and models of the analysis, as well as "matched pairs"-analyses. In these analyses, all samples of transgenic animals were then simultaneously compared to those of their associated non-transgenic controls, irrespective of their affiliation to a respective model or stage of investigation. In summary, the investigational strategies applied according to the experimental design of the present study, the different performed analyses and their respective results are considered to provide a reliable basis for detection of shared glomerular gene expression profiles, associated with defined stages of glomerular alteration in different animal experimental models of nephropathy.

5.5.5 Relative depletion of podocytic RNA in samples of hypertrophied glomeruli: A potential pitfall of interpretation of glomerular gene expression profiles

Finally, a special aspect of potentially problematic interpretation of gene expression data from samples of isolated glomeruli has to be addressed. Although investigations were performed on glomerulus isolates of highest purities and almost identical quantities, the lower abundance of podocytes in relation to the total number of glomerular cells in samples of transgenic animals might inherit the danger of nonobservance or of misinterpretation of signals derived from "differentially expressed" transcripts of podocytic origin.

As demonstrated by the results of the performed stereological examinations, the absolute number of podocytes per glomerulus did not differ between specimens derived from transgenic animals and their associated control mice, whereas the numbers of mesangial and endothelial cells per glomerulus typically increased significantly during development of glomerular hypertrophy in transgenic animals. For performance of transcript profiling analysis, total RNA was isolated from glomerulus isolates, each consisting of nearly identical numbers of approximately 1000 isolated glomeruli both in samples of transgenic and control mice. Thus, the resulting RNA isolates derived from glomerulus isolates of transgenic animals contained the RNA of a number of podocytes comparable to that present in the samples of control mice. However, in glomerular samples of transgenic animals the amount of total RNA isolated from other glomerular cell types than podocytes derived from a significant larger number of cells than in the respective non-transgenic animals. If one assumes that there were neither general differences concerning the effectiveness of RNA isolation from glomerulus isolates derived from transgenic and non-transgenic animals, nor individual differences in the effectiveness of RNA isolation from different glomerular cell types, then the abundances of podocyte derived RNAs within the different samples of either transgenic mice <u>or</u> control animals should be comparable. However, these assumptions cannot be taken for granted, as the attained yields of total RNA, isolated from glomerular samples of transgenic animals vs. their associated controls did not display explicit significant differences in the investigated mouse models of nephropathy. As expression profiles have necessarily to be identified by investigation and comparison of samples of approximately identical amounts of total RNA of both wild-type and transgenic animals, this might potentially lead to an artificial under-representation of transcripts of podocytic origin. The effects of this circumstance might then theoretically result in either a nonobservance of "upregulated" podocytic transcripts, or the misinterpretation of a detected "down-regulation" of a respective podocyte derived transcript, whose abundance per podocyte might actually not be altered. These eventual circumstances would predominantly impair the detection and interpretation of expression levels of transcripts exclusively derived from podocytes. Apart from a potential nonobservance of "upregulated" podocytic transcripts, problems concerning the interpretability or reliability of expression levels of podocyte-specific transcripts affect only those with a detected lower abundance in glomerular samples of transgenic animals.

Using the available data sets, none of the various different factors that potentially might exhibit an influence on the described situation can directly be examined. Thus, the problem can neither be addressed itself, nor a reliable statement can be made if it actually is present. As well, the problem has yet not been described. Strategies as " in silico- microdissection" (Schmid et al. 2003), which use podocyte specific "housekeeping" transcripts for evaluation of regulated expression levels of other podocyte specific transcripts by real-time PCR can only partially address the problem, as the application of this approach requires reliable knowledge that the respective target transcript is actually exclusively expressed in podocytes. If any, this can only be confirmed by performance of in situ hybridization or comparable methods. Therefore this strategy should be applied in studies that focus on investigation of distinct podocyte-specific transcripts and their potential involvement in podocyte function or in pathways implicated in development of podocyte damage. In a holistic approach as in the present study, a comprehensive consideration of all of these conditions currently can not be regarded. In the follow up studies however, the problem will have to be addressed at least by identification of the patterns of cellular and sub-cellular distribution of expression of single transcripts of interest in the glomerular compartment.

5.6.1 Bioinformatical analyses

Performance of bioinformatical analyses on the known functions of the 21 genes, that displayed a congeneric common differential expression in all samples of GIPR^{dn}-transgenic and GH-transgenic animals in both investigated stages of glomerular alteration revealed a number of genes (their corresponding gene products, respectively), that had already been described to be involved in development of several forms of glomerulopathies, as well as of some that had yet not been subject of investigations in this context. Gene products with known involvement in development of glomerulopathy comprise those with a known function of e. g. cell adhesion molecules (CD44), cytokines (Fractalkine) and mediators of events of inflammatory character (C1QB, FCGR1) or regulators of extracellular matrix turnover (CTSH).

The Gene Ontologies of the products of commonly differentially expressed glomerular genes that have yet not been extensively described in the context of development of glomerular lesions assign them to functional categories of cell adhesion molecules (XLKD1, MSR1), proteins related to an altered metabolism of lipids (MSR1, FABP4, TGH2), as well as some which are known or supposed to be constituents of the cytoskeleton (MYO1F, TNNT2, RIKEN cDNA 2810484G07 gene) or involved the regulation of the function of the cytoskeleton (FILIP1, DNAI1) and other mechanisms of intracellular signal transduction (GNG2).

In the following sections, the supposed involvement of 18 of these different gene products in appearance of glomerulopathies and their potential interactions are addressed, according to their affiliation to distinct mechanisms of known or supposed pathogenetic significance. These mechanisms include alterations of molecular pathways involved in lipid metabolism, oxidative stress, cytokine and chemokine signalling pathways, regulation of extracellular matrix turnover, cell-matrix adhesions, cytoskeletal functions, G-protein coupled signal transduction and immunological events (Gomez-Guerrero et al. 2005, Pavenstadt et al. 2003, Schlondorff 1993).

5.6.2 Commonly differentially expressed genes involved in lipid metabolism

In the present study, performance of micro-array experiments indicated an elevated expression of transcripts coding for MSR1 and FABP4 and a decreased expression of the Expressed sequence AU018778 in glomerular samples of GIPR^{dn}-transgenic and bGH-transgenic mice. For Msr1 and Fabp4, this was additionally confirmed by performance of real-time PCR, also in independent sample materials of isolated glomeruli. Therefore, the results of these experiments strongly indicate a differential expression of the Msr1 and the FABP4 gene in glomerular cells during development of glomerular hypertrophy and beginning albuminuria in the investigated mouse models of nephropathy.

MSR1, FABP4 and TGH-2 (triacylglycerol hydrolase 2, the protein corresponding to the Expressed sequence AU018778) participate in molecular pathways linked to lipid metabolism. Alterations of the lipid metabolism as hyperlipidaemias are thought to play a role in the progression of various renal diseases, including diabetes mellitus (Schlondorff 1993).

The macrophage scavenger receptor 1 (MSR1, also known as class A macrophage scavenger receptor or CD204) was originally identified as a transmembrane receptor on macrophages that binds and internalizes modified lipoproteins (Fukuda et al. 1986, Goldstein et al. 1979). MSR1 has also been shown to be expressed on microglia and perivascular macrophages in the brain (mato cells) (Tomokiyo et al. 2002). Macrophage scavenger receptors mediate the binding, internalization, and processing of a wide range of negatively charged macromolecules (Doi et al. 1993, Emi et al. 1993, Platt and Gordon 2001). MSR1 mediated adhesion might play an important role in macrophage retention, specifically at sites of tissue injury. Several components of the extracellular matrix, including modified types of collagen and certain proteoglycans, present at sites of inflammation, have been identified as adhesion substrates for MSR1 (el Khoury et al. 1994, Gowen et al. 2000, Gowen et al. 2001, Santiago-Garcia et al. 2003).

Recent studies suggest, that (human) mesangial glomerular cells may also express an inducible class A macrophage scavenger receptor, by which cells can acquire lipids as LDL and convert to foam cells in developing glomerulosclerosis (Ruan et al. 1999). Other studies indicate potential common patterns of transcriptional regulation of Msr1 expression with other genes (gene products) of the commonly differentially expressed genes in stage I and II of this study.

An interesting finding is the observation, that advanced glycation end products, as glycated albumin, a powerful contributor to diabetic angiopathy and atherosclerosis in patients with diabetes mellitus (Sakaguchi et al. 1998), induces the expression of both CD44 and macrophage scavenger receptors on monocytes. Furthermore, CD44 crosslinking and/or glycated albumin enhances the uptake of oxidized-low density lipoprotein in monocytes, which in turn enhances foam cell transformation (Kishikawa et al. 2006). For these reasons it appears most likely that the increased expression abundances of glomerular transcripts coding for MSR1 in GIPR[dn]-transgenic and bGH-transgenic mice actually represent a common consequence of different factors that contribute to the development of glomerular alteration in diabetic and non diabetic nephropathy. Moreover, the known functions of MSR1 expressed on mesangial glomerular cells as well suggest a pathogenetically significant role of MSR1 during development of early glomerular alterations.

Fatty acid binding proteins (FABPs) are a family of small, cytoplasmatic carrier proteins. They bind long-chain fatty acids and other hydrophobic ligands such as eicosanoids and retinoids (Chmurzynska 2006, Hotamisligil et al. 1996), provide their solubility and intracellular trafficking (Coe and Bernlohr 1998, Zimmerman and Veerkamp 2002). They facilitate fatty acid uptake, the transfer of fatty acids between extra- and intracellular membranes (Weisiger 2002) and their metabolism. Some members of the fatty acid binding protein family are also believed to transport lipophilic molecules from outer cell membrane to certain intracellular receptors such as peroxisome proliferator-activated receptors (PPARs) (Tan et al. 2002). In nephrology, FABPs (predominantly liver-type fatty acid binding protein, which is expressed in human proximal tubules and appears in the urine of patients with CKD) are seen as useful clinical biomarkers to predict and monitor the progression of chronic glomerular diseases (Kamijo-Ikemori et al. 2006, Kamijo et al. 2004, Kamijo et al. 2006). As well, they are employed as diagnostic indicators for segregation of different entities of glomerular abnormalities (Nakamura et al. 2006).

FABP4 is also known as A-FABP or AP2. It is primarily expressed in adipocytes and macrophages (Baxa et al. 1989), acts on metabolic and inflammatory pathways and plays an important role in obesity and glucose metabolism. Although the role of FABP4 in development of CKD or especially the development of glomerular alterations has yet not been subject of extended studies, there are several findings indicating a potential involvement of FABP4 in this context. Expression of macrophage FABP4 is induced on Toll-like receptor (TLR) activation (Kazemi et al. 2005). Several processes of pathogenetic importance in developing glomerulopathies (e. g. mesangial cell proliferation) have been identified to be mediated by activation of TLR (Chow et al. 2005). Activation of macrophages by TLR ligands increases low-density lipoprotein (LDL) uptake and cholesterol content, leading to foam cell formation (Funk et al. 1993, Oiknine and Aviram 1992), which has been shown to be involved in development of glomerulosclerosis (Abrass 2006). Expression of the Fabp4 gene is enhanced in macrophage cell lines treated with low levels of oxidized LDL, HDL, or PPAR-gamma agonists (Cabrero et al. 2003, Fu et al. 2000, Han et al. 2002) and was shown to be likely to be regulated through peroxisome proliferator-responsive elements (PPREs) located in Fabp4 gene promoter region (Fu et al. 2006).

Activation of PPAR-gamma dependent pathways has been shown to be associated with regulation of glomerular cell proliferation, hypertrophy and mesangial matrix expansion during development of glomerulosclerosis (Izzedine et al. 2005, Ma et al. 2001) and treatment with PPAR-gamma agonists has shown beneficial effects in several studies on diverse forms of glomerular diseases, including diabetic nephropathy (Guan and Breyer 2001, Isshiki et al. 2000, Kanjanabuch et al. 2007, Okada et al. 2006, Yang et al. 2006). These findings strongly support the assumption that the enhanced glomerular Fabp4 expressions in GIPR[dn]-transgenic and bGH-transgenic mice are actually a consequence of specific transcriptional programs, commonly activated during development of early stages of glomerulosclerotic alterations. Furthermore, overexpression of the FABP4 gene in macrophage foam cells was shown to enhance the accumulations of cholesterol and triglycerides, probably due to an increased expression of MSR1 (Fu et al. 2006). Deficiency of FABP4 enhances PPAR-gamma activity, which is leading to an enhanced uptake of modified low density lipoprotein in macrophages. In parallel, FABP4 deficient macrophages display reduced NF-kappa ß activity, resulting in suppression of inflammatory function and impaired production of inflammatory cytokines (Makowski et al. 2001, Makowski et al. 2005).

Activation of NF-kappa ß pathways and elevated expression of cytokines in the kidney have been shown to be important features in the development of diabetic nephropathy (Cohen et al. 2006, Mezzano et al. 2004, Sakai et al. 2005, Schrijvers et al. 2004). Therefore, FABP4 and MSR1 can be supposed to regulate central molecular pathways to coordinate lipid trafficking and inflammatory activity in glomerular cells.

Another of the 21 identified commonly differentially expressed glomerular genes of the present study with a known participation in lipid metabolism is the unannotated gene corresponding to the Expressed sequence AU018778. Recently the protein encoded by this gene was identified and tentatively designated as triacylglycerol hydrolase 2 (TGH-2) (Okazaki et al. 2006), due to its remarkable structural resemblance to TGH-1 (Lehner and Vance 1999, Lehner and Verger 1997). Both TGH-1 and TGH-2 are members of the carboxylesterase family and involved in molecular mechanisms that mediate lipolysis.

Therefore, both the elevated common differential glomerular expressions of Msr1 and Fabp4 in GIPR[dn]-transgenic and bGH-transgenic mice, as well as the decreased glomerular abundances of transcripts coding for TGH-2 could be regarded to reflect concordant alterations of the glomerular lipid metabolism. So far, TGH-2 has not been described in the context of nephropathy.

Although the precise effects of MSR1, FABP4 and TGH2 during development of glomerular hypertrophy are not known, the common differential expression of transcripts of these genes in glomerular cells might indicate a potential pathogenetic significance of their gene products and of the molecular pathways they participate in. Further inside views will be gained by detection of the cellular distribution of expression patterns of these transcripts within the glomerular compartment. As mesangial glomerular cells possess a number of macrophage-like characteristics (Gomez-Guerrero et al. 2005), these studies will also have to address the important question, if the detected differential expression of glomerular transcripts coding for MSR1, FABP4 and TGH-2 in the investigated early stages of glomerular alterations of GIPR[dn]-transgenic and bGH-transgenic mice can actually be related to intrinsic glomerular cells (e. g. mesangial cells and resident macrophages), or derives from other types of cells (leucocytes) infiltrating the glomerulus.

5.6.3 Commonly differentially expressed genes involved in oxidative stress

In the present study, transcripts coding for the cytochrome b-245 beta polypeptide (CYBB) were identified to be commonly differentially expressed in glomerular samples of transgenic animals of both investigated animal models and stages of glomerular alteration. As part of the NADPH oxidase system, CYBB displays oxidoreductase activity and is involved in production of reactive oxygen species (ROS) as superoxide radicals, oxygen radicals, hydrogen peroxide, hydroxyl radicals, and lipid hydroperoxides. Several reports have evaluated the direct and indirect damaging effects of reactive oxygen species (ROS) on renal structural integrity (Gomez-Guerrero et al. 2005, Gwinner and Grone 2000) in different kidney diseases. Enhanced generation of ROS has been detected in several human and experimental glomerular diseases (Binder et al. 1999, Gaertner et al. 2002, Gwinner and Grone 2000, Neale et al. 1993, Pavenstadt et al. 2003, Ricardo et al. 1994, Shah 1988), leading to oxidatively modified proteins in podocytes, mesangial cells, and basement membranes (Grone et al. 1997).

ROS may also alter collagen structures, which facilitates GBM degradation and leads to activation of proteinases or complement components (Gomez-Guerrero et al. 2005). Excess oxidized LDL are supposed to act as cytotoxic agents on mesangial, epithelial, and endothelial cells, thereby contributing to a vicious cycle of cell damage and sclerosis (Schlondorff 1993). Recent evidences implicate ROS as signaling molecules (Budisavljevic et al. 2003, Suzuki et al. 1997), through which oxidative stress can also cause glomerular injury by regulation of intracellular signaling cascades in mitogenic pathways (Budisavljevic et al. 2003). In inflammatory glomerular diseases, there is also evidence of ROS activation also by immune complexes (IC) in mesangial cells, which includes release of O_2^- and H_2O_2 (Gomez-Guerrero et al. 1993, Satriano et al. 1997, Satriano et al. 1993, Sedor et al. 1987, Suzuki et al. 2003) as well as NADPH-dependent oxidase and superoxide dismutase (SOD) activation (Satriano et al. 1993, Stephanz et al. 1996). Finally, ROS are also known to mediate several processes that lead to podocyte damage (Pavenstadt et al. 2003). Podocytes seem to be not only the target but also the source of ROS in different forms of nephropathy (Binder et al. 1999, Greiber et al. 2002, Ricardo et al. 1994, Shankland 2006, Vega-Warner et al. 2004).

In podocytes, ROS itself changes several signaling cascades, which then may maintain podocyte injury by mechanisms distinct from ROS and might also modulate cellular properties of glomerular endothelial cells or immune cells in a paracrine fashion through release of podocyte derived signaling molecules. For example, it was shown that exogenous ROS causes a marked increase in the induction of granulocyte macrophage colony-stimulating factor (GM-CSF) mRNA as well as GM-CSF protein release in cultured differentiated mouse podocytes (refer to chapter 5.6.4), which in vivo might modulate cellular properties of glomerular endothelial cells in a paracrine fashion (Greiber et al. 2002). Although the involvement of molecular processes related to oxidative stress in development of glomerular damage is generally accepted, a causative participation of elevated expression levels of transcripts coding for cytochrome b-245 beta polypeptide in processes leading to glomerular hypertrophy and subsequent albuminuria can not be concluded from the available data.

5.6.4 Commonly differentially expressed genes involved in cytokine and chemokine signaling pathways

In the present study, several transcripts of genes with a described known or supposed affiliation to cytokine and chemokine signaling pathways displayed a congeneric common differential expression in the investigated glomerular samples of transgenic animals of GIPR^{dn}- and bGH-transgenic animals in early stages of glomerular alteration, e. g. the Colony stimulating factor 2 receptor beta (CSF2RB) and the Chemokine (CX3C motif) ligand 1 (CX3CL1, also known as Fractalkine).

Cytokine and chemokine signaling pathways are considered to be involved in several aspects of development of renal lesions through a broad variety of different chronic kidney diseases (Gomez-Guerrero et al. 2005, Kamanna et al. 1996, Pavenstadt et al. 2003). Many studies have described the glomerular expression of various chemokines and cytokines in CKD (e.g. monocyte chemoattractant protein 1, RANTES, macrophage inflammatory protein 1α, cytokine-induced neutrophil chemoattractant and fractalkine), as reviewed in Gomez-Guerrero et al. (2005). In inflammatory glomerular disease, chemokines and pro-inflammatory cytokines, which can be locally secreted, play important roles in recruitment of leukocytes toward the site of tissue injury (Rovin and Phan 1998, Segerer et al. 2000, Wenzel and Abboud 1995) and participate in leukocyte adhesion to vascular endothelium and transendothelial migration (Anders et al. 2003, Segerer et al. 2000).

Next to induction of chemokine release by mesangial cells through pro-inflammatory stimuli as tumor necrosis factor alpha (TNF-alpha) (Anders et al. 2003, Schwarz et al. 1997, Segerer et al. 2000, Wolf et al. 1993, Wu et al. 1995) or oxidized LDL (Segerer et al. 2000), release and production of chemokines and adhesion molecules can also be triggered by generation of ROS (Anders et al. 2003, Satriano et al. 1997, Satriano et al. 1993, Schlondorff 1995, Wolf et al. 1993). Mesangial cell-leukocyte interaction is supposed to be mediated by receptor-mediated adhesion molecule pathways (Gauer et al. 1997, Wuthrich 1992), as well as through mechanisms, promoted by chemoattractants and cytokines, such as granulocyte macrophage-colony-stimulating factor (GM-CSF) (Brady et al. 1992, Gauer et al. 1997) or TNF-alpha (Adler and Brady 1999, Brady et al. 1992, Denton et al. 1991, Gauer et al. 1997, Satriano et al. 1997).

The granulocyte macrophage colony-stimulating factor receptor (CSFR) is a transmembrane receptor for GM-CSF. GM-CSF is a cytokine secreted by macrophages, T cells, mast cells, endothelial cells and fibroblasts.

As well, glomerular cells as mesangial cells and podocytes differentially express and produce GM-CSF (Greiber et al. 2002) according to manifold stimuli (Schlondorff and Mori 1990), mediated by several factors with known pathogenetic importance in development of glomerulosclerosis. In the context of inflammatory and other glomerular diseases, the GM-CSF pathways are involved in cellular processes as proliferation, differentiation and growth of mononuclear phagocytes and the functions of glomerular mesangial cells (Pavenstadt et al. 2003, Gomez-Guerrero et al. 2005, Kamanna, et al. 1996). Next to the mentioned (refer to chapter 5.6.3) induction of GM-CSF mRNA and GM-CSF protein release in podocytes by ROS (Greiber et al. 2002), for example also LDL (Pai et al. 1995), or proinflammatory cytokines such as TNF-alpha were shown to induce CSF production by mesangial cells, which then regulates the differentiation of monocytes into macrophages and proliferation within the mesangium (Kamanna et al. 1996). Next to leucocytes, CSFR is also expressed on the cell surface of mesangial glomerular cells (Mori et al. 1990). The increased glomerular expression abundances of CSF2RB mRNA in GIPR^{dn}-transgenic and bGH-transgenic mice might therefore as well be involved in growth processes of mesangial and other glomerular cells during development of glomerular hypertrophy.

CX3CL1 (Fractalkine) is a small cytokine, which is the only known member of the CX3C chemokine family (Bazan et al. 1997, Pan et al. 1997). The fractalkine molecule can exist in two forms, as membrane-anchored or as a soluble glycoprotein. Soluble fractalkine potently chemoattracts T cells and monocytes, while the cell-bound chemokine promotes strong adhesion of leukocytes to the surface of activated endothelial cells, where it is primarily expressed (Bazan et al. 1997). Therefore, Cx3CL1 can function both as a chemoattractant and as an adhesion molecule for cells expressing its receptor, CX3CR1 (Haskell et al. 1999, Imai et al. 1997). By interacting with CX3CR1, fractalkine elicits its adhesive and migratory functions (Imai et al. 1997). It appears likely, that CX3CR1 functions predominantly as an adhesion molecule, functioning in the processes of firm adhesion and extravasation of leukocytes from the circulation (Segerer et al. 2002). Expression of CX3CR1 and migration towards CX3CL1 has been demonstrated for a wide variety of cells, including monocytes and macrophages, as well as other types of leucocytes, neurons and microglia (Fong et al. 1998, Foussat et al. 2000, Harrison et al. 1998, Imai et al. 1997, Tong et al. 2000). Upon stimulation, Fractalkine (CX3CL1) is also expressed by mesangial cells in vitro (Anders et al. 2003, Segerer et al. 2000).

In vivo expression of fractalkine was demonstrated in human glomeruli, tubular epithelial cells and peritubular capillaries in settings of acute crescentic glomerulonephritis or acute renal allograft rejection accompanied by prominent parenchymal infiltration by mononuclear leukocytes, but not in normal kidneys or in biopsies of patients with non-inflammatory diseases such as minimal change disease (Cockwell et al. 2002). Complementary to these findings, other studies showed that (human) leukocytes bear the appropriate fractalkine receptor in similar disease settings (Segerer et al. 2002). Glomerular production of fractalkine in mesangial cells was also detected in an animal model of glomerulonephritis (Chen et al. 2003). The expression of fractalkine in mesangial cells is increased by factors as for example TNF-alpha, a process which is least in partially mediated via the Nfk-ß signalling pathway (Chen et al. 2003). In response to inflammatory cytokines, mesangial cells do also express fractalkine recognizing chemokine receptors, such as CXCR1 (Segerer et al. 2006), indicating that intrinsic renal cells are also targets for the chemokines, secreted during the initial phase of injury (Banas et al. 2002, Romagnani et al. 1999). In fact, CX3CR1 is expressed on both interstitial, and in the two most common groups of glomerular infiltrating leukocytes in inflammatory kidney diseases, T cells and macrophages (Imai et al. 1997). Experimental data in animal models suggest an important role of the chemokine-receptor pair of CX3CL1-CX3CR1 in various inflammatory glomerular diseases and make it an attractive target for therapeutic interventions (Cook et al. 2001, Feng et al. 1999, Jung et al. 2000, Robinson et al. 2000). There is growing evidence that inflammatory processes participate also in development of diabetic nephropathy, as inflammatory cells are observed at every stage of this disease (Galkina and Ley 2006). Renal tissue macrophages, T cells, and neutrophils produce various reactive oxygen species, proinflammatory cytokines, metalloproteinases, and growth factors, which modulate the local response and increase inflammation within the diabetic kidney (Bending et al. 1988, Furuta et al. 1993, Gomez-Guerrero et al. 2005, Moriya et al. 2004). Within this context, chemokines as Fractalkine are supposed to be crucially involved in leukocyte migration in diabetic nephropathy (Galkina and Ley 2006). Glomerular-produced chemokines have been implicated not only to induce recruitment of inflammatory cells, but also to alter functions of resident glomerular cells. Expression of several functional active chemokine receptors, including CXCR1 have been detected in human differentiated podocytes.

Ligands of these chemokine receptors increase the intracellular calcium concentration and stimulate the generation of superoxide anion in podocytes, suggesting that activation of these receptors may be involved in the pathogenesis of podocyte injury (Huber et al. 2002). It also has been demonstrated that podocytes are able to produce ligands for the CXCR1/CXCR2 receptor, so that the CXCR1 receptor in podocytes may be activated in an autocrine fashion (Huber et al. 2002). With regard to the known mesangial expression patterns of Fractalkine, it appears likely that the elevated expression of glomerular transcripts coding for Fraktalkine might also be pathogenetically involved in the, in first instance non-inflammatory, development of early stages of glomerular lesions in both $GIPR^{dn}$- and bGH-transgenic mice.

5.6.5 Commonly differentially expressed genes involved in extracellular matrix turnover

A common pathological feature of progressive glomerulosclerosis leading to renal insufficiency is an accumulation of extracellular glomerular matrix proteins, predominantly collagens of type IV and V, laminin, fibronectin, and proteoglycans (Mene et al. 1989, Schlondorff 1987). This prominent histological abnormality is present in nearly all types of chronic, progressive glomerular disease (Kashgarian and Sterzel 1992). Mesangial matrix accumulation leading to glomerulosclerosis is seen as a consequence of an imbalance between matrix production and degradation. This (in)-balance is apparently influenced by the activity of glomerular proteinases as cathepsins, which are involved in the degradation of these extracellular matrix components. Inter alia, cathepsins are expressed in glomerular cells (Teschner et al. 1992) tubular (Schaefer et al. 1996) and juxtaglomerular cells (Matsuba et al. 1989) of the kidney. They are crucially involved in remodeling processes of the extracellular matrix (ECM) in physiological nephrogenesis (Vattimo Mde and Santos 2005) as well as in the development of chronic renal diseases (Huang et al. 1992, Schaefer et al. 1996, Schaefer et al. 1992, Teschner et al. 1992). Next to their function in glomerular extracellular matrix turnover, recent findings also demonstrated the participation of Cathepsins (Cathepsin L) in the development of podocyte damage in several proteinuric kidney diseases, including diabetic nephropathy (Sever et al. 2007). The same study also identified the proteolytic activity of cytoplasmatic Cathepsin L in podocytes to be an important mediator of development of podocyte foot process effacement and proteinuria in an experimental mouse model.

The cysteine proteinase Catepsin H plays an important role in proteolytic processes. Reduced glomerular Cathepsin H expression levels and activities were demonstrated by several studies in animal models of glomerulosclerosis, probably representing a common pathogenetic mechanism leading to extracellular matrix accumulation (Huang et al. 1992, Schaefer et al. 1996, Schaefer et al. 1992, Teschner et al. 1992). Thus, these findings are congruent to the detected decreased glomerular expression of transcripts coding for Catepsin H in GIPR^{dn}-transgenic and bGH-transgenic mice in both investigated stages of glomerular alteration of the present study.

5.6.6 Commonly differentially expressed genes involved in mediation of cell-matrix contacts

In the present study, a congeneric common elevated expression of two genes coding for the CD44 molecule and the lymphatic vessel endothelial hyaluronan receptor 1 (LYVE1, syn. extra cellular link domain-containing 1, XLKD1; cell surface retention sequence binding protein-1, CRSBP1) was independently detected in glomerular samples of all investigated GIPR^{dn}- and bGH-transgenic animals in both stages of early glomerular alteration. The known molecular functions of CD44 and LYVE1 associate these gene products to molecular pathways which, inter alia, participate in mediation of cell-matrix contacts and are involved in cellular processes of movement and adhesion.

Both CD44 and LYVE-1 act as receptors for hyaluronic acid (HA), an ubiquitous extracellular matrix molecule (Laurent and Fraser 1992) with proinflammatory, angiogenic, and cell-migratory functions (Lee and Spicer 2000, Savani et al. 2001). HA has been described to be involved in several processes linked to the development of diverse glomerular lesions observed in a variety of different chronic kidney diseases, including diabetic nephropathy (Dunlop and Muggli 2002, Hallgren et al. 1987, Johnsson et al. 1996, Mahadevan et al. 1995, Nishikawa et al. 1993, Turney et al. 1991, Wuthrich 1999). Unlike other matrix components, hyaluronan (HA) is turned over rapidly. HA is cleaved into fragments of low and intermediate molecular weight by specific hyaluronidases (Wuthrich 1999), or via the action of reactive oxygen species (Li et al. 1997). Different HA degradation products have biological functions distinct from those of the native high-molecular-weight polymer (Noble 2002).

High-molecular-weight HA polymers are known to possess anti-inflammatory and anti-fibrotic functions (Yevdokimova 2006), whereas many of the reported effects of hyaluronan at a number of inflammatory sites are seen as a consequence of inflammatory modification of hyaluronan to forms of lower molecular mass (Li et al. 1997). Expansion of the glomerular mesangial matrix and proliferation of mesangial cells is a feature of several forms of human and experimental glomerulopathy, including that seen in diabetes. High-glucose conditions lead to thrombospondin-1 mediated activation of transforming growth factor beta 1 (TGFβ1) in mesangial glomerular cells, which triggers the accumulation of matrix proteins and increased synthesis of HA of high molecular weight (Crawford et al. 1998, Hugo 2003, Yevdokimova et al. 2001, Yevdokimova 2006). This is seen as an important regulative molecular mechanism in diabetic nephropathy. However, it remains unclear, whether the phenomenon of increased generation of HA in mesangial cells provides a promotional, passive or defensive function. The dysregulation of the metabolism of glycosaminoglycan and protein components of extracellular matrix (ECM) is also a typical feature of diabetic complications. High glucose-induced enrichment of ECM with hyaluronan not only affects tissue structural integrity, but influences cell metabolic response due to the variety of effects depending on the HA polymer molecular weight. HA fragments of lower molecular weight (LMW) accumulate during inflammatory processes and induce the expression of inflammatory genes in macrophages, resulting in production of proinflammatory cytokines, chemokines and adhesion molecules. These processes are likely to be mediated by CD44 binding to the LMW-HA fragments (McKee et al. 1996). Increased HA synthesis was described within the glomeruli of diabetic rat kidney (Mahadevan et al. 1995). HA-enriched mesangial extracellular matrix stimulates monocyte and macrophage adhesion (Wang and Hascall 2004), formally promoting the inflammatory response and progression of diabetic nephropathy (Yevdokimova 2006). Recent studies have also reported of increased hyaluronan production in diabetes-related arterial sclerosis, diabetic nephropathy (Chajara et al. 2000, Heickendorff et al. 1994, Jones et al. 2001) and diabetic microangiopathy (Mine et al. 2006).

The protein encoded by the Cd44 gene is an integral cell-surface membrane glycoprotein, involved in cell to cell and cell to matrix interactions and adhesions, including inflammatory cell recruitment and cell activation (Aruffo et al. 1990, Borland et al. 1998, DeGrendele et al. 1996, Hodge-Dufour et al. 1997, McKee et al. 1996).

The genomic structure of Cd44 is remarkably complex and transcripts of this gene can undergo alternative splicing that results in many functionally distinct isoforms (Borland et al. 1998, Gunthert 1993, Screaton et al. 1992), mirroring the structural and functional diversity of CD44. Under physiological conditions, inter alia, CD44 is expressed in the (rat) kidney by medullary tubules, some distal tubules and thick ascending limbs of Henle, dendritic-like cells around Bowman's capsule, some interstitial cells and occasionally within the glomerular compartment (Nikolic-Paterson et al. 1996). Other studies found constitutive CD44 expression in normal kidney tissue by resident glomerular macrophages and parietal epithelial cells (Jun et al. 1997). The adhesion mediated by the binding of CD44 to HA is relatively weak in comparison to other cell adhesion mechanisms, such as those involving integrins for example. This has led to the suggestion that CD44 does not have a primary role in promoting attachments that strongly anchor cells to the matrix. Instead, it may facilitate transient associations that allow for the activation of intracellular cascades involved in processes required for cell activities such cell proliferation or migration (Savani et al. 2001). CD44 is also discussed to be involved in the presentation of cytokines/growth factors to other cell types (e. g. leucocytes), which then results in their adhesion (Borland et al. 1998). The CD44-variant CD44v3 for example is capable of binding growth factors and presents these factors to their high-affinity receptors (Bennett et al. 1995, Jackson et al. 1995). Interestingly, HA fragments accumulate in the absence of CD44 at the site of injury (Teder et al. 2002), suggesting a role for CD44 in the clearance of HA.

An increased expression of CD44 was detected in several studies investigating in diverse chronic kidney diseases. Early glomerular influx of CD44+ macrophages and de novo CD44 expression by proliferating mesangial cells was found in a rat model of glomerulonephritis (Nikolic-Paterson et al. 1996). As the CD44 expression was restricted to the transient period of mesangial cell proliferation, a functional interaction between the CD44/hyaluronan receptor-ligand pair during mesangial cell proliferation was suggested (Nikolic-Paterson et al. 1996). As mentioned, development of glomerular hypertrophy is as well characterized by proliferation of mesangial cells. Therefore, although the investigations in the present study were not performed in glomerulonephritis models of nephropathy, an involvement of increased glomerular Cd44 expression, as observed in glomerular samples of GIPR[dn]-transgenic and bGH-transgenic mice, in the development glomerular hypertrophy could probably be suggested as well.

In another study on an experimental rat model of glomerulonephritis, hyaluronan deposition in areas of fibrosis, such as glomerular crescents, was accompanied by the presence of many CD44+ infiltrating monocytes and lymphocytes, which adhered to activated endothelium and displayed high levels of CD44, expressed on their surface (Jun et al. 1997). It was concluded that CD44 is constitutively expressed in the normal kidney and is dramatically up-regulated in glomerulonephritis, suggesting a possible role for the CD44-hyaluronan interaction in leucocyte recruitment and development of fibrosis during the induction and progression of disease (Jun et al. 1997). Next to HA, also other constituents of the mesangial extracellular matrix as fibronectin and collagens, matrix metalloproteinases (MMPs) and osteopontin have been identified as binding ligands for different CD44 variants (Bennett et al. 1995, Jalkanen and Jalkanen 1992, Noiri et al. 1999, Ophascharoensuk et al. 1999, Weber et al. 1996, Yang et al. 1994). CD44 was also shown to be directly involved in modulation of molecular pathways as of transforming growth factor-ß1 (Yu and Stamenkovic 2000), hepatocyte growth factor (Rouschop et al. 2004), MMPs and tissue inhibitors of MMP (TIMP) (Duymelinck et al. 2000, Oda et al. 2001), which are important determinants of progression of chronic renal diseases.

LYVE-1, a CD44 homologue transmembrane receptor binds to both soluble and immobilized hyaluronan (Banerji et al. 1999) with greater specificity than CD44 and is also involved in the uptake of hyaluronan by lymphatic endothelial cells. LYVE-1 was considered to be the first HA receptor present on lymph vessels but completely absent from blood vessels (Jackson et al. 2001).

Next to its expression in lymphatic vessels (Prevo et al. 2001), it also appears in normal hepatic blood sinusoidal endothelial cells in mice and humans, suggesting that LYVE-1 has functions beyond the lymph vascular system (Mouta Carreira et al. 2001). This suggestion is supported by the finding that CRSBP-1, a membrane glycoprotein that was found to be identical to LYVE-1 , can mediate cell-surface retention of secreted growth factors containing CRS motifs such as platelet derived growth factor-B and is suggested to play a role in autocrine regulation of cell growth mediated by growth regulators containing CRS motifs (Huang et al. 2003). Expression of LYVE-1 in glomerular cells has not been reported so far.

However, due to the similarity of LYVE-1 to CD44 and due to the steadily growing numbers of identified ligands for different CD44 variants (Bennett et al. 1995, Jalkanen and Jalkanen 1992, Weber et al. 1996, Yang et al. 1994) it is supposable, that there might be more further functions and ligands for CD44 and LYVE-1, than the ones yet described.

Due to these manifold cross-links of yet described CD44 functions with other well known mechanisms that contribute to development of glomerular alterations in various chronic kidney diseases and in experimental models of nephropathy, a potential pathogenetically relevant involvement of CD44, and probably of LYVE1, in the development of the investigated early stages of glomerular alterations might also be assumed for GIPR^{dn}-transgenic and bGH-transgenic mice. As the development of glomerular hypertrophy and subsequent albuminuria in the investigated murine nephropathy models is not accompanied by a noticeable appearance of inflammatory cells infiltrating the glomerulus, the detection of the cellular origin of glomerular Cd44 and Xlkd1 gene expression will provide further inside views into their assumed pathogenetical significance.

5.6.7 Commonly differentially expressed genes involved in cytoskeletal functions

Cytoskeletal reorganization is fundamental for cell shape change, signalling, locomotion, and many other important dynamic cellular processes and plays an important role in development of glomerulosclerotic lesions due to podocyte damage (Pavenstadt et al. 2003, Shankland 2006). In the present study performance of microarray experiments on samples of isolated glomeruli of GIPR^{dn}- and bGH-transgenic mice identified an elevated common congeneric expression of several glomerular transcripts of genes, whose related proteins have a known function as structural components of the cytoskeleton (Myo1f, Tnnt2, cDNA 2810484G07 gene) or act as regulators of the organization of cytoskleletal components (Filip1, Dnai1). Filamin A interacting protein 1 (FILIP1) is crucially involved in the regulation and control of function and cellular content of Filamin A, as it induces its degradation (Nagano et al. 2002). Filamin A, is a widely expressed actin-binding protein that regulates the reorganization of the actin cytoskeleton.

Cytoskeletal reorganization is fundamental for cell shape change, signaling, and many other important dynamic cellular processes, which are known to be altered in development of glomerulosclerotic lesions due to podocyte damage (Pavenstadt et al. 2003, Shankland 2006). Filamin A is known to interact with various proteins, including integrins (Loo et al. 1998), transmembrane receptor complexes (Awata et al. 2001, Hjalm et al. 2001, Lin et al. 2001) and signal transduction molecules (Scott et al. 2006, Stossel et al. 2001). It crosslinks actin filaments into orthogonal networks in the cortical cytoplasm and participates in the anchoring of membrane proteins for the actin cytoskeleton. Filamin provides a scaffold for small GTPases that regulate cytoskeletal organization and are crucially involved in signaling mechanisms that target the cytoskeleton in development of podocyte damage (Kobayashi et al. 2004, Shirato et al. 1996, Togawa et al. 1999). Filamin also interacts directly with caveolin (Gorlin et al. 1990, Stahlhut and van Deurs 2000), a protein component of caveolae, plasma membrane microdomains containing receptors and associated signalling molecules as G proteins and calcium receptors that are thought to serve as cellular "message centres" (Schlegel et al. 1998). Finally, Filamin is involved in protein trafficking and contributes to localization and cycling of proteins in the cell (Li et al. 2000, Liu et al. 1997). Most of the Filamin associated signaling pathways are at least partially known to play key roles in the pathogenesis of podocyte and mesangial cell damage during development of glomerular lesions in various chronic kidney diseases (Gomez-Guerrero et al. 2005, Pavenstadt et al. 2003). The Filamin A interacting protein 1 (FILIP1) is crucially involved in the regulation, the control of function and the cellular content of Filamin A, as it induces its degradation (Nagano et al. 2002). Therefore, a pathogenetically important participation of FilaminA/FILIP1 in the development of the early investigated stages of glomerulosclerotic alterations in GIPR[dn]-transgenic and bGH-transgenic mice might as well be assumed.

Further identified "cytoskeleton-associated transcripts" that displayed an elevated common differential expression across all investigated glomerular samples of GIPR[dn]- and bGH-transgenic mice were coding for the intermediate polypeptide of axonemal dynein, Myosin 1F, Troponin T type 2 (cardiac) and the gene product of the RIKEN cDNA 2810484G07 (similar to beta tubulin 1, class VI) -gene.

The respective proteins have known functions as structural components of the cytoskeleton and participate in cellular functions as adhesion, cell-matrix contacts, motility (Kim et al. 2006), calcium signaling pathways, mitosis, cytokinesis, vesicular transport and maintenance of the structure of podocyte foot processes (Kobayashi et al. 2001).

Dyneins are involved in cellular processes of ciliary beating, intracellular transport, organelle transport, mitosis and cell polarization. Based on both functional and structural criteria, dyneins fall into two major classes, cytoplasmic and axonemal dyneins. Dynein isoformspecific intermediate chains are found in some axonemal dyneins as well as in cytoplasmic dynein (Hook and Vallee 2006). Dyneins are crucially involved in the development, maintenance and modulation of the podocyte cytoskeleton and foot process architecture. Therefore, they play important roles in both physiological podocyte function, as well as in the pathogenesis of podocyte damage during development of glomerular lesions (Kobayashi et al. 2004, Kobayashi and Mundel 1998).

Actin-associated motor proteins like myosin allow for isometric or isotonic contraction of the bundles in muscle and non-muscle cells (Gordon et al. 2000). The Myo1f-gene is widely expressed in adult mouse tissues (Crozet et al. 1997), predominantly in the mammalian immune system. Also non-muscle cells as myofibroblasts express many homologues of sarcomeric proteins. Myofibroblasts are cells of mesenchymal origin that are characterized by a fibroblastic appearance with some ultrastructural features of muscle cells. Glomerular mesangial cells are myofibroblasts (Johnson et al. 1992), that contract and relax in response to vasoactive agents (Badr et al. 1989, Schlondorff 1987, Schlondorff et al. 1984). Their contractile properties are thought to control the rate of glomerular filtration by changing capillary surface area. They play a key role in processes leading to development of glomerular alterations (Skalli and Gabbiani 1988), as they are involved in the generation of mediators of inflammation, synthesis of cytokines, production and breakdown of basement membranes, as well as uptake of macromolecules (Abboud 1991, Elema et al. 1976, Martin et al. 1989, Ohyama et al. 1990).

The Troponin T type 2 (cardiac) protein encoded by the Tnnt2 gene is the tropomyosin-binding subunit of the troponin complex, which is located on the thin filament of striated muscles and regulates muscle contraction in response to alterations in intracellular calcium ion concentration.

Cardiac troponin T is a very sensitive and specific marker of myocardial damage (Bozbas et al. 2006) However, in the absence of a major clinically evident cardiac injury, troponins are found to be elevated in several clinical conditions, including ESRD (Dierkes et al. 2000, Donaldson and Cove-Smith 2001).

Finally, also transcripts corresponding to the RIKEN cDNA 2810484G07 gene (similar to beta tubulin 1, class VI) displayed an increased common differential expression in the investigated glomerulus isolates of GIPR[dn]-transgenic and bGH-transgenic mice in both stages of glomerular alteration. Beta-tubulins are constituents of microtubules, structural cellular components which are involved in processes as e. g. mitosis, cytokinesis, and vesicular transport. In glomerular cells, they are essential for an intact structure of major podocyte processes, since they connect the cell body with the GBM-anchored actin network in foot processes (Kobayashi et al. 2001).

Taken together, although they have yet not been described in this particular context, the deduced proteins of the Myo1f, Tnnt2 and the RIKEN cDNA 2810484G07 -gene might be supposed to be important for physiological glomerular function. Their detected common differential glomerular expression in GIPR[dn]-transgenic and bGH-transgenic mice might therefore reflect important changes of the cytoskeletal architecture of glomerular cells during development of glomerular hypertrophy.

5.6.8 Commonly differentially expressed genes involved in G-protein dependent signaling processes

Transcripts coding for GNG2, a subunit of a heterotrimeric G-protein protein, commonly displayed increased differential expressions in the investigated glomerular samples of all transgenic mice in the present study. The biological function of heterotrimeric G-protein proteins is to act as signal transducers in G-protein coupled receptor signaling pathways. G-protein signaling participates in cellular processes as mitogenesis, chemotaxis, migration, aggregation, proliferation, formation, endocytosis, formation of focal adhesions adhesion and actin stress fibers and rearrangement of the actin cytoskeleton. Moreover, G-protein protein dependent signaling processes are involved in regulation of several downstream pathways, which are considered to play important roles in podocyte (Pavenstadt et al. 2003) and mesangial cell damage (Gomez-Guerrero et al. 2005) during development of glomerulosclerosis.

GTP-binding proteins have been identified to be involved in the mediation of several effects (Schlondorff et al. 1989) of the various known factors (Ruiz-Ortega et al. 2001) involved in regulation of mesangial cell growth, proliferation, hypertrophy and increased synthesis and accumulation of extracellular matrix proteins and are therefore considered to be important molecules for maintenance of glomerular function and mediation of a variety of processes participating in development of glomerular lesions. Since an affection of single specific molecular pathways in this context can not be concluded directly from detection of elevated glomerular expression of transcripts coding for GNG2, it remains speculative, if the observed common differential expression of the Gng2 gene reflects a pathogenetically important process in development of glomerular hypertrophy, or mirrors just epiphenomenous changes of the glomerular transcription profiles.

5.6.9 Commonly differentially expressed genes involved in immunological events

In the microarray experiments of the present study, a congeneric common elevated expression of transcripts coding for the beta polypeptide of the complement subcomponent 1 Q, (C1QB) and the high affinity Fc gamma (IgG) receptor 1 (FCGR1) was detected in glomerular samples of all investigated GIPR^{dn}- and bGH-transgenic animals in both stages of early glomerular alteration.

The known molecular functions of C1QB and FCGR1 associate these gene products to processes of immunological and inflammatory character. It has been widely accepted that immune reactions are centrally involved in the development of glomerular disease (Gomez-Guerrero et al. 2005). In this context, the involvement of the complement system and the importance of immune complex (IC) formation/localization to the mesangium in the pathogenesis of kidney diseases have been studied intensively. C1QB is a constituent of the first component of the serum complement system, C1. The C1q complex is potentially multivalent for attachment to the complement fixation sites of immunoglobulin. C1QB is expressed in a large variety of tissues, including the kidney and neuronal cells (Rozovsky et al. 1994, Spielman et al. 2002). FCGR1 is a type of integral membrane glycoprotein that binds monomeric IgG-type antibodies with high affinity. Fc receptors are most important for inducing phagocytosis of opsonized antigens (Hulett and Hogarth 1998). FCGR1 is predominantly found on macrophages and monocytes.

In glomerulonephritis, deposition of ICs and complement activation in the glomerulus has been regarded to be responsible for the initiation of glomerular injury, although cell-mediated immunity also plays an essential role in initiation and perpetuation of glomerular inflammation (Radeke and Resch 1992). IC-mediated injury is seen in a large number of different nephropathies, such as idiopathic membranous and membranoproliferative glomerulonephritis, IgA nephropathy, postinfectious glomerulonephritis, and other disease entities (Ambrus and Sridhar 1997). The initial phase of immune-mediated glomerular inflammation depends on the interaction of ICs with specific Fc receptors and/or complement receptors in infiltrating leukocytes and resident mesangial cells (MC), the ability of immune complexes to activate the complement system and on local inflammatory processes (Gomez-Guerrero et al. 2005). IC-bound activated C1Q has the potential to interact with cellular C1Q-receptors (C1Q-R) (Anders et al. 2003), which are expressed by monocytes, macrophages, polymorphonuclear cells, lymphocytes, endothelial cells, MC (van den Dobbelsteen et al. 1993) and podocytes (Anders et al. 2003, Brady et al. 1992, Denton et al. 1991, Nolasco et al. 1987, van den Dobbelsteen et al. 1993). Several studies also confirmed the expression of functional Fc gamma receptors also on glomerular mesangial cells (Neuwirth et al. 1988, Santiago et al. 1991, Schlondorff and Mori 1990, van den Dobbelsteen et al. 1993). The expression of Fc receptors for IgG on MC was found to be influenced by several factors with known implication in the pathogenesis of glomerular disease, including GM-CSF and complement C1q (Daha 2000, Santiago et al. 1991, Schlondorff and Mori 1990, Singhal et al. 1990, van den Dobbelsteen et al. 1996). Further studies indicated cooperative effects between Fc gamma receptors and C1Q-receptors on MC in the recognition of immune complexes (van den Dobbelsteen et al. 1993). After an initial activation through IC and complement, mesangial cells express or release numerous biologically active molecules, most of which are mediators of inflammation, leading to amplification of the injury (Tarzi and Cook 2003, Veis 1993). Binding and uptake of IgG-containing IC, or soluble aggregates by mesangial cells triggers the release of a wide array of mediators involved in inflammation (Chen et al. 1994, Gomez-Chiarri et al. 1993, Gomez-Guerrero et al. 1994, Leung et al. 2003, Matsumoto and Hatano 1991, Radeke and Resch 1992), proliferation (Gomez-Guerrero et al. 1994), migration and matrix production (Lai et al. 2003, Lopez-Armada et al. 1996, Wang et al. 2004).

Deficiency of C1q has been associated with auto-immune disease and glomerulonephritis in humans, as well as in studies of experimental animal models (Hannema et al. 1984), indicating a protective effect of C1Q from immune-mediated glomerular injury and development of glomerulosclerotic kidney lesions (Robson et al. 2001, Turnberg et al. 2006). There is also increasing evidence from in vivo and in vitro studies, that the complement system is important in mediating renal injury in proteinuric diseases and that complement activation is a crucial step in the development of complement-mediated podocyte injury in various, predominantly inflammatory nephropathies (Gomez-Guerrero et al. 2005, Pavenstadt et al. 2003). The precise mechanisms by which complement activation causes podocyte damage and proteinuria are unclear. Although podocytes seem to be resistant to cell lysis by C5b-9, C5b-9 induces podocytes to produce reactive oxygen radicals. This, as well as other mechanisms induced by complement-mediated glomerular injury (McMillan et al. 1996, Shankland et al. 1996) leads to an alteration of the properties of the glomerular filtration barrier and overproduction of matrix (Kerjaschki and Neale 1996, Shankland et al. 1996).

As the investigated forms of nephropathies developing in GIPR^{dn}- and bGH-transgenic mice are in first instance of non-inflammatory character and not associated with any observed appearance of immune complexes, a significant pathogenetic participation of the detected elevated glomerular expression abundances of Fcgr1 and C1qb in the development of early stages of glomerulosclerotic alteration in these models of nephropathy has to be doubted. As approximatively 2% of all mesangial cells are Fc receptor expressing phagocytes (Venkatachalam and Kriz 1992), the increased differential glomerular expression of these genes might probably result from the presence of increased numbers of mesangial cells in hypertrophied glomeruli.

5.7 Conclusions and future prospects

The results of the present study demonstrate that the development of characteristic early comparable stages of glomerular alterations in completely different transgenic mouse models of nephropathy is characterized by shared expression signatures of glomerular genes. Appliance of a sophisticated experimental design and stringent parameters for characterization of the investigated stages of morphological and functional glomerular alteration allowed for their identification.

The data generated in the present study provide a basis for detailed further investigations in the single investigated animal models, as well as in the identified shared glomerular expression profiles of both experimental models. The bioinformatical analyses indicate a participation both of molecules with an already known pathogenetic significance in development of glomerular damage, as CD44 or Fraktalkine, but also a potential involvement of gene products which have yet not been subject of comprehensive investigations in this context (e.g. FABP4, MSR1, TGH2, LYVE1). Further studies will focus on the participation of single of these molecules in the pathogenesis of glomerular hypertrophy and/or onset of albuminuria. The questions to be addressed in the next analyses concern the cellular origin of commonly differentially expressed glomerular genes on the RNA and protein level in order to evaluate the contribution of single glomerular cell types (podocytes, mesangial cells, endothelial cells and resident or immigrated cells of the immune system) to the altered glomerular expression profiles.

These further studies will help to reveal the relevance of these shared expression signatures for our understanding of the molecular pathogenesis of early stages of progressive glomerulopathies, potential mechanisms of intraglomerular communication of different glomerular cell types, as well as the potential use of single identified transcripts or corresponding proteins as diagnostic markers or therapeutic targets. Additional investigations will identify causative (common) molecular mechanisms and pathways that trigger the development of early glomerular lesions in chronic kidney diseases of the investigated animal models, their potential involvement in the pathogenesis of human renal disease, as well as the regulatory networks that underlie the detected patterns of differential glomerular gene expression.

6. Summary

Development of glomerulosclerotic alterations is a common pathological feature of various progressive kidney diseases. The earliest stages of these different disease entities are characterized by common morphological and functional alterations of the glomeruli, such as glomerular hypertrophy and consecutive development of albuminuria. The present study addressed the question, if such common patterns of morphological and functional glomerular alterations would also find a reflection in common glomerular gene expression profiles. Therefore differential gene expression profiles of samples of isolated kidney glomeruli from two different transgenic mouse models of nephropathy were identified. Microarray experiments were performed in two defined comparable early stages of glomerular alteration. Investigated transgenic murine models of nephropathy consisted of a novel model of diabetes mellitus, transgenic mice expressing a dominant negative glucose-dependent insulinotropic polypeptide receptor (GIPR^{dn}), bred on the genetic background of the CD1 outbred stock; and growth hormone-transgenic mice (bGH), bred on a NMRI background. Transgenic animals of both models develop glomerular hypertrophy and micro-albuminuria. Pairs of male transgenic mice and their corresponding non-transgenic littermate control animals were investigated in two early comparable stages of glomerular alteration. These stages were defined as the stage of glomerular hypertrophy (stage I), characterized by a significant increase (40 – 60%) of the mean glomerular volume of the transgenic animals compared to the respective controls; and as stage II, the stage of onset of albuminuria. Transgenic animals assigned to stage II also had to display a significant increase of their mean glomerular volumes, as well as an onset of albuminuria, determined by repeated SDS-PAGE based urine analyses of urine samples taken on consecutive time points. Albuminuria was verified by Western blot and ELISA experiments. At both stages transgenic mice displayed a significant increase in numbers of mesangial and endothelial cells per glomerulus, determined by quantitative stereology, while numbers of podocytes per glomerulus remained almost unchanged. Glomerulus isolation was performed according to a modified magnetic isolation procedure, using spherical superparamagnetic beads for perfusion.

Total RNA of high quality was extracted from glomerulus isolates and processed for Affymetrix® GeneChip microarray analysis according to standard procedures. In each group (GIPR^{dn} and bGH) and stage (I & II), transcripts that displayed a significant differential abundance (False discovery rate < 0.049%) between transgenic animals

and their corresponding controls were identified and assigned to their respective genes. Commonly differentially expressed genes, representing the intersections of congeneric differentially expressed genes in both groups in comparable stages of glomerular alteration, were identified. The numbers of these commonly differentially expressed genes were found to be significantly enriched compared to random data sets. Transcripts of 21 genes were congeneric differentially expressed in all groups and stages. Differential expression of 5 of these transcripts (coding for Cx3cl1, Ctsh, Fabp4, Cd44 and Msr1) was confirmed by real-time PCR. RNA of sample materials that had previously been investigated in the array experiment, as well as RNA samples of an independent control cohort of same size, was evaluated.

Irrespective of type of transgene or genetic background of the different investigated animal models, common patterns of glomerular gene expression profiles in early stages of glomerular alteration were identified. Within these common expression profiles, genes/transcripts with already known involvement in development of glomerular lesions, as well as some that have not yet been described in this context were identified. The gene products with known involvement in development of nephropathy comprise those with Gene ontology functions assigned to cell adhesion molecules, cytokines and mediators of inflammation and regulators of extracellular matrix turnover. Functional catagories assigned to novel gene products in the context of glomerular alterations include cell adhesion molecules, lipid metabolism, cytoskeletal dynamics and intracellular signal transduction.

These datasets provide the basis for further studies, with the aim to integrate these shared expression signatures in our understanding of the molecular pathogenesis of early stages of progressive glomerulopathies to define therapeutic targets. A potential clinical application could be in their suitability as early diagnostic markers of glomerular damage.

7. Zusammenfassung

Progressive glomerulosklerotische Alterationen treten bei Mensch und Tier als gemeinsames histopathologisches Erscheinungsbild bei diversen systemischen Grunderkrankungen sowie verschiedensten Nephropathien mit Tendenz zur Entwicklung eines terminalen Nierenversagens auf. Glomeruläre Hypertrophie und konsekutiv einsetzende Mikroalbuminurie sind charakteristische frühstadiale glomeruläre Alterationsformen, welchen im Rahmen der Entwicklung der progressiven Glomerulosklerose eine entscheidende pathogenetische Relevanz zugesprochen wird.

Ziel der vorliegenden Arbeit war es aufzuklären, ob die in verschiedenen Nephropathiemodellen uniform auftretenden Alterationsstadien der 1.) glomerulären Hypertrophie und 2.) glomerulären Hypertrophie mit Mikroalbuminurie eine Entsprechung in gemeinsamen glomerulären Genexpressionsprofilen finden würden. Zu diesem Zwecke wurden in den beiden Alterationsstadien Microarray-basierte Genexpressionsanalysen an Proben isolierter Glomerula von männlichen transgenen Tieren und nicht-transgenen Kontrolltieren zweier muriner Nephropathiemodelle durchgeführt. Bei diesen Nephropathiemodellen handelte es sich zum einen um Wachstumshormon-transgene Mäuse (NMRI Hintergrund), welche das bovine Wachstumshormongen unter der transkriptionellen Kontrolle des Promotors des Phosphoenolpyruvat-carboxykinasegens der Ratte exprimieren. Sie repräsentieren ein gut charakterisiertes Modell zum Studium der progressiven Glomerulosklerose. Als zweites Modell dienten diabetische transgene Mäuse (CD1 Hintergrund), welche einen dominant negativen Glucose-dependent Insulinotropic Polypeptide Receptor (GIPR^{dn}) unter der transkriptionellen Kontrolle des Insulingenpromotors der Ratte in den pankreatischen ß-Zellen exprimieren. Diese Tiere stellen ein Modell für Diabetes mellitus-assoziierte Nierenveränderungen dar.

Die untersuchten Stadien der glomerulären Hypertrophie und der einsetzenden Mikroalbuminurie wurden durch jeweils vergleichbare Grade morphologischer und funktioneller glomerulärer Veränderungen der transgenen Individuen eines jeden Tiermodelles definiert. Als Bedingung für die Untersuchung im Stadium der glomerulären Hypertrophie wurde eine mittels quantitativ stereologischer Untersuchungen objektiv erfasste signifikante Zunahme (40 – 60%) des mittleren glomerulären Volumens der transgenen Tiere gegenüber dem der nicht-transgenen Kontrolltiere festgelegt.

Im zweiten Untersuchungsstadium hatten die transgenen Tiere beider untersuchter Modelle neben bestehender glomerulärer Hypertrophie zusätzlich das Merkmal einer einsetzenden, nicht transienten Mikroalbuminurie aufzuweisen. Hierzu wurden in definierten Zeitabständen gewonnene Spontanurinproben sämtlicher Tiere durch SDS-PAGE basierte Urinproteinanalysen untersucht. Die Mikroalbuminurie wurden durch Western-blot- sowie ELISA- Analysen bestätigt.

Im Vergleich zu nicht-transgenen Kontrolltieren war die mittels quantitativer Stereologie bestimmte durchschnittliche Gesamtzellzahl pro Glomerulum bei transgenen Tieren beider Modelle in beiden untersuchten Stadien erhöht. Diese für die Entwicklung der glomerulären Hypertrophie charakteristische Veränderung war durch eine Erhöhung der Anzahl der endothelialen und mesangialen glomerulären Zellen pro Glomerulum gekennzeichnet, wohingegen die Anzahl der Podozyten unverändert blieb.

Zur Gewinnung von Glomerulumisolaten, welche den qualitativen und quantitativen Anforderungen einer umfassenden Genexpressionsanalyse genügen, wurde ein in umfangreichen Vorversuchen modifiziertes und optimiertes Protokoll einer jüngst entwickelten Methode der magnetischen Isolation von murinen Glomerula angewandt. Aus den generierten Glomerulumisolaten extrahierte, qualitativ hochwertige RNA wurde unter Anwendung von Standardmethoden prozessiert und auf Affymetrix GeneChip® Arrays hybridisiert. Die statistische Auswertung der Arraydaten erfolgte unter Festlegung eines stringenten Signifikanzniveaus (false discovery rate < 0,049%).

Transkripte, welche in den glomerulären Proben von transgenen und nicht-transgenen Tieren eines Tiermodelles und Alterationsstadiums in signifikant differentieller Abundanz vorlagen wurden identifiziert und den ihnen entsprechenden Genen zugeordnet. In beiden untersuchten Stadien konnten signifkant angereicherte Schnittmengen der Anzahlen von in beiden Tiermodellen gleichartig differentiell exprimierten Genen identifiziert werden. Ferner wurden in den untersuchten Glomerulumisolaten beider Nephropathiemodelle Transkripte von 21 Genen identifiziert, welche in beiden Untersuchungsstadien gemeinsam differentiell abundant vorlagen. Diese repräsentieren somit ein gemeinsames glomeruläres Expressionsprofil der Entwicklung glomerulärer Hypertrophie und des Einsetzens der Mikroalbuminurie.

Zur Verifikation der Ergebnisse der Arrayanalysen wurde die glomeruläre Expression von fünf ausgewählten, in beiden Untersuchungsstadien gemeinsam differentiell exprimierten Genen (CD44, Fractalkine, Fatty acid binding protein 4, Macrophage scavenger receptor 1, Cathepsin H) durch quantitative real-time PCR untersucht. Die gemeinsame differentielle glomeruläre Expression dieser Gene konnte sowohl in dem im Array-Experiment untersuchten Material als auch in Proben einer unabhängigen Kontrollkohorte gleichen Probenumfanges bestätigt werden.

Einige der im Rahmen der vorliegenden Studie identifizierten 21 gemeinsam differentiell glomerulär exprimierten Gene beziehungsweise ihre Genprodukte sind bereits im Zusammenhang mit verschiedenen Nephropathieformen beschrieben worden. Sie besitzen bekannte Funktionen als Zytokine, Zelladhäsionsmoleküle, zytoskelettale Elemente und als Matrixproteinasen. Die bislang nicht im Kontext von Glomerulopathien beschriebenen Gene kodieren für weitere Zelladhäsionsmoleküle sowie für Proteine mit Funktionen im Lipidstoffwechsel, der intrazellulären Signaltransduktion oder der Regulation der Organisation des Zytoskelettes. Ihre potenzielle pathogenetische Relevanz im Hinblick auf die Entwicklung der glomerulären Alterationen der untersuchten Tiermodelle sowie ihre Bedeutung im Rahmen chronischer Nierenerkrankungen des Menschen wird Gegenstand weiterführender Studien sein.

Die Ergebnisse der vorliegenden Arbeit zeigen, dass vergleichbare, in verschiedenartigen Nephropathiemodellen auftretende frühe morphologische und funktionelle Stadien glomerulärer Alterationen auf molekularer Ebene durch gemeinsame differentielle glomeruläre Genexpressionsprofile gekennzeichnet sind. Die erzielten Resultate stellen somit die Grundlage für die weitere Aufklärung der an der Entwicklung frühstadialer glomerulärer Alterationen beteiligten molekularen Mechanismen sowie die Identifizierung regulativer Schlüsselmoleküle, potenzieller Marker und therapeutischer Angriffspunkte dar.

.

8 References

Abbate, M., Zoja, C., Morigi, M., Rottoli, D., Angioletti, S., Tomasoni, S., Zanchi, C., Longaretti, L., Donadelli, R., and Remuzzi, G. 2002. Transforming growth factor-beta1 is up-regulated by podocytes in response to excess intraglomerular passage of proteins: a central pathway in progressive glomerulosclerosis. *Am J Pathol* 161:2179-2193.

Abboud, H.E. 1991. Resident glomerular cells in glomerular injury: mesangial cells. *Semin Nephrol* 11:304-311.

Abitbol, C., Zilleruelo, G., Freundlich, M., and Strauss, J. 1990. Quantitation of proteinuria with urinary protein/creatinine ratios and random testing with dipsticks in nephrotic children. *J Pediatr* 116:243-247.

Abrass, C.K. 2006. Lipid metabolism and renal disease. *Contrib Nephrol* 151:106-121.

Adler, S., and Brady, H.R. 1999. Cell adhesion molecules and the glomerulopathies. *Am J Med* 107:371-386.

Affymetrix Manual. GeneChip Essentials - How Affymetrix Genechip® Gene Expression Microarrays Work. http://www.affymetrix.com/corporate/media/genechip_essentials/gene_expression/Matchmaker __Matchmaker.affx

Afonina, I., Zivarts, M., Kutyavin, I., Lukhtanov, E., Gamper, H., and Meyer, R.B. 1997. Efficient priming of PCR with short oligonucleotides conjugated to a minor groove binder. *Nucleic Acids Res* 25:2657-2660.

Akalin, E., Hendrix, R.C., Polavarapu, R.G., Pearson, T.C., Neylan, J.F., Larsen, C.P., and Lakkis, F.G. 2001. Gene expression analysis in human renal allograft biopsy samples using high-density oligoarray technology. *Transplantation* 72:948-953.

Alcorta, D.A., Prakash, K., Waga, I., Sasai, H., Munger, W., Jennette, J.C., and Falk, R.J. 2000. Future molecular approaches to the diagnosis and treatment of glomerular disease. *Semin Nephrol* 20:20-31.

Alebiosu, C.O., and Ayodele, O.E. 2005. The global burden of chronic kidney disease and the way forward. *Ethn Dis* 15:418-423.

Amann, K., Irzyniec, T., Mall, G., and Ritz, E. 1993. The effect of enalapril on glomerular growth and glomerular lesions after subtotal nephrectomy in the rat: a stereological analysis. *J Hypertens* 11:969-975.

Ambrus, J.L., Jr., and Sridhar, N.R. 1997. Immunologic aspects of renal disease. *Jama* 278:1938-1945.

Anders, H., and Schlondorff, D. 2000. Murine models of renal disease: possibilities and problems in studies using mutant mice. *Exp Nephrol* 8:181-193.

Anders, H.J., Vielhauer, V., and Schlondorff, D. 2003. Chemokines and chemokine receptors are involved in the resolution or progression of renal disease. *Kidney Int* 63:401-415.

Anderson, S., Meyer, T.W., Rennke, H.G., and Brenner, B.M. 1985. Control of glomerular hypertension limits glomerular injury in rats with reduced renal mass. *J Clin Invest* 76:612-619.

Anderson, S., Rennke, H.G., and Brenner, B.M. 1986. Therapeutic advantage of converting enzyme inhibitors in arresting progressive renal disease associated with systemic hypertension in the rat. *J Clin Invest* 77:1993-2000.

Artacho-Perula, E., Roldan-Villalobos, R., Salcedo-Leal, I., and Vaamonde-Lemos, R. 1993. Stereological estimates of volume-weighted mean glomerular volume in streptozotocin-diabetic rats. *Lab Invest* 68:56-61.

Aruffo, A., Stamenkovic, I., Melnick, M., Underhill, C.B., and Seed, B. 1990. CD44 is the principal cell surface receptor for hyaluronate. *Cell* 61:1303-1313.

Arya, M., Shergill, I.S., Williamson, M., Gommersall, L., Arya, N., and Patel, H.R. 2005. Basic principles of real-time quantitative PCR. *Expert Rev Mol Diagn* 5:209-219.

Asanuma, K., and Mundel, P. 2003. The role of podocytes in glomerular pathobiology. *Clin Exp Nephrol* 7:255-259.

Atkins, R.C. 2005. The epidemiology of chronic kidney disease. *Kidney Int Suppl*:S14-18.

Awata, H., Huang, C., Handlogten, M.E., and Miller, R.T. 2001. Interaction of the calcium-sensing receptor and filamin, a potential scaffolding protein. *J Biol Chem* 276:34871-34879.

Babinet, C. 2000. Transgenic mice: an irreplaceable tool for the study of mammalian development and biology. *J Am Soc Nephrol* 11 Suppl 16:S88-94.

Badr, K.F., Murray, J.J., Breyer, M.D., Takahashi, K., Inagami, T., and Harris, R.C. 1989. Mesangial cell, glomerular and renal vascular responses to endothelin in the rat kidney. Elucidation of signal transduction pathways. *J Clin Invest* 83:336-342.

Baelde, H.J., Bergijk, E.C., and Bruijn, J.A. 1990. Isolation and characterization of mouse glomerular basement membrane. *J Clin Lab Immunol* 33:17-20.

Baelde, H.J., Eikmans, M., Doran, P.P., Lappin, D.W., de Heer, E., and Bruijn, J.A. 2004. Gene expression profiling in glomeruli from human kidneys with diabetic nephropathy. *Am J Kidney Dis* 43:636-650.

Baelde, J.J., Bergijk, E.C., Hoedemaeker, P.J., de Heer, E., and Bruijn, J.A. 1994. Optimal method for RNA extraction from mouse glomeruli. *Nephrol Dial Transplant* 9:304-308.

Baldwin, D.S. 1982. Chronic glomerulonephritis: nonimmunologic mechanisms of progressive glomerular damage. *Kidney Int* 21:109-120.

Banas, B., Wornle, M., Berger, T., Nelson, P.J., Cohen, C.D., Kretzler, M., Pfirstinger, J., Mack, M., Lipp, M., Grone, H.J., and Schlondorff, D. 2002. Roles of SLC/CCL21 and CCR7 in human kidney for mesangial proliferation, migration, apoptosis, and tissue homeostasis. *J Immunol* 168:4301-4307.

Banerji, S., Ni, J., Wang, S.X., Clasper, S., Su, J., Tammi, R., Jones, M., and Jackson, D.G. 1999. LYVE-1, a new homologue of the CD44 glycoprotein, is a lymph-specific receptor for hyaluronan. *J Cell Biol* 144:789-801.

Barati, M.T., Merchant, M.L., Kain, A.B., Jevans, A.W., McLeish, K.R., and Klein, J.B. 2007. Proteomic analysis defines altered cellular redox pathways and advanced glycation end-product metabolism in glomeruli of db/db diabetic mice. *Am J Physiol Renal Physiol* 293:F1157-1165.

Barisoni, L., Kriz, W., Mundel, P., and D'Agati, V. 1999. The dysregulated podocyte phenotype: a novel concept in the pathogenesis of collapsing idiopathic focal segmental glomerulosclerosis and HIV-associated nephropathy. *J Am Soc Nephrol* 10:51-61.

Baxa, C.A., Sha, R.S., Buelt, M.K., Smith, A.J., Matarese, V., Chinander, L.L., Boundy, K.L., and Bernlohr, D.A. 1989. Human adipocyte lipid-binding protein: purification of the protein and cloning of its complementary DNA. *Biochemistry* 28:8683-8690.

Bazan, J.F., Bacon, K.B., Hardiman, G., Wang, W., Soo, K., Rossi, D., Greaves, D.R., Zlotnik, A., and Schall, T.J. 1997. A new class of membrane-bound chemokine with a CX3C motif. *Nature* 385:640-644.

Bellush, L.L., Doublier, S., Holland, A.N., Striker, L.J., Striker, G.E., and Kopchick, J.J. 2000. Protection against diabetes-induced nephropathy in growth hormone receptor/binding protein gene-disrupted mice. *Endocrinology* 141:163-168.

Bending, J.J., Lobo-Yeo, A., Vergani, D., and Viberti, G.C. 1988. Proteinuria and activated T-lymphocytes in diabetic nephropathy. *Diabetes* 37:507-511.

Benigni, A., Corna, D., Zoja, C., Longaretti, L., Gagliardini, E., Perico, N., Coffman, T.M., and Remuzzi, G. 2004. Targeted deletion of angiotensin II type 1A receptor does not protect mice from progressive nephropathy of overload proteinuria. *J Am Soc Nephrol* 15:2666-2674.

Benigni, A., Gagliardini, E., Tomasoni, S., Abbate, M., Ruggenenti, P., Kalluri, R., and Remuzzi, G. 2004. Selective impairment of gene expression and assembly of nephrin in human diabetic nephropathy. *Kidney Int* 65:2193-2200.

Bennett, K.L., Jackson, D.G., Simon, J.C., Tanczos, E., Peach, R., Modrell, B., Stamenkovic, I., Plowman, G., and Aruffo, A. 1995. CD44 isoforms containing exon V3 are responsible for the presentation of heparin-binding growth factor. *J Cell Biol* 128:687-698.

Bergstein, J.M. 1999. A practical approach to proteinuria. *Pediatr Nephrol* 13:697-700.

Bertani, T., Cutillo, F., Zoja, C., Broggini, M., and Remuzzi, G. 1986. Tubulo-interstitial lesions mediate renal damage in adriamycin glomerulopathy. *Kidney Int* 30:488-496.

Bertani, T., Rocchi, G., Sacchi, G., Mecca, G., and Remuzzi, G. 1986. Adriamycin-induced glomerulosclerosis in the rat. *Am J Kidney Dis* 7:12-19.

Beynon, R.J., and Hurst, J.L. 2004. Urinary proteins and the modulation of chemical scents in mice and rats. *Peptides* 25:1553-1563.

Bhathena, D.B. 2003. Glomerular basement membrane length to podocyte ratio in human nephronopenia: implications for focal segmental glomerulosclerosis. *Am J Kidney Dis* 41:1179-1188.

Binder, C.J., Weiher, H., Exner, M., and Kerjaschki, D. 1999. Glomerular overproduction of oxygen radicals in Mpv17 gene-inactivated mice causes podocyte foot process flattening and proteinuria: A model of steroid-resistant nephrosis sensitive to radical scavenger therapy. *Am J Pathol* 154:1067-1075.

Block, C. 2007. Differential Proteomic analysis of isolated glomeruli from two murine nephropathy models at early stages of glomerulosclerosis. In *Institute of Veterinary Pathology*. Munich: Ludwig-Maximilians-University.

Block, C., Blutke, A., Berendt, F., Kemter, E., Herbach, N., Wanke, R., and Arnold, G.J. 2006. 2D DIGE based subproteome analysis of renal glomeruli from two murine nephropathy

models. Abstract in *Proceedings of the 7th Siena Meeting - From Genome to Proteome: Back to the future.* Siena, Italy.

Block, C. 2008. Differential Proteomic analysis of isolated glomeruli from two murine nephropathy models at early stages of glomerulosclerosis. Inaugural – Dissertation to achieve the doctor title of veterinary medicine at the Faculty of Veterinary Medicine of the Ludwig-Maximilians-University, Munich. Currently under revision. 1-150.

Blutke, A. 2006. Perfusionsanordnung. Gebrauchsmusterschrift. Aktenzeichen DE 20 2006 001 542.6. Eintragungstag 20.04.2006. Bekanntmachung im Patentblatt des Deutsches Patent- und Markenamtes (DPMA) der Bundesrepublik Deutschland.

Blutke, A., Block, C., Kemter, E., Wolf, E., Herbach, N., and Wanke, R. 2005. Large scale isolation of glomeruli from murine kidneys: Comparison of different methods and solutions for methodological problems. Abstract in *Proceedings of the 23rd Meeting of the European Society of Veterinary Pathology*. Neaples, Italy. 36.

Bonvalet, J.P., Champion, M., Courtalon, A., Farman, N., Vandewalle, A., and Wanstok, F. 1977. Number of glomeruli in normal and hypertrophied kidneys of mice and guinea-pigs. *J Physiol* 269:627-641.

Borland, G., Ross, J.A., and Guy, K. 1998. Forms and functions of CD44. *Immunology* 93:139-148.

Bottinger, E.P., Novetsky, A., and Zavadil, J. 2003. RNA labeling and hybridization of DNA microarrays. *Methods Mol Med* 86:275-284.

Bozbas, H., Yildirir, A., and Muderrisoglu, H. 2006. Cardiac enzymes, renal failure and renal transplantation. *Clin Med Res* 4:79-84.

Brady, H.R., Denton, M.D., Jimenez, W., Takata, S., Palliser, D., and Brenner, B.M. 1992. Chemoattractants provoke monocyte adhesion to human mesangial cells and mesangial cell injury. *Kidney Int* 42:480-487.

Brem, G., Wanke, R., Wolf, E., Buchmuller, T., Muller, M., Brenig, B., and Hermanns, W. 1989. Multiple consequences of human growth hormone expression in transgenic mice. *Mol Biol Med* 6:531-547.

Brenner, B.M. 1983. Hemodynamically mediated glomerular injury and the progressive nature of kidney disease. *Kidney Int* 23:647-655.

Brenner, B.M., Meyer, T.W., and Hostetter, T.H. 1982. Dietary protein intake and the progressive nature of kidney disease: the role of hemodynamically mediated glomerular injury in the pathogenesis of progressive glomerular sclerosis in aging, renal ablation, and intrinsic renal disease. *N Engl J Med* 307:652-659.

Breyer, M.D., Bottinger, E., Brosius, F.C., 3rd, Coffman, T.M., Harris, R.C., Heilig, C.W., and Sharma, K. 2005. Mouse models of diabetic nephropathy. *J Am Soc Nephrol* 16:27-45.

Breyer, M.D., Bottinger, E., Brosius, F.C., Coffman, T.M., Fogo, A., Harris, R.C., Heilig, C.W., and Sharma, K. 2005. Diabetic nephropathy: of mice and men. *Adv Chronic Kidney Dis* 12:128-145.

Bronson, S.K., and Smithies, O. 1994. Altering mice by homologous recombination using embryonic stem cells. *J Biol Chem* 269:27155-27158.

Budisavljevic, M.N., Hodge, L., Barber, K., Fulmer, J.R., Durazo-Arvizu, R.A., Self, S.E., Kuhlmann, M., Raymond, J.R., and Greene, E.L. 2003. Oxidative stress in the pathogenesis of experimental mesangial proliferative glomerulonephritis. *Am J Physiol Renal Physiol* 285:F1138-1148.

Cabrero, A., Cubero, M., Llaverias, G., Jove, M., Planavila, A., Alegret, M., Sanchez, R., Laguna, J.C., and Carrera, M.V. 2003. Differential effects of peroxisome proliferator-activated receptor activators on the mRNA levels of genes involved in lipid metabolism in primary human monocyte-derived macrophages. *Metabolism* 52:652-657.

Camerini-Davalos, R.A., Oppermann, W., Treser, G., Ehrenreich, T., Lange, K., and Levine, R. 1968. Glomerulosclerosis in a strain of genetically diabetic mice. *Diabetes* 17:301.

Caramori, M.L., Fioretto, P., and Mauer, M. 2000. The need for early predictors of diabetic nephropathy risk: is albumin excretion rate sufficient? *Diabetes* 49:1399-1408.

Cardullo, R.A., Agrawal, S., Flores, C., Zamecnik, P.C., and Wolf, D.E. 1988. Detection of nucleic acid hybridization by nonradiative fluorescence resonance energy transfer. *Proc Natl Acad Sci U S A* 85:8790-8794.

Carlson, E.C., Audette, J.L., Klevay, L.M., Nguyen, H., and Epstein, P.N. 1997. Ultrastructural and functional analyses of nephropathy in calmodulin-induced diabetic transgenic mice. *Anat Rec* 247:9-19.

Carraro, M., Zennaro, C., Artero, M., Candiano, G., Ghiggeri, G.M., Musante, L., Sirch, C., Bruschi, M., and Faccini, L. 2004. The effect of proteinase inhibitors on glomerular albumin permeability induced in vitro by serum from patients with idiopathic focal segmental glomerulosclerosis. *Nephrol Dial Transplant* 19:1969-1975.

Caulfield, J.B. 1957. Effects of varying the vehicle for OsO4 in tissue fixation. *J Biophys Biochem Cytol* 3:827-830.

Cavaggioni, A., and Mucignat-Caretta, C. 2000. Major urinary proteins, alpha(2U)-globulins and aphrodisin. *Biochim Biophys Acta* 1482:218-228.

Chajara, A., Raoudi, M., Delpech, B., Leroy, M., Basuyau, J.P., and Levesque, H. 2000. Increased hyaluronan and hyaluronidase production and hyaluronan degradation in injured aorta of insulin-resistant rats. *Arterioscler Thromb Vasc Biol* 20:1480-1487.

Chavers, B.M., Bilous, R.W., Ellis, E.N., Steffes, M.W., and Mauer, S.M. 1989. Glomerular lesions and urinary albumin excretion in type I diabetes without overt proteinuria. *N Engl J Med* 320:966-970.

Chen, A., Chen, W.P., Sheu, L.F., and Lin, C.Y. 1994. Pathogenesis of IgA nephropathy: in vitro activation of human mesangial cells by IgA immune complex leads to cytokine secretion. *J Pathol* 173:119-126.

Chen, H.M., Liu, Z.H., Zeng, C.H., Li, S.J., Wang, Q.W., and Li, L.S. 2006. Podocyte lesions in patients with obesity-related glomerulopathy. *Am J Kidney Dis* 48:772-779.

Chen, P.Y., St John, P.L., Kirk, K.A., Abrahamson, D.R., and Sanders, P.W. 1993. Hypertensive nephrosclerosis in the Dahl/Rapp rat. Initial sites of injury and effect of dietary L-arginine supplementation. *Lab Invest* 68:174-184.

Chen, Y.M., Hu-Tsai, M.I., Lin, S.L., Tsai, T.J., and Hsieh, B.S. 2003. Expression of CX3CL1/fractalkine by mesangial cells in vitro and in acute anti-Thy1 glomerulonephritis in rats. *Nephrol Dial Transplant* 18:2505-2514.

Chmurzynska, A. 2006. The multigene family of fatty acid-binding proteins (FABPs): function, structure and polymorphism. *J Appl Genet* 47:39-48.

Chow, E.K., O'Connell R, M., Schilling, S., Wang, X.F., Fu, X.Y., and Cheng, G. 2005. TLR agonists regulate PDGF-B production and cell proliferation through TGF-beta/type I IFN crosstalk. *Embo J* 24:4071-4081.

Churg, J., and Sobin, L.H. 1982. *Renal disease: Classification and atlas of glomerular diseases*. Tokyo, New York: Igaku-Shoin.

Cockwell, P., Chakravorty, S.J., Girdlestone, J., and Savage, C.O. 2002. Fractalkine expression in human renal inflammation. *J Pathol* 196:85-90.

Coe, N.R., and Bernlohr, D.A. 1998. Physiological properties and functions of intracellular fatty acid-binding proteins. *Biochim Biophys Acta* 1391:287-306.

Cohen, C.D., Calvaresi, N., Armelloni, S., Schmid, H., Henger, A., Ott, U., Rastaldi, M.P., and Kretzler, M. 2005. CD20-positive infiltrates in human membranous glomerulonephritis. *J Nephrol* 18:328-333.

Cohen, C.D., Frach, K., Schlondorff, D., and Kretzler, M. 2002. Quantitative gene expression analysis in renal biopsies: a novel protocol for a high-throughput multicenter application. *Kidney Int* 61:133-140.

Cohen, C.D., Grone, H.J., Grone, E.F., Nelson, P.J., Schlondorff, D., and Kretzler, M. 2002. Laser microdissection and gene expression analysis on formaldehyde-fixed archival tissue. *Kidney Int* 61:125-132.

Cohen, C.D., Klingenhoff, A., Boucherot, A., Nitsche, A., Henger, A., Brunner, B., Schmid, H., Merkle, M., Saleem, M.A., Koller, K.P., Werner, T., Grone, H.J., Nelson, P.J., and Kretzler, M. 2006. Comparative promoter analysis allows de novo identification of specialized cell junction-associated proteins. *Proc Natl Acad Sci U S A* 103:5682-5687.

Cohen, C.D., and Kretzler, M. 2002. Gene expression analysis in microdissected renal tissue. Current challenges and strategies. *Nephron* 92:522-528.

Cohen, C.D., and Kretzler, M. 2003. Gene-Expression Analysis of Microdissected Renal Biopsies. In *Renal disease: Techniques and Protokols*. M.S. Goligorsky, editor. Totowa, New Jersey: Humana Press Inc. 285-293.

Cook, D.N., Chen, S.C., Sullivan, L.M., Manfra, D.J., Wiekowski, M.T., Prosser, D.M., Vassileva, G., and Lira, S.A. 2001. Generation and analysis of mice lacking the chemokine fractalkine. *Mol Cell Biol* 21:3159-3165.

Cortes, P., Dumler, F., Goldman, J., and Levin, N.W. 1987. Relationship between renal function and metabolic alterations in early streptozocin-induced diabetes in rats. *Diabetes* 36:80-87.

Crawford, S.E., Stellmach, V., Murphy-Ullrich, J.E., Ribeiro, S.M., Lawler, J., Hynes, R.O., Boivin, G.P., and Bouck, N. 1998. Thrombospondin-1 is a major activator of TGF-beta1 in vivo. *Cell* 93:1159-1170.

Creutzfeldt, W. 1979. The incretin concept today. *Diabetologia* 16:75-85.

Creutzfeldt, W., and Nauck, M. 1992. Gut hormones and diabetes mellitus. *Diabetes Metab Rev* 8:149-177.

Crozet, F., el Amraoui, A., Blanchard, S., Lenoir, M., Ripoll, C., Vago, P., Hamel, C., Fizames, C., Levi-Acobas, F., Depetris, D., Mattei, M.G., Weil, D., Pujol, R., and Petit, C. 1997. Cloning of the genes encoding two murine and human cochlear unconventional type I myosins. *Genomics* 40:332-341.

Cui, S., Li, C., Ema, M., Weinstein, J., and Quaggin, S.E. 2005. Rapid isolation of glomeruli coupled with gene expression profiling identifies downstream targets in Pod1 knockout mice. *J Am Soc Nephrol* 16:3247-3255.

D'Amico, G., and Bazzi, C. 2003. Pathophysiology of proteinuria. *Kidney Int* 63:809-825.

Daha, M.R. 2000. Mechanisms of mesangial injury in glomerular diseases. *J Nephrol* 13 Suppl 3:S89-95.

Daniels, B.S., and Hostetter, T.H. 1990. Adverse effects of growth in the glomerular microcirculation. *Am J Physiol* 258:F1409-1416.

Deen, W.M., Lazzara, M.J., and Myers, B.D. 2001. Structural determinants of glomerular permeability. *Am J Physiol Renal Physiol* 281:F579-596.

DeGrendele, H.C., Estess, P., Picker, L.J., and Siegelman, M.H. 1996. CD44 and its ligand hyaluronate mediate rolling under physiologic flow: a novel lymphocyte-endothelial cell primary adhesion pathway. *J Exp Med* 183:1119-1130.

Denton, M.D., Marsden, P.A., Luscinskas, F.W., Brenner, B.M., and Brady, H.R. 1991. Cytokine-induced phagocyte adhesion to human mesangial cells: role of CD11/CD18 integrins and ICAM-1. *Am J Physiol* 261:F1071-1079.

Diamond, J.R., and Karnovsky, M.J. 1986. Focal and segmental glomerulosclerosis following a single intravenous dose of puromycin aminonucleoside. *Am J Pathol* 122:481-487.

Dierkes, J., Domrose, U., Westphal, S., Ambrosch, A., Bosselmann, H.P., Neumann, K.H., and Luley, C. 2000. Cardiac troponin T predicts mortality in patients with end-stage renal disease. *Circulation* 102:1964-1969.

Ding, C., and Cantor, C.R. 2004. Quantitative analysis of nucleic acids--the last few years of progress. *J Biochem Mol Biol* 37:1-10.

Dische, F.E. 1992. Measurement of glomerular basement membrane thickness and its application to the diagnosis of thin-membrane nephropathy. *Arch Pathol Lab Med* 116:43-49.

Doi, T., Higashino, K., Kurihara, Y., Wada, Y., Miyazaki, T., Nakamura, H., Uesugi, S., Imanishi, T., Kawabe, Y., Itakura, H., and et al. 1993. Charged collagen structure mediates the recognition of negatively charged macromolecules by macrophage scavenger receptors. *J Biol Chem* 268:2126-2133.

Doi, T., Striker, L.J., Gibson, C.C., Agodoa, L.Y., Brinster, R.L., and Striker, G.E. 1990. Glomerular lesions in mice transgenic for growth hormone and insulinlike growth factor-I. I. Relationship between increased glomerular size and mesangial sclerosis. *Am J Pathol* 137:541-552.

Doi, T., Striker, L.J., Quaife, C., Conti, F.G., Palmiter, R., Behringer, R., Brinster, R., and Striker, G.E. 1988. Progressive glomerulosclerosis develops in transgenic mice chronically expressing growth hormone and growth hormone releasing factor but not in those expressing insulinlike growth factor-1. *Am J Pathol* 131:398-403.

Donaldson, A., and Cove-Smith, R. 2001. Cardiac troponin levels in patients with impaired renal function. *Hosp Med* 62:86-89.

Drenckhahn, D., and Franke, R.P. 1988. Ultrastructural organization of contractile and cytoskeletal proteins in glomerular podocytes of chicken, rat, and man. *Lab Invest* 59:673-682.

Drummond, K., and Mauer, M. 2002. The early natural history of nephropathy in type 1 diabetes: II. Early renal structural changes in type 1 diabetes. *Diabetes* 51:1580-1587.

Drumond, M.C., Kristal, B., Myers, B.D., and Deen, W.M. 1994. Structural basis for reduced glomerular filtration capacity in nephrotic humans. *J Clin Invest* 94:1187-1195.

Dunlop, M.E., and Muggli, E.E. 2002. Hyaluronan increases glomerular cyclooxygenase-2 protein expression in a p38 MAP-kinase-dependent process. *Kidney Int* 61:1729-1738.

Duymelinck, C., Dauwe, S.E., De Greef, K.E., Ysebaert, D.K., Verpooten, G.A., and De Broe, M.E. 2000. TIMP-1 gene expression and PAI-1 antigen after unilateral ureteral obstruction in the adult male rat. *Kidney Int* 58:1186-1201.

Dworkin, L.D., Benstein, J.A., Parker, M., Tolbert, E., and Feiner, H.D. 1993. Calcium antagonists and converting enzyme inhibitors reduce renal injury by different mechanisms. *Kidney Int* 43:808-814.

Eddy, A.A. 1989. Interstitial nephritis induced by protein-overload proteinuria. *Am J Pathol* 135:719-733.

Eddy, A.A., and Michael, A.F. 1988. Acute tubulointerstitial nephritis associated with aminonucleoside nephrosis. *Kidney Int* 33:14-23.

Ehrlein, J. 1993. Darstellung von Wachstumshormon mRNA und Wachstumshormon mittels nicht-radioaktiver In-situ-Hybridisierung und Immunhistochemie: Untersuchungen zur Transgenexpression bei Wachstumshormon-transgenen Mäusen. Inaugural – Dissertation to achieve the doctor title of veterinary medicine at the Faculty of Veterinary Medicine of the Ludwig-Maximilians-University, Munich.

Eisen, M.B., Spellman, P.T., Brown, P.O., and Botstein, D. 1998. Cluster analysis and display of genome-wide expression patterns. *Proc Natl Acad Sci U S A* 95:14863-14868.

Eknoyan, G., Lameire, N., Barsoum, R., Eckardt, K.U., Levin, A., Levin, N., Locatelli, F., MacLeod, A., Vanholder, R., Walker, R., and Wang, H. 2004. The burden of kidney disease: improving global outcomes. *Kidney Int* 66:1310-1314.

El-Aouni, C., Herbach, N., Blattner, S.M., Henger, A., Rastaldi, M.P., Jarad, G., Miner, J.H., Moeller, M.J., St-Arnaud, R., Dedhar, S., Holzman, L.B., Wanke, R., and Kretzler, M. 2006. Podocyte-specific deletion of integrin-linked kinase results in severe glomerular basement membrane alterations and progressive glomerulosclerosis. *J Am Soc Nephrol* 17:1334-1344.

el Khoury, J., Thomas, C.A., Loike, J.D., Hickman, S.E., Cao, L., and Silverstein, S.C. 1994. Macrophages adhere to glucose-modified basement membrane collagen IV via their scavenger receptors. *J Biol Chem* 269:10197-10200.

el Nahas, A.M. 1989. Glomerulosclerosis: insights into pathogenesis and treatment. *Nephrol Dial Transplant* 4:843-853.

Elema, J.D., Hoyer, J.R., and Vernier, R.L. 1976. The glomerular mesangium: uptake and transport of intravenously injected colloidal carbon in rats. *Kidney Int* 9:395-406.

Elema, J.D., Weening, J.J., and Grond, J. 1988. Focal glomerular hyalinosis and sclerosis in aminonucleoside and adriamycin nephrosis: pathogenetic and therapeutic considerations. *Contrib Nephrol* 60:73-82.

Emi, M., Asaoka, H., Matsumoto, A., Itakura, H., Kurihara, Y., Wada, Y., Kanamori, H., Yazaki, Y., Takahashi, E., Lepert, M., and et al. 1993. Structure, organization, and chromosomal mapping of the human macrophage scavenger receptor gene. *J Biol Chem* 268:2120-2125.

Eremina, V., Baelde, H.J., and Quaggin, S.E. 2007. Role of the VEGF--a signaling pathway in the glomerulus: evidence for crosstalk between components of the glomerular filtration barrier. *Nephron Physiol* 106:p32-37.

Eremina, V., Cui, S., Gerber, H., Ferrara, N., Haigh, J., Nagy, A., Ema, M., Rossant, J., Jothy, S., Miner, J.H., and Quaggin, S.E. 2006. Vascular endothelial growth factor a signaling in the podocyte-endothelial compartment is required for mesangial cell migration and survival. *J Am Soc Nephrol* 17:724-735.

Eremina, V., Sood, M., Haigh, J., Nagy, A., Lajoie, G., Ferrara, N., Gerber, H.P., Kikkawa, Y., Miner, J.H., and Quaggin, S.E. 2003. Glomerular-specific alterations of VEGF-A expression lead to distinct congenital and acquired renal diseases. *J Clin Invest* 111:707-716.

Fehmann, H.C., Goke, R., and Goke, B. 1995. Cell and molecular biology of the incretin hormones glucagon-like peptide-I and glucose-dependent insulin releasing polypeptide. *Endocr Rev* 16:390-410.

Feng, L., Chen, S., Garcia, G.E., Xia, Y., Siani, M.A., Botti, P., Wilson, C.B., Harrison, J.K., and Bacon, K.B. 1999. Prevention of crescentic glomerulonephritis by immunoneutralization of the fractalkine receptor CX3CR1 rapid communication. *Kidney Int* 56:612-620.

Finlayson, J.S., Asofsky, R., Potter, M., and Runner, C.C. 1965. Major urinary protein complex of normal mice: origin. *Science* 149:981-982.

Fisch, T. 2004. Effects of insulin-like growth factor-binding protein-2 (IGFBP2) overexpression on adrenal and renal growth processes and functions: findings in transgenic mouse models. Inaugural – Dissertation to achieve the doctor title of veterinary medicine at the Faculty of Veterinary Medicine of the Ludwig-Maximilians-University, Munich. 1-155.

Floege, J., Burns, M.W., Alpers, C.E., Yoshimura, A., Pritzl, P., Gordon, K., Seifert, R.A., Bowen-Pope, D.F., Couser, W.G., and Johnson, R.J. 1992. Glomerular cell proliferation and PDGF expression precede glomerulosclerosis in the remnant kidney model. *Kidney Int* 41:297-309.

Fogo, A., and Ichikawa, I. 1989. Evidence for the central role of glomerular growth promoters in the development of sclerosis. *Semin Nephrol* 9:329-342.

Fogo, A., and Ichikawa, I. 1991. Evidence for a pathogenic linkage between glomerular hypertrophy and sclerosis. *Am J Kidney Dis* 17:666-669.

Fogo, A., Yoshida, Y., Glick, A.D., Homma, T., and Ichikawa, I. 1988. Serial micropuncture analysis of glomerular function in two rat models of glomerular sclerosis. *J Clin Invest* 82:322-330.

Fogo, A.B. 1999. Mesangial matrix modulation and glomerulosclerosis. *Exp Nephrol* 7:147-159.

Fogo, A.B. 2000. Glomerular hypertension, abnormal glomerular growth, and progression of renal diseases. *Kidney Int Suppl* 75:S15-21.

Fogo, A.B. 2001. Minimal change disease and focal segmental glomerulosclerosis. *Nephrol Dial Transplant* 16 Suppl 6:74-76.

Fogo, A.B. 2003. Animal models of FSGS: lessons for pathogenesis and treatment. *Semin Nephrol* 23:161-171.

Fogo, A.B. 2006. Progression versus regression of chronic kidney disease. *Nephrol Dial Transplant* 21:281-284.

Fong, A.M., Robinson, L.A., Steeber, D.A., Tedder, T.F., Yoshie, O., Imai, T., and Patel, D.D. 1998. Fractalkine and CX3CR1 mediate a novel mechanism of leukocyte capture, firm adhesion, and activation under physiologic flow. *J Exp Med* 188:1413-1419.

Förster, V.T. 1948. Zwischenmolekulare Energiewanderung und Fluoreszenz. *Annals of Physics (Leipzig)* 2:55-75.

Foussat, A., Coulomb-L'Hermine, A., Gosling, J., Krzysiek, R., Durand-Gasselin, I., Schall, T., Balian, A., Richard, Y., Galanaud, P., and Emilie, D. 2000. Fractalkine receptor expression by T lymphocyte subpopulations and in vivo production of fractalkine in human. *Eur J Immunol* 30:87-97.

Fries, J.W., Roth, T., Dienes, H.P., Weber, M., and Odenthal, M. 2003. A novel evaluation method for paraffinized human renal biopsies using quantitative analysis of microdissected glomeruli and VCAM-1 as marker of inflammatory mesangial cell activation. *Nephrol Dial Transplant* 18:710-716.

Fries, J.W., Sandstrom, D.J., Meyer, T.W., and Rennke, H.G. 1989. Glomerular hypertrophy and epithelial cell injury modulate progressive glomerulosclerosis in the rat. *Lab Invest* 60:205-218.

Fu, Y., Luo, L., Luo, N., and Garvey, W.T. 2006. Lipid metabolism mediated by adipocyte lipid binding protein (ALBP/aP2) gene expression in human THP-1 macrophages. *Atherosclerosis* 188:102-111.

Fu, Y., Luo, N., and Lopes-Virella, M.F. 2000. Oxidized LDL induces the expression of ALBP/aP2 mRNA and protein in human THP-1 macrophages. *J Lipid Res* 41:2017-2023.

Fujimoto, M., Maezawa, Y., Yokote, K., Joh, K., Kobayashi, K., Kawamura, H., Nishimura, M., Roberts, A.B., Saito, Y., and Mori, S. 2003. Mice lacking Smad3 are protected against streptozotocin-induced diabetic glomerulopathy. *Biochem Biophys Res Commun* 305:1002-1007.

Fukuda, S., Horiuchi, S., Tomita, K., Murakami, M., Morino, Y., and Takahashi, K. 1986. Acetylated low-density lipoprotein is endocytosed through coated pits by rat peritoneal macrophages. *Virchows Arch B Cell Pathol Incl Mol Pathol* 52:1-13.

Funk, J.L., Feingold, K.R., Moser, A.H., and Grunfeld, C. 1993. Lipopolysaccharide stimulation of RAW 264.7 macrophages induces lipid accumulation and foam cell formation. *Atherosclerosis* 98:67-82.

Furuta, T., Saito, T., Ootaka, T., Soma, J., Obara, K., Abe, K., and Yoshinaga, K. 1993. The role of macrophages in diabetic glomerulosclerosis. *Am J Kidney Dis* 21:480-485.

Gaertner, S.A., Janssen, U., Ostendorf, T., Koch, K.M., Floege, J., and Gwinner, W. 2002. Glomerular oxidative and antioxidative systems in experimental mesangioproliferative glomerulonephritis. *J Am Soc Nephrol* 13:2930-2937.

Galkina, E., and Ley, K. 2006. Leukocyte recruitment and vascular injury in diabetic nephropathy. *J Am Soc Nephrol* 17:368-377.

Garcia, C.D., Bittencourt, V.B., Tumelero, A., Antonello, J.S., Malheiros, D., and Garcia, V.D. 2006. Plasmapheresis for recurrent posttransplant focal segmental glomerulosclerosis. *Transplant Proc* 38:1904-1905.

Gaspari, F., Perico, N., Ruggenenti, P., Mosconi, L., Amuchastegui, C.S., Guerini, E., Daina, E., and Remuzzi, G. 1995. Plasma clearance of nonradioactive iohexol as a measure of glomerular filtration rate. *J Am Soc Nephrol* 6:257-263.

Gauer, S., Yao, J., Schoecklmann, H.O., and Sterzel, R.B. 1997. Adhesion molecules in the glomerular mesangium. *Kidney Int* 51:1447-1453.

Gauthier, V.J., and Mannik, M. 1988. A method for isolation of mouse glomeruli for quantitation of immune deposits. *Kidney Int* 33:897-899.

Gehrig, A., Langmann, T., Horling, F., Janssen, A., Bonin, M., Walter, M., Poths, S., and Weber, B.H. 2007. Genome-wide expression profiling of the retinoschisin-deficient retina in early postnatal mouse development. *Invest Ophthalmol Vis Sci* 48:891-900.

Genomatix's ChipInspector Manual.
http://www.genomatix.de/download/software/ChipInspector_manual.pdf.

Gibson, U.E., Heid, C.A., and Williams, P.M. 1996. A novel method for real time quantitative RT-PCR. *Genome Res* 6:995-1001.

Gilbert, T., Lelievre-Pegorier, M., Malienou, R., Meulemans, A., and Merlet-Benichou, C. 1987. Effects of prenatal and postnatal exposure to gentamicin on renal differentiation in the rat. *Toxicology* 43:301-313.

Gilbertson, D.T., Liu, J., Xue, J.L., Louis, T.A., Solid, C.A., Ebben, J.P., and Collins, A.J. 2005. Projecting the number of patients with end-stage renal disease in the United States to the year 2015. *J Am Soc Nephrol* 16:3736-3741.

Glasser, R.J., Velosa, J.A., and Michael, A.F. 1977. Experimental model of focal sclerosis. I. Relationship to protein excretion in aminonucleoside nephrosis. *Lab Invest* 36:519-526.

Goldstein, J.L., Ho, Y.K., Basu, S.K., and Brown, M.S. 1979. Binding site on macrophages that mediates uptake and degradation of acetylated low density lipoprotein, producing massive cholesterol deposition. *Proc Natl Acad Sci U S A* 76:333-337.

Goldszer, R.C., Sweet, J., and Cotran, R.S. 1984. Focal segmental glomerulosclerosis. *Annu Rev Med* 35:429-449.

Gomez-Chiarri, M., Hamilton, T.A., Egido, J., and Emancipator, S.N. 1993. Expression of IP-10, a lipopolysaccharide- and interferon-gamma-inducible protein, in murine mesangial cells in culture. *Am J Pathol* 142:433-439.

Gomez-Guerrero, C., Gonzalez, E., Hernando, P., Ruiz-Ortega, M., and Egido, J. 1993. Interaction of mesangial cells with IgA and IgG immune complexes: a possible mechanism of glomerular injury in IgA nephropathy. *Contrib Nephrol* 104:127-137.

Gomez-Guerrero, C., Hernandez-Vargas, P., Lopez-Franco, O., Ortiz-Munoz, G., and Egido, J. 2005. Mesangial cells and glomerular inflammation: from the pathogenesis to novel therapeutic approaches. *Curr Drug Targets Inflamm Allergy* 4:341-351.

Gomez-Guerrero, C., Lopez-Armada, M.J., Gonzalez, E., and Egido, J. 1994. Soluble IgA and IgG aggregates are catabolized by cultured rat mesangial cells and induce production of TNF-alpha and IL-6, and proliferation. *J Immunol* 153:5247-5255.

Gordon, A.M., Homsher, E., and Regnier, M. 2000. Regulation of contraction in striated muscle. *Physiol Rev* 80:853-924.

Gorlin, J.B., Yamin, R., Egan, S., Stewart, M., Stossel, T.P., Kwiatkowski, D.J., and Hartwig, J.H. 1990. Human endothelial actin-binding protein (ABP-280, nonmuscle filamin): a molecular leaf spring. *J Cell Biol* 111:1089-1105.

Goulter, A.B., Harmer, D.W., and Clark, K.L. 2006. Evaluation of low density array technology for quantitative parallel measurement of multiple genes in human tissue. *BMC Genomics* 7:34.

Gowen, B.B., Borg, T.K., Ghaffar, A., and Mayer, E.P. 2000. Selective adhesion of macrophages to denatured forms of type I collagen is mediated by scavenger receptors. *Matrix Biol* 19:61-71.

Gowen, B.B., Borg, T.K., Ghaffar, A., and Mayer, E.P. 2001. The collagenous domain of class A scavenger receptors is involved in macrophage adhesion to collagens. *J Leukoc Biol* 69:575-582.

Gowri, P.M., Yu, J.H., Shaufl, A., Sperling, M.A., and Menon, R.K. 2003. Recruitment of a repressosome complex at the growth hormone receptor promoter and its potential role in diabetic nephropathy. *Mol Cell Biol* 23:815-825.

Greiber, S., Muller, B., Daemisch, P., and Pavenstadt, H. 2002. Reactive oxygen species alter gene expression in podocytes: induction of granulocyte macrophage-colony-stimulating factor. *J Am Soc Nephrol* 13:86-95.

Gretz, N., Meisinger, E., and Strauch, M. 1988. Partial nephrectomy and chronic renal failure: the 'mature' rat model. *Contrib Nephrol* 60:46-55.

Griffin, S.V., Petermann, A.T., Durvasula, R.V., and Shankland, S.J. 2003. Podocyte proliferation and differentiation in glomerular disease: role of cell-cycle regulatory proteins. *Nephrol Dial Transplant* 18 Suppl 6:vi8-13.

Grond, J., Weening, J.J., and Elema, J.D. 1984. Glomerular sclerosis in nephrotic rats. Comparison of the long-term effects of adriamycin and aminonucleoside. *Lab Invest* 51:277-285.

Grone, H.J., Walli, A., Grone, E., Niedmann, P., Thiery, J., Seidel, D., and Helmchen, U. 1989. Induction of glomerulosclerosis by dietary lipids. A functional and morphologic study in the rat. *Lab Invest* 60:433-446.

Grone, H.J., Walli, A.K., and Grone, E.F. 1997. The role of oxidatively modified lipoproteins in lipid nephropathy. *Contrib Nephrol* 120:160-175.

Gross, M.L., Ritz, E., Schoof, A., Adamczak, M., Koch, A., Tulp, O., Parkman, A., El-Shakmak, A., Szabo, A., and Amann, K. 2004. Comparison of renal morphology in the Streptozotocin and the SHR/N-cp models of diabetes. *Lab Invest* 84:452-464.

Guan, Y., and Breyer, M.D. 2001. Peroxisome proliferator-activated receptors (PPARs): novel therapeutic targets in renal disease. *Kidney Int* 60:14-30.

Gundersen, H.J. 1986. Stereology of arbitrary particles. A review of unbiased number and size estimators and the presentation of some new ones, in memory of William R. Thompson. *J Microsc* 143:3-45.

Gunthert, U. 1993. CD44: a multitude of isoforms with diverse functions. *Curr Top Microbiol Immunol* 184:47-63.

Gurley, S.B., Clare, S.E., Snow, K.P., Hu, A., Meyer, T.W., and Coffman, T.M. 2006. Impact of genetic background on nephropathy in diabetic mice. *Am J Physiol Renal Physiol* 290:F214-222.

Gwinner, W., and Grone, H.J. 2000. Role of reactive oxygen species in glomerulonephritis. *Nephrol Dial Transplant* 15:1127-1132.

Habener, J.F. 1993. The incretin notion and its relevance to diabetes. *Endocrinol Metab Clin North Am* 22:775-794.

Habib, R. 1973. Editorial: Focal glomerular sclerosis. *Kidney Int* 4:355-361.

Hallgren, R., Engstrom-Laurent, A., and Nisbeth, U. 1987. Circulating hyaluronate. A potential marker of altered metabolism of the connective tissue in uremia. *Nephron* 46:150-154.

Hammad, S.M., Hazen-Martin, D.J., Sohn, M., Eldridge, L., Powell-Braxton, L., Won, W., and Lyons, T.J. 2003. Nephropathy in a hypercholesterolemic mouse model with streptozotocin-induced diabetes. *Kidney Blood Press Res* 26:351-361.

Hammerman, M.R. 1989. The growth hormone-insulin-like growth factor axis in kidney. *Am J Physiol* 257:F503-514.

Han, J., Hajjar, D.P., Zhou, X., Gotto, A.M., Jr., and Nicholson, A.C. 2002. Regulation of peroxisome proliferator-activated receptor-gamma-mediated gene expression. A new mechanism of action for high density lipoprotein. *J Biol Chem* 277:23582-23586.

Hannema, A.J., Kluin-Nelemans, J.C., Hack, C.E., Eerenberg-Belmer, A.J., Mallee, C., and van Helden, H.P. 1984. SLE like syndrome and functional deficiency of C1q in members of a large family. *Clin Exp Immunol* 55:106-114.

Haraldsson, B., and Sorensson, J. 2004. Why do we not all have proteinuria? An update of our current understanding of the glomerular barrier. *News Physiol Sci* 19:7-10.

Harrison, J.K., Jiang, Y., Chen, S., Xia, Y., Maciejewski, D., McNamara, R.K., Streit, W.J., Salafranca, M.N., Adhikari, S., Thompson, D.A., Botti, P., Bacon, K.B., and Feng, L. 1998. Role for neuronally derived fractalkine in mediating interactions between neurons and CX3CR1-expressing microglia. *Proc Natl Acad Sci U S A* 95:10896-10901.

Haskell, C.A., Cleary, M.D., and Charo, I.F. 1999. Molecular uncoupling of fractalkine-mediated cell adhesion and signal transduction. Rapid flow arrest of CX3CR1-expressing cells is independent of G-protein activation. *J Biol Chem* 274:10053-10058.

Hayden, M.R., Whaley-Connell, A., and Sowers, J.R. 2005. Renal redox stress and remodeling in metabolic syndrome, type 2 diabetes mellitus, and diabetic nephropathy: paying homage to the podocyte. *Am J Nephrol* 25:553-569.

Heickendorff, L., Ledet, T., and Rasmussen, L.M. 1994. Glycosaminoglycans in the human aorta in diabetes mellitus: a study of tunica media from areas with and without atherosclerotic plaque. *Diabetologia* 37:286-292.

Heid, C.A., Stevens, J., Livak, K.J., and Williams, P.M. 1996. Real time quantitative PCR. *Genome Res* 6:986-994.

Henger, A., Kretzler, M., Doran, P., Bonrouhi, M., Schmid, H., Kiss, E., Cohen, C.D., Madden, S., Porubsky, S., Grone, E.F., Schlondorff, D., Nelson, P.J., and Grone, H.J. 2004. Gene expression fingerprints in human tubulointerstitial inflammation and fibrosis as prognostic markers of disease progression. *Kidney Int* 65:904-917.

Heptinstall, R.H. 1992. End-stage renal disease. In *Pathology of the kidney*. R.H. Heptinstall, editor. 713-778.

Herbach, N. 2002. Clinical and pathological characterization of a novel animal model of diabetes mellitus expressing a dominant negative glucose-dependent insulinotropic polypeptide receptor (GIPR^{dn}). Inaugural – Dissertation to achieve the doctor title of veterinary medicine at the Faculty of Veterinary Medicine of the Ludwig-Maximilians-University, Munich. 1-165.

Herbach, N., Goeke, B., Schneider, M., Hermanns, W., Wolf, E., and Wanke, R. 2005. Overexpression of a dominant negative GIP receptor in transgenic mice results in disturbed postnatal pancreatic islet and beta-cell development. *Regul Pept* 125:103-117.

Herbach, N., Göke, B., Hermanns, W., Wolf, E., and Wanke, R. 2003. Diabetes-associated kidney lesions in GIPR^{dn} transgenic mice, a novel animal model of diabetes mellitus. . *Diabetes 52,* Suppl. 1:A186.

Hermanns, W., Liebig, K., and Schulz, L.C. 1981. Postembedding immunohistochemical demonstration of antigen in experimental polyarthritis using plastic embedded whole joints. *Histochemistry* 73:439-446.

Higgins, D.F., Lappin, D.W., Kieran, N.E., Anders, H.J., Watson, R.W., Strutz, F., Schlondorff, D., Haase, V.H., Fitzpatrick, J.M., Godson, C., and Brady, H.R. 2003. DNA oligonucleotide microarray technology identifies fisp-12 among other potential fibrogenic genes following murine unilateral ureteral obstruction (UUO): modulation during epithelial-mesenchymal transition. *Kidney Int* 64:2079-2091.

Higgins, J.P., Wang, L., Kambham, N., Montgomery, K., Mason, V., Vogelmann, S.U., Lemley, K.V., Brown, P.O., Brooks, J.D., and van de Rijn, M. 2004. Gene expression in the normal adult human kidney assessed by complementary DNA microarray. *Mol Biol Cell* 15:649-656.

Hirose, K., Osterby, R., Nozawa, M., and Gundersen, H.J. 1982. Development of glomerular lesions in experimental long-term diabetes in the rat. *Kidney Int* 21:689-695.

Hjalm, G., MacLeod, R.J., Kifor, O., Chattopadhyay, N., and Brown, E.M. 2001. Filamin-A binds to the carboxyl-terminal tail of the calcium-sensing receptor, an interaction that participates in CaR-mediated activation of mitogen-activated protein kinase. *J Biol Chem* 276:34880-34887.

Hodge-Dufour, J., Noble, P.W., Horton, M.R., Bao, C., Wysoka, M., Burdick, M.D., Strieter, R.M., Trinchieri, G., and Pure, E. 1997. Induction of IL-12 and chemokines by hyaluronan requires adhesion-dependent priming of resident but not elicited macrophages. *J Immunol* 159:2492-2500.

Hoeflich, A., Nedbal, S., Blum, W.F., Erhard, M., Lahm, H., Brem, G., Kolb, H.J., Wanke, R., and Wolf, E. 2001. Growth inhibition in giant growth hormone transgenic mice by overexpression of insulin-like growth factor-binding protein-2. *Endocrinology* 142:1889-1898.

Holland, P.M., Abramson, R.D., Watson, R., and Gelfand, D.H. 1991. Detection of specific polymerase chain reaction product by utilizing the 5'----3' exonuclease activity of Thermus aquaticus DNA polymerase. *Proc Natl Acad Sci U S A* 88:7276-7280.

Holzman, L.B., St John, P.L., Kovari, I.A., Verma, R., Holthofer, H., and Abrahamson, D.R. 1999. Nephrin localizes to the slit pore of the glomerular epithelial cell. *Kidney Int* 56:1481-1491.

Hong, S.W., Isono, M., Chen, S., Iglesias-De La Cruz, M.C., Han, D.C., and Ziyadeh, F.N. 2001. Increased glomerular and tubular expression of transforming growth factor-beta1, its type II receptor, and activation of the Smad signaling pathway in the db/db mouse. *Am J Pathol* 158:1653-1663.

Hook, P., and Vallee, R.B. 2006. The dynein family at a glance. *J Cell Sci* 119:4369-4371.

Hostetter, T.H., Olson, J.L., Rennke, H.G., Venkatachalam, M.A., and Brenner, B.M. 1981. Hyperfiltration in remnant nephrons: a potentially adverse response to renal ablation. *Am J Physiol* 241:F85-93.

Hotamisligil, G.S., Johnson, R.S., Distel, R.J., Ellis, R., Papaioannou, V.E., and Spiegelman, B.M. 1996. Uncoupling of obesity from insulin resistance through a targeted mutation in aP2, the adipocyte fatty acid binding protein. *Science* 274:1377-1379.

Huang, S., Reisch, S., Schaefer, L., Teschner, M., Heidland, A., and Schaefer, R.M. 1992. Effect of dietary protein on glomerular proteinase activities. *Miner Electrolyte Metab* 18:84-88.

Huang, S.S., Tang, F.M., Huang, Y.H., Liu, I.H., Hsu, S.C., Chen, S.T., and Huang, J.S. 2003. Cloning, expression, characterization, and role in autocrine cell growth of cell surface retention sequence binding protein-1. *J Biol Chem* 278:43855-43869.

Huber, T.B., Reinhardt, H.C., Exner, M., Burger, J.A., Kerjaschki, D., Saleem, M.A., and Pavenstadt, H. 2002. Expression of functional CCR and CXCR chemokine receptors in podocytes. *J Immunol* 168:6244-6252.

Hugo, C. 2003. The thrombospondin 1-TGF-beta axis in fibrotic renal disease. *Nephrol Dial Transplant* 18:1241-1245.

Hulett, M.D., and Hogarth, P.M. 1998. The second and third extracellular domains of FcgammaRI (CD64) confer the unique high affinity binding of IgG2a. *Mol Immunol* 35:989-996.

Ichikawa, I., Ikoma, M., and Fogo, A. 1991. Glomerular growth promoters, the common key mediator for progressive glomerular sclerosis in chronic renal diseases. *Adv Nephrol Necker Hosp* 20:127-148.

Ichikawa, I., Ma, J., Motojima, M., and Matsusaka, T. 2005. Podocyte damage damages podocytes: autonomous vicious cycle that drives local spread of glomerular sclerosis. *Curr Opin Nephrol Hypertens* 14:205-210.

Ikoma, M., Kawamura, T., Kakinuma, Y., Fogo, A., and Ichikawa, I. 1991. Cause of variable therapeutic efficiency of angiotensin converting enzyme inhibitor on glomerular lesions. *Kidney Int* 40:195-202.

Imai, T., Hieshima, K., Haskell, C., Baba, M., Nagira, M., Nishimura, M., Kakizaki, M., Takagi, S., Nomiyama, H., Schall, T.J., and Yoshie, O. 1997. Identification and molecular characterization of fractalkine receptor CX3CR1, which mediates both leukocyte migration and adhesion. *Cell* 91:521-530.

Inokuchi, S., Shirato, I., Kobayashi, N., Koide, H., Tomino, Y., and Sakai, T. 1996. Re-evaluation of foot process effacement in acute puromycin aminonucleoside nephrosis. *Kidney Int* 50:1278-1287.

Irizarry, R.A., Hobbs, B., Collin, F., Beazer-Barclay, Y.D., Antonellis, K.J., Scherf, U., and Speed, T.P. 2003. Exploration, normalization, and summaries of high density oligonucleotide array probe level data. *Biostatistics* 4:249-264.

Iseki, K., Kinjo, K., Iseki, C., and Takishita, S. 2004. Relationship between predicted creatinine clearance and proteinuria and the risk of developing ESRD in Okinawa, Japan. *Am J Kidney Dis* 44:806-814.

Isshiki, K., Haneda, M., Koya, D., Maeda, S., Sugimoto, T., and Kikkawa, R. 2000. Thiazolidinedione compounds ameliorate glomerular dysfunction independent of their insulin-sensitizing action in diabetic rats. *Diabetes* 49:1022-1032.

Izzedine, H., Launay-Vacher, V., Buhaescu, I., Heurtier, A., Baumelou, A., and Deray, G. 2005. PPAR-gamma-agonists' renal effects. *Minerva Urol Nefrol* 57:247-260.

Jackson, D.G., Bell, J.I., Dickinson, R., Timans, J., Shields, J., and Whittle, N. 1995. Proteoglycan forms of the lymphocyte homing receptor CD44 are alternatively spliced variants containing the v3 exon. *J Cell Biol* 128:673-685.

Jackson, D.G., Prevo, R., Clasper, S., and Banerji, S. 2001. LYVE-1, the lymphatic system and tumor lymphangiogenesis. *Trends Immunol* 22:317-321.

Jacot, T.A., Striker, G.E., Stetler-Stevenson, M., and Striker, L.J. 1996. Mesangial cells from transgenic mice with progressive glomerulosclerosis exhibit stable, phenotypic changes including undetectable MMP-9 and increased type IV collagen. *Lab Invest* 75:791-799.

Jalkanen, S., and Jalkanen, M. 1992. Lymphocyte CD44 binds the COOH-terminal heparin-binding domain of fibronectin. *J Cell Biol* 116:817-825.

Jani, A., Polhemus, C., Corrigan, G., Kwon, O., Myers, B.D., and Pavlakis, M. 2002. Determinants of hypofiltration during acute renal allograft rejection. *J Am Soc Nephrol* 13:773-778.

Jensen, E.B., Gundersen, H.J., and Osterby, R. 1979. Determination of membrane thickness distribution from orthogonal intercepts. *J Microsc* 115:19-33.

Johnson, D., al-Shawi, R., and Bishop, J.O. 1995. Sexual dimorphism and growth hormone induction of murine pheromone-binding proteins. *J Mol Endocrinol* 14:21-34.

Johnson, R.J., Floege, J., Yoshimura, A., Iida, H., Couser, W.G., and Alpers, C.E. 1992. The activated mesangial cell: a glomerular "myofibroblast"? *J Am Soc Nephrol* 2:S190-197.

Johnsson, C., Tufveson, G., Wahlberg, J., and Hallgren, R. 1996. Experimentally-induced warm renal ischemia induces cortical accumulation of hyaluronan in the kidney. *Kidney Int* 50:1224-1229.

Johnstone, D.B., and Holzman, L.B. 2006. Clinical impact of research on the podocyte slit diaphragm. *Nat Clin Pract Nephrol* 2:271-282.

Jones, S., Jones, S., and Phillips, A.O. 2001. Regulation of renal proximal tubular epithelial cell hyaluronan generation: implications for diabetic nephropathy. *Kidney Int* 59:1739-1749.

Jun, Z., Hill, P.A., Lan, H.Y., Foti, R., Mu, W., Atkins, R.C., and Nikolic-Paterson, D.J. 1997. CD44 and hyaluronan expression in the development of experimental crescentic glomerulonephritis. *Clin Exp Immunol* 108:69-77.

Jung, S., Aliberti, J., Graemmel, P., Sunshine, M.J., Kreutzberg, G.W., Sher, A., and Littman, D.R. 2000. Analysis of fractalkine receptor CX(3)CR1 function by targeted deletion and green fluorescent protein reporter gene insertion. *Mol Cell Biol* 20:4106-4114.

Kalluri, R. 2006. Proteinuria with and without renal glomerular podocyte effacement. *J Am Soc Nephrol* 17:2383-2389.

Kamanna, V.S., Pai, R., Bassa, B., and Kirschenbaum, M.A. 1996. Activation of mesangial cells with TNF-alpha stimulates M-CSF gene expression and monocyte proliferation: evidence for involvement of protein kinase C and protein tyrosine kinase. *Biochim Biophys Acta* 1313:161-172.

Kamijo-Ikemori, A., Sugaya, T., and Kimura, K. 2006. Urinary fatty acid binding protein in renal disease. *Clin Chim Acta* 374:1-7.

Kamijo, A., Sugaya, T., Hikawa, A., Okada, M., Okumura, F., Yamanouchi, M., Honda, A., Okabe, M., Fujino, T., Hirata, Y., Omata, M., Kaneko, R., Fujii, H., Fukamizu, A., and Kimura, K. 2004. Urinary excretion of fatty acid-binding protein reflects stress overload on the proximal tubules. *Am J Pathol* 165:1243-1255.

Kamijo, A., Sugaya, T., Hikawa, A., Yamanouchi, M., Hirata, Y., Ishimitsu, T., Numabe, A., Takagi, M., Hayakawa, H., Tabei, F., Sugimoto, T., Mise, N., Omata, M., and Kimura, K. 2006. Urinary liver-type fatty acid binding protein as a useful biomarker in chronic kidney disease. *Mol Cell Biochem* 284:175-182.

Kamme, F., Salunga, R., Yu, J., Tran, D.T., Zhu, J., Luo, L., Bittner, A., Guo, H.Q., Miller, N., Wan, J., and Erlander, M. 2003. Single-cell microarray analysis in hippocampus CA1: demonstration and validation of cellular heterogeneity. *J Neurosci* 23:3607-3615.

Kanjanabuch, T., Ma, L.J., Chen, J., Pozzi, A., Guan, Y., Mundel, P., and Fogo, A.B. 2007. PPAR-gamma agonist protects podocytes from injury. *Kidney Int* 71:1232-1239.

Karnovsky, M.J., and Ainsworth, S.K. 1972. The structural basis of glomerular filtration. *Adv Nephrol Necker Hosp* 2:35-60.

Kashgarian, M., and Sterzel, R.B. 1992. The pathobiology of the mesangium. *Kidney Int* 41:524-529.

Kasiske, B.L., Cleary, M.P., O'Donnell, M.P., and Keane, W.F. 1985. Effects of genetic obesity on renal structure and function in the Zucker rat. *J Lab Clin Med* 106:598-604.

Kazemi, M.R., McDonald, C.M., Shigenaga, J.K., Grunfeld, C., and Feingold, K.R. 2005. Adipocyte fatty acid-binding protein expression and lipid accumulation are increased during activation of murine macrophages by toll-like receptor agonists. *Arterioscler Thromb Vasc Biol* 25:1220-1224.

Kerjaschki, D. 2001. Caught flat-footed: podocyte damage and the molecular bases of focal glomerulosclerosis. *J Clin Invest* 108:1583-1587.

Kerjaschki, D., Miettinen, A., and Farquhar, M.G. 1987. Initial events in the formation of immune deposits in passive Heymann nephritis. gp330-anti-gp330 immune complexes form in epithelial coated pits and rapidly become attached to the glomerular basement membrane. *J Exp Med* 166:109-128.

Kerjaschki, D., and Neale, T.J. 1996. Molecular mechanisms of glomerular injury in rat experimental membranous nephropathy (Heymann nephritis). *J Am Soc Nephrol* 7:2518-2526.

Kestila, M., Lenkkeri, U., Mannikko, M., Lamerdin, J., McCready, P., Putaala, H., Ruotsalainen, V., Morita, T., Nissinen, M., Herva, R., Kashtan, C.E., Peltonen, L., Holmberg, C., Olsen, A., and Tryggvason, K. 1998. Positionally cloned gene for a novel glomerular protein--nephrin--is mutated in congenital nephrotic syndrome. *Mol Cell* 1:575-582.

Kieffer, T.J., and Habener, J.F. 1999. The glucagon-like peptides. *Endocr Rev* 20:876-913.

Kieran, N.E., Doran, P.P., Connolly, S.B., Greenan, M.C., Higgins, D.F., Leonard, M., Godson, C., Taylor, C.T., Henger, A., Kretzler, M., Burne, M.J., Rabb, H., and Brady, H.R. 2003. Modification of the transcriptomic response to renal ischemia/reperfusion injury by lipoxin analog. *Kidney Int* 64:480-492.

Kim, S.V., Mehal, W.Z., Dong, X., Heinrich, V., Pypaert, M., Mellman, I., Dembo, M., Mooseker, M.S., Wu, D., and Flavell, R.A. 2006. Modulation of cell adhesion and motility in the immune system by Myo1f. *Science* 314:136-139.

Kim, Y.H., Goyal, M., Kurnit, D., Wharram, B., Wiggins, J., Holzman, L., Kershaw, D., and Wiggins, R. 2001. Podocyte depletion and glomerulosclerosis have a direct relationship in the PAN-treated rat. *Kidney Int* 60:957-968.

Kimmelstiel, P., and Wilson, C. 1936. Intercapillary lesions in the glomeruli of the kidney. *Am J Pathol* 12:83-96.

Kiritoshi, S., Nishikawa, T., Sonoda, K., Kukidome, D., Senokuchi, T., Matsuo, T., Matsumura, T., Tokunaga, H., Brownlee, M., and Araki, E. 2003. Reactive oxygen species from mitochondria induce cyclooxygenase-2 gene expression in human mesangial cells: potential role in diabetic nephropathy. *Diabetes* 52:2570-2577.

Kishikawa, H., Mine, S., Kawahara, C., Tabata, T., Hirose, A., Okada, Y., and Tanaka, Y. 2006. Glycated albumin and cross-linking of CD44 induce scavenger receptor expression and uptake of oxidized LDL in human monocytes. *Biochem Biophys Res Commun* 339:846-851.

Klahr, S., Schreiner, G., and Ichikawa, I. 1988. The progression of renal disease. *N Engl J Med* 318:1657-1666.

Kleinknecht, C., Laouari, D., and Burtin, M. 1988. Uremic rat model: experience with young rats. *Contrib Nephrol* 60:27-38.

Kobayashi, N., Gao, S.Y., Chen, J., Saito, K., Miyawaki, K., Li, C.Y., Pan, L., Saito, S., Terashita, T., and Matsuda, S. 2004. Process formation of the renal glomerular podocyte: is there common molecular machinery for processes of podocytes and neurons? *Anat Sci Int* 79:1-10.

Kobayashi, N., Mominoki, K., Wakisaka, H., Shimazaki, Y., and Matsuda, S. 2001. Morphogenetic activity of extracellular matrices on cultured podocytes. Laminin accelerates podocyte process formation in vitro. *Ital J Anat Embryol* 106:423-430.

Kobayashi, N., and Mundel, P. 1998. A role of microtubules during the formation of cell processes in neuronal and non-neuronal cells. *Cell Tissue Res* 291:163-174.

Koletsky, S., and Goodsitt, A.M. 1960. Natural history and pathogenesis of renal ablation hypertension. *Arch Pathol* 69:654-662.

Krakower, C.A., and Greenspon, S.A. 1951. Localization of the nephrotoxic antigen within the isolated renal glomerulus. *AMA Arch Pathol* 51:629-639.

Kretzler, M., Cohen, C.D., Doran, P., Henger, A., Madden, S., Grone, E.F., Nelson, P.J., Schlondorff, D., and Grone, H.J. 2002. Repuncturing the renal biopsy: strategies for molecular diagnosis in nephrology. *J Am Soc Nephrol* 13:1961-1972.

Kretzler, M., Koeppen-Hagemann, I., and Kriz, W. 1994. Podocyte damage is a critical step in the development of glomerulosclerosis in the uninephrectomised-desoxycorticosterone hypertensive rat. *Virchows Arch* 425:181-193.

Kriz, W. 1996. Progressive renal failure--inability of podocytes to replicate and the consequences for development of glomerulosclerosis. *Nephrol Dial Transplant* 11:1738-1742.

Kriz, W. 2002. Podocyte is the major culprit accounting for the progression of chronic renal disease. *Microsc Res Tech* 57:189-195.

Kriz, W., Elger, M., Hosser, H., Hahnel, B., Provoost, A., Kranzlin, B., and Gretz, N. 1999. How does podocyte damage result in tubular damage? *Kidney Blood Press Res* 22:26-36.

Kriz, W., Elger, M., Mundel, P., and Lemley, K.V. 1995. Structure-stabilizing forces in the glomerular tuft. *J Am Soc Nephrol* 5:1731-1739.

Kriz, W., Elger, M., Nagata, M., Kretzler, M., Uiker, S., Koeppen-Hageman, I., Tenschert, S., and Lemley, K.V. 1994. The role of podocytes in the development of glomerular sclerosis. *Kidney Int Suppl* 45:S64-72.

Kriz, W., Kretzler, M., Nagata, M., Provoost, A.P., Shirato, I., Uiker, S., Sakai, T., and Lemley, K.V. 1996. A frequent pathway to glomerulosclerosis: deterioration of tuft architecture-podocyte damage-segmental sclerosis. *Kidney Blood Press Res* 19:245-253.

Kriz, W., and LeHir, M. 2005. Pathways to nephron loss starting from glomerular diseases-insights from animal models. *Kidney Int* 67:404-419.

Kriz, W., Mundel, P., and Elger, M. 1994. The contractile apparatus of podocytes is arranged to counteract GBM expansion. *Contrib Nephrol* 107:1-9.

Krolewski, A.S. 1999. Genetics of diabetic nephropathy: evidence for major and minor gene effects. *Kidney Int* 55:1582-1596.

Kutyavin, I.V., Lukhtanov, E.A., Gamper, H.B., and Meyer, R.B. 1997. Oligonucleotides with conjugated dihydropyrroloindole tripeptides: base composition and backbone effects on hybridization. *Nucleic Acids Res* 25:3718-3723.

Lafferty, H.M., and Brenner, B.M. 1990. Are glomerular hypertension and "hypertrophy" independent risk factors for progression of renal disease? *Semin Nephrol* 10:294-304.

Lai, K.N., Tang, S.C., Guh, J.Y., Chuang, T.D., Lam, M.F., Chan, L.Y., Tsang, A.W., and Leung, J.C. 2003. Polymeric IgA1 from patients with IgA nephropathy upregulates transforming growth factor-beta synthesis and signal transduction in human mesangial cells via the renin-angiotensin system. *J Am Soc Nephrol* 14:3127-3137.

Lakowicz, J.R. 1983. Energy Transfer. In *Principles of Flourescent Spectroscopy*. New York: Plenum Press. 303-339.

Lane, P.H., Steffes, M.W., and Mauer, S.M. 1992. Estimation of glomerular volume: a comparison of four methods. *Kidney Int* 41:1085-1089.

Laurent, T.C., and Fraser, J.R. 1992. Hyaluronan. *Faseb J* 6:2397-2404.

Lax, D.S., Benstein, J.A., Tolbert, E., and Dworkin, L.D. 1992. Effects of salt restriction on renal growth and glomerular injury in rats with remnant kidneys. *Kidney Int* 41:1527-1534.

Lee, J.Y., and Spicer, A.P. 2000. Hyaluronan: a multifunctional, megaDalton, stealth molecule. *Curr Opin Cell Biol* 12:581-586.

Lehner, R., and Vance, D.E. 1999. Cloning and expression of a cDNA encoding a hepatic microsomal lipase that mobilizes stored triacylglycerol. *Biochem J* 343 Pt 1:1-10.

Lehner, R., and Verger, R. 1997. Purification and characterization of a porcine liver microsomal triacylglycerol hydrolase. *Biochemistry* 36:1861-1868.

Lemley, K.V. 2003. A basis for accelerated progression of diabetic nephropathy in Pima Indians. *Kidney Int Suppl*:S38-42.

Leung, J.C., Tang, S.C., Chan, L.Y., Tsang, A.W., Lan, H.Y., and Lai, K.N. 2003. Polymeric IgA increases the synthesis of macrophage migration inhibitory factor by human mesangial cells in IgA nephropathy. *Nephrol Dial Transplant* 18:36-45.

Lewis, E.J., Hunsicker, L.G., Bain, R.P., and Rohde, R.D. 1993. The effect of angiotensin-converting-enzyme inhibition on diabetic nephropathy. The Collaborative Study Group. *N Engl J Med* 329:1456-1462.

Li, M., Bermak, J.C., Wang, Z.W., and Zhou, Q.Y. 2000. Modulation of dopamine D(2) receptor signaling by actin-binding protein (ABP-280). *Mol Pharmacol* 57:446-452.

Li, M., Rosenfeld, L., Vilar, R.E., and Cowman, M.K. 1997. Degradation of hyaluronan by peroxynitrite. *Arch Biochem Biophys* 341:245-250.

Liao, J., Kobayashi, M., Kanamuru, Y., Nakamura, S., Makita, Y., Funabiki, K., Horikoshi, S., and Tomino, Y. 2003. Effects of candesartan, an angiotensin II type 1 receptor blocker, on diabetic nephropathy in KK/Ta mice. *J Nephrol* 16:841-849.

Lin, R., Karpa, K., Kabbani, N., Goldman-Rakic, P., and Levenson, R. 2001. Dopamine D2 and D3 receptors are linked to the actin cytoskeleton via interaction with filamin A. *Proc Natl Acad Sci U S A* 98:5258-5263.

Liu, G., Thomas, L., Warren, R.A., Enns, C.A., Cunningham, C.C., Hartwig, J.H., and Thomas, G. 1997. Cytoskeletal protein ABP-280 directs the intracellular trafficking of furin and modulates proprotein processing in the endocytic pathway. *J Cell Biol* 139:1719-1733.

Loo, D.T., Kanner, S.B., and Aruffo, A. 1998. Filamin binds to the cytoplasmic domain of the beta1-integrin. Identification of amino acids responsible for this interaction. *J Biol Chem* 273:23304-23312.

Lopez-Armada, M.J., Gomez-Guerrero, C., and Egido, J. 1996. Receptors for immune complexes activate gene expression and synthesis of matrix proteins in cultured rat and human mesangial cells: role of TGF-beta. *J Immunol* 157:2136-2142.

Lu, M., Wheeler, M.B., Leng, X.H., and Boyd, A.E., 3rd. 1993. The role of the free cytosolic calcium level in beta-cell signal transduction by gastric inhibitory polypeptide and glucagon-like peptide I(7-37). *Endocrinology* 132:94-100.

Ma, L.J., Marcantoni, C., Linton, M.F., Fazio, S., and Fogo, A.B. 2001. Peroxisome proliferator-activated receptor-gamma agonist troglitazone protects against nondiabetic glomerulosclerosis in rats. *Kidney Int* 59:1899-1910.

MacLeod, J.N., Pampori, N.A., and Shapiro, B.H. 1991. Sex differences in the ultradian pattern of plasma growth hormone concentrations in mice. *J Endocrinol* 131:395-399.

Madaio, M.P. 1990. Renal biopsy. *Kidney Int* 38:529-543.

Madsen, K.M., and Tisher, C.C. 1996. The Nephron. In *The Kidney.* B.M. Brenner, editor. Philadelphia: Elsevier. 8-18.

Mahadevan, P., Larkins, R.G., Fraser, J.R., Fosang, A.J., and Dunlop, M.E. 1995. Increased hyaluronan production in the glomeruli from diabetic rats: a link between glucose-induced prostaglandin production and reduced sulphated proteoglycan. *Diabetologia* 38:298-305.

Makino, H., Miyamoto, Y., Sawai, K., Mori, K., Mukoyama, M., Nakao, K., Yoshimasa, Y., and Suga, S. 2006. Altered gene expression related to glomerulogenesis and podocyte structure in early diabetic nephropathy of db/db mice and its restoration by pioglitazone. *Diabetes* 55:2747-2756.

Makowski, L., Boord, J.B., Maeda, K., Babaev, V.R., Uysal, K.T., Morgan, M.A., Parker, R.A., Suttles, J., Fazio, S., Hotamisligil, G.S., and Linton, M.F. 2001. Lack of macrophage fatty-acid-binding protein aP2 protects mice deficient in apolipoprotein E against atherosclerosis. *Nat Med* 7:699-705.

Makowski, L., Brittingham, K.C., Reynolds, J.M., Suttles, J., and Hotamisligil, G.S. 2005. The fatty acid-binding protein, aP2, coordinates macrophage cholesterol trafficking and inflammatory activity. Macrophage expression of aP2 impacts peroxisome proliferator-activated receptor gamma and IkappaB kinase activities. *J Biol Chem* 280:12888-12895.

Mansouri, A. 2001. Determination of gene function by homologous recombination using embryonic stem cells and knockout mice. *Methods Mol Biol* 175:397-413.

Marinides, G.N., Groggel, G.C., Cohen, A.H., and Border, W.A. 1990. Enalapril and low protein reverse chronic puromycin aminonucleoside nephropathy. *Kidney Int* 37:749-757.

Marshall, T., and Williams, K.M. 1998. Clinical analysis of human urinary proteins using high resolution electrophoretic methods. *Electrophoresis* 19:1752-1770.

Martin, J., Davies, M., Thomas, G., and Lovett, D.H. 1989. Human mesangial cells secrete a GBM-degrading neutral proteinase and a specific inhibitor. *Kidney Int* 36:790-801.

Martin, J., Steadman, R., Knowlden, J., Williams, J., and Davies, M. 1998. Differential regulation of matrix metalloproteinases and their inhibitors in human glomerular epithelial cells in vitro. *J Am Soc Nephrol* 9:1629-1637.

Maschio, G., Alberti, D., Janin, G., Locatelli, F., Mann, J.F., Motolese, M., Ponticelli, C., Ritz, E., and Zucchelli, P. 1996. Effect of the angiotensin-converting-enzyme inhibitor benazepril on the progression of chronic renal insufficiency. The Angiotensin-Converting-Enzyme Inhibition in Progressive Renal Insufficiency Study Group. *N Engl J Med* 334:939-945.

Matsuba, H., Watanabe, T., Watanabe, M., Ishii, Y., Waguri, S., Kominami, E., and Uchiyama, Y. 1989. Immunocytochemical localization of prorenin, renin, and cathepsins B, H, and L in juxtaglomerular cells of rat kidney. *J Histochem Cytochem* 37:1689-1697.

Matsumoto, K., and Hatano, M. 1991. Soluble immune complexes stimulate production of interleukin-1 by cultured rat glomerular mesangial cells. *Am J Nephrol* 11:138-143.

Mauer, S.M., Lane, P., Zhu, D., Fioretto, P., and Steffes, M.W. 1992. Renal structure and function in insulin-dependent diabetes mellitus in man. *J Hypertens Suppl* 10:S17-20.

Mauer, S.M., Steffes, M.W., Ellis, E.N., Sutherland, D.E., Brown, D.M., and Goetz, F.C. 1984. Structural-functional relationships in diabetic nephropathy. *J Clin Invest* 74:1143-1155.

Mayo, K.E., Miller, L.J., Bataille, D., Dalle, S., Goke, B., Thorens, B., and Drucker, D.J. 2003. International Union of Pharmacology. XXXV. The glucagon receptor family. *Pharmacol Rev* 55:167-194.

McGrane, M.M., de Vente, J., Yun, J., Bloom, J., Park, E., Wynshaw-Boris, A., Wagner, T., Rottman, F.M., and Hanson, R.W. 1988. Tissue-specific expression and dietary regulation of a chimeric phosphoenolpyruvate carboxykinase/bovine growth hormone gene in transgenic mice. *J Biol Chem* 263:11443-11451.

McKee, C.M., Penno, M.B., Cowman, M., Burdick, M.D., Strieter, R.M., Bao, C., and Noble, P.W. 1996. Hyaluronan (HA) fragments induce chemokine gene expression in alveolar macrophages. The role of HA size and CD44. *J Clin Invest* 98:2403-2413.

McMillan, J.I., Riordan, J.W., Couser, W.G., Pollock, A.S., and Lovett, D.H. 1996. Characterization of a glomerular epithelial cell metalloproteinase as matrix metalloproteinase-9 with enhanced expression in a model of membranous nephropathy. *J Clin Invest* 97:1094-1101.

Mene, P., Simonson, M.S., and Dunn, M.J. 1989. Physiology of the mesangial cell. *Physiol Rev* 69:1347-1424.

Mezzano, S., Aros, C., Droguett, A., Burgos, M.E., Ardiles, L., Flores, C., Schneider, H., Ruiz-Ortega, M., and Egido, J. 2004. NF-kappaB activation and overexpression of regulated genes in human diabetic nephropathy. *Nephrol Dial Transplant* 19:2505-2512.

Mine, S., Okada, Y., Kawahara, C., Tabata, T., and Tanaka, Y. 2006. Serum hyaluronan concentration as a marker of angiopathy in patients with diabetes mellitus. *Endocr J* 53:761-766.

Misra, R.P. 1972. Isolation of glomeruli from mammalian kidneys by graded sieving. *Am J Clin Pathol* 58:135-139.

Mitka, M. 2005. Kidney failure rates end 20-year climb. *Jama* 294:2563.

Moeller, M.J., Soofi, A., Hartmann, I., Le Hir, M., Wiggins, R., Kriz, W., and Holzman, L.B. 2004. Podocytes populate cellular crescents in a murine model of inflammatory glomerulonephritis. *J Am Soc Nephrol* 15:61-67.

Moerth, C., Schneider, M.R., Renner-Mueller, I., Blutke, A., Elmlinger, M.W., Erben, R.G., Camacho-Hubner, C., Hoeflich, A., and Wolf, E. 2007. Postnatally elevated levels of insulin-like growth factor (IGF)-II fail to rescue the dwarfism of IGF-I-deficient mice except kidney weight. *Endocrinology* 148:441-451.

Mogensen, C.E., Christensen, C.K., and Vittinghus, E. 1983. The stages in diabetic renal disease. With emphasis on the stage of incipient diabetic nephropathy. *Diabetes* 32 Suppl 2:64-78.

Mori, T., Bartocci, A., Satriano, J., Zuckerman, A., Stanley, R., Santiago, A., and Schlondorff, D. 1990. Mouse mesangial cells produce colony-stimulating factor-1 (CSF-1) and express the CSF-1 receptor. *J Immunol* 144:4697-4702.

Moriya, R., Manivel, J.C., and Mauer, M. 2004. Juxtaglomerular apparatus T-cell infiltration affects glomerular structure in Type 1 diabetic patients. *Diabetologia* 47:82-88.

Morrison, T.B., Weis, J.J., and Wittwer, C.T. 1998. Quantification of low-copy transcripts by continuous SYBR Green I monitoring during amplification. *Biotechniques* 24:954-958, 960, 962.

Mouta Carreira, C., Nasser, S.M., di Tomaso, E., Padera, T.P., Boucher, Y., Tomarev, S.I., and Jain, R.K. 2001. LYVE-1 is not restricted to the lymph vessels: expression in normal liver blood sinusoids and down-regulation in human liver cancer and cirrhosis. *Cancer Res* 61:8079-8084.

Mueller, O., Hahnenberger, K., Dittmann, M., Yee, H., Dubrow, R., Nagle, R., and Ilsley, D. 2000. A microfluidic system for high-speed reproducible DNA sizing and quantitation. *Electrophoresis* 21:128-134.

Mundel, P., and Shankland, S.J. 2002. Podocyte biology and response to injury. *J Am Soc Nephrol* 13:3005-3015.

Nagano, T., Yoneda, T., Hatanaka, Y., Kubota, C., Murakami, F., and Sato, M. 2002. Filamin A-interacting protein (FILIP) regulates cortical cell migration out of the ventricular zone. *Nat Cell Biol* 4:495-501.

Nagata, M., Hattori, M., Hamano, Y., Ito, K., Saitoh, K., and Watanabe, T. 1998. Origin and phenotypic features of hyperplastic epithelial cells in collapsing glomerulopathy. *Am J Kidney Dis* 32:962-969.

Nakagawa, T., Sato, W., Glushakova, O., Heinig, M., Clarke, T., Campbell-Thompson, M., Yuzawa, Y., Atkinson, M.A., Johnson, R.J., and Croker, B. 2007. Diabetic endothelial nitric oxide synthase knockout mice develop advanced diabetic nephropathy. *J Am Soc Nephrol* 18:539-550.

Nakamura, T., Sugaya, T., Kawagoe, Y., Ueda, Y., Osada, S., and Koide, H. 2006. Urinary liver-type fatty acid-binding protein levels for differential diagnosis of idiopathic focal glomerulosclerosis and minor glomerular abnormalities and effect of low-density lipoprotein apheresis. *Clin Nephrol* 65:1-6.

Neale, T.J., Ullrich, R., Ojha, P., Poczewski, H., Verhoeven, A.J., and Kerjaschki, D. 1993. Reactive oxygen species and neutrophil respiratory burst cytochrome b558 are produced by

kidney glomerular cells in passive Heymann nephritis. *Proc Natl Acad Sci U S A* 90:3645-3649.

Neuwirth, R., Singhal, P., Diamond, B., Hays, R.M., Lobmeyer, L., Clay, K., and Schlondorff, D. 1988. Evidence for immunoglobulin Fc receptor-mediated prostaglandin2 and platelet-activating factor formation by cultured rat mesangial cells. *J Clin Invest* 82:936-944.

Nikolic-Paterson, D.J., Jun, Z., Tesch, G.H., Lan, H.Y., Foti, R., and Atkins, R.C. 1996. De novo CD44 expression by proliferating mesangial cells in rat anti-Thy-1 nephritis. *J Am Soc Nephrol* 7:1006-1014.

Nishikawa, K., Andres, G., Bhan, A.K., McCluskey, R.T., Collins, A.B., Stow, J.L., and Stamenkovic, I. 1993. Hyaluronate is a component of crescents in rat autoimmune glomerulonephritis. *Lab Invest* 68:146-153.

Noble, P.W. 2002. Hyaluronan and its catabolic products in tissue injury and repair. *Matrix Biol* 21:25-29.

Noiri, E., Dickman, K., Miller, F., Romanov, G., Romanov, V.I., Shaw, R., Chambers, A.F., Rittling, S.R., Denhardt, D.T., and Goligorsky, M.S. 1999. Reduced tolerance to acute renal ischemia in mice with a targeted disruption of the osteopontin gene. *Kidney Int* 56:74-82.

Nolasco, F.E., Cameron, J.S., Hartley, B., Coelho, R.A., Hildredth, G., and Reuben, R. 1987. Abnormal podocyte CR-1 expression in glomerular diseases: association with glomerular cell proliferation and monocyte infiltration. *Nephrol Dial Transplant* 2:304-312.

Norgaard, J.O. 1976. A new method for the isolation of ultrastructurally preserved glomeruli. *Kidney Int* 9:278-285.

Norstedt, G., and Palmiter, R. 1984. Secretory rhythm of growth hormone regulates sexual differentiation of mouse liver. *Cell* 36:805-812.

Nyengaard, J.R. 1999. Stereologic methods and their application in kidney research. *J Am Soc Nephrol* 10:1100-1123.

Nyengaard, J.R., and Bendtsen, T.F. 1992. Glomerular number and size in relation to age, kidney weight, and body surface in normal man. *Anat Rec* 232:194-201.

O'Donnell, M.P., Kasiske, B.L., Schmitz, P.G., and Keane, W.F. 1990. High protein intake accelerates glomerulosclerosis independent of effects on glomerular hemodynamics. *Kidney Int* 37:1263-1269.

Oda, T., Jung, Y.O., Kim, H.S., Cai, X., Lopez-Guisa, J.M., Ikeda, Y., and Eddy, A.A. 2001. PAI-1 deficiency attenuates the fibrogenic response to ureteral obstruction. *Kidney Int* 60:587-596.

Ohyama, K., Seyer, J.M., Raghow, R., and Kang, A.H. 1990. Extracellular matrix phenotype of rat mesangial cells in culture. Biosynthesis of collagen types I, III, IV, and V and a low molecular weight collagenous component and their regulation by dexamethasone. *J Lab Clin Med* 116:219-227.

Oiknine, J., and Aviram, M. 1992. Increased susceptibility to activation and increased uptake of low density lipoprotein by cholesterol-loaded macrophages. *Arterioscler Thromb* 12:745-753.

Okada, T., Wada, J., Hida, K., Eguchi, J., Hashimoto, I., Baba, M., Yasuhara, A., Shikata, K., and Makino, H. 2006. Thiazolidinediones ameliorate diabetic nephropathy via cell cycle-dependent mechanisms. *Diabetes* 55:1666-1677.

Okazaki, H., Igarashi, M., Nishi, M., Tajima, M., Sekiya, M., Okazaki, S., Yahagi, N., Ohashi, K., Tsukamoto, K., Amemiya-Kudo, M., Matsuzaka, T., Shimano, H., Yamada, N., Aoki, J., Morikawa, R., Takanezawa, Y., Arai, H., Nagai, R., Kadowaki, T., Osuga, J., and Ishibashi, S. 2006. Identification of a novel member of the carboxylesterase family that hydrolyzes triacylglycerol: a potential role in adipocyte lipolysis. *Diabetes* 55:2091-2097.

Olson, J.L. 1992 (a). The nephrotic syndrome. In Pathology of the kidney (Heptinstall, R.H. ed.), Little, Brown, Boston, Toronto, London, pp. 779-870.

Olson, J.L. 1992 (b). *Diabetes mellitus. In Pathology of the kiney (Heptinstall, R.H. ed.), Little, Brown, Boston, Toronto, London, pp. 1715-1764.*

Olson, J.L., de Urdaneta, A.G., and Heptinstall, R.H. 1985. Glomerular hyalinosis and its relation to hyperfiltration. *Lab Invest* 52:387-398.

Olson, J.L., and Heptinstall, R.H. 1988. Nonimmunologic mechanisms of glomerular injury. *Lab Invest* 59:564-578.

Ophascharoensuk, V., Giachelli, C.M., Gordon, K., Hughes, J., Pichler, R., Brown, P., Liaw, L., Schmidt, R., Shankland, S.J., Alpers, C.E., Couser, W.G., and Johnson, R.J. 1999. Obstructive uropathy in the mouse: role of osteopontin in interstitial fibrosis and apoptosis. *Kidney Int* 56:571-580.

Osawa, G., Kimmelstiel, P., and Seiling, V. 1966. Thickness of glomerular basement membranes. *Am J Clin Pathol* 45:7-20.

Oser, B.M., and Boesken, W.H. 1993. [Rational diagnosis in kidney diseases]. *Z Arztl Fortbild (Jena)* 87:211-215.

Osterby, R., and Gundersen, H.J. 1975. Glomerular size and structure in diabetes mellitus. I. Early abnormalities. *Diabetologia* 11:225-229.

Pagtalunan, M.E., Miller, P.L., Jumping-Eagle, S., Nelson, R.G., Myers, B.D., Rennke, H.G., Coplon, N.S., Sun, L., and Meyer, T.W. 1997. Podocyte loss and progressive glomerular injury in type II diabetes. *J Clin Invest* 99:342-348.

Pai, R., Kirschenbaum, M.A., and Kamanna, V.S. 1995. Low-density lipoprotein stimulates the expression of macrophage colony-stimulating factor in glomerular mesangial cells. *Kidney Int* 48:1254-1262.

Palmiter, R.D., Brinster, R.L., Hammer, R.E., Trumbauer, M.E., Rosenfeld, M.G., Birnberg, N.C., and Evans, R.M. 1982. Dramatic growth of mice that develop from eggs microinjected with metallothionein-growth hormone fusion genes. *Nature* 300:611-615.

Pan, Y., Lloyd, C., Zhou, H., Dolich, S., Deeds, J., Gonzalo, J.A., Vath, J., Gosselin, M., Ma, J., Dussault, B., Woolf, E., Alperin, G., Culpepper, J., Gutierrez-Ramos, J.C., and Gearing, D. 1997. Neurotactin, a membrane-anchored chemokine upregulated in brain inflammation. *Nature* 387:611-617.

Pavenstadt, H., Kriz, W., and Kretzler, M. 2003. Cell biology of the glomerular podocyte. *Physiol Rev* 83:253-307.

Pease, A.C., Solas, D., Sullivan, E.J., Cronin, M.T., Holmes, C.P., and Fodor, S.P. 1994. Light-generated oligonucleotide arrays for rapid DNA sequence analysis. *Proc Natl Acad Sci U S A* 91:5022-5026.

Pesce, C. 1998. Glomerular number and size: facts and artefacts. *Anat Rec* 251:66-71.

Peten, E.P., Garcia-Perez, A., Terada, Y., Woodrow, D., Martin, B.M., Striker, G.E., and Striker, L.J. 1992. Age-related changes in alpha 1- and alpha 2-chain type IV collagen mRNAs in adult mouse glomeruli: competitive PCR. *Am J Physiol* 263:F951-957.

Peterson, J.C., Adler, S., Burkart, J.M., Greene, T., Hebert, L.A., Hunsicker, L.G., King, A.J., Klahr, S., Massry, S.G., and Seifter, J.L. 1995. Blood pressure control, proteinuria, and the progression of renal disease. The Modification of Diet in Renal Disease Study. *Ann Intern Med* 123:754-762.

Phimister, B. 1999. A note on nomenclature (editorial). *Nature Genetics* volume 21 no.1 supplement:1.

Platt, N., and Gordon, S. 2001. Is the class A macrophage scavenger receptor (SR-A) multifunctional? - The mouse's tale. *J Clin Invest* 108:649-654.

Prevo, R., Banerji, S., Ferguson, D.J., Clasper, S., and Jackson, D.G. 2001. Mouse LYVE-1 is an endocytic receptor for hyaluronan in lymphatic endothelium. *J Biol Chem* 276:19420-19430.

Radeke, H.H., and Resch, K. 1992. The inflammatory function of renal glomerular mesangial cells and their interaction with the cellular immune system. *Clin Investig* 70:825-842.

Raij, L., Azar, S., and Keane, W. 1984. Mesangial immune injury, hypertension, and progressive glomerular damage in Dahl rats. *Kidney Int* 26:137-143.

Ramage, I.J., Howatson, A.G., McColl, J.H., Maxwell, H., Murphy, A.V., and Beattie, T.J. 2002. Glomerular basement membrane thickness in children: a stereologic assessment. *Kidney Int* 62:895-900.

Rastaldi, M.P., Armelloni, S., Berra, S., Calvaresi, N., Corbelli, A., Giardino, L.A., Li, M., Wang, G.Q., Fornasieri, A., Villa, A., Heikkila, E., Soliymani, R., Boucherot, A., Cohen, C.D., Kretzler, M., Nitsche, A., Ripamonti, M., Malgaroli, A., Pesaresi, M., Forloni, G.L., Schlondorff, D., Holthofer, H., and D'Amico, G. 2006. Glomerular podocytes contain neuron-like functional synaptic vesicles. *Faseb J* 20:976-978.

Rastaldi, M.P., Armelloni, S., Berra, S., Li, M., Pesaresi, M., Poczewski, H., Langer, B., Kerjaschki, D., Henger, A., Blattner, S.M., Kretzler, M., Wanke, R., and D'Amico, G. 2003. Glomerular podocytes possess the synaptic vesicle molecule Rab3A and its specific effector rabphilin-3a. *Am J Pathol* 163:889-899.

Reddi, A.S., Oppermann, W., Velasco, C.A., and Camerini-Davalos, R.A. 1977. Diabetic microangiopathy in KK mice. II. Suppression of Glomerulosclerosis by pyridinolcarbamate. *Exp Mol Pathol* 26:325-339.

Reddi, A.S., Velasco, C.A., Reddy, P.R., Khan, M.Y., and Camerini-Davalos, R.A. 1990. Diabetic microangiopathy in KK mice. VI. Effect of glycemic control on renal glycoprotein metabolism and established glomerulosclerosis. *Exp Mol Pathol* 53:140-151.

Reddi, A.S., Wehner, H., Khan, M.Y., and Camerini-Davalos, R.A. 1988. Kidney disease in KK mice: structural, biochemical and functional relationships. *Adv Exp Med Biol* 246:135-145.

Remuzzi, A., Fassi, A., Bertani, T., Perico, N., and Remuzzi, G. 1999. ACE inhibition induces regression of proteinuria and halts progression of renal damage in a genetic model of progressive nephropathy. *Am J Kidney Dis* 34:626-632.

Remuzzi, A., Gagliardini, E., Donadoni, C., Fassi, A., Sangalli, F., Lepre, M.S., Remuzzi, G., and Benigni, A. 2002. Effect of angiotensin II antagonism on the regression of kidney disease in the rat. *Kidney Int* 62:885-894.

Remuzzi, A., Mazerska, M., Gephardt, G.N., Novick, A.C., Brenner, B.M., and Remuzzi, G. 1995. Three-dimensional analysis of glomerular morphology in patients with subtotal nephrectomy. *Kidney Int* 48:155-162.

Remuzzi, G. 1995. Abnormal protein traffic through the glomerular barrier induces proximal tubular cell dysfunction and causes renal injury. *Curr Opin Nephrol Hypertens* 4:339-342.

Remuzzi, G., Benigni, A., and Remuzzi, A. 2006. Mechanisms of progression and regression of renal lesions of chronic nephropathies and diabetes. *J Clin Invest* 116:288-296.

Remuzzi, G., and Bertani, T. 1990. Is glomerulosclerosis a consequence of altered glomerular permeability to macromolecules? *Kidney Int* 38:384-394.

Remuzzi, G., Ruggenenti, P., and Perico, N. 2002. Chronic renal diseases: renoprotective benefits of renin-angiotensin system inhibition. *Ann Intern Med* 136:604-615.

Rennke, H.G., and Klein, P.S. 1989. Pathogenesis and significance of nonprimary focal and segmental glomerulosclerosis. *Am J Kidney Dis* 13:443-456.

Reynolds, E.S. 1963. The use of lead citrate at high pH as an electron-opaque stain in electron microscopy. *J Cell Biol* 17:208-212.

Ricardo, S.D., Bertram, J.F., and Ryan, G.B. 1994. Antioxidants protect podocyte foot processes in puromycin aminonucleoside-treated rats. *J Am Soc Nephrol* 4:1974-1986.

Risdon, R.A., Sloper, J.C., and De Wardener, H.E. 1968. Relationship between renal function and histological changes found in renal-biopsy specimens from patients with persistent glomerular nephritis. *Lancet* 2:363-366.

Ritz, E., Mehls, O., Gilli, G., and Heuck, C.C. 1978. Protein restriction in the conservative management of uremia. *Am J Clin Nutr* 31:1703-1711.

Robert, C.P., and Casella, G. 2004. *Monte Carlo Statistical Methods*. New York: Springer-Verlag.

Robinson, L.A., Nataraj, C., Thomas, D.W., Howell, D.N., Griffiths, R., Bautch, V., Patel, D.D., Feng, L., and Coffman, T.M. 2000. A role for fractalkine and its receptor (CX3CR1) in cardiac allograft rejection. *J Immunol* 165:6067-6072.

Robson, M.G., Cook, H.T., Botto, M., Taylor, P.R., Busso, N., Salvi, R., Pusey, C.D., Walport, M.J., and Davies, K.A. 2001. Accelerated nephrotoxic nephritis is exacerbated in C1q-deficient mice. *J Immunol* 166:6820-6828.

Romagnani, P., Beltrame, C., Annunziato, F., Lasagni, L., Luconi, M., Galli, G., Cosmi, L., Maggi, E., Salvadori, M., Pupilli, C., and Serio, M. 1999. Role for interactions between IP-10/Mig and CXCR3 in proliferative glomerulonephritis. *J Am Soc Nephrol* 10:2518-2526.

Romen, W. 1976. [On the pathogenesis of the glomerulosclerosis ultrastructural and autoradiographic investigations on the rat kidney (author's transl)]. *Veroff Pathol*:1-101.

Rouschop, K.M., Claessen, N., Pals, S.T., Weening, J.J., and Florquin, S. 2006. CD44 disruption prevents degeneration of the capillary network in obstructive nephropathy via reduction of TGF-beta1-induced apoptosis. *J Am Soc Nephrol* 17:746-753.

Rouschop, K.M., Sewnath, M.E., Claessen, N., Roelofs, J.J., Hoedemaeker, I., van der Neut, R., Aten, J., Pals, S.T., Weening, J.J., and Florquin, S. 2004. CD44 deficiency increases tubular damage but reduces renal fibrosis in obstructive nephropathy. *J Am Soc Nephrol* 15:674-686.

Rovin, B.H., and Phan, L.T. 1998. Chemotactic factors and renal inflammation. *Am J Kidney Dis* 31:1065-1084.

Rozovsky, I., Morgan, T.E., Willoughby, D.A., Dugichi-Djordjevich, M.M., Pasinetti, G.M., Johnson, S.A., and Finch, C.E. 1994. Selective expression of clusterin (SGP-2) and complement C1qB and C4 during responses to neurotoxins in vivo and in vitro. *Neuroscience* 62:741-758.

Ruan, X.Z., Varghese, Z., Powis, S.H., and Moorhead, J.F. 1999. Human mesangial cells express inducible macrophage scavenger receptor. *Kidney Int* 56:440-451.

Ruiz-Ortega, M., Lorenzo, O., Ruperez, M., Esteban, V., Mezzano, S., and Egido, J. 2001. Renin-angiotensin system and renal damage: emerging data on angiotensin II as a proinflammatory mediator. *Contrib Nephrol*:123-137.

Rumpelt, H.J., and Thoenes, W. 1974. Focal and segmental sclerosing glomerulopathy (-nephritis). *Virchows Arch A Pathol Anat Histol* 362:265-282.

Ruotsalainen, V., Ljungberg, P., Wartiovaara, J., Lenkkeri, U., Kestila, M., Jalanko, H., Holmberg, C., and Tryggvason, K. 1999. Nephrin is specifically located at the slit diaphragm of glomerular podocytes. *Proc Natl Acad Sci U S A* 96:7962-7967.

Sadlier, D.M., Connolly, S.B., Kieran, N.E., Roxburgh, S., Brazil, D.P., Kairaitis, L., Wang, Y., Harris, D.C., Doran, P., and Brady, H.R. 2004. Sequential extracellular matrix-focused and baited-global cluster analysis of serial transcriptomic profiles identifies candidate modulators of renal tubulointerstitial fibrosis in murine adriamycin-induced nephropathy. *J Biol Chem* 279:29670-29680.

Sakaguchi, H., Takeya, M., Suzuki, H., Hakamata, H., Kodama, T., Horiuchi, S., Gordon, S., van der Laan, L.J., Kraal, G., Ishibashi, S., Kitamura, N., and Takahashi, K. 1998. Role of macrophage scavenger receptors in diet-induced atherosclerosis in mice. *Lab Invest* 78:423-434.

Sakai, N., Wada, T., Furuichi, K., Iwata, Y., Yoshimoto, K., Kitagawa, K., Kokubo, S., Kobayashi, M., Hara, A., Yamahana, J., Okumura, T., Takasawa, K., Takeda, S., Yoshimura, M., Kida, H., and Yokoyama, H. 2005. Involvement of extracellular signal-regulated kinase and p38 in human diabetic nephropathy. *Am J Kidney Dis* 45:54-65.

Sanden, S.K., Wiggins, J.E., Goyal, M., Riggs, L.K., and Wiggins, R.C. 2003. Evaluation of a thick and thin section method for estimation of podocyte number, glomerular volume, and glomerular volume per podocyte in rat kidney with Wilms' tumor-1 protein used as a podocyte nuclear marker. *J Am Soc Nephrol* 14:2484-2493.

Santiago-Garcia, J., Kodama, T., and Pitas, R.E. 2003. The class A scavenger receptor binds to proteoglycans and mediates adhesion of macrophages to the extracellular matrix. *J Biol Chem* 278:6942-6946.

Santiago, A., Mori, T., Satriano, J., and Schlondorff, D. 1991. Regulation of Fc receptors for IgG on cultured rat mesangial cells. *Kidney Int* 39:87-94.

Sarwal, M., Chua, M.S., Kambham, N., Hsieh, S.C., Satterwhite, T., Masek, M., and Salvatierra, O., Jr. 2003. Molecular heterogeneity in acute renal allograft rejection identified by DNA microarray profiling. *N Engl J Med* 349:125-138.

Satriano, J.A., Banas, B., Luckow, B., Nelson, P., and Schlondorff, D.O. 1997. Regulation of RANTES and ICAM-1 expression in murine mesangial cells. *J Am Soc Nephrol* 8:596-603.

Satriano, J.A., Shuldiner, M., Hora, K., Xing, Y., Shan, Z., and Schlondorff, D. 1993. Oxygen radicals as second messengers for expression of the monocyte chemoattractant protein, JE/MCP-1, and the monocyte colony-stimulating factor, CSF-1, in response to tumor necrosis factor-alpha and immunoglobulin G. Evidence for involvement of reduced nicotinamide adenine dinucleotide phosphate (NADPH)-dependent oxidase. *J Clin Invest* 92:1564-1571.

Savani, R.C., Cao, G., Pooler, P.M., Zaman, A., Zhou, Z., and DeLisser, H.M. 2001. Differential involvement of the hyaluronan (HA) receptors CD44 and receptor for HA-mediated motility in endothelial cell function and angiogenesis. *J Biol Chem* 276:36770-36778.

Schaefer, L., Meier, K., Hafner, C., Teschner, M., Heidland, A., and Schaefer, R.M. 1996. Protein restriction influences glomerular matrix turnover and tubular hypertrophy by modulation of renal proteinase activities. *Miner Electrolyte Metab* 22:162-167.

Schaefer, R.M., Paczek, L., Huang, S., Teschner, M., Schaefer, L., and Heidland, A. 1992. Role of glomerular proteinases in the evolution of glomerulosclerosis. *Eur J Clin Chem Clin Biochem* 30:641-646.

Schairer, I. 2006. Diabetes-assoziierte Nierenveränderungen bei GIPR[dn]-transgenen Mäusen verschiedener Lebensaltersstufen. Inaugural – Dissertation to achieve the doctor title of veterinary medicine at the Faculty of Veterinary Medicine of the Ludwig-Maximilians-University, Munich.1-107.

Schena, M., Shalon, D., Davis, R.W., and Brown, P.O. 1995. Quantitative monitoring of gene expression patterns with a complementary DNA microarray. *Science* 270:467-470.

Schieppati, A., and Remuzzi, G. 2005. Chronic renal diseases as a public health problem: epidemiology, social, and economic implications. *Kidney Int Suppl*:S7-S10.

Schlegel, A., Volonte, D., Engelman, J.A., Galbiati, F., Mehta, P., Zhang, X.L., Scherer, P.E., and Lisanti, M.P. 1998. Crowded little caves: structure and function of caveolae. *Cell Signal* 10:457-463.

Schlondorff, D. 1987. The glomerular mesangial cell: an expanding role for a specialized pericyte. *Faseb J* 1:272-281.

Schlondorff, D. 1993. Cellular mechanisms of lipid injury in the glomerulus. *Am J Kidney Dis* 22:72-82.

Schlondorff, D. 1995. The role of chemokines in the initiation and progression of renal disease. *Kidney Int Suppl* 49:S44-47.

Schlondorff, D., and Mori, T. 1990. Contributions of mesangial cells to glomerular immune functions. *Klin Wochenschr* 68:1138-1144.

Schlondorff, D., Satriano, J.A., Hagege, J., Perez, J., and Baud, L. 1984. Effect of platelet-activating factor and serum-treated zymosan on prostaglandin E2 synthesis, arachidonic acid release, and contraction of cultured rat mesangial cells. *J Clin Invest* 73:1227-1231.

Schlondorff, D., Singhal, P., Hassid, A., Satriano, J.A., and DeCandido, S. 1989. Relationship of GTP-binding proteins, phospholipase C, and PGE2 synthesis in rat glomerular mesangial cells. *Am J Physiol* 256:F171-178.

Schmid, H., Boucherot, A., Yasuda, Y., Henger, A., Brunner, B., Eichinger, F., Nitsche, A., Kiss, E., Bleich, M., Grone, H.J., Nelson, P.J., Schlondorff, D., Cohen, C.D., and Kretzler, M. 2006. Modular activation of nuclear factor-kappaB transcriptional programs in human diabetic nephropathy. *Diabetes* 55:2993-3003.

Schmid, H., Cohen, C.D., Henger, A., Irrgang, S., Schlondorff, D., and Kretzler, M. 2003. Validation of endogenous controls for gene expression analysis in microdissected human renal biopsies. *Kidney Int* 64:356-360.

Schmid, H., Cohen, C.D., Henger, A., Schlondorff, D., and Kretzler, M. 2004. Gene expression analysis in renal biopsies. *Nephrol Dial Transplant* 19:1347-1351.

Schmid, H., Henger, A., Cohen, C.D., Frach, K., Grone, H.J., Schlondorff, D., and Kretzler, M. 2003. Gene expression profiles of podocyte-associated molecules as diagnostic markers in acquired proteinuric diseases. *J Am Soc Nephrol* 14:2958-2966.

Schmid, H., Henger, A., and Kretzler, M. 2006. Molecular approaches to chronic kidney disease. *Curr Opin Nephrol Hypertens* 15:123-129.

Schmid, H., Nitschko, H., Gerth, J., Kliem, V., Henger, A., Cohen, C.D., Schlondorff, D., Grone, H.J., and Kretzler, M. 2005. Polyomavirus DNA and RNA detection in renal allograft biopsies: results from a European multicenter study. *Transplantation* 80:600-604.

Schrijvers, B.F., De Vriese, A.S., and Flyvbjerg, A. 2004. From hyperglycemia to diabetic kidney disease: the role of metabolic, hemodynamic, intracellular factors and growth factors/cytokines. *Endocr Rev* 25:971-1010.

Schroppel, B., Huber, S., Horster, M., Schlondorff, D., and Kretzler, M. 1998. Analysis of mouse glomerular podocyte mRNA by single-cell reverse transcription-polymerase chain reaction. *Kidney Int* 53:119-124.

Schwartz, M.M., and Bidani, A.K. 1993. Comparison of glomerular injury in juvenile versus mature rats in a remnant kidney model. *J Lab Clin Med* 121:348-355.

Schwartz, M.M., Bidani, A.K., and Lewis, E.J. 1987. Glomerular epithelial cell function and pathology following extreme ablation of renal mass. *Am J Pathol* 126:315-324.

Schwartz, M.M., and Lewis, E.J. 1985. Focal segmental glomerular sclerosis: the cellular lesion. *Kidney Int* 28:968-974.

Schwarz, M., Radeke, H.H., Resch, K., and Uciechowski, P. 1997. Lymphocyte-derived cytokines induce sequential expression of monocyte- and T cell-specific chemokines in human mesangial cells. *Kidney Int* 52:1521-1531.

Scott, M.G., Pierotti, V., Storez, H., Lindberg, E., Thuret, A., Muntaner, O., Labbe-Jullie, C., Pitcher, J.A., and Marullo, S. 2006. Cooperative regulation of extracellular signal-regulated kinase activation and cell shape change by filamin A and beta-arrestins. *Mol Cell Biol* 26:3432-3445.

Screaton, G.R., Bell, M.V., Jackson, D.G., Cornelis, F.B., Gerth, U., and Bell, J.I. 1992. Genomic structure of DNA encoding the lymphocyte homing receptor CD44 reveals at least 12 alternatively spliced exons. *Proc Natl Acad Sci U S A* 89:12160-12164.

Seaquist, E.R., Goetz, F.C., Rich, S., and Barbosa, J. 1989. Familial clustering of diabetic kidney disease. Evidence for genetic susceptibility to diabetic nephropathy. *N Engl J Med* 320:1161-1165.

Sedor, J.R., Carey, S.W., and Emancipator, S.N. 1987. Immune complexes bind to cultured rat glomerular mesangial cells to stimulate superoxide release. Evidence for an Fc receptor. *J Immunol* 138:3751-3757.

Seefeldt, T., Bohman, S.O., Jorgen, H., Gundersen, H.J., Maunsbach, A.B., Petersen, V.P., and Olsen, S. 1981. Quantitative relationship between glomerular foot process width and proteinuria in glomerulonephritis. *Lab Invest* 44:541-546.

Segerer, S., Henger, A., Schmid, H., Kretzler, M., Draganovici, D., Brandt, U., Noessner, E., Nelson, P.J., Kerjaschki, D., Schlondorff, D., and Regele, H. 2006. Expression of the chemokine receptor CXCR1 in human glomerular diseases. *Kidney Int* 69:1765-1773.

Segerer, S., Hughes, E., Hudkins, K.L., Mack, M., Goodpaster, T., and Alpers, C.E. 2002. Expression of the fractalkine receptor (CX3CR1) in human kidney diseases. *Kidney Int* 62:488-495.

Segerer, S., Nelson, P.J., and Schlondorff, D. 2000. Chemokines, chemokine receptors, and renal disease: from basic science to pathophysiologic and therapeutic studies. *J Am Soc Nephrol* 11:152-176.

Sever, S., Altintas, M.M., Nankoe, S.R., Moller, C.C., Ko, D., Wei, C., Henderson, J., del Re, E.C., Hsing, L., Erickson, A., Cohen, C.D., Kretzler, M., Kerjaschki, D., Rudensky, A., Nikolic, B., and Reiser, J. 2007. Proteolytic processing of dynamin by cytoplasmic cathepsin L is a mechanism for proteinuric kidney disease. *J Clin Invest* 117:2095-2104.

Seyer-Hansen, K., Hansen, J., and Gundersen, H.J. 1980. Renal hypertrophy in experimental diabetes. A morphometric study. *Diabetologia* 18:501-505.

Shah, S.V. 1988. Evidence suggesting a role for hydroxyl radical in passive Heymann nephritis in rats. *Am J Physiol* 254:F337-344.

Shahan, K., Denaro, M., Gilmartin, M., Shi, Y., and Derman, E. 1987. Expression of six mouse major urinary protein genes in the mammary, parotid, sublingual, submaxillary, and lachrymal glands and in the liver. *Mol Cell Biol* 7:1947-1954.

Shankland, S.J. 2006. The podocyte's response to injury: role in proteinuria and glomerulosclerosis. *Kidney Int* 69:2131-2147.

Shankland, S.J., Pippin, J., Pichler, R.H., Gordon, K.L., Friedman, S., Gold, L.I., Johnson, R.J., and Couser, W.G. 1996. Differential expression of transforming growth factor-beta isoforms and receptors in experimental membranous nephropathy. *Kidney Int* 50:116-124.

Sharma, M., Sharma, R., McCarthy, E.T., and Savin, V.J. 1999. "The FSGS factor:" enrichment and in vivo effect of activity from focal segmental glomerulosclerosis plasma. *J Am Soc Nephrol* 10:552-561.

Shimamura, T., and Morrison, A.B. 1975. A progressive glomerulosclerosis occurring in partial five-sixths nephrectomized rats. *Am J Pathol* 79:95-106.

Shirato, I. 2002. Podocyte process effacement in vivo. *Microsc Res Tech* 57:241-246.

Shirato, I., Sakai, T., Kimura, K., Tomino, Y., and Kriz, W. 1996. Cytoskeletal changes in podocytes associated with foot process effacement in Masugi nephritis. *Am J Pathol* 148:1283-1296.

Shumway, J.T., and Gambert, S.R. 2002. Diabetic nephropathy-pathophysiology and management. *Int Urol Nephrol* 34:257-264.

Singhal, P.C., Santiago, A., Satriano, J., Hays, R.M., and Schlondorff, D. 1990. Effects of vasoactive agents on uptake of immunoglobulin G complexes by mesangial cells. *Am J Physiol* 258:F589-596.

Sitek, B., Potthoff, S., Schulenborg, T., Stegbauer, J., Vinke, T., Rump, L.C., Meyer, H.E., Vonend, O., and Stuhler, K. 2006. Novel approaches to analyse glomerular proteins from smallest scale murine and human samples using DIGE saturation labelling. *Proteomics* 6:4337-4345.

Skalli, O., and Gabbiani, G. 1988. The biology of myofibroblasts: relationships to wound contraction and fibrocontractive diseases. In *The Molecular and Cellular Biology of Wound Repair*. R.M.F. Clarck, and P.M. Henson, editors. New York: Plenum Publishing Corp. 373-402.

Spielman, L., Winger, D., Ho, L., Aisen, P.S., Shohami, E., and Pasinetti, G.M. 2002. Induction of the complement component C1qB in brain of transgenic mice with neuronal overexpression of human cyclooxygenase-2. *Acta Neuropathol (Berl)* 103:157-162.

Spiro, R.G. 1967. Studies on the renal glomerular basement membrane. Preparation and chemical composition. *J Biol Chem* 242:1915-1922.

Stahlhut, M., and van Deurs, B. 2000. Identification of filamin as a novel ligand for caveolin-1: evidence for the organization of caveolin-1-associated membrane domains by the actin cytoskeleton. *Mol Biol Cell* 11:325-337.

Steffes, M.W., Brown, D.M., and Mauer, S.M. 1978. Diabetic glomerulopathy following unilateral nephrectomy in the rat. *Diabetes* 27:35-41.

Steffes, M.W., Schmidt, D., McCrery, R., and Basgen, J.M. 2001. Glomerular cell number in normal subjects and in type 1 diabetic patients. *Kidney Int* 59:2104-2113.

Steg, A., Wang, W., Blanquicett, C., Grunda, J.M., Eltoum, I.A., Wang, K., Buchsbaum, D.J., Vickers, S.M., Russo, S., Diasio, R.B., Frost, A.R., LoBuglio, A.F., Grizzle, W.E., and Johnson, M.R. 2006. Multiple gene expression analyses in paraffin-embedded tissues by TaqMan low-density array: Application to hedgehog and Wnt pathway analysis in ovarian endometrioid adenocarcinoma. *J Mol Diagn* 8:76-83.

Stephanz, G.B., Gwinner, W., Cannon, J.K., Tisher, C.C., and Nick, H.S. 1996. Heat-aggregated IgG and interleukin-1-beta stimulate manganese superoxide dismutase in mesangial cells. *Exp Nephrol* 4:151-158.

Sterio, D.C. 1984. The unbiased estimation of number and sizes of arbitrary particles using the disector. *J Microsc* 134:127-136.

Stierle, H.E., Oser, B., and Boesken, W.H. 1990. Improved classification of proteinuria by semiautomated ultrathin SDS polyacrylamide gel electrophoresis. *Clin Nephrol* 33:168-173.

Stossel, T.P., Condeelis, J., Cooley, L., Hartwig, J.H., Noegel, A., Schleicher, M., and Shapiro, S.S. 2001. Filamins as integrators of cell mechanics and signalling. *Nat Rev Mol Cell Biol* 2:138-145.

Striker, G.E., and Striker, L.J. 1985. Glomerular cell culture. *Lab Invest* 53:122-131.

Susztak, K., Bottinger, E., Novetsky, A., Liang, D., Zhu, Y., Ciccone, E., Wu, D., Dunn, S., McCue, P., and Sharma, K. 2004. Molecular profiling of diabetic mouse kidney reveals novel genes linked to glomerular disease. *Diabetes* 53:784-794.

Suto, J., Matsuura, S., Imamura, K., Yamanaka, H., and Sekikawa, K. 1998. Genetic analysis of non-insulin-dependent diabetes mellitus in KK and KK-Ay mice. *Eur J Endocrinol* 139:654-661.

Suzuki, D., Miyazaki, M., Jinde, K., Koji, T., Yagame, M., Endoh, M., Nomoto, Y., and Sakai, H. 1997. In situ hybridization studies of matrix metalloproteinase-3, tissue inhibitor of metalloproteinase-1 and type IV collagen in diabetic nephropathy. *Kidney Int* 52:111-119.

Suzuki, D., Miyazaki, M., Naka, R., Koji, T., Yagame, M., Jinde, K., Endoh, M., Nomoto, Y., and Sakai, H. 1995. In situ hybridization of interleukin 6 in diabetic nephropathy. *Diabetes* 44:1233-1238.

Suzuki, Y., Gomez-Guerrero, C., Shirato, I., Lopez-Franco, O., Gallego-Delgado, J., Sanjuan, G., Lazaro, A., Hernandez-Vargas, P., Okumura, K., Tomino, Y., Ra, C., and Egido, J. 2003. Pre-existing glomerular immune complexes induce polymorphonuclear cell recruitment through an Fc receptor-dependent respiratory burst: potential role in the perpetuation of immune nephritis. *J Immunol* 170:3243-3253.

Suzuki, Y.J., Forman, H.J., and Sevanian, A. 1997. Oxidants as stimulators of signal transduction. *Free Radic Biol Med* 22:269-285.

Takahashi, M., Rhodes, D.R., Furge, K.A., Kanayama, H., Kagawa, S., Haab, B.B., and Teh, B.T. 2001. Gene expression profiling of clear cell renal cell carcinoma: gene identification and prognostic classification. *Proc Natl Acad Sci U S A* 98:9754-9759.

Takemoto, M., Asker, N., Gerhardt, H., Lundkvist, A., Johansson, B.R., Saito, Y., and Betsholtz, C. 2002. A new method for large scale isolation of kidney glomeruli from mice. *Am J Pathol* 161:799-805.

Takemoto, M., He, L., Norlin, J., Patrakka, J., Xiao, Z., Petrova, T., Bondjers, C., Asp, J., Wallgard, E., Sun, Y., Samuelsson, T., Mostad, P., Lundin, S., Miura, N., Sado, Y., Alitalo, K., Quaggin, S.E., Tryggvason, K., and Betsholtz, C. 2006. Large-scale identification of genes implicated in kidney glomerulus development and function. *Embo J* 25:1160-1174.

Tan, N.S., Shaw, N.S., Vinckenbosch, N., Liu, P., Yasmin, R., Desvergne, B., Wahli, W., and Noy, N. 2002. Selective cooperation between fatty acid binding proteins and peroxisome proliferator-activated receptors in regulating transcription. *Mol Cell Biol* 22:5114-5127.

Tarnow, L., Rossing, P., Nielsen, F.S., Fagerudd, J.A., Poirier, O., and Parving, H.H. 2000. Cardiovascular morbidity and early mortality cluster in parents of type 1 diabetic patients with diabetic nephropathy. *Diabetes Care* 23:30-33.

Tarzi, R.M., and Cook, H.T. 2003. Role of Fcgamma receptors in glomerulonephritis. *Nephron Exp Nephrol* 95:e7-12.

Teder, P., Vandivier, R.W., Jiang, D., Liang, J., Cohn, L., Pure, E., Henson, P.M., and Noble, P.W. 2002. Resolution of lung inflammation by CD44. *Science* 296:155-158.

Teschner, M., Schaefer, R.M., Paczek, L., and Heidland, A. 1992. Effect of renal disease on glomerular proteinases. *Miner Electrolyte Metab* 18:92-96.

Togawa, A., Miyoshi, J., Ishizaki, H., Tanaka, M., Takakura, A., Nishioka, H., Yoshida, H., Doi, T., Mizoguchi, A., Matsuura, N., Niho, Y., Nishimune, Y., Nishikawa, S., and Takai, Y. 1999. Progressive impairment of kidneys and reproductive organs in mice lacking Rho GDIalpha. *Oncogene* 18:5373-5380.

Tomokiyo, R., Jinnouchi, K., Honda, M., Wada, Y., Hanada, N., Hiraoka, T., Suzuki, H., Kodama, T., Takahashi, K., and Takeya, M. 2002. Production, characterization, and interspecies reactivities of monoclonal antibodies against human class A macrophage scavenger receptors. *Atherosclerosis* 161:123-132.

Tong, N., Perry, S.W., Zhang, Q., James, H.J., Guo, H., Brooks, A., Bal, H., Kinnear, S.A., Fine, S., Epstein, L.G., Dairaghi, D., Schall, T.J., Gendelman, H.E., Dewhurst, S., Sharer, L.R., and Gelbard, H.A. 2000. Neuronal fractalkine expression in HIV-1 encephalitis: roles for macrophage recruitment and neuroprotection in the central nervous system. *J Immunol* 164:1333-1339.

Toyoda, M., Suzuki, D., Honma, M., Uehara, G., Sakai, T., Umezono, T., and Sakai, H. 2004. High expression of PKC-MAPK pathway mRNAs correlates with glomerular lesions in human diabetic nephropathy. *Kidney Int* 66:1107-1114.

Trumper, A., Trumper, K., Trusheim, H., Arnold, R., Goke, B., and Horsch, D. 2001. Glucose-dependent insulinotropic polypeptide is a growth factor for beta (INS-1) cells by pleiotropic signaling. *Mol Endocrinol* 15:1559-1570.

Trumper, K., Trumper, A., Trusheim, H., Arnold, R., Goke, B., and Horsch, D. 2000. Integrative mitogenic role of protein kinase B/Akt in beta-cells. *Ann N Y Acad Sci* 921:242-250.

Tryggvason, K., and Wartiovaara, J. 2005. How does the kidney filter plasma? *Physiology (Bethesda)* 20:96-101.

Tseng, C.C., and Zhang, X.Y. 1998. Role of regulator of G protein signaling in desensitization of the glucose-dependent insulinotropic peptide receptor. *Endocrinology* 139:4470-4475.

Turnberg, D., Lewis, M., Moss, J., Xu, Y., Botto, M., and Cook, H.T. 2006. Complement activation contributes to both glomerular and tubulointerstitial damage in adriamycin nephropathy in mice. *J Immunol* 177:4094-4102.

Turney, J.H., Davison, A.M., Forbes, M.A., and Cooper, E.H. 1991. Hyaluronic acid in end-stage renal failure treated by haemodialysis: clinical correlates and implications. *Nephrol Dial Transplant* 6:566-570.

Tusher, V.G., Tibshirani, R., and Chu, G. 2001. Significance analysis of microarrays applied to the ionizing radiation response. *Proc Natl Acad Sci U S A* 98:5116-5121.

Usdin, T.B., Mezey, E., Button, D.C., Brownstein, M.J., and Bonner, T.I. 1993. Gastric inhibitory polypeptide receptor, a member of the secretin-vasoactive intestinal peptide receptor family, is widely distributed in peripheral organs and the brain. *Endocrinology* 133:2861-2870.

USRDS. 2004. U.S. Renal Data System, USRDS 2004 Annual Data Report: Atlas of End-Stage Renal Disease in the United States,National Institutes of Health, National Institute of Diabetes and Digestive and Kidney Diseases, Bethesda, MD.

Valeri, A., Barisoni, L., Appel, G.B., Seigle, R., and D'Agati, V. 1996. Idiopathic collapsing focal segmental glomerulosclerosis: a clinicopathologic study. *Kidney Int* 50:1734-1746.

van den Dobbelsteen, M.E., van der Woude, F.J., Schroeijers, W.E., Klar-Mohamad, N., van Es, L.A., and Daha, M.R. 1993. C1Q, a subunit of the first component of complement, enhances the binding of aggregated IgG to rat renal mesangial cells. *J Immunol* 151:4315-4324.

van den Dobbelsteen, M.E., van der Woude, F.J., Schroeijers, W.E., Klar-Mohamad, N., van Es, L.A., and Daha, M.R. 1996. Both IgG- and C1q-receptors play a role in the enhanced binding of IgG complexes to human mesangial cells. *J Am Soc Nephrol* 7:573-581.

van Goor, H., Fidler, V., Weening, J.J., and Grond, J. 1991. Determinants of focal and segmental glomerulosclerosis in the rat after renal ablation. Evidence for involvement of macrophages and lipids. *Lab Invest* 64:754-765.

Van Vliet, A., Baelde, H.J., Vleming, L.J., de Heer, E., and Bruijn, J.A. 2001. Distribution of fibronectin isoforms in human renal disease. *J Pathol* 193:256-262.

Vattimo Mde, F., and Santos, O.F. 2005. Functional interface between cathepsins and growth factors in the kidney development. *Ren Fail* 27:615-622.

Vega-Warner, V., Ransom, R.F., Vincent, A.M., Brosius, F.C., and Smoyer, W.E. 2004. Induction of antioxidant enzymes in murine podocytes precedes injury by puromycin aminonucleoside. *Kidney Int* 66:1881-1889.

Veis, J.H. 1993. An overview of mesangial cell biology. *Contrib Nephrol* 104:115-126.

Velling, T., Risteli, J., Wennerberg, K., Mosher, D.F., and Johansson, S. 2002. Polymerization of type I and III collagens is dependent on fibronectin and enhanced by integrins alpha 11beta 1 and alpha 2beta 1. *J Biol Chem* 277:37377-37381.

Venkatachalam, M.A., and Kriz, W. 1992. Anatomy. In *Pathology of the Kidney*. R.H. Heptinstall, editor. Boston/Toronto/London: Little, Brown and Company. 1-92.

Volz, A. 1997. Klonierung und funktionelle Charakterisierung des humanen GIP-Rezeptors. Inaugural – Dissertation to achieve the doctor title of biology at the University of Marburg. 1-159.

Wada, J., Zhang, H., Tsuchiyama, Y., Hiragushi, K., Hida, K., Shikata, K., Kanwar, Y.S., and Makino, H. 2001. Gene expression profile in streptozotocin-induced diabetic mice kidneys undergoing glomerulosclerosis. *Kidney Int* 59:1363-1373.

Waldherr, R., and Derks, H. 1989. [Clinical pathology of the glomerulus--from phenomenon to entity. Focal sclerosis]. *Verh Dtsch Ges Pathol* 73:71-82.

Wang, A., and Hascall, V.C. 2004. Hyaluronan structures synthesized by rat mesangial cells in response to hyperglycemia induce monocyte adhesion. *J Biol Chem* 279:10279-10285.

Wang, Y., Zhao, M.H., Zhang, Y.K., Li, X.M., and Wang, H.Y. 2004. Binding capacity and pathophysiological effects of IgA1 from patients with IgA nephropathy on human glomerular mesangial cells. *Clin Exp Immunol* 136:168-175.

Wanke, R. 1996. Zur Morpho- und Pathogenese der progressiven Glomerulosklerose. Ludwig-Maximilians-Universität München. 1-257.

Wanke, R., Hermanns, W., Folger, S., Wolf, E., and Brem, G. 1991. Accelerated growth and visceral lesions in transgenic mice expressing foreign genes of the growth hormone family: an overview. *Pediatr Nephrol* 5:513-521.

Wanke, R., Kahnt, E., Weis, S., Wolf, E., Brem, G., and Hermanns, W. 1993. Pathological and quantitative morphological changes in the kidney of mice transgenic for growth hormone. *Exp Clin Endocrinol* 101:115.

Wanke, R., Milz, S., Rieger, N., Ogiolda, L., Renner-Muller, I., Brem, G., Hermanns, W., and Wolf, E. 1999. Overgrowth of skin in growth hormone transgenic mice depends on the presence of male gonads. *J Invest Dermatol* 113:967-971.

Wanke, R., Wolf, E., Brem, G., and Hermanns, W. 1996. Physiology and pathology of growth-studies in GH transgenic mice. *J Anim Breed Genet* 113:445-456.

Wanke, R., Wolf, E., Brem, G., and Hermanns, W. 2001. [Role of podocyte damage in the pathogenesis of glomerulosclerosis and tubulointerstitial lesions: findings in the growth hormone transgenic mouse model of progressive nephropathy]. *Verh Dtsch Ges Pathol* 85:250-256.

Wanke, R., Wolf, E., Hermanns, W., Folger, S., Buchmuller, T., and Brem, G. 1992. The GH-transgenic mouse as an experimental model for growth research: clinical and pathological studies. *Horm Res* 37 Suppl 3:74-87.

Wartiovaara, J., Ofverstedt, L.G., Khoshnoodi, J., Zhang, J., Makela, E., Sandin, S., Ruotsalainen, V., Cheng, R.H., Jalanko, H., Skoglund, U., and Tryggvason, K. 2004. Nephrin strands contribute to a porous slit diaphragm scaffold as revealed by electron tomography. *J Clin Invest* 114:1475-1483.

Weber, G.F., Ashkar, S., Glimcher, M.J., and Cantor, H. 1996. Receptor-ligand interaction between CD44 and osteopontin (Eta-1). *Science* 271:509-512.

Wehbi, G.J., Zimpelmann, J., Carey, R.M., Levine, D.Z., and Burns, K.D. 2001. Early streptozotocin-diabetes mellitus downregulates rat kidney AT2 receptors. *Am J Physiol Renal Physiol* 280:F254-265.

Weibel, E.R. 1979. *Stereological methods. I. Practical methods for biologicalmorphometry. Academic Press, London.*

Weibel, E.R. 1980. *Stereological Methods II. Theoretical foundations*. London: Academic press

Weibel, E.R., and Gomez, D.M. 1962. A principle for counting tissue structures on random sections. *J Appl Physiol* 17:343-348.

Weisiger, R.A. 2002. Cytosolic fatty acid binding proteins catalyze two distinct steps in intracellular transport of their ligands. *Mol Cell Biochem* 239:35-43.

Wenzel, U.O., and Abboud, H.E. 1995. Chemokines and renal disease. *Am J Kidney Dis* 26:982-994.

Wharram, B.L., Goyal, M., Wiggins, J.E., Sanden, S.K., Hussain, S., Filipiak, W.E., Saunders, T.L., Dysko, R.C., Kohno, K., Holzman, L.B., and Wiggins, R.C. 2005. Podocyte depletion causes glomerulosclerosis: diphtheria toxin-induced podocyte depletion in rats expressing human diphtheria toxin receptor transgene. *J Am Soc Nephrol* 16:2941-2952.

White, K.E., Bilous, R.W., Marshall, S.M., El Nahas, M., Remuzzi, G., Piras, G., De Cosmo, S., and Viberti, G. 2002. Podocyte number in normotensive type 1 diabetic patients with albuminuria. *Diabetes* 51:3083-3089.

White, S.L., Cass, A., Atkins, R.C., and Chadban, S.J. 2005. Chronic kidney disease in the general population. *Adv Chronic Kidney Dis* 12:5-13.

Wiggins, J.E., Goyal, M., Sanden, S.K., Wharram, B.L., Shedden, K.A., Misek, D.E., Kuick, R.D., and Wiggins, R.C. 2005. Podocyte hypertrophy, "adaptation," and "decompensation" associated with glomerular enlargement and glomerulosclerosis in the aging rat: prevention by calorie restriction. *J Am Soc Nephrol* 16:2953-2966.

Wiggins, R.C. 2007. The spectrum of podocytopathies: a unifying view of glomerular diseases. *Kidney Int* 71:1205-1214.

Wild, S., Roglic, G., Green, A., Sicree, R., and King, H. 2004. Global prevalence of diabetes: estimates for the year 2000 and projections for 2030. *Diabetes Care* 27:1047-1053.

Wolf, E., Kahnt, E., Ehrlein, J., Hermanns, W., Brem, G., and Wanke, R. 1993. Effects of long-term elevated serum levels of growth hormone on life expectancy of mice: lessons from transgenic animal models. *Mech Ageing Dev* 68:71-87.

Wolf, E., and Wanke, R. 1997. Growth hormone overproduction in transgenic mice: Phenotypic alterations and deduced animal models. In *Welfare aspects of transgenic animals*. L.F.M. van Zutphen, and M. van der Meer, editors. Berlin: Springer Verlag.

Wolf, G., Aberle, S., Thaiss, F., Nelson, P.J., Krensky, A.M., Neilson, E.G., and Stahl, R.A. 1993. TNF alpha induces expression of the chemoattractant cytokine RANTES in cultured mouse mesangial cells. *Kidney Int* 44:795-804.

Wolf, G., Chen, S., and Ziyadeh, F.N. 2005. From the periphery of the glomerular capillary wall toward the center of disease: podocyte injury comes of age in diabetic nephropathy. *Diabetes* 54:1626-1634.

Wolf, G., and Ziyadeh, F.N. 2007. Cellular and molecular mechanisms of proteinuria in diabetic nephropathy. *Nephron Physiol* 106:p26-31.

Wu, X., Dolecki, G.J., and Lefkowith, J.B. 1995. GRO chemokines: a transduction, integration, and amplification mechanism in acute renal inflammation. *Am J Physiol* 269:F248-256.

Wuthrich, R.P. 1992. Vascular cell adhesion molecule-1 (VCAM-1) expression in murine lupus nephritis. *Kidney Int* 42:903-914.

Wuthrich, R.P. 1999. The proinflammatory role of hyaluronan-CD44 interactions in renal injury. *Nephrol Dial Transplant* 14:2554-2556.

Yamada, K., Kurosawa, T., Okamoto, M., Yue, B.F., Mizuno, S., and Naiki, M. 1994. [Pathogenesis of spontaneous nephrosis in mice--urinary protein in nephrotic mice]. *Jikken Dobutsu* 43:527-534.

Yamamoto, Y., Kato, I., Doi, T., Yonekura, H., Ohashi, S., Takeuchi, M., Watanabe, T., Yamagishi, S., Sakurai, S., Takasawa, S., Okamoto, H., and Yamamoto, H. 2001. Development and prevention of advanced diabetic nephropathy in RAGE-overexpressing mice. *J Clin Invest* 108:261-268.

Yang, B., Hall, C.L., Yang, B.L., Savani, R.C., and Turley, E.A. 1994. Identification of a novel heparin binding domain in RHAMM and evidence that it modifies HA mediated locomotion of ras-transformed cells. *J Cell Biochem* 56:455-468.

Yang, H.C., Ma, L.J., Ma, J., and Fogo, A.B. 2006. Peroxisome proliferator-activated receptor-gamma agonist is protective in podocyte injury-associated sclerosis. *Kidney Int* 69:1756-1764.

Yano, N., Endoh, M., Fadden, K., Yamashita, H., Kane, A., Sakai, H., and Rifai, A. 2000. Comprehensive gene expression profile of the adult human renal cortex: analysis by cDNA array hybridization. *Kidney Int* 57:1452-1459.

Yasuda, Y., Boucherot, A., Schmid, H., Eichinger, F., Henger, A., and Cohen, C.D. 2005. Conserved expression signatures in murine and human
disease imply a shared transcriptome regulated in renal failure. *Nephron News* 09/05:110.

Yasuda, Y., Cohen, C.D., Henger, A., and Kretzler, M. 2006. Gene expression profiling analysis in nephrology: towards molecular definition of renal disease. *Clin Exp Nephrol* 10:91-98.

Yevdokimova, N., Wahab, N.A., and Mason, R.M. 2001. Thrombospondin-1 is the key activator of TGF-beta1 in human mesangial cells exposed to high glucose. *J Am Soc Nephrol* 12:703-712.

Yevdokimova, N.Y. 2006. Elevated level of ambient glucose stimulates the synthesis of high-molecular-weight hyaluronic acid by human mesangial cells. The involvement of transforming growth factor beta1 and its activation by thrombospondin-1. *Acta Biochim Pol* 53:383-393.

Yoshida, T., Tang, S.S., Hsiao, L.L., Jensen, R.V., Ingelfinger, J.R., and Gullans, S.R. 2002. Global analysis of gene expression in renal ischemia-reperfusion in the mouse. *Biochem Biophys Res Commun* 291:787-794.

Yoshida, Y., Fogo, A., Shiraga, H., Glick, A.D., and Ichikawa, I. 1988. Serial micropuncture analysis of single nephron function in subtotal renal ablation. *Kidney Int* 33:855-867.

Yoshida, Y., Kawamura, T., Ikoma, M., Fogo, A., and Ichikawa, I. 1989. Effects of antihypertensive drugs on glomerular morphology. *Kidney Int* 36:626-635.

Young, B.A., Maynard, C., and Boyko, E.J. 2003. Racial differences in diabetic nephropathy, cardiovascular disease, and mortality in a national population of veterans. *Diabetes Care* 26:2392-2399.

Yu, Q., and Stamenkovic, I. 2000. Cell surface-localized matrix metalloproteinase-9 proteolytically activates TGF-beta and promotes tumor invasion and angiogenesis. *Genes Dev* 14:163-176.

Yuan, H.T., Suri, C., Yancopoulos, G.D., and Woolf, A.S. 1999. Expression of angiopoietin-1, angiopoietin-2, and the Tie-2 receptor tyrosine kinase during mouse kidney maturation. *J Am Soc Nephrol* 10:1722-1736.

Zatz, R., Meyer, T.W., Rennke, H.G., and Brenner, B.M. 1985. Predominance of hemodynamic rather than metabolic factors in the pathogenesis of diabetic glomerulopathy. *Proc Natl Acad Sci U S A* 82:5963-5967.

Zhao, H.J., Wang, S., Cheng, H., Zhang, M.Z., Takahashi, T., Fogo, A.B., Breyer, M.D., and Harris, R.C. 2006. Endothelial nitric oxide synthase deficiency produces accelerated nephropathy in diabetic mice. *J Am Soc Nephrol* 17:2664-2669.

Zheng, F., Cheng, Q.L., Plati, A.R., Ye, S.Q., Berho, M., Banerjee, A., Potier, M., Jaimes, E.A., Yu, H., Guan, Y.F., Hao, C.M., Striker, L.J., and Striker, G.E. 2004. The glomerulosclerosis of aging in females: contribution of the proinflammatory mesangial cell phenotype to macrophage infiltration. *Am J Pathol* 165:1789-1798.

Zimmerman, A.W., and Veerkamp, J.H. 2002. New insights into the structure and function of fatty acid-binding proteins. *Cell Mol Life Sci* 59:1096-1116.

Zoja, C., Abbate, M., and Remuzzi, G. 2006. Progression of chronic kidney disease: insights from animal models. *Curr Opin Nephrol Hypertens* 15:250-257.

9. Appendix

9.1 Protocol for silver staining of SDS-PAGE gels

Silver stain for SDS-PAGE gels	
1.) **Fixation solution**	60 minutes
99.6 % Ethanol (Roth, Germany)	500 ml
Glacial acetic acid (Sigma, Germany)	120 ml
37% Formaldehyde (Roth, Germany)	0.5 ml
ad 1000 ml distilled water	
2.) **Washing in 50 % Ethanol**	3 x 20 minutes
3.) **Pre-treatment**	1 minute
Sodium thiosulphate (Merck, Germany)	0.05 g
ad 50 ml distilled water	
4.) **Washing in distilled water**	3 x 20 seconds
5.) **Impregnation**	20 minutes
Silver nitrate (Roth, Germany)	0.05 g
37% Formaldehyde (Roth, Germany)	35 µl
ad 50 ml distilled water	
6.) **Washing in distilled water**	2x 20 seconds
7.) **Develop**	until bands become visible
Sodium carbonate (Roth, Germany)	3 g
Sodium thiosulphate (Merck, Germany)	0.2 mg
37% Formaldehyde (Roth, Germany)	50 µl
ad 1000 ml distilled water	
8.) **Washing in distilled water**	20 seconds
9.) **Stop solution**	
0.1 M EDTA (Sigma, Germany)	

9.2 Drying of SDS-PAGE gels

The DryEase^{TM} Mini-Gel Drying System (DryEase Mini-Gel Dryer Frame, DryEase Mini-Gel Drying Base, DryEase Mini Cellophane and Gel-Dry Drying Solution; Novex, Germany) was used for drying polyacrylamid gels. Stained gels were washed in distilled water 3 times for 2 minutes and then equilibrated in Gel-dry Solution for 15-20 minutes on a rotary shaker (Heidolph, Germany). Rough edges of the gel were cutt off, using a razor blade. 2 pieces of cellophane were pre-wetted in Gel-Drying Solution for 15-20 seconds. A DryEase gel drying frame was placed on the gel dryer base and covered with one cellophane piece. The gel was placed in the centre of the cellophane sheet; no air was to be trapped between the gel and the cellophane sheet. The gel was covered with a second layer of pre-wetted cellophane. No air was to be trapped between gel and the cellophane sheets. Wrinkles were removed with a gloved hand. The remaining frame was aligned so that its corner pins fit into the holes on the bottom frame. Plastic clamps were pushed onto the four edges of the frame. The assembly was to stand upright on a benchtop. Gels were dried for 12-36 hours; drafts were avoided. The gel/cellophane sandwich was removed and excess cellophane was trimmed off. Dried gels were pressed between pages of a book for approximately 2 days and then stored in a cassette.

9.3 Preparation of murine albumin standard dilutions (range: 7.8 - 500 ng/ml) for quantification of urine albumin concentrations by ELISA (mouse albumin ELISA-kit Bethyl E90-134, Bethyl, USA)

step	ng/ml	Calibrator	sample diluent
0	10,000	2 µl	9 ml
1	500	0.5 ml from step 0	9.5 ml
2	250	1 ml from step 1	1 ml
3	125	1 ml from step 2	1 ml
4	62.5	1 ml from step 3	1 ml
5	31.25	1 ml from step 4	1 ml
6	15.625	1 ml from step 5	1 ml
7	7.8	1 ml from step 6	1 ml

9.4 Pattern of photography of glomerular peripheral capillary loops (TEM)

Pattern of photography of glomerular peripheral capillary loops (TEM)

☐   **area of view at respective factor of magnification**

📷   **photo**

⬅   **2 x ½ turns of stage handle**
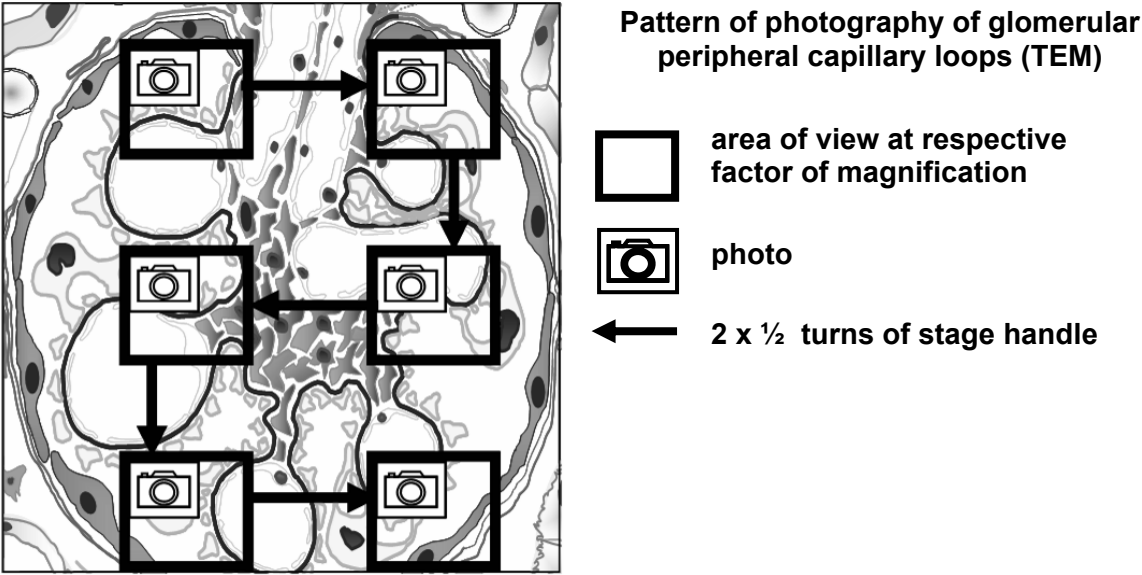
Figure 9.1. Systematic pattern of photography of glomerular peripheral capillary loops in transmission electron microscopy (TEM) for determination of the filtration slit frequency (FSF) and estimation of the thickness of the glomerular basement membrane (GBM).

9.5.1 Dimensions of the logarithmic ruler for measurement of the thickness of the glomerular basement membrane

<div style="border:1px solid black; padding:1em;">

Dimensions of Ruler
(Divisions Equidistant on Log Reciprocal Scale)

Class	Lower Limit, *mm*	1 / Lower Limit, *mm*	Midpoint, *mm*
Class A	2.0000	0.5000	0.4375
Class 1	2.6667	0.3750	0.3281
Class 2	3.5556	0.2813	0.2461
Class 3	4.7407	0.2109	0.1846
Class 4	6.3210	0.1582	0.1384
Class 5	8.4280	0.1187	0.1038
Class 6	11.2373	0.0890	0.0779
Class 7	14.9831	0.0667	0.0584
Class 8	19.9774	0.0501	0.0438
Class 9	26.6366	0.0375	0.0328
Class 10	35.5155	0.0282	0.0246
Class 11	47.3539	0.0211	0.0211

Class A: the initial division in which no measurements of the glomerular basement membrane (GBM) can be contained.
Class 1 – 11: classes of ruler into which measurements are placed.
Lower Limit: begin of next (upper) class of ruler, measured from the origin of the ruler.
Midpoint of Class n:
((1/Lower Limit of Class n) + (1/Lower Limit of Class n+1))/2

</div>

9.5.2 Example for calculation of the true harmonic mean thickness (Th) of the GBM

This example was performed using a pocket calculator. For regular use, a suitably programmed computer "spreadsheet" (e.g. Microsoft®-EXCEL) is more convenient.

Example

	Glomerulus 1				Glomerulus 2			
	N° of Observations	Midpoints	Midpoints x N° of Observations		N° of Observations	Midpoints	Midpoints x N° of Observations	
Class A	0	0.4375	0.4375 x 0	0	0	0.4375	0.4375 x 0	0
Class 1	0	0.3281	0.3281 x 0	0	0	0.3281	0.3281 x 0	0
Class 2	0	0.2461	0.2461 x 0	0	2	0.2461	0.2461 x2	0.4922
Class 3	6	0.1846	0.1846 x 6	1.1074	7	0.1846	0.1846 x 7	1.2920
Class 4	77	0.1384	0.1384 x 77	10.658	82	0.1384	0.1384 x 82	11.351
Class 5	69	0.1038	0.1038 x 69	7.1636	79	0.1038	0.1038 x 79	8.2018
Class 6	15	0.0779	0.0779 x 15	1.1680	22	0.0779	0.0779 x 22	1.7130
Class 7	2	0.0584	0.0584 x 2	0.1168	3	0.0584	0.0584 x 3	0.1752
Class 8	1	0.0438	0.0438 x 1	0.0438	1	0.0438	0.0438 x 1	0.0438
Class 9	0	0.0328	0.0328 x 0	0	0	0.0328	0.0328 x 0	0
Class	0	0.0246	0.0246 x 0	0	0	0.0246	0.0246 x 0	0
Class	0	0.0211	0.0211 x 0	0	0	0.0211	0.0211 x 0	0
Sum of Column	**170**			**20.2586**	**196**			**23.2691**

	Glomerulus 1			Glomerulus 2	
$\overline{\ell}_h$. mm	8.3915		$\overline{\ell}_h$. mm	8.4232	
M	45000		M	45000	
$T_h 1$. nm	158.3		$T_h 2$. nm	158.9	

Mean Th.=(Th1+Th2)/2=(158.3+158.9)/2 =158.6 nm

Calibration:
cross grating : 2160 divisions/ mm
1 cm = 10 mm = 10000 µm = 10.000.000 nm
1 division of cross grating = 1 mm / 2160 divisions per mm = 462.962963 nm
10 divisions of cross grating = 4629.63 nm = 0.000462963 cm
factor of magnification = measured 10 divisions of cross grating in magnified print in cm/0.000462963 cm

10 divisions of cross grating, measured in magnified print, *cm*
} 20.9 cm   (first calibration print, first plane)
  20.8 cm   (first calibration print, 90 ° to first plane)

mean 10 divisions = (20.9 cm + 20.8 cm) / 2 = 20.85 cm
factor of final magnification = 20.85 cm / 0.000462963 cm = 45000
M = 45000

9.6 Preparation of amplified, biotin-labeled cDNA from total RNA for gene expression analysis by Affymetrix GeneChip® arrays, using the Ovation™ Biotin-RNA Amplification and Labeling System (NuGEN Technologies, Inc., USA)

Generation of first strand cDNA: First strand cDNA is prepared from total RNA using a unique first strand DNA/RNA chimeric primer and reverse transcriptase. The primer has a DNA portion that hybridizes to the 5′ portion of the poly A sequence. The resulting cDNA/mRNA hybrid molecule contains a unique RNA sequence at the 5′ end of the cDNA strand. **Generation of a DNA/RNA heteroduplex double strand cDNA:** Fragmentation of the mRNA within the cDNA/mRNA complex creates priming sites for DNA polymerase to synthesize a second strand, which includes DNA complementary to the 5′ unique sequence from the first strand chimeric primer. The result is a double stranded cDNA with a unique DNA/RNA heteroduplex at one end. **SPIA™ amplification:** SPIA™ amplification is a linear isothermal DNA amplification process developed by NuGEN™ (NuGen Inc., USA). It uses a SPIA™ DNA/RNA chimeric primer, DNA polymerase and RNase H in a homogeneous isothermal assay that provides highly efficient amplification of DNA sequences. RNase H is used to degrade RNA in the DNA/RNA heteroduplex at the 5′ end of the first cDNA strand. This results in the exposure of a DNA sequence that is available for binding a second SPIA™ DNA/RNA chimeric primer. DNA polymerase then initiates replication at the 3′ end of the primer, displacing the existing forward strand. The RNA portion at the 5′ end of the newly synthesized strand is again removed by RNase H, exposing part of the unique priming site for initiation of the next round of cDNA synthesis. The process of SPIA™ DNA/RNA primer binding, DNA replication, strand displacement and RNA cleavage is repeated, resulting in rapid accumulation of cDNA with sequence complementary to the original mRNA. The size of the majority of the products produced by the Ribo-SPIA™ amplification process is between 200 bases and 2.0 Kb. **cDNA fragmentation and biotin labeling:** A proprietary two-step process is used to fragment and biotin label the single-stranded cDNA generated during the amplification process. The first step is an enzymatic fragmentation that produces product mostly below 250 bases with an average length ranging from 50-100 bases. The fragmented product is then labeled with biotin.

The procedure is schematically illustrated below.

RNA Amplification and Biotin labeling Processes

First strand synthesis   *Elapsed time*

total RNA

reverse transcriptase

first strand primer

mRNA cDNA duplex

1.5 hours

Second strand synthesis   *DNA polymerase*

double stranded cDNA

0.75 hours

SPIA^{TM} isothermal linear amplification   *RNAse H*

DNA polymerase   3' ◼▬ 5' **SPIA^{TM} primer**

RNAse H

DNA polymerase   3' ◼▬ 5' **SPIA^{TM} primer**

1.25 hours
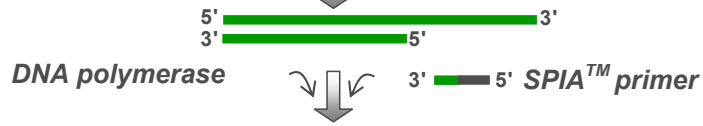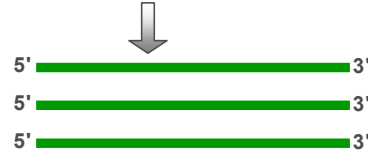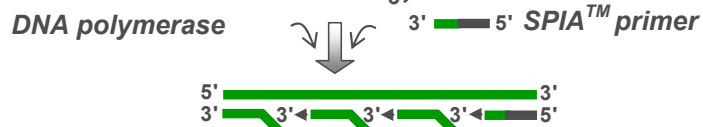
cDNA Fragmentation and labeling   *fragmentation*

biotynilation

*fragmented,
biotin-labeled cDNA*
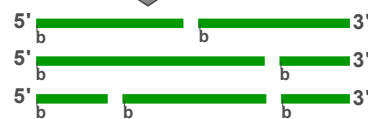
1.0 hours

▬ **RNA**
▬ **cDNA**

9.7 Principle of relative quantification of real-time PCR results using the ΔC_T method (Example)

Figure 9.2

Principle of relative quantification of real-time PCR results using the ΔC_T method

Real-time PCR results for housekeeping- and target-sequences in 8 samples (4 wt and 4 tg)
-samples of groups to be compared (wt vs. tg) are run on identical plates-

A *"housekeeper"*

ΔRn

treshold

no template controls

ⓐ ⓑ ⓒ ⓓ ⓔ

PCR cycle number

B *"target"*

ΔRn

treshold

no template controls

ⓐ ⓑ ⓒ ⓓ ⓔ

PCR cycle number

a: plateau phase, b: linear phase, c: exponential (geometric) phase, d: background, e: baseline; identical threshold lines were manually set in the exponential phase of the amplification.

Calculation of the mean C_T from each of the duplicate measurements of each sample for housekeeping- and target-sequences; e.g. for sample 1 (wt) and sample 2 (tg)

C *"housekeeper"*

ΔRn

sample 1

treshold

sample 2

no template controls

PCR cycle number

C_T (sample 2) = 20
C_T (sample 1) = 15

D *"target"*

ΔRn

sample 1

treshold

sample 2

no template controls

PCR cycle number

C_T (sample 2) = 21
C_T (sample 1) = 19

E **Calculation of ΔC_T for each sample, e.g. for sample 1 (wt) and sample 2 (tg)**

ΔC_T (sample 1) = C_T (housekeeper) - C_T (housekeeper) = 15 - 19 = - 4
ΔC_T (sample 2) = C_T (housekeeper) - C_T (housekeeper) = 20 - 21 = - 1

F **Calculation of $2^{\Delta C_T}$ for each sample, e.g. for sample 1 (wt) and sample 2 (tg)**

$2^{\Delta C_T}$ (sample 1) = 2^{-4} = 0.0625
$2^{\Delta C_T}$ (sample 2) = 2^{-1} = 0.5

G **Group-wise comparison of $2^{\Delta C_T}$ values (wt vs. tg)**

wt-group	tg-group
$2^{\Delta C_T}$ (sample 1) = 0.0625	$2^{\Delta C_T}$ (sample 2) = 0.5
$2^{\Delta C_T}$ (sample 3) = 0.0800	$2^{\Delta C_T}$ (sample 4) = 0.6
$2^{\Delta C_T}$ (sample 5) = 0.0552	$2^{\Delta C_T}$ (sample 6) = 0.4
$2^{\Delta C_T}$ (sample 7) = 0.0652	$2^{\Delta C_T}$ (sample 8) = 0.7
mean = 0,0663	mean = 0,5500
SD = 0.0102	SD = 0.1290

H $2^{\Delta C_T}$

**

wt   tg

Figure 9.2 (page 223): The ΔC_T method for relative quantification of real-time PCR results is demonstrated, using the following (fictitious) example: Expression abundances of a specific target transcript in each 4 RNA samples of two groups (wt and tg), relative to the respective expression of a reference transcript in each sample (housekeeping transcript) are compared. Through reverse transcription of RNA, cDNA samples were obtained. Real-time PCR was performed each for quantitation of the target-, as well as for the housekeeping-transcript, running all samples of the respective groups to be compared on the identical plate. The respective measurements were performed in duplicates, no template controls served as negative references. **A**, **B**: Amplification plots of both real-time PCR runs. Data exhibit the "typical " amplification curves (a-e). ΔRn is the difference between the normalized reporter fluorescence in the sample and in the no template control (NTC) wells. The software generated amplification plot result view displays a plot of ΔRn as a function of cycle number. The C_T (= threshold cycle) is the calculated fractional cycle number at which the PCR product crosses the threshold of detection. The Threshold line is the level of detection at which a reaction reaches a fluorescent intensity above background (d). Identical threshold lines were manually set in the exponential phase (c) of the amplification. **C**, **D**: The mean C_T from each of the duplicate measurements of each sample for housekeeping-(**C**) and target-sequences (**D**) is calculated, as demonstrated for sample 1 (wt) and sample 2 (tg).**E**: ΔC_T value is calculated by subtraction of the mean C_T value of the target transcript from that of the housekeeping gene of the sample. **F**, **G**: The $2^{\text{mean }\Delta C_T}$-value is calculated for each sample in the respective groups. Means and standard deviation (SD) of these values are calculated for each group and compared, using a two sided Students t-test. **H**: graphical presentation of the result of comparison (means and SD; **, $p<0.01$).

9.8 Estimation of statistical enrichment of numbers of commonly differentially expressed genes by performance of Monte Carlo Simulation

Experimentally observed situation

Expected situation by computized simulation of purely randomly conditions (10,000 simulations)

GIPR^{dn} x CD1

glomerulus isolation,
RNA-extraction,
microarray-analysis

bGH x NMRI

wt   tg

wt   tg

expressed glomerular genes
(à 26,000)

group 1

26000

group 2

26000

26000 unique numbers
(1 – 26000) represent the
numbers and ID's of all
expressed glomerular genes

comparison of
expressed glomerular genes
wt vs. tg

numbers of
differentially
regulated genes
wt vs. tg

2600

5200

generation of (n) unique
random numbers in each
group, each ranging from
1-26000

n=2600

n=5200

comparison of ID's of differentially
regulated genes and the respective
direction of regulation (up- or down-
regulation)

comparison of ID's (value) of
the respective random
numbers generated for each
group

620 commonly congeneric differentially
regulated genes GIPR^{dn} vs. bGH

X = number of unique random numbers
(values = ID's), found in both groups of
random numbers in one of 10,000 random
simulations. Arithmetic mean and standard
deviation of these numbers are calculated.

Assuming purely randomly conditions, the population of numbers of commonly differentially regulated genes in this example displays a normal distribution of values with an average of µ=570.74 (=expected value) and a standard deviation of ɕ=20.00. The statistical probability of observing a number of 620 commonly differentially regulated genes (experimentally identified number = observed value $\varkappa$) within this population is calculated and indicated by a p-value and a z-score.

$$f_{(x,\mu,\sigma)} = \frac{1}{\sqrt{2\pi}\sigma} e^{-\left(\frac{(x-\mu)^2}{2\sigma^2}\right)}$$

$$z = \frac{x - \mu}{\sigma}$$

$$p = 1 - f_{(\varkappa;\,\mu;\,\sigma)} = 0.0069 \qquad z = 2.463$$

Distribution of numbers of common random numbers in 10,000 simulations

$f_{n(\varkappa)}$

expected value (µ = 570.74)

observed value
$\varkappa$ = 620

standard deviation
ɕ = 20.00

*number of common random numbers
in 10,000 simulations*
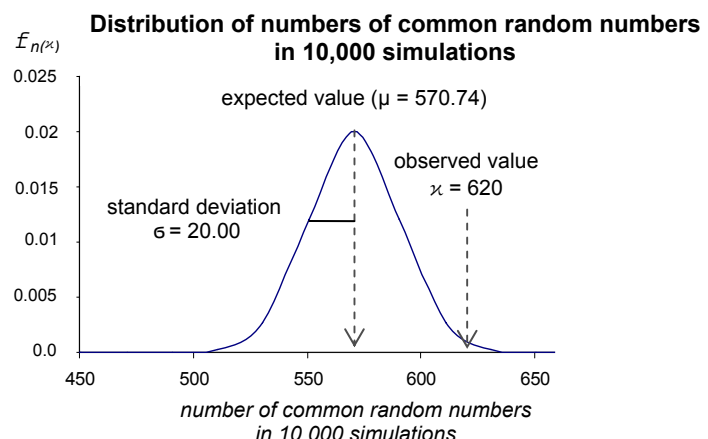
Figure 9.3 (page 225): Illustration of application of a Monte Carlo simulation for estimation of statistical enrichment of numbers of commonly differentially regulated genes in two independent and different sized groups of differentially regulated genes (2600 and 5200, respectively). In the given example, the application of a Monte Carlo simulation confirms, that the experimentally detected number of 620 commonly differentially regulated genes is very unlikely (p= 0.0069) to be just a result of coincidence. The randomly expected number of commonly differentially regulated genes (570.74), and the normal distribution of these values in the given example was estimated by 10,000 random trials, using the numbers indicated (representing the total numbers of expressed glomerular genes and differentially regulated genes).

9.9.1 Commonly differentially expressed genes in stage I (GIPR^{dn} vs. bGH)

Table 9.1 (pages 226-229) : Commonly differentially expressed genes in stage I: [GIPR^{dn} stage I, wt vs. tg] vs. [bGH stage I, wt vs. tg]. Genes displaying a statistically significant (FDR ≤0.045 %) increase or decrease in signal changes relative to controls were identified in both groups of stage I (wt vs. tg), using the ChipInspector 1.2 software, Genomatix$^{®}$, Germany. A number of 86 genes displayed a congeneric differential expression in both groups of stage I. $^{(*)}$ The indicated mean expression ratio logs were calculated as arithmetic means of expression ratio log values (with identical algebraic signs) of the respective differentially expressed genes in the single groups (GIPR^{dn}-group and bGH-group) of stage I of investigation.

Commonly differentially expressed genes in stage I (GIPR^{dn} vs. bGH)

Entrez Gene ID	official symbol	official full name	mean ratio log $^{(*)}$
225642	**Grp**	gastrin releasing peptide	1.38
23792	**Adam23**	a disintegrin and metallopeptidase domain 23 zinc finger and BTB domain	0.94
235320	**Zbtb16**	containing 16	0.87
114332	**Xlkd1**	extra cellular link domain-containing 1	0.85
11770	**Fabp4**	fatty acid binding protein 4, adipocyte	0.67
56760	**Clec1b**	C-type lectin domain family 1, member b	0.65
106068	**Slc45a4**	solute carrier family 45, member 4	0.65
12260	**C1qb**	complement component 1, q subcomponent, beta polypeptide	0.64
60361	**Ms4a4b**	membrane-spanning 4-domains, subfamily A, member 4B	0.59
68922	**Dnaic1**	dynein, axonemal, intermediate chain 1	0.58
65973	**Asph**	aspartate-beta-hydroxylase	0.58
12167	**Bmpr1b**	bone morphogenetic protein receptor, type 1B	0.56
72817	**2810484G07Rik**	RIKEN cDNA 2810484G07 gene	0.53
21384	**Tbx15**	T-box 15	0.53
20312	**Cx3cl1**	chemokine (C-X3-C motif) ligand 1	0.53
20887	**Sult1a1**	sulfotransferase family 1A, phenol-preferring, member 1	0.52
16589	**Uhmk1**	U2AF homology motif (UHM) kinase 1	0.51
70598	**Filip1**	filamin A interacting protein 1	0.50
12983	**Csf2rb1**	colony stimulating factor 2 receptor, beta 1, low-affinity (granulocyte-macrophage)	0.49
268481	**Krt222**	keratin 222	0.49
21956	**Tnnt2**	troponin T2, cardiac	0.49
29809	**Rabgap1l**	RAB GTPase activating protein 1-like	0.48
58860	**Adamdec1**	ADAM-like, decysin 1	0.48
20288	**Msr1**	macrophage scavenger receptor 1	0.46
216233	**Socs2**	suppressor of cytokine signaling 2	0.46
12505	**Cd44**	CD44 antigen	0.46
70065	**1700030G11Rik**	RIKEN cDNA 1700030G11 gene	0.46

Commonly differentially expressed genes in stage I (continued)

Entrez Gene ID	official symbol	official full name	mean ratio log [*]
14406	**Gabrg2**	gamma-aminobutyric acid (GABA-A) receptor, subunit gamma 2	0.45
74446	**4933425K02Rik**	RIKEN cDNA 4933425K02 gene	0.44
14129	**Fcgr1**	Fc receptor, IgG, high affinity I	0.44
18676	**Phf2**	PHD finger protein 2	0.44
13058	**Cybb**	cytochrome b-245, beta polypeptide	0.44
57754	**Cend1**	cell cycle exit and neuronal differentiation 1	0.43
212937	**BC027057**	cDNA sequence BC027057	0.43
56619	**Clec4e**	C-type lectin domain family 4, member e	0.43
11519	**Add2**	adducin 2 (beta)	0.43
110876	**Scn2a1**	sodium channel, voltage-gated, type II, alpha 1	0.43
17916	**Myo1f**	myosin IF	0.43
80890	**Trim2**	neural activity-related ring finger protein; tripartite motif protein TRIM2	0.42
20728	**Spic**	Spi-C transcription factor (Spi-1/PU.1 related)	0.42
70806	**D19Ertd652e**	DNA segment, Chr 19, ERATO Doi 652, expressed	0.42
20975	**Synj2**	synaptojanin 2	0.41
14702	**Gng2**	guanine nucleotide binding protein (G protein), gamma 2 subunit	0.41
13175	**Dcamkl1**	double cortin and calcium/calmodulin-dependent protein kinase-like 1	0.41
14025	**Bcl11a**	B-cell CLL/lymphoma 11A (zinc finger protein)	0.41
216543	**Cep68**	centrosomal protein 68	0.41
75458	**Cklf**	chemokine-like factor	0.41
72832	**Crtac1**	cartilage acidic protein 1	0.40
56809	**Gmeb1**	glucocorticoid modulatory element binding protein 1	0.40
12936	**Pcdha4**	protocadherin alpha 4; cadherin-related neuronal receptor 1	0.40
17203	**Mc5r**	melanocortin 5 receptor	0.40
27214	**Dbf4**	DBF4 homolog (S. cerevisiae)	0.39
18575	**Pde1c**	phosphodiesterase 1C	0.39
52570	**Ccdc69**	coiled-coil domain containing 69	0.39
268281	**Shprh**	SNF2 histone linker PHD RING helicase	0.39
101488	**Slco2b1**	solute carrier organic anion transporter family, member 2b1	0.38
20970	**Sdc3**	syndecan 3	0.38
320799	**Zhx3**	zinc fingers and homeoboxes 3	0.37
16508	**Kcnd2**	potassium voltage-gated channel, Shal-related family, member 2	0.33
77252	**9430038I01Rik**	RIKEN cDNA 9430038I01 gene	0.33

Commonly differentially expressed genes in stage I (continued)

Entrez Gene ID	official symbol	official full name	mean ratio log [*]
216558	**Ugp2**	UDP-glucose pyrophosphorylase 2	-0.34
68642	**2810441K11Rik**	RIKEN cDNA 2810441K11 gene	-0.40
18645	**Pfn2**	profilin 2	-0.41
193116	**Slu7**	SLU7 splicing factor homolog (S. cerevisiae)	-0.42
75619	**Fastkd2**	FAST kinase domains 2	-0.44
26419	**Mapk8**	mitogen activated protein kinase 8	-0.47
320271	**A930041I02Rik**	RIKEN cDNA A930041I02 gene	-0.48
22359	**Vldlr**	very low density lipoprotein receptor	-0.53
13649	**Egfr**	epidermal growth factor receptor	-0.53
103503	**BB001228**	expressed sequence BB001228	-0.54
66970	**Ssbp2**	single-stranded DNA binding protein 2	-0.54
13036	**Ctsh**	cathepsin H	-0.54
101160	**AI838057**	expressed sequence AI838057	-0.54
54722	**Dfna5h**	deafness, autosomal dominant 5 homolog (human)	-0.56
18109	**Mycn**	v-myc myelocytomatosis viral related oncogene, neuroblastoma derived (avian)	-0.57
58998	**Pvrl3**	poliovirus receptor-related 3	-0.57
223473	**Npal2**	NIPA-like domain containing 2	-0.60
21817	**Tgm2**	transglutaminase 2, C polypeptide	-0.60
103784	**AI553587**	expressed sequence AI553587	-0.60
71306	**Mfap3l**	microfibrillar-associated protein 3-like	-0.66
11936	**Fxyd2**	FXYD domain-containing ion transport regulator 2	-0.67
67389	**C1qdc2**	C1q domain containing 2	-0.68
234564	**AU018778**	expressed sequence AU018778	-0.78
210463	**BC026439**	cDNA sequence BC026439	-0.82
74087	**Slc7a13**	solute carrier family 7, (cationic amino acid transporter, y+ system) member 13	-1.00

9.9.2 Commonly differentially expressed genes in stage II (GIPR^{dn} vs. bGH)

Table 9.2 (page 230-241): Commonly differentially expressed genes in stage II: [GIPR^{dn} stage II, wt vs. tg] vs. [bGH stage II, wt vs. tg]. Genes displaying a statistically significant (FDR ≤0.045 %) increase or decrease in signal changes relative to controls were identified in both groups of stage II (wt vs. tg), using the ChipInspector 1.2 software, Genomatix$^®$, Germany. A number of 86 genes displayed a congeneric differential expression in both groups of stage II. [*] The indicated mean expression ratio logs were calculated as arithmetic means of expression ratio log values (with identical algebraic signs) of the respective differentially expressed genes in the single groups (GIPR^{dn}-group and bGH-group) of stage II of investigation.

Commonly differentially expressed genes in stage II (GIPR^{dn} vs. bGH)

Entrez Gene ID	official symbol	official full name	mean ratio log [*]
73230	**Bmper**	BMP-binding endothelial regulator	1.35
12260	**C1qb**	complement component 1, q subcomponent, beta polypeptide	1.16
74499	**Sost**	sclerostin	1.15
107765	**Ankrd1**	ankyrin repeat domain 1 (cardiac muscle)	1.09
192188	**Stab2**	stabilin 2	1.09
78709	**Spink8**	serine peptidase inhibitor, Kazal type 8	1.07
11770	**Fabp4**	fatty acid binding protein 4, adipocyte	1.06
100689	**Spon2**	spondin 2, extracellular matrix protein	1.04
320012	**B930023M13Rik**	RIKEN cDNA B930023M13 gene	1.00
68453	**Gpihbp1**	GPI-anchored HDL-binding protein 1	1.00
22341	**Vegfc**	vascular endothelial growth factor C	0.97
16854	**Lgals3**	lectin, galactose binding, soluble 3	0.97
21825	**Thbs1**	thrombospondin 1	0.97
13040	**Ctss**	cathepsin S	0.95
11602	**Angpt4**	angiopoietin 4	0.93
18436	**P2rx1**	purinergic receptor P2X, ligand-gated ion channel, 1	0.93
12772	**Ccr2**	chemokine (C-C motif) receptor 2	0.91
20715	**Serpina3g**	serine (or cysteine) peptidase inhibitor, clade A, member 3G	0.91
15370	**Nr4a1**	nuclear receptor subfamily 4, group A, member 1	0.88
14955	**H19**	H19 fetal liver mRNA	0.86
268859	**A2bp1**	ataxin 2 binding protein 1	0.85
73149	**Clec4a3**	C-type lectin domain family 4, member a3	0.84
17384	**Mmp10**	matrix metallopeptidase 10	0.83
13924	**Ptprv**	protein tyrosine phosphatase, receptor type, V	0.83
114332	**Xlkd1**	extra cellular link domain-containing 1	0.83

Commonly differentially expressed genes in stage II (continued)

Entrez Gene ID	official symbol	official full name	mean ratio log [*]
381413	**Gpr176**	G protein-coupled receptor 176	0.78
246256	**Fcgr3a**	Fc fragment of IgG, low affinity IIIa, receptor	0.78
60361	**Ms4a4b**	membrane-spanning 4-domains, subfamily A, member 4B	0.77
14289	**Fpr-rs2**	formyl peptide receptor, related sequence 2	0.77
17476	**Mpeg1**	macrophage expressed gene 1	0.77
14599	**Gh**	growth hormone	0.76
14961	**H2-Ab1**	histocompatibility 2, class II antigen A, beta 1	0.76
14129	**Fcgr1**	Fc receptor, IgG, high affinity I	0.76
14573	**Gdnf**	glial cell line derived neurotrophic factor	0.74
110595	**Timp4**	tissue inhibitor of metalloproteinase 4	0.73
103511	**BB146404**	expressed sequence BB146404	0.73
20339	**Sele**	selectin, endothelial cell	0.73
22177	**Tyrobp**	TYRO protein tyrosine kinase binding protein	0,68
11601	**Angpt2**	angiopoietin 2	0.67
16852	**Lgals1**	lectin, galactose binding, soluble 1	0,67
17084	**Ly86**	lymphocyte antigen 86	0,67
66873	**1200009O22Rik**	RIKEN cDNA 1200009O22 gene	0.66
14825	**Cxcl1**	chemokine (C-X-C motif) ligand 1	0.66
14696	**Gnb4**	guanine nucleotide binding protein, beta 4	0.65
18106	**Cd244**	CD244 natural killer cell receptor 2B4	0.65
12505	**Cd44**	CD44 antigen	0.64
21956	**Tnnt2**	troponin T2, cardiac	0.64
54392	**Ncapg**	on-SMC condensin I complex, subunit G	0.64
226652	**Arhgap30**	Rho GTPase activating protein 30	0.64
14127	**Fcer1g**	Fc receptor, IgE, high affinity I, gamma polypeptide	0.64
56191	**Tro**	trophinin	0.64
227929	**Pscdbp**	pleckstrin homology, Sec7 and coiled-coil domains, binding protein	0.64
16792	**Laptm5**	lysosomal-associated protein transmembrane 5	0.63
213002	**Ifitm6**	interferon induced transmembrane protein 6	0.62
52614	**Emr4**	EGF-like module containing, mucin-like, hormone receptor-like sequence 4	0.,61
245527	**Eda2r**	ectodysplasin A2 isoform receptor	0.61
23796	**Agtrl1**	angiotensin receptor-like 1	0.60
56050	**Cyp39a1**	cytochrome P450, family 39, subfamily a, polypeptide 1	0.60
16007	**Cyr61**	cysteine rich protein 61	0.60
109050	**6530418L21Rik**	RIKEN cDNA 6530418L21 gene	0.60
69638	**2310040A07Rik**	RIKEN cDNA 2310040A07 gene	0.60
12319	**Car8**	carbonic anhydrase 8	0,60
246707	**Emilin2**	elastin microfibril interfacer 2	0.59
52276	**Cdca8**	cell division cycle associated 8	0.59
12721	**Coro1a**	coronin, actin binding protein 1A	0.59

Commonly differentially expressed genes in stage II (continued)

Entrez Gene ID	official symbol	official full name	mean ratio log [*]
12316	**Aspm**	asp (abnormal spindle)-like, microcephaly associated (Drosophila)	0.59
18845	**Plxna2**	plexin A2	0.59
13733	**Emr1**	EGF-like module containing, mucin-like, hormone receptor-like sequence 1	0.58
59126	**Nek6**	NIMA (never in mitosis gene a)-related expressed kinase 6	0.58
70695	**3830408D24Rik**	RIKEN cDNA 3830408D24 gene	0.57
12579	**Cdkn2b**	cyclin-dependent kinase inhibitor 2B (p15, inhibits CDK4)	0.57
224840	**Treml4**	triggering receptor expressed on myeloid cells-like 4	0.57
22778	**Zfpn1a1**	zinc finger protein, subfamily 1A, 1 (Ikaros)	0.56
15162	**Hck**	hemopoietic cell kinase	0,56
13038	**Ctsk**	cathepsin K	0,56
223650	**Eppk1**	epiplakin 1	0,56
66102	**Cxcl16**	chemokine (C-X-C motif) ligand 16	0,55
21809	**Tgfb3**	transforming growth factor, beta 3	0.55
69810	**Clec4b1**	C-type lectin domain family 4, member b1	0.55
66857	**1100001H23Rik**	RIKEN cDNA 1100001H23 gene	0.55
13803	**Enc1**	ectodermal-neural cortex 1	0.55
414087	**A330068G13Rik**	RIKEN cDNA A330068G13 gene	0.55
192187	**Stab1**	stabilin 1	0.55
13800	**Enah**	enabled homolog (Drosophila)	0.54
17133	**Maff**	v-maf musculoaponeurotic fibrosarcoma oncogene family, protein F (avian)	0.54
12759	**Clu**	clusterin	0.54
15213	**Hey1**	hairy/enhancer-of-split related with YRPW motif 1	0.54
104885	**Tmem179**	transmembrane protein 179	0.54
21898	**Tlr4**	toll-like receptor 4	0.53
27405	**Abcg3**	ATP-binding cassette, sub-family G (WHITE), member 3	0.53
66929	**Asf1b**	ASF1 anti-silencing function 1 homolog B (S. cerevisiae)	0.53
236604	**4933439C20Rik**	RIKEN cDNA 4933439C20 gene	0.53
15077	**Hist2h3c1**	histone 2, H3c1	0.53
12571	**Cdk6**	cyclin-dependent kinase 6	0.53
58801	**Pmaip1**	phorbol-12-myristate-13-acetate-induced protein 1	0.53
17130	**Smad6**	MAD homolog 6 (Drosophila)	0.53
20312	**Cx3cl1**	chemokine (C-X3-C motif) ligand 1	0.52
19076	**Prim2**	DNA primase, p58 subunit	0.52
12983	**Csf2rb1**	colony stimulating factor 2 receptor, beta 1, low-affinity (granulocyte-macrophage)	0.51
432868	-	hypothetical gene supported by AK052160	0.51
104759	**Pld4**	phospholipase D family, member 4	0.51
20305	**Ccl6**	chemokine (C-C motif) ligand 6	0.51
78887	**Sfi1**	Sfi1 homolog, spindle assembly associated (yeast)	0.51
72925	**March1**	membrane-associated ring finger (C3HC4) 1	0.51
14702	**Gng2**	guanine nucleotide binding protein (G protein), gamma 2 subunit	0.51
74782	**Glt8d2**	glycosyltransferase 8 domain containing 2	0.51

Commonly differentially expressed genes in stage II (continued)

Entrez Gene ID	official symbol	official full name	mean ratio log (*)
94045	P2rx5	purinergic receptor P2X, ligand-gated ion channel, 5	0.50
14230	Fkbp10	FK506 binding protein 10	0.50
104009	Qscn6	quiescin Q6	0.50
21938	Tnfrsf1b	tumor necrosis factor receptor superfamily, member 1b	0.50
17035	Lxn	latexin	050
74748	Slamf8	SLAM family member 8	0.50
229521	Syt11	synaptotagmin XI	0.50
67849	Cdca5	cell division cycle associated 5	0.50
74041	4632434I11Rik	RIKEN cDNA 4632434I11 gene	0.49
71086	4933412E12Rik	RIKEN cDNA 4933412E12 gene	0.48
474332	Dnm3os	dynamin 3, opposite strand	0.48
101351	A130022J15Rik	RIKEN cDNA A130022J15 gene	0.48
26931	Ppp2r5c	protein phosphatase 2, regulatory subunit B (B56), gamma isoform	0.48
13058	Cybb	cytochrome b-245, beta polypeptide	0.48
12394	Runx1	runt related transcription factor 1	0.47
22793	Zyx	zyxin	0.47
14191	Fgr	Gardner-Rasheed feline sarcoma viral (Fgr) oncogene homolog	0.47
14086	Fscn1	fascin homolog 1, actin bundling protein (Strongylocentrotus purpuratus)	0.47
20454	St3gal5	ST3 beta-galactoside alpha-2,3-sialyltransferase 5	0.47
104732	4930427A07Rik	RIKEN cDNA 4930427A07 gene	0.47
20288	Msr1	macrophage scavenger receptor 1	0.47
52187	Rragd	Ras-related GTP binding D	0.47
17158	Man2a1	mannosidase 2, alpha 1	0.47
20965	Syn2	synapsin II	0.47
26943	Serinc3	serine incorporator 3	0.46
74013	Rftn2	raftlin family member 2	0.46
72817	2810484G07Rik	RIKEN cDNA 2810484G07 gene	0.46
67468	Mmd	monocyte to macrophage differentiation-associated	0.46
12929	Crkl	v-crk sarcoma virus CT10 oncogene homolog (avian)-like	0.46
226421	5430435G22Rik	RIKEN cDNA 5430435G22 gene	0.46
110611	Hdlbp	high density lipoprotein (HDL) binding protein	0.46
268390	1110064P04Rik	RIKEN cDNA 1110064P04 gene	0.45
66686	Dcbld1	discoidin, CUB and LCCL domain containing 1	0.45
18718	Pip5k2a	phosphatidylinositol-4-phosphate 5-kinase, type II, alpha	0.45
68922	Dnaic1	dynein, axonemal, intermediate chain 1	0.45
66468	2810433K01Rik	RIKEN cDNA 2810433K01 gene	0.45
19252	Dusp1	dual specificity phosphatase 1	0.45
56318	Acpp	acid phosphatase, prostate	0.44
217303	Cd300a	CD300A antigen	0.44
18590	Pdgfa	platelet derived growth factor, alpha	0.44
94346	Tmem40	transmembrane protein 40	0.44

Commonly differentially expressed genes in stage II (continued)

Entrez Gene ID	official symbol	official full name	mean ratio log [*]
140497	**Cd300d**	Cd300D antigen	0.44
12506	**Cd48**	CD48 antigen	0.44
17916	**Myo1f**	myosin IF	0.44
12223	**Btc**	betacellulin, epidermal growth factor family member	0.43
110920	**Stch**	stress 70 protein chaperone, microsome-associated, human homolog	0.43
105855	**Nckap1l**	NCK associated protein 1 like	0.43
22061	**Trp63**	transformation related protein 63	0.43
211187	**Lrtm2**	leucine-rich repeats and transmembrane domains 2	0.43
245386	**6430550H21Rik**	RIKEN cDNA 6430550H21 gene	0.43
57357	**Srd5a2l**	steroid 5 alpha-reductase 2-like	0.43
70065	**1700030G11Rik**	RIKEN cDNA 1700030G11 gene	0.42
231633	**Tmem119**	transmembrane protein 119	0.42
108099	**Prkag2**	protein kinase, AMP-activated, gamma 2 non-catalytic subunit	0.42
12267	**C3ar1**	complement component 3a receptor 1	0.42
78832	**2700078E11Rik**	RIKEN cDNA 2700078E11 gene	0.42
76788	**2410127E18Rik**	RIKEN cDNA 2410127E18 gene	0.42
14594	**Ggta1**	glycoprotein galactosyltransferase alpha 1, 3	0.42
22589	**Atrx**	alpha thalassemia/mental retardation syndrome X-linked homolog (human)	0.42
70598	**Filip1**	filamin A interacting protein 1	0.42
72333	**Palld**	palladin, cytoskeletal associated protein	0.42
72080	**2010317E24Rik**	RIKEN cDNA 2010317E24 gene	0.42
103220	**Gnn**	Grp94 neighboring nucleotidase variant 4	0.41
73635	**1700113I22Rik**	RIKEN cDNA 1700113I22 gene	0.41
170749	**Mtmr4**	myotubularin related protein 4	0.41
12978	**Csf1r**	colony stimulating factor 1 receptor	0.41
20344	**Selp**	selectin, platelet	0.41
277010	**Marveld1**	MARVEL (membrane-associating) domain containing 1	0.40
14131	**Fcgr3**	Fc receptor, IgG, low affinity III	0.40
72795	**Ttc19**	tetratricopeptide repeat domain 19	0.40
217169	**Tns4**	tensin 4	0.40
14257	**Flt4**	FMS-like tyrosine kinase 4	0.40
70829	**Ccdc93**	coiled-coil domain containing 93	0.40
329739	**B430201A12Rik**	RIKEN cDNA B430201A12 gene	0.40
73130	**Tmed5**	transmembrane emp24 protein transport domain containing 5	0.40
15902	**Id2**	inhibitor of DNA binding 2	0.40
71085	**Arhgap19**	Rho GTPase activating protein 19	0.40
109019	**5830411E10Rik**	RIKEN cDNA 5830411E10 gene	0.39
52855	**Lair1**	leukocyte-associated Ig-like receptor 1	0.39
171504	**Apob48r**	apolipoprotein B48 receptor	0.38
17921	**Myo7a**	myosin VIIa	0.38
23984	**Pde10a**	phosphodiesterase 10A	0.38
228602	**4930402H24Rik**	RIKEN cDNA 4930402H24 gene	0.38

Commonly differentially expressed genes in stage II (continued)

Entrez Gene ID	official symbol	official full name	mean ratio log [*]
20776	**Tmie**	transmembrane inner ear	0.38
18008	**Nes**	nestin	0.37
14219	**Ctgf**	connective tissue growth factor	0.37
14293	**Fpr1**	formyl peptide receptor 1	0.37
239273	**Abcc4**	ATP-binding cassette, sub-family C (CFTR/MRP), member 4	0.35
68048	**Isg20l1**	interferon stimulated exonuclease gene 20-like 1	0.34
17210	**Mcl1**	myeloid cell leukemia sequence 1	0.34
77593	**Usp45**	ubiquitin specific petidase 45	0.34
20375	**Sfpi1**	SFFV proviral integration 1	0.34
108958	**5730472N09Rik**	RIKEN cDNA 5730472N09 gene	0.34
11520	**Adfp**	adipose differentiation related protein	0.33
109346	**Ankrd39**	ankyrin repeat domain 39	0.33
18640	**Pfkfb2**	6-phosphofructo-2-kinase/fructose-2,6-biphosphatase 2	0.32
78829	**Tsc22d4**	TSC22 domain family 4	0.32
76813	**Armc6**	armadillo repeat containing 6	0.29
55944	**Eif3s7**	eukaryotic translation initiation factor 3, subunit 7 (zeta)	-0.27
56484	**Foxo3a**	forkhead box O3a	-0.28
21841	**Tia1**	cytotoxic granule-associated RNA binding protein 1	-0.31
68904	**Abhd13**	abhydrolase domain containing 13	-0.31
69499	**Tsr2**	TSR2, 20S rRNA accumulation, homolog (S. cerevisiae)	-0.31
56424	**Stub1**	STIP1 homology and U-Box containing protein 1	-0.31
211401	**Mtss1**	metastasis suppressor 1	-0.32
77605	**H2afv**	H2A histone family, member V	-0.32
94178	**Mcoln1**	mucolipin 1	-0.32
67393	**Cxxc5**	CXXC finger 5	-0.32
217732	**2310044G17Rik**	RIKEN cDNA 2310044G17 gene	-0.32
233908	**Fus**	fusion, derived from t(12;16) malignant liposarcoma (human)	-0.33
104263	**Jmjd1a**	jumonji domain containing 1A	-0.33
16553	**Kif13a**	kinesin family member 13A	-0.33
68077	**Gltscr2**	glioma tumor suppressor candidate region gene 2	-0.33
11564	**Adsl**	adenylosuccinate lyase	-0.33
445007	**Nup85**	nucleoporin 85	-0.33
19357	**Rad21**	RAD21 homolog (S. pombe)	-0.33
74682	**Wdr35**	WD repeat domain 35	-0.33
231279	**Guf1**	GUF1 GTPase homolog (S. cerevisiae)	-0.33
16601	**Klf9**	Kruppel-like factor 9	-0.33
224902	**Safb2**	scaffold attachment factor B2	-0.34
77626	**Smpd4**	sphingomyelin phosphodiesterase 4	-0.34
56031	**Ppie**	peptidylprolyl isomerase E (cyclophilin E)	-0.34
76155	**6330509M23Rik**	RIKEN cDNA 6330509M23 gene	-0.34
71713	**Cdc40)**	cell division cycle 40 homolog (yeast)	-0.34

Commonly differentially expressed genes in stage II (continued)

Entrez Gene ID	official symbol	official full name	mean ratio log [*]
26554	**Cul3**	cullin 3	-0.34
28019	**Ing4**	inhibitor of growth family, member 4	-0.34
22232	**Slc35a2**	solute carrier family 35 (UDP-galactose transporter), member 2	-0.34
228866	**F730014I05Rik**	RIKEN cDNA F730014I05 gene	-0.35
75560	**Ep400**	E1A binding protein p400	-0.35
121021	**Cspg4**	chondroitin sulfate proteoglycan 4	-0.35
50794	**Klf13**	Kruppel-like factor 13	-0.35
20658	**Son**	Son cell proliferation protein	-0.35
27528	**D0H4S114**	DNA segment, human D4S114	-0.35
66870	**Serbp1**	Serpine1 mRNA binding protein 1	-0.35
93681	**Zfp192**	zinc finger protein 192	-0.35
76917	**2810417J12Rik**	RIKEN cDNA 2810417J12 gene	-0.35
19687	**Recc1**	replication factor C 1	-0.36
64009	**Syne1**	synaptic nuclear envelope 1	-0.36
408063	**LOC432868**	hypothetical gene supported by AK052160	-0.36
107932	**Chd4**	chromodomain helicase DNA binding protein 4	-0.36
18744	**Pja1**	praja1, RING-H2 motif containing	-0.36
230908	**Tardbp**	TAR DNA binding protein	-0.37
20361	**Sema7a**	sema domain, immunoglobulin domain (Ig), and GPI membrane anchor, (semaphorin) 7A	-0.38
67623	**Tm7sf3**	transmembrane 7 superfamily member 3	-0.38
14571	**Gpd2**	glycerol phosphate dehydrogenase 2, mitochondrial	-0.38
93834	**Peli2**	pellino 2	-0.38
21888	**Tle4**	transducin-like enhancer of split 4, homolog of Drosophila E(spl)	-0.38
239364	**Tspyl5**	testis-specific protein, Y-encoded-like 5	-0.38
57431	**Dnajc4**	DnaJ (Hsp40) homolog, subfamily C, member 4	-0.38
78656	**Brd8**	bromodomain containing 8	-0.38
56809	**Gmeb1**	glucocorticoid modulatory element binding protein 1	-0.39
18230	**Nxn**	nucleoredoxin	-0.39
195018	**Zzef1**	zinc finger, ZZ-type with EF hand domain 1	-0.39
109979	**Art3**	ADP-ribosyltransferase 3	-0.39
67705	**1810058I24Rik**	RIKEN cDNA 1810058I24 gene	-0.39
71807	**Tars2**	threonyl-tRNA synthetase 2, mitochondrial (putative)	-0.39
66892	**Eif4e3**	eukaryotic translation initiation factor 4E member 3	-0.39
18029	**Nfic**	nuclear factor I/C	-0.39
432442	**Akap7**	A kinase (PRKA) anchor protein 7	-0.40
68490	**Zfp579**	zinc finger protein 579	-0.40
68346	**Sirt5**	sirtuin 5 (silent mating type information regulation 2 homolog) 5 (S. cerevisiae)	-0.40
67463	**1200014M14Rik**	RIKEN cDNA 1200014M14 gene	-0.40
110784	**Nr3c2**	nuclear receptor subfamily 3, group C, member 2	-0.40
103135	**Usp52**	ubiquitin specific peptidase 52	-0.40
21833	**Thra**	thyroid hormone receptor alpha	-0.40

Commonly differentially expressed genes in stage II (continued)

Entrez Gene ID	official symbol	official full name	mean ratio log (*)
68070	**Pdzd2**	PDZ domain containing 2	-0.40
72508	**Rps6kb1**	ribosomal protein S6 kinase, polypeptide 1	-0.40
72061	**2010111I01Rik**	RIKEN cDNA 2010111I01 gene	-0.41
12803	**Cntf**	ciliary neurotrophic factor	-0.41
12040	**Bckdhb**	branched chain ketoacid dehydrogenase E1, beta polypeptide	-0.41
22289	**Utx**	ubiquitously transcribed tetratricopeptide repeat gene, X chromosome	-0.41
53605	**Nap1l1**	nucleosome assembly protein 1-like 1	-0.41
17984	**Ndn**	necdin	-0.41
27223	**Trp53bp1**	transformation related protein 53 binding protein 1	-0.41
77492	**8030456M14Rik**	RIKEN cDNA 8030456M14 gene	-0.41
16987	**Lss**	lanosterol synthase	-0.41
108100	**Baiap2**	brain-specific angiogenesis inhibitor 1-associated protein 2	-0.42
71891	**Cdadc1**	cytidine and dCMP deaminase domain containing 1	-0.42
19934	**Rpl22**	ribosomal protein L22	-0.42
73181	**Nfatc4**	nuclear factor of activated T-cells, cytoplasmic, calcineurin-dependent 4	-0.42
12484	**Cd24a**	CD24a antigen	-0.42
26365	**Ceacam1**	CEA-related cell adhesion molecule 1	-0.42
11877	**Arvcf**	armadillo repeat gene deleted in velo-cardio-facial syndrome	-0,42
103406	**9130206N08Rik**	RIKEN cDNA 9130206N08 gene	-0.42
77853	**Msl2l1**	male-specific lethal 2-like 1 (Drosophila)	-0.43
19317	**Qk**	quaking	-0.43
319190	**Hist2h2be**	histone cluster 2, H2be	-0.43
209497	**Tmem164**	transmembrane protein 164	-0.43
70757	**Ptplb**	protein tyrosine phosphatase-like (proline instead of catalytic arginine), member b	-0.43
68617	**1110012J17Rik**	RIKEN cDNA 1110012J17 gene	-0,.43
14609	**Gja1**	gap junction membrane channel protein alpha 1	-0.43
20844	**Stam**	signal transducing adaptor molecule (SH3 domain and ITAM motif) 1	-0.43
234725	**Zfp612**	zinc finger protein 612	-0.43
381217	**Gm967**	gene model 967, (NCBI)	-0.43
107351	**Ankrd15**	ankyrin repeat domain 15	-0.43
57915	**Tbc1d1**	TBC1 domain family, member 1	-0.43
22682	**Zfand5**	zinc finger, AN1-type domain 5	-0.44
16468	**Jarid2**	jumonji, AT rich interactive domain 2	-0.44
23966	**Odz4**	odd Oz/ten-m homolog 4 (Drosophila)	-0.44
233806	**8430420C20Rik**	RIKEN cDNA 8430420C20 gene	-0.44
19277	**Ptpro**	protein tyrosine phosphatase, receptor type, O	-0.44
229055	**Zbtb10**	zinc finger and BTB domain containing 10	-0.44
622434	**4631416L12Rik**	RIKEN cDNA 4631416L12 gene	-0.45
100273	**Osbpl9**	oxysterol binding protein-like 9	-0.45
235493	**BC031353**	cDNA sequence BC031353	-0.45
319934	**Sbf2**	SET binding factor 2	-0.45

Commonly differentially expressed genes in stage II (continued)

Entrez Gene ID	official symbol	official full name	mean ratio log [*]
67197	Zcrb1	zinc finger CCHC-type and RNA binding motif 1	-0.46
67733	Itgb3bp	integrin beta 3 binding protein (beta3-endonexin)	-0.46
54613	St3gal6	ST3 beta-galactoside alpha-2,3-sialyltransferase 6	-0.46
245474	Dkc1	dyskeratosis congenita 1, dyskerin homolog (human)	-0.46
224088	Atp13a3	ATPase type 13A3	-0.46
22781	Ikzf4	IKAROS family zinc finger	-0.46
104184	Blmh	bleomycin hydrolase	-0.46
20668	Sox13	SRY-box containing gene 13	-0.46
12874	Cpd	carboxypeptidase D	-0.47
74760	Rab3il1	RAB3A interacting protein (rabin3)-like 1	-0,47
13082	Cyp26a1	cytochrome P450, family 26, subfamily a, polypeptide 1	-0,47
109135	Plekha5	pleckstrin homology domain containing, family A member 5	-0.47
66625	5730406M06Rik	RIKEN cDNA 5730406M06 gene	-0.47
77465	C030027H14Rik	RIKEN cDNA C030027H14 gene	-0.47
233878	Sez6l2	seizure related 6 homolog like 2	-0.47
52428	Rhpn2	rhophilin, Rho GTPase binding protein 2	-0.48
18578	Pde4b	phosphodiesterase 4B, cAMP specific	-0.48
21944	Tnfsf12	tumor necrosis factor (ligand) superfamily, member 12	-0.48
208650	Cblb	Casitas B-lineage lymphoma b	-0.48
94187	Zfp423	zinc finger protein 423	-0.48
235582	6230410P16Rik	RIKEN cDNA 6230410P16 gene	-0.48
59028	Rcl1	RNA terminal phosphate cyclase-like 1	-0.49
18799	Plcd1	phospholipase C, delta 1	-0.49
20495	Slc12a1	solute carrier family 12, member 1	-0.49
12593	Cdyl	chromodomain protein, Y chromosome-like	-0.49
14611	Gja3	gap junction membrane channel protein alpha 3	-0.49
20259	Scin	scinderin	-0.49
68979	Nol11	nucleolar protein 11	-0.50
11443	Chrnb1	cholinergic receptor, nicotinic, beta polypeptide 1 (muscle)	-0.50
231440	9130213B05Rik	RIKEN cDNA 9130213B0 gene	-0.50
13360	Dhcr7	7-dehydrocholesterol reductase	-0.50
56217	Mpp5	membrane protein, palmitoylated 5 (MAGUK p55 subfamily member 5)	-0.50
20681	Sox8	SRY-box containing gene 8	-0.50
213480	OTTMUSG00000015049	predicted gene, OTTMUSG00000015049	-0.51
380912	Zfp395	zinc finger protein 395	-0.51
353310	Zfp703	zinc finger protein 703	-0.51
26360	Angptl2	angiopoietin-like 2	-0.51
67332	Snrpd3	small nuclear ribonucleoprotein D3	-0.52
103142	Rdh9	retinol dehydrogenase 9	-0,52
13555	E2f1	E2F transcription factor 1	-0.52
67101	2310039H08Rik	RIKEN cDNA 2310039H08 gene	-0.52

Commonly differentially expressed genes in stage II (continued)

Entrez Gene ID	official symbol	official full name	mean ratio log [*]
16656	Hivep3	human immunodeficiency virus type I enhancer binding protein 3	-0.52
230259	E130308A19Rik	RIKEN cDNA E130308A19 gene	-0.52
72810	2810455D13Rik	RIKEN cDNA 2810455D13 gene	-0.53
67198	2810022L02Rik	RIKEN cDNA 2810022L02 gene	-0.53
74492	5430433E21Rik	RIKEN cDNA 5430433E21 gene	-0.53
407821	Znrf3	zinc and ring finger 3	-0.53
232798	Leng8	leukocyte receptor cluster (LRC) member 8	-0.54
19737	Rgs5	regulator of G-protein signaling 5	-0.54
20677	Sox4	SRY-box containing gene 4	-0.55
50781	Dkk3	dickkopf homolog 3 (Xenopus laevis)	-0.55
13134	Dach1	dachshund 1 (Drosophila)	-0.55
20620	Plk2	polo-like kinase 2 (Drosophila)	-0.55
13717	Eln	elastin	-0.55
18654	Pgf	placental growth factor	-0.56
50770	Atp11a	ATPase, class VI, type 11A	-0.56
12843	Col1a2	procollagen, type I, alpha 2	-0.56
70267	2010109K09Rik	RIKEN cDNA 2010109K09 gene	-0.56
381339	Tmem182	transmembrane protein 182	-0.56
18166	Npy1r	neuropeptide Y receptor Y1	-0.57
60345	Nrip2	nuclear receptor interacting protein 2	-0.57
14402	Gabrb3	gamma-aminobutyric acid (GABA-A) receptor, subunit beta 3	-0.57
72842	2810488G03Rik	RIKEN cDNA 2810488G03 gene	-0.57
11551	Adra2a	adrenergic receptor, alpha 2a	-0.58
13611	Edg6	endothelial differentiation, G-protein-coupled receptor 6	-0.58
330267	Thsd7a	thrombospondin, type I, domain containing 7A	-0.58
19736	Rgs4	regulator of G-protein signaling 4	-0.58
16658	Mafb	v-maf musculoaponeurotic fibrosarcoma oncogene family, protein B (avian)	-0.58
74842	4833419G08Rik	RIKEN cDNA 4833419G08 gene	-0.59
12006	Axin2	axin2	-0.59
13645	Egf	epidermal growth factor	-0.59
69852	Tcf23	transcription factor 23	-0.60
18004	Nek1	NIMA (never in mitosis gene a)-related expressed kinase 1	-0.60
22418	Wnt5a	wingless-related MMTV integration site 5A	-0.60
71151	Exod1	exonuclease domain containing 1	-0.60
70673	Prdm16	PR domain containing 16	-0.60
11899	Astn1	astrotactin 1	-0.61
70727	Rasgef1a	RasGEF domain family, member 1A	-0.61
329385	C130021I20Rik	RIKEN cDNA C130021I20 gene	-0.61
22673	Zfp185	zinc finger protein 185	-0.62
66222	Serpinb1a	serine (or cysteine) peptidase inhibitor, clade B, member 1a	-0.62
74182	Prei4	preimplantation protein 4	-0.62

Commonly differentially expressed genes in stage II (continued)

Entrez Gene ID	official symbol	official full name	mean ratio log $^{(*)}$
66425	Pcp4l1	Purkinje cell protein 4-like 1	-0.62
14563	Gdf5	growth differentiation factor 5	-0.62
16497	Kcnab1	potassium voltage-gated channel, shaker-related subfamily, beta member 1	-0.62
218038	Amph	amphiphysin	-0.63
20745	Spock1	sparc/osteonectin, cwcv and kazal-like domains proteoglycan 1	-0.63
78892	Crispld2	cysteine-rich secretory protein LCCL domain containing 2	-0.64
17288	Mep1b	meprin 1 beta	-0.64
320840	Negr1	neuronal growth regulator 1	-0.65
68713	Ifitm1	interferon induced transmembrane protein 1	-0.65
75400	Defb29	defensin beta 29	-0.65
240725	Sulf1	sulfatase 1	-0.66
18546	Pcp4	Purkinje cell protein 4	-0.66
11997	Akr1b7	aldo-keto reductase family 1, member B7	-0.66
101160	AI838057	expressed sequence AI838057	-0.66
70784	Rasl12	RAS-like, family 12	-0.66
223473	Npal2	NIPA-like domain containing 2	-0.67
15229	Foxd1	forkhead box D1	-0.67
72361	2210023G05Rik	RIKEN cDNA 2210023G05 gene	-0,67
217265	Abca5	ATP-binding cassette, sub-family A (ABC1), member 5	-0.67
12522	Cd83	CD83 antigen	-0.68
16716	Ky	kyphoscoliosis peptidase	-0.68
224997	Dlgap1	discs, large (Drosophila) homolog-associated protein 1	-0.68
12351	Car4	carbonic anhydrase 4	-0,69
69908	Rab3b	RAB3B, member RAS oncogene family	-0.69
74644	4930426D05Rik	RIKEN cDNA 4930426D05 gene	-0.70
235135	Tmem45b	transmembrane protein 45b	-0.70
276829	D130058I21Rik	RIKEN cDNA D130058I21 gene	-0.71
74333	4122401K19Rik	RIKEN cDNA 4122401K19 gene	-0.71
13036	Ctsh	cathepsin H	-0.71
170772	Glcci1	glucocorticoid induced transcript 1	-0.72
237858	Tusc5	tumor suppressor candidate 5	-0.72
69849	2010007H06Rik	RIKEN cDNA 2010007H06 gene	-0.72
108073	Grm7	glutamate receptor, metabotropic 7	-0.74
22042	Tfrc	transferrin receptor	-0.76
15478	Hs3st3a1	heparan sulfate (glucosamine) 3-O-sulfotransferase 3A1	-0.77
83408	Gimap3	GTPase, IMAP family member 3	-0.79
17967	Ncam1	neural cell adhesion molecule 1	-0.81
320158	Zmat4	zinc finger, matrin type 4	-0.82
18552	Pcsk5	proprotein convertase subtilisin/kexin type 5	-0.82
212539	Gm266	gene model 266, (NCBI)	-0.82
22242	Umod	uromodulin	-0.84

Commonly differentially expressed genes in stage II (continued)

Entrez Gene ID	official symbol	official full name	mean ratio log [*]
110310	**Krt2-7**	keratin complex 2, basic, gene 7	-0.85
59095	**Fxyd6**	FXYD domain-containing ion transport regulator 6	-0.88
18205	**Ntf3**	neurotrophin 3	-0.89
654812	**Angptl7**	angiopoietin-like 7	-0.89
66696	**4631426E05Rik**	RIKEN cDNA 4631426E05 gene	-0.90
12425	**Cckar**	cholecystokinin A receptor	-0.90
15483	**Hsd11b1**	hydroxysteroid 11-beta dehydrogenase 1	-0.90
16069	**Igj**	immunoglobulin joining chain	-0.90
96938	**R74740**	expressed sequence R74740	-0.94
20216	**Acsm3**	acyl-CoA synthetase medium-chain family member 3	-1.01
20272	**Scn7a**	sodium channel, voltage-gated, type VII, alpha	-1.03
56808	**Cacna2d2**	calcium channel, voltage-dependent, alpha 2/delta subunit 2	-1.07
21743	**Inmt**	indolethylamine N-methyltransferase	-1.12
19217	**Ptger2**	prostaglandin E receptor 2 (subtype EP2)	-1.20
14181	**Fgfbp1**	fibroblast growth factor binding protein 1	-1.31
277753	**Cyp4a12**	cytochrome P450, family 4, subfamily a, polypeptide 12	-1.33
28248	**Slco1a1**	solute carrier organic anion transporter family, member 1a1	-1.37
234564	**AU018778**	expressed sequence AU018778	-1.43

Acknowledgements

Curriculum vitae

Name	Andreas Falko Blutke
Date of birth	1st of April 1976
Place of birth	Stuttgart Bad Cannstatt
Citizenship	german
Home adress	Friedrich Engelsbogen 5
	Germany-81735 Munich
Institutional adress	Institute of Veterinary Pathology
	Ludwig-Maximilians-University, Munich
	Veterinärstrasse 13
	80539 Munich
E-mail	blutke@patho.vetmed.uni-muenchen.de
1982 – 1986	Eichendorff Grundschule, Böblingen
1986 – 1990	Albert Einstein Gymnasium, Böblingen
1990 – 1995	Otto Hahn Gymnasium, Böblingen
29.06.1995	Allgemeine Hochschulreife (1.6).
1995 - 1997	Basic military service, then service as professional soldier, last at Geb.Art.Btl.225/ Geb.Jg.Brgd. 23.
1997 – 2003	Student of veterinary medicine, Ludwig-Maximilian-University, Munich.
1999-2001	Employee at the Institute for Veterinary Anatomy of the Veterinary faculty of the Ludwig-Maximilians-University, Munich
2002	Employee at the Institute for Internal Medicine - Dpt. of diseases of the pig - of the Veterinary Faculty of the Ludwig-Maximilians-University, Munich.
10.10.2003	Final exams (1.44).
26.01.2004	Approbation.
February - July 2004	Employee at the Institute for Molecular Animal Breeding and Biotechnology (Gene Center) of the Veterinary Faculty of the Ludwig-Maximilians-University, Munich.
Since February 2004	Investigations of renal and cutaneous alterations in IGF-1 deficient, bGH- transgenic mice.

Since October 2004	Begin of this doctorate "Molecular pathogenesis of progressive glomerulosclerosis - Differential transcript profiling analysis in two murine models of nephropathy" at the Institute of Veterinary Pathology, Ludwig-Maximilians-University, Munich.
	This study is performed in the framework of the graduate college "Functional genomics in veterinary medicine" (grk 1029), supported by the Deutsche Forschungsgemeinschaft, DFG.
2006, 2007	Repeated residences at the University of Michigan, USA as part of the collaboration with the group of Prof. Dr. Kretzler, Dept. of Nephrology.